# Bacteria nanoparticle toxicity testing:

# Toward the use of original methods and complex matrices.

By

**Florian Mallevre**

A thesis submitted for the degree of

Doctor of Philosophy

School of Life Sciences, Heriot-Watt University

Edinburgh, United-Kingdom

February 2016

## Abstract

The development and use of engineered nanoparticles (NPs) has continuously expanded over the last two decades. Despite clear beneficial aspects of NPs, their extensive use and hardly regulated dissemination has raised concern regarding their potential adverse effects. Reports on the environmental release of NPs in wastes, waters, and wastewaters have emerged as well as ecotoxicity related information to a diverse range of model microorganisms (*e.g*. crustaceans, worms, algae, bacteria). However, in spite of growing knowledge in nanoecotoxicology there is limited evidence to draw conclusive statements about the toxicity and fate of NPs, especially in real matrices, in part due to a lack of appropriate methodologies. In this context, this work aimed to investigate the ecotoxicity of widely used and potentially antimicrobial inorganic NPs (Ag, ZnO, CuO, $TiO_2$) to environmentally relevant bacteria (*Pseudomonas putida*) in various matrices (microbiological growth medium, artificial wastewater, real crude and final wastewaters). Complementary planktonic (*i.e*. using a luminescent switch-off bioreporter in a microtitre plate format) and biofilm (*i.e*. using mono and multi-species structures in flow-cell reactors) based assays were used. In addition, the implementation of microcantilever (μCT) and surface plasmon resonance imaging (SPRi) biosensor technologies were piloted. Toxicity of NPs was discussed across approaches (when applicable) in light of their physico-chemical characterisation (using dynamic light scattering, atomic absorption spectroscopy, and ultraviolet-visible spectrophotometry) in used matrices of exposure.

This work provides both practical and fundamental insights about water/wastewater related ecotoxicology of NPs using bacteria. Overall outputs highlighted the suitability of original methods for testing of NPs in or with complex (*i.e*. real) materials and emphasised further the possible limited impact of NPs below the mg $L^{-1}$ level to bacteria (as planktonic or biofilms) in the environment, especially with ageing of NPs (as reported with the Ag NPs), or considering the potential of recovery of bacterial structures (as shown with the biofilms). In addition, the workability of SPRi for testing of NPs was reported for the first time with bacteria, offering new opportunities of further real-time and high throughput biosensor based applications in nanoecotoxicology.

## Acknowledgements

I would like to thank first my supervisors Doctor Thomas J. Aspray and Professor Teresa F. Fernandes for their support during those three years. Thank you Teresa for giving me the chance to compete for a funding when I was looking for opportunities back in 2012 and for welcoming me in your group in 2013. Tom, it was just a great pleasure to work with you, I could not thank you enough for your time, commitment, feedbacks as well as for the freedom and opportunities you offered to me.

This research project would literally not have been possible without the financial support from Heriot-Watt University (HWU). I therefore deeply acknowledge HWU for originally providing me with a James Watt Scholarship (2013-2016) then for further supporting some aspects of my PhD *via* two travel grants (the Alumni Fund 2014 and the Annual Fund 2015). I acknowledge also the Society for Applied Microbiology (SfAM) as well as the MODENA COST action for provided me with, respectively, a R&D Grant in 2013 and a Short-Term Scientific Mission (STSM) Grant in 2015. This work was also supported by the European Union's Seventh Framework Programme [FP7 2007-2013] under EC-GA No. 263215 MARINA, for the provision of the nanomaterials.

I would like to thank the members of the NanoSafety group and of the School of Life Sciences (SLS) as a whole for having unavoidably endured one of my talks, posters, questions, requests or favours at some point. I am especially grateful to Professor Vicki Stone, Doctor Helinor Johnston, Doctor Theodore Henry, Doctor Birgit Gaiser, Doctor David Brown, Doctor Sebastian Hennige, Doctor Nilesh Kanase and Doctor John Kinross for being available to discuss my research. A sincere thank you, as well, to the helpful technical team (Paul, Margaret, Douglas, Sean, Vicky and Robert) and the administrative staff (Kenia, Maggie, Helen and Lesley).

I am glad that collaborators put faith in my proposals. I am particularly grateful to Doctor Will Shu and his team (especially Isaac) from HWU for the trials with the microcantilevers, to Doctors Thierry Livache and Arnaud Buhot and their team (especially Vincent Templier and Raphael Mathey) from the CEA for the trials of surface plasmon resonance imaging, and to Professor Gary Bending and his team, especially Dr Sally Hilton, from Warwick

University for the trials of next generation sequencing. I am also pleased to acknowledge Scottish Water, Craig Milne and Simon Gillespie for their support with the wastewater samples and their insights regarding the water/wastewater industry. I am very grateful as well to Emeritus Professor Nick Christofi for the donation of the *Pseudomonas putida* bioreporter and for keeping a keen eye on me and my project.

Thank you to Professor Susan Dewar and Doctor Derek Jamieson from HWU for taking me along demonstrating in their courses in Microbiology and Molecular Biology, respectively.

Thanks to Doctor Maiwenn Kersaudhi and Doctor Helen Bridle from HWU and to the Bang Goes To the Borders organisers for the two editions of "World of Microfluidics" we had in Melrose S$^{t}$ Mary's Primary School.

Thanks to my mates Richard, Sam, Virginia, Majhed, Joanne, Maria and Cris for the friendly and cheerful atmosphere in the office, the laboratory and beyond. Thanks to Lea and Flora for the rewarding time past together working on the post-graduate student representative duties.

Most importantly again, I have very warm memories of relatives visiting us in Scotland (Laurent & Marie-Laure, Seb & Claire, J-C & Alice, Gregoire & Nadine) and of Scots welcoming us as part of the family (Jimmy, Fiona, James, Isobel, Sarah, Chris and the wees); thank you so much for being part of our live and of our Scot adventure.

Finally, I have a moved thought to my family, parents and brother (always supportive), and deceased grandparents when looking at the accomplished. Family is the most important no matter what; a deep and sincere thought to Melanie with whom we built this project abroad and much more.

# Declaration Statement

ACADEMIC REGISTRY
**Research Thesis Submission**

| | | | |
|---|---|---|---|
| Name: | FLORIAN MALLEVRE | | |
| School/PGI: | School of Life Sciences | | |
| Version: *(i.e. First, Resubmission, Final)* | | Degree Sought (Award **and** Subject area) | PhD in Microbiology & Nanoecotoxicology |

**Declaration**

In accordance with the appropriate regulations I hereby submit my thesis and I declare that:

1) the thesis embodies the results of my own work and has been composed by myself
2) where appropriate, I have made acknowledgement of the work of others and have made reference to work carried out in collaboration with other persons
3) the thesis is the correct version of the thesis for submission and is the same version as any electronic versions submitted*.
4) my thesis for the award referred to, deposited in the Heriot-Watt University Library, should be made available for loan or photocopying and be available via the Institutional Repository, subject to such conditions as the Librarian may require
5) I understand that as a student of the University I am required to abide by the Regulations of the University and to conform to its discipline.

* *Please note that it is the responsibility of the candidate to ensure that the correct version of the thesis is submitted.*

| | | | |
|---|---|---|---|
| Signature of Candidate: | | Date: | |

**Submission**

| | |
|---|---|
| Submitted By *(name in capitals)*: | |
| Signature of Individual Submitting: | |
| Date Submitted: | |

**For Completion in the Student Service Centre (SSC)**

| | | | |
|---|---|---|---|
| Received in the SSC by (name in capitals): | | | |
| Method of Submission (Handed in to SSC; posted through internal/external mail): | | | |
| E-thesis Submitted (**mandatory for final theses**) | | | |
| Signature: | | Date: | |

# Table of Contents

# List of Tables and Figures

CHAPTER 1



CHAPTER 2

CHAPTER 3



CHAPTER 4

CHAPTER 5



APPENDIX A



APPENDIX B



APPENDIX C

APPENDIX D



APPENDIX E

# List of Abbreviations

| Acronym | Definition |
|---|---|
| AAS | Atomic Absorption Spectroscopy |
| AFM | Atomic Force Microscopy |
| Ag | Silver |
| ASTM | American Society for Testing and Materials |
| AW | Artificial Wastewater |
| BOD | Biochemical Oxygen Demand |
| BSA | Bovine Serum Albumin |
| BSI | British Standards Institute |
| C | Carbon |
| CCD | Charge Coupled Device |
| CCM | Culture-Capture-Measure |
| CEA | Alternative Energies and Atomic Energy Commission |
| CFU | Colony Forming Unit |
| CLSM | Confocal Laser Scanning Microscopy |
| COD | Chemical Oxygen Demand |
| Cu (CuO) | Copper (Copper Oxide) |
| CW | Crude Wastewater |
| DLS | Dynamic Light Scattering |
| DNA | Deoxyribonucleic Acid |
| ΔR | Variation of Reflectivity |
| EPS | Extracellular Polymeric Substance |
| FW | Final Wastewater |
| Glc | D-glucose |
| GMB | Genetically Modified Bacteria |
| GMM | Genetically Modified Microorganism |
| HWU | Heriot-Watt University |
| IC | Inhibitory Concentration |
| KLH | Keyhole Limpet Hemocyanin |
| LB | Luria-Bertani |
| LPS | Lipopolysaccharide |
| NGS | Next Generation Sequencing |

| | |
|---|---|
| NM | Nanomaterial |
| NP | Nanoparticle |
| OD | Optical Density |
| OECD | Organisation for Economic Co-operation and Development |
| OTU | Operational Taxonomic Unit |
| § | Paragraph (section) |
| PBS | Phosphate Buffered Saline |
| PCR | Polymerase Chain Reaction |
| PdI | Polydispersity Index |
| PEEK | Polyether-Ether-Ketone |
| pH | Potential Hydrogen |
| PIA | *Pseudomonas* Isolation Agar |
| PID | Proportional Integral Derivative |
| PMT | Photomultiplier |
| Ppy | Polypyrrole |
| PSD | Position Sensitive Detector |
| RI | Reflectivity Index |
| ROS | Reactive Oxygen Species |
| SD | Standard Deviation |
| SEM | Standard Error of the Mean |
| SPRi | Surface Plasmon Resonance imaging |
| $T_D$ | Detection Time |
| $T_G$ | Generation Time |
| $TiO_2$ | Titanium Dioxide |
| T-RFLP | Terminal Restriction Fragment Length Polymorphism |
| TSS | Total Suspended Solids |
| UV-Vis. | Ultraviolet - Visible |
| WWTP | Wastewater Treatment Plant |
| µCT | Microcantilever |
| Zn (ZnO) | Zinc (Zinc Oxide) |

# CHAPTER 1: Introduction and Aims

This chapter presents the relevant scientific milestones supporting the performed and herein reported research. Firstly, general information on "Nanomaterials and nanoparticles" will be presented. Secondly, "Nanoecotoxicology" will be introduced. Information on "Bacteria" followed by a comprehensive literature review focussing on the use of "Bacteria as model microorganisms in nanoecotoxicology" will then be proposed. In light of this, the "Aims" of the research project will finally be formulated.

## 1.1 Introduction

### 1.1.1 Nanomaterials and nanoparticles

#### 1.1.1.1 Definition

Nanomaterials (NMs) are defined by the European Commission as "*materials containing particles, in an unbound state or as an aggregate or as an agglomerate and where, for 50 % or more of the particles in the number size distribution, one or more external dimensions is in the size range 1 - 100 nm"* [1]. In the absence of specific definition for the following, this indistinctively encompasses as well nanotubes, nanorods and nanoparticles. Nanoparticles (NPs) are therefore commonly reported as materials with a least one external dimension in the nanoscale (*i.e*. 1 - 100 nm) in the literature [2]. However, NPs are also reported as materials exhibiting at least two or all three external dimensions in the nanoscale by different standards dedicated organisms such as the American Society for Testing and Materials (ASTM) International and the British Standards Institution (BSI), respectively. In the absence of a consensus regarding the terminology of NPs [3], the latter and less conservative definition from the BSI [4] will be preferred herein, as previously proposed [5].

As shown in Fig. 1.1, on a sole size basis the NMs/NPs could be artificially positioned on a scale alongside deoxyribonucleic acid (DNA) and proteins (*e.g*. antibodies). Overall NPs are therefore more equivalent (*i.e*. in size terms) to the fundamental biological molecules, such as DNA and proteins, than to the cells themselves.

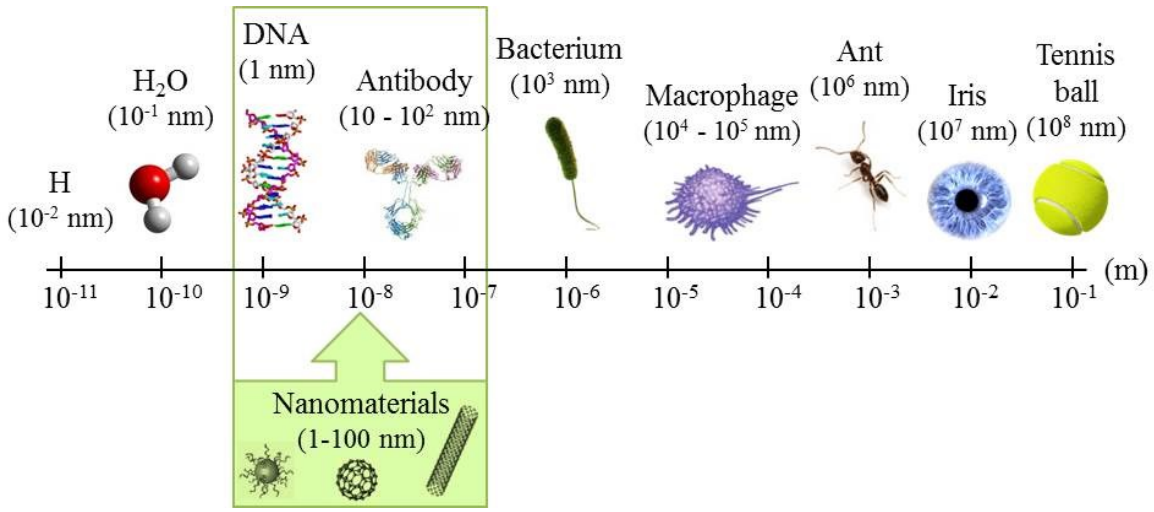


**Fig. 1.1: Relative position of NMs on a size based scale diagram.** Adapted from Klaine *et al*. (2008) [2].

#### 1.1.1.2 Origin and classification

NMs occur naturally (*e.g*. volcanic eruptions, forest fires, soil erosion or ocean sprays) and artificially (*e.g*. as primary products of intentional anthropogenic syntheses and uses or as by-products of industrial processes, mining and combustion engines) in the environment [1, 2, 5, 6].

NMs are classified as: 1) organic, including carbon nanotubes (single and multi-walled) and related materials (*e.g*. fullerenes), or 2) inorganic, including metal and metal oxide NPs (*e.g*. silver (Ag), titanium dioxide ($TiO_2$), zinc oxide (ZnO) and copper oxide (CuO)), quantum dots (*e.g*. cadmium selenide (CdSe) and cadmium telluride (CdTe)), zero-valent metals (*e.g*. zero valent iron (nZVI)) and polymers (*e.g*. dendrimers).

The past few decades witnessed the major expansion of the nanotechnology domain (*i.e*. which encompasses the understanding and development of the fundamental and applied physics, chemistry, biology and technology of NMs) leading, notably, to the omnipresence of manufactured products containing engineered NMs. As a result, the anthropogenic NMs are certainly the most discussed nowadays [2, 3, 5-7].

#### 1.1.1.3 Anthropogenic production

The manufacture of NMs is commonly performed *via* bottom-up and top-down based approaches which respective principle is schematised in Fig. 1.2. Variant biological based methods (referred to as biosynthesis or green synthesis) as well as "safer by design" NPs are nonetheless being increasingly reported [8, 9]. Surprisingly, clear figures on the quantities of NPs produced are hardly available. Piccinno *et al*. (2012) [10] reported values of 550 - 5500, 55 - 550, and 5.5 - 55 tonnes *per* year for $TiO_2$, ZnO and Ag NPs, respectively (based on a survey sent to producing companies). Sun *et al*. (2014) [7] discussed annual European production data *ca*. 10000, 1600 and 30 tonnes for same NPs, respectively, compiling several reports for the year 2012.

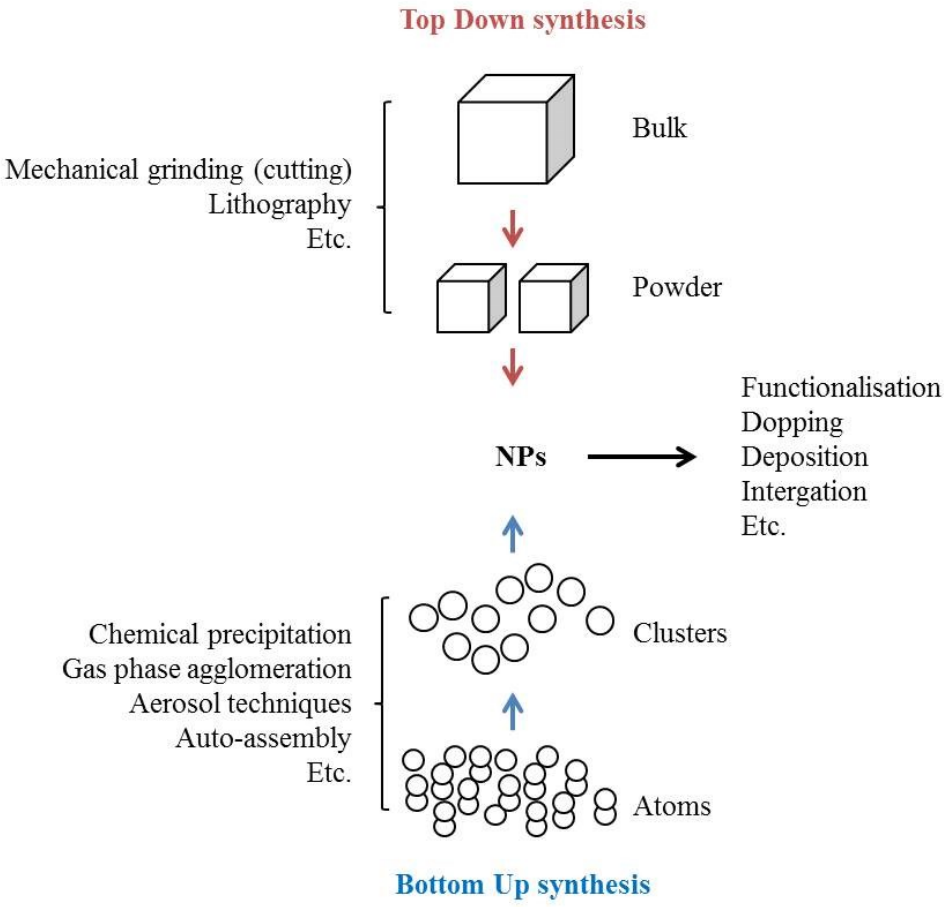


**Fig. 1.2: Different ways of synthesising NPs.** Adapted from Ju-Nam and Lead (2008) [5].

#### 1.1.1.4 Societal implications

Due to their size, NMs show unique physico-chemical (*e.g*. electrical, physical, catalytic, optical, photoactive) properties compared to their bulk counterparts [5, 6, 11]. This makes NMs particularly attractive to develop products or technologies with new or enhanced specificities and applications. As of December 01 2015, there were more than 1820 products listed in the Consumer Products Inventory (CPI). The CPI (non-exhaustive *per se*) is itself being improved in order to support a better referencing of those accumulating products containing engineered NMs [12].

Inorganic NMs such as metal and metal oxide NPs (*e.g*. Ag, $TiO_2$, ZnO and CuO) are among the most used NMs for applications in a wide range of industries such as cosmetic, electronic and sensor, plastic and packaging, textile, paint or water treatment [5-7, 12-16]. The development of metal and metal oxide NPs has been supported further because of their potential antimicrobial properties [17]. Applications in nanomedicine (*i.e*. directly as drugs or as carriers) represent another major interest of NPs, especially with the recrudescence of antibiotic microbial resistance [18, 19].

Continually expanding, the contribution of nanotechnology to the global economy was expected to reach more than $3 trillion by 2015 [20]. Societal implications and benefits of NMs to twenty first century living are therefore clear and considered worldwide [21, 22]; such are their possible subsequent environmental implications.

#### 1.1.1.5 Release and toxicological concern

The life cycle assessment of NPs is intricate [23]. NPs can be released into the environment during their production process or while being transferred between sites for example; or again while being integrated to products or from the actual use, misuse, recycling or disposal of those products containing NPs [24]. Such processes may lead to low rate based but continuous (and potentially accumulating) release [25]. The deliberate use of NPs for some environmental applications (*e.g*. water treatment and environmental remediation) is inevitably leading to their recurrent release too [2, 5, 6, 26, 27]. Finally, massive incidental (or voluntary) releases may also occur therefore leading, conversely, to a temporary but high dose exposure to the microbiota.

As mentioned previously (§ 1.1.1.4), inorganic NPs such as Ag, ZnO, and $TiO_2$ NPs are widely used materials and well known antimicrobial agents for some; their case should be therefore prioritised in nanoecotoxicology. Modelled and measured environmental concentrations of Ag, ZnO and $TiO_2$ NPs range from $10^{-2}$ - $10^{-3}$ µg $L^{-1}$, $10^{-2}$ µg $L^{-1}$ and $10^{0}$ - $10^{-1}$ µg $L^{-1}$ in surface waters and $10^{-1}$ - $10^{-2}$ µg $L^{-1}$, $10^{-2}$ µg $L^{-1}$ and $10^{-1}$ µg $L^{-1}$ in effluent wastewaters as recently discussed by Gottschalk *et al*. (2013) [28]. However, those authors also mentioned than concentrations of inorganic NPs above the mg $L^{-1}$ level could easily be reached in cases of massive releases.

Sources and types of nanowaste (*e.g*. pure NMs, contaminated items or equipment, liquid suspensions and solids containing NMs) as well as their possible fluxes were recently discussed by Marcoux *et al*. (2013) [29]. Those authors emphasised that NMs were a concern in every type of waste and therefore an emerging challenge in waste management aggravated by the uncertainty surrounding quantification, production, and release figures. A scheme of the possible flow of Ag NPs in the environment was proposed by Gottschalk and co-workers (2009) [30], more recently adopted again by Chernousova and Epple (2013) [31] and Sun *et al*. (2014) [7], and here reported in Fig. 1.3.

It was suggested that wastewater treatments plants (WWTPs) were the central but temporal recipients of manufactured NPs while lands, soils and sediments were the terminal sinks. This was highlighted further in the recent reports by Westerhoff *et al*. (2013) [32] and Duester *et al*. (2014) [33]. Additional schemes about ZnO and $TiO_2$ NPs as well as nanotubes were also discussed by Sun *et al*. (2014) [7].

Consequently, the environmental dissemination of manufactured NPs is evident. Concomitant to the continuous development of the nanotechnology sector, the release levels are expected to further increase. As an adverse result, the exposure of the environment to NPs is increasing, inevitably rising potential ecotoxicological concerns [34]. Most studies carried out to date have focused on human health [35, 36], especially on respiratory or inflammatory effects; comparatively little work has been done in the environmental area [2, 5, 6, 29, 33]. Kahru and Ivask (2013) [37] indicated for example that for every 1 000 papers on manufactured NPs about 10 were related to toxicology while only 1 was actually dedicated to ecotoxicological testing. Similarly, the need for minimal

physico-chemical characterisation of NPs (along with toxicity assessment) in used matrices of exposure is increasingly emphasised.

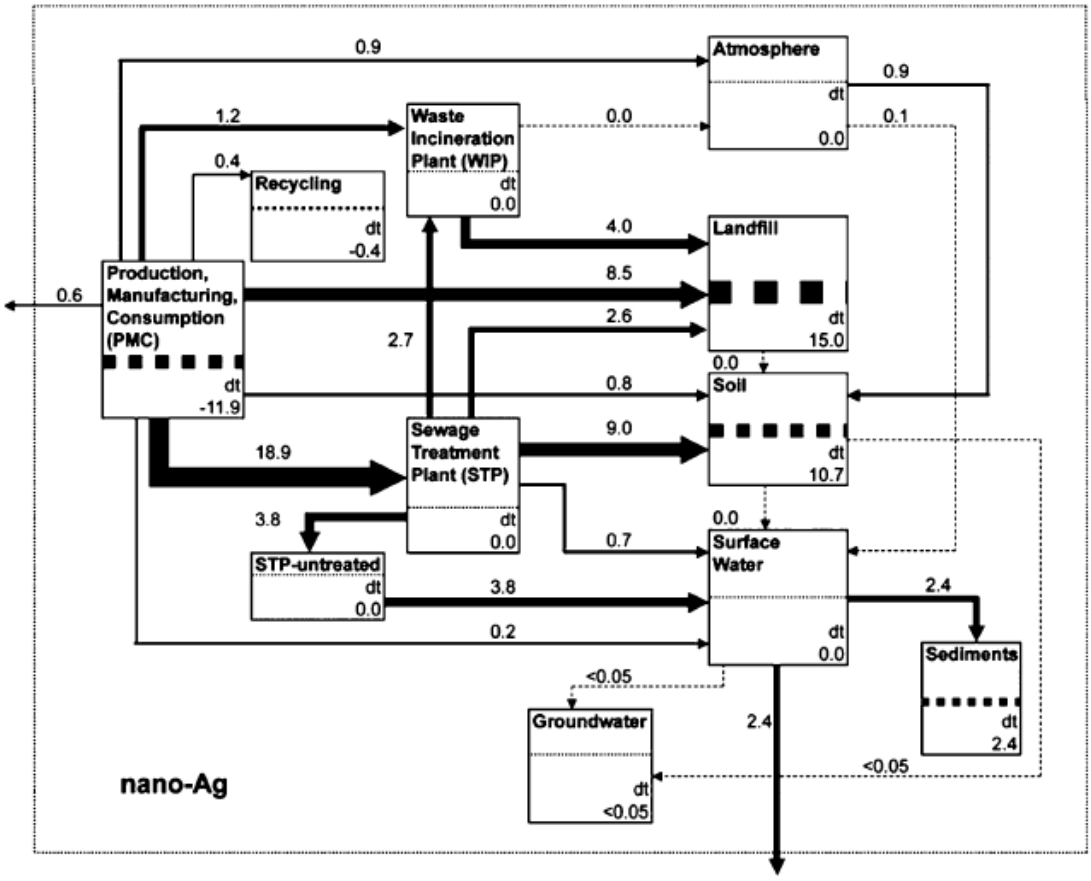


**Fig. 1.3: Scheme of possible NPs (Ag) flow in the environment.** Taken from Gottschalk *et al*. (2009) [30]. Data are mode values (> 0.0005) in tonnes *per* year for the United States of America.

### 1.1.1.6 Usual NP physico-chemical characterisation

#### *1.1.1.6.1 UV-visible spectroscopy*

NPs have optical properties (including absorbance properties) that are sensitive to various parameters such as size, shape, concentration and agglomeration state which may vary with the medium of exposure used. As such, the UV-visible spectroscopy (UV-vis) has shown to be a valuable and inexpensive technique for characterising NPs in aqueous media [38-40].

*1.1.1.6.2 Dynamic Light Scattering*

1.1.1.6.2.1 Z-Average

When particles in suspension are exposed to a monochromatic laser beam part of the photons is deviated due to interactions with the electric field of the particles. The deviated photons constitute the scattered light. It has been demonstrated that the scattered light intensity from a particle was related to its hydrodynamic diameter $d_H$ (*i.e*. the bigger the particle is, the more intense the scattered signal is) [40-42].

The Dynamic Light Scattering (DLS) technique is based on the measurement of the scattered light intensity from excited particles and informs on the averaged derived $d_H$, also referred to as z-average, of the analysed suspension. The z-average value is therefore generally superior to the actual core diameter of the analysed particles (*i.e*. considering the primary particle size derived from dry based microscopy characterisation) as the particles may be directly impacted by the physico-chemical properties of the medium used for exposure as well as the presence of any impurities in the analysed suspension.

The Polydispersity Index (PdI, dimensionless) is generally proposed along with every measurement performed by DLS in order to upraise the significance of the produced data. According to the manufacturer, PdI > 0.7 attests that the analysed suspension is too polydisperse for being suitable with DLS measurements. Conversely, PdI < 0.3 characterise monodisperse colloidal suspensions.

1.1.1.6.2.2 Zeta Potential

When an electric field is applied to a colloidal suspension, the particles bearing charges (due to processes of surface ionisation and/or adsorption of charged particles) exhibit an electrophoretic mobility towards the counter-charged electrode. By measuring this electrophoretic mobility, the DLS (using dedicated cuvettes bearing electrodes) can derive zeta potential values of particle suspensions [40-42].

The zeta potential represents the potential in the slipping plane of a particle (*i.e*. the plane which separates the mobile fluid from the fluid that remains attached to the surface). The zeta potential value can be positive or negative (generally between -30 mV and +30 mV)

and may be directly impacted by the physico-chemical properties of the medium used for exposure. Regardless of the charge, the zeta potential measures the magnitude of attraction/repulsion between the particles. High absolute values will therefore attest to the stability (*i.e*. due to important repulsion between particles) of the analysed suspension, and conversely with low absolute values.

##### *1.1.1.6.3 Atomic Spectroscopy*

Atomic Spectroscopy techniques such as Atomic Absorption Spectroscopy (AAS), Inductively Coupled Plasma Optical Emission Spectroscopy (ICP-OES) and Inductively Coupled Plasma Mass Spectrometry (ICP-MS) are analytical methods used to determine the concentration of a particular metal element (*e.g*. Ag, Zn, Cu) within a sample based on its electromagnetic or mass spectrum [40, 41].

##### *1.1.1.6.4 Electron Microscopy*

Particle size, shape and surface features are critical NP properties which are commonly characterised using Scanning Electron Microscopy (SEM) and Transmission Electron Microscopy (TEM) [40, 43]. Electron microscopy works by bombarding a sample with a stream of electrons and monitoring either the resulting scattering (SEM) or transmission (TEM) effects. The main difference in outputs of both techniques is the way in which the images are resolved. However from a practical viewpoint, SEM is associated with shorter sample preparation and analysis than TEM, whereas TEM delivers greater resolution than TEM.

### 1.1.2 Nanoecotoxicology

#### 1.1.2.1 Definition

Toxicology is the branch of science concerned with the nature, effects, and detection of poisons (*i.e*. substances that are capable of causing the illness or death of a living organism when introduced or absorbed). Ecotoxicology is a sub-branch dedicated to the environment related living organisms. Nanoecotoxicology is, specifically, the ecotoxicology of NMs. Not only the nomenclature is interconnected, the domain itself derives from the others as

reported by Karhu and Dubourguier (2010) [14] in "From ecotoxicology to nanoecotoxicology".

#### 1.1.2.2 "State of the art"

Nanoecotoxicology emerged *ca.* 10 years ago and developed across a plethora of model organisms (*e.g.* crustaceans, bacteria, worms, algae, fishes, plants) screening an overwhelming panel of NPs (*e.g.* of different type, size, charge, coating, surfactant) *via* diverse approaches (*e.g.* varying methodologies, media, endpoints, concentrations) [2, 14, 16, 44-46].

Overall, it was demonstrated that different model organisms have different sensitivity to NPs; algae and crustaceans (natural filters) being the most sensitive. The toxicity of NPs was shown to vary from one material to another; generally attesting to great toxicity of Ag, ZnO and CuO NPs compared to $TiO_2$ NPs, regardless of the testing model. In case of the soluble NPs, ions were generally reported as more toxic than the NP counterparts and the toxicity therefore often reported has mainly driven by the released ions [47]. Otherwise, NPs were widely described to exhibit very versatile physico-chemical properties (*i.e.* corona related) function of, especially, the environment they are in/with [48, 49]. Size and shape of NPs have shown to impact their eventual toxicity [50-55], and so have pH, salt, ionic strength, temperature and light variations [56-59]. The media of exposure were shown to have direct impacts on the NP toxicity [60-66]. Protein containing media (such as Luria Bertani or LB medium) may for example result in the underestimation of NP toxicity as proteins may adsorb on the surface of the NPs potentially altering the metal/ion release or sensibly modifying their size or leading to more aggregation. Similarly, the presence of organic matter has shown to diminish the toxicity of NPs [67, 68].

Despite the above information and despite being clearly associated with protein, membrane, oxidative and DNA damage, the mechanisms (especially in kinetics terms) by which NPs are toxic is not yet deciphered [34, 69]. Consequently, the "state of the art" mainly highlights how little we understand about the actual behaviour and toxicity of NP in real matrices despite critical works have accumulated and nanoecotoxicological trends have emerged during the last decade.

#### 1.1.2.3 Current needs

Nanoecotoxicological studies are particularly challenging since the behaviour, bioavailability and toxicity of NMs are governed by their physico-chemical properties (*e.g.* size, shape, charge, surface area, coating/corona) which are greatly versatile with their environment. This leads to particularly complex studies and to a lack of consistency between results [2, 63, 69-72], challenging further the global understanding and formulation of undergoing mechanisms or principles. Consequently, both the importance and need of standardised approach development and NM characterisation were especially emphasised in nanoecotoxicology during the past few years [6, 27, 34, 69, 70, 72, 73]. Due to the extent of the screening task to perform, the need for high throughput systems has been highlighted too; and so was the need for more frequent assays in real matrices (*e.g.* wastewaters) or questioning potential long term effects of NMs [33, 46, 72, 74, 75].

### 1.1.3 Bacteria

#### 1.1.3.1 Definition

Bacteria are ubiquitous prokaryotic microorganisms constituting a highly diversified although still uncomplete (*e.g.* unknown and non-culturable bacteria) phyla. Gram positive (Gram+) bacteria are characterised by a single external membrane covered with a thick peptidoglycan based layer while Gram negative (Gram-) bacteria exhibit a double membrane (with only a thin peptidoglycan layer intercalated) covered with lipopolysaccharides (LPS).

Bacteria may be encountered as planktonic or biofilm forms [71, 76]. Biofilms are defined as accretions of mono or multi communities of bacteria at biological or non-biological interfaces embedded in a self-produced extracellular polymeric (EPS) matrix [77, 78]. Biofilms are generally referenced as complex, organised and dynamic structures as well as being the main living form of bacteria in the environment [71, 76-78]. Conversely, the planktonic form of bacteria will therefore refer to their non-biofilm organisation when they are “freely floating” (Fig. 1.4).

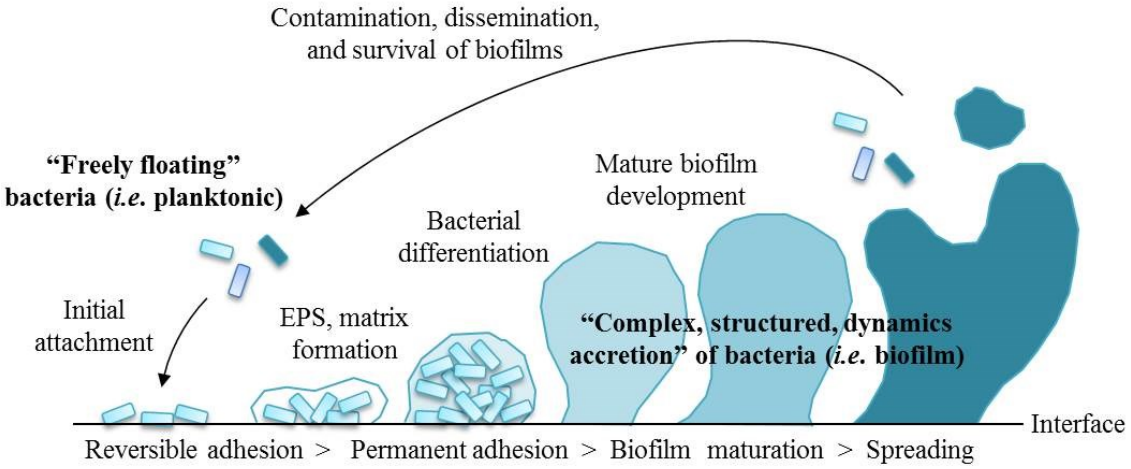


**Fig. 1.4: Planktonic and biofilm living forms of bacteria.** Adapted from Saleh *et al*. (2015) [71].

In addition, compared to planktonic bacteria, biofilms can have gradients of electron donors and acceptors within their structure for example. They also can exhibit both highly active and dormant cells, simultaneously, or show coordinate behaviour in response to particular events; all governed by a highly regulated signalling system known as the quorum sensing [71, 76-79]. The different living style of planktonic and biofilm bacteria have been associated with different transcriptomic patterns [80, 81]. Even their tolerance to antibacterial agents such as antibiotics has been found to be different [77, 79, 82, 83]; the biofilm bacteria being generally more resilient than the planktonic bacteria.

Bacteria are known environmental facilitators at the bottom of the food chain. They may be symbiotic or pathogenic microorganisms for plants and animals (including human beings) and may therefore have both beneficial (*e.g.* wastewater treatment, bioremediation, flora) and problematic (*e.g.* biofouling, infections) implications. Consequently, bacteria (as both planktonic and biofilm forms) represent essential environmental model microorganisms (as well as potentially key clinical targets from a health prospective).

#### 1.1.3.2 Using bacteria as model microorganisms in ecotoxicology

Examples of application of bacteria as model microorganisms in ecotoxicology are numerous as attested, for example, by the review of Robbens *et al*. (2010) [84]. Concomitant with the apex of the molecular biology in the 90s, a plethora of bespoke

genetically modified bacteria (GMB, *e.g*. luminescence emitting bioreporters) have been designed and reported [85-87]. A non-exhaustive list of such bioreporters (considering *ca*. 70 different GMB potentially applicable in nanoecotoxicology) is proposed in Appendix A (Table S1.1). The interest of developing GMB is generally supported by the scientific community [88-90] even if strict regulations are globally limiting their broader applicability so far [91].

Ecotoxicology is also a domain in which the implementation of technologies (*i.e*. integrated along with the use of bacteria) was initiated in order to help developing portable devices suitable for remote testing or integrating multiplex platforms for high throughput analyses of samples for example [92-96].

With such a strong background in ecotoxicology and in light of their aforementioned relevance, the use of bacteria in nanoecotoxicology may seem legitimate; some additional reasons were nonetheless recently highlighted.

#### 1.1.3.3 Reasons for using bacteria in nanoecotoxicology

Holden and co-workers (2014) [97] recently discussed five reasons for using bacteria in nanoecotoxicology. Theses authors outlined evidence suggesting that NMs can "*reduce bacterial community diversity*" and "*alter bacterial physiology and thus nutrient cycling*". In addition, they reported that bacteria may "*affect NM physical characteristics*", "*degrade NMs*", and "*initiate NM trophic transfer to higher organisms*". They notably concluded that routinely using bacteria for assessing NMs would promote effective management of their environmental risk.

Additional advantages could be mentioned regarding bacteria, such as their ease of handling, their rapid growth, the diversity of their phylum, and as aforementioned their potency of being engineered by molecular biology or of being integrated with biosensor technologies as reported in ecotoxicology. Their dual relevance in both environmental and health related sciences makes bacteria very interesting model microorganisms too.

### 1.1.4 Bacteria as model microorganisms in nanoecotoxicology

As widely used and potentially antimicrobial NMs (§ 1.1.1), the following will focus on the inorganic NPs.

#### 1.1.4.1 Toxicity and mode of action

Several reviews have discussed bacteria based toxicity data and the possible mode of action of metal and metal oxide NPs recently [16, 31, 40, 43, 71, 98, 99]. In light of this dedicated literature, it appears that the mechanism(s) by which the NPs are toxic is overall unclear and that conflicting information exist because of, often, differences in the NP dose and solubility or to the methodology used (*e.g*. NP dispersion method, media of exposure, presence of additives, endpoints).

More specifically, the toxicity mechanism(s) of metal and metal oxide NPs to bacteria is generally associated with oxidative stress (*e.g*. generation of reactive oxygen species, ROS), membrane stress (*e.g*. accumulation at the bacterial surface and potential alterations), DNA stress (*e.g*. up and down regulation of genes) as well as released ion based effects and potential internalisation of NPs. The kinetics of those mechanisms is globally unknown; their real implication as causes of toxicity is sometimes debated, especially for the NP internalisation which in the absence of endocytosis phenomenon in bacteria may be seen either as a consequence of the toxic impact or as a methodological artefact.

ROS-induced damage are widely reported to bacteria [98], the causal link between NP properties and ROS generation (by the NPs and/or by the bacteria) is nevertheless unclear. The commonly incriminated ROS species are radical and non-radical forms of high energy chemical species such as singlet oxygen ($^1O_2$), hydroxyl radical (•OH), superoxide ions ($•O_2^-$) and hydrogen peroxide ($H_2O_2$) [100, 101]. Additional information may be found in the detailed review on the implications of oxidative stress induced by inorganic NPs in bacteria [98].

The bacterial membrane alteration is a more debated mechanism. Whereas the interaction between the NPs and the cell wall (*e.g*. adsorption *via* van der Walls or electrostatic

interactions as well as *via* specific groups of moieties depending on the NP coating) seems to be an important factor contributing to the toxicity [53, 102], the sparsely reported internalisation of NPs is not widely accepted [43, 103]. Alteration of the membrane permeability, viscosity and transport exchanges capability were proposed as consequences of such interactions [104, 105].

The toxicity of soluble NPs such as Ag, ZnO and CuO is commonly associated with released ion (*e.g.* $Ag^{+}$, $Zn^{2+}$ and $Cu^{2+}$) based effects [47]. The bacterial case is not different as emphasised by the recent review by Juganson *et al*. (2015) [16] and reported elsewhere [106-108]. The ions are notably thought to be capable of diffusion through the bacterial membrane (*via* porines for example) directly impacting the cell homeostasis and metabolism. $Ag^{+}$ has shown to be able to interact with thiol groups and to form adducts with enzymes, DNA and membrane associated proteins, thereby altering their function [109]. Detailed information may be found in the thorough review proposed by Chernousova and Epple (2013) [31] focussing on Ag (NPs and ions) as antimicrobial agent.

The aforementioned stresses have been further supported by the recent use of genomics and transcriptomics emphasising, in addition, the occurrence of nucleic acid related stresses [110-112].

A graphical abstract of the involved mechanisms reported in the NP toxicity is shown in Fig. 1.5.

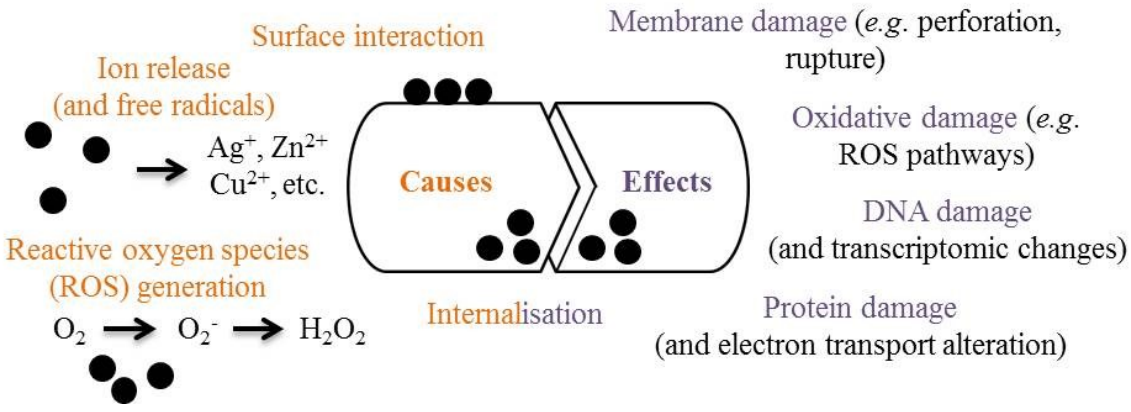


**Fig. 1.5: Graphical abstract of the main reported mechanisms of toxicity of NPs to bacteria.** Adapted from von Moos and Slaveykova (2014) [98].

In addition, Gram+ and Gram- bacteria have shown to be differently tolerant to NPs, the Gram+ being generally reported as the most sensitive [106]. The complex LPS extracellular surface of the double membrane of the Gram- bacteria may confer better protection overall [43]. Some bacteria may also be naturally better equipped than others with, for example, metal resistance genes (*e.g*. to Ag, Zn or Cu) therefore mitigating the potential impact of the released ions in this case. Catalase positive bacteria have also shown to be more tolerant to oxidative stresses than catalase negative ones [98].

Consequently, different bacteria may have different susceptibility to NPs, further challenging the general understanding of the toxicity related mode of action of NPs which still remain to be clearly deciphered.

#### 1.1.4.2 Review of the methodological habits

As the methodology appeared to be a recurrently discussed issue within the nanoecotoxicological domain and as bacteria have intrinsic advantages from a development prospective, a comprehensive literature review has been performed focussing on the actual methodological habits of scientists when using bacteria for NP testing. Main goals of this review were to highlight the common approaches, species, media and techniques used over the last decade; mapping their emergence, questioning their relevance and identifying the potential gaps.

##### *1.1.4.2.1 Overall snapshot*

The following considers 250+ publications dedicated to the testing of inorganic NPs using bacteria over the period 2005-2015. Similarly to Juganson *et al*. (2015) [16] before, existing research studies were mapped by the author using Web of Science™ (Thomson Reuters) with key search term combinations (*e.g*. bacteri* AND nano* AND *toxic*, bacteri* AND nano* AND *toxic* AND eco*). The list of selected relevant publications was cross-checked and completed with the references from the aforementioned reviews [16, 31, 40, 43, 71, 98, 99] reporting on toxicity and mode of action of NPs to bacteria in order to ensure maximal relevance.

The first observation is that about 70 % [50, 52-55, 57, 59-63, 66, 74, 102-105, 108, 110-269] of the considered literature is based on planktonic bacteria (Fig. 1.6). Works with biofilms emerged relatively recently and represents slightly less than 20 % [71, 270-315] of the total reviewed information. A third section, named here as "microcosms", using both planktonic and biofilm forms of bacteria (without directly referring to them) was also identified. Representing slightly more than 10 % [316-347] of the research done so far, mainly in the very recent years, this field is only emerging.

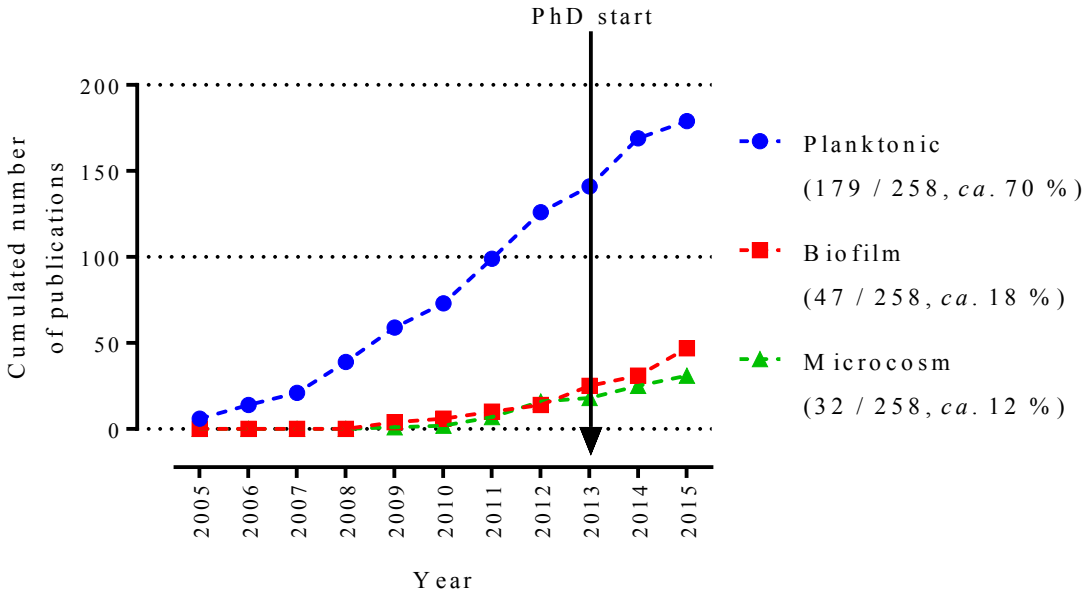


**Fig. 1.6: Mapping the use of bacteria as model microorganisms in nanoecotoxicology during the 2005 - 2015 period.** The cumulated appearance of the planktonic, biofilm and microcosm based methods using bacteria considering 250+ dedicated publications is plotted above.

This quick snapshot attests to the wide use of bacteria in nanoecotoxicology, especially as planktonic cultures; biofilms nonetheless are the common living form of bacteria in the environment (§ 1.1.3). In addition, those figures do not take into account additional papers identified as using bacteria (mainly *via* planktonic means too) but focussing first on the process of biosynthesis (or green synthesis) of NPs (*e.g.* [348-352]). Similarly, information on NP coated surfaces or NP embedding films is not considered, neither are the papers using cyanobacteria or the emerging ones reporting on hybrid or composite NPs (*e.g.* [353-357]). The above therefore certainly underestimates the use of the planktonic based

methods, further unbalancing the actual situation. The emergence of more realistic studies using complex models such as biofilms and microcosms is nevertheless representative of the trend of proposing more relevant data in nanoecotoxicology over the years as previously highlighted (§ 1.1.2).

As shown in Fig. 1.7 A, this effort of proposing more relevant data is also certainly substantiated by the multiplication of the real matrices of exposure (*e.g*. soils, wastewaters, freshwaters, seawaters) being used, especially in the very recent years [59, 118, 123, 125-127, 132-134, 136, 156, 158, 184, 191, 204, 205, 227, 280, 290, 306, 312, 316-319, 321-332, 334-337, 339-342, 344, 346, 347]. However, those are minority cases as the overall picture attests that more than 80 % of the research with bacteria (all methods considered) has been performed in non-real matrices so far. Some distinctions have nonetheless to be made. The rich and undefined microbiological media (*e.g*. Luria Bertani, Tryptone Soja Broth, Nutrient Broth) represent *ca*. 50 % of the matrices used, followed by a group composed of water, water supplemented with NaCl and PBS (phosphate buffered saline) representing *ca*. 25 %. Then come the minimal defined microbiological media (*e.g*. Minimal Davis Medium, TSM, M9, HEPES Minimal Medium, *ca*. 15 %) and the synthetic waters mimicking real-matrices (*e.g*. freshwaters, wastewaters, seawaters, *ca*. 10 %).

Regarding the bacterial species commonly used for the testing of NPs (Fig. 1.7 B), *Escherichia coli*, *Pseudomonas* spp., *Staphylococcus* spp. and *Bacillus* spp. are the most frequently used bacteria (*ca*. 30, 13, 10 and 9 % respectively). Altogether with an additional section called “mix community” (*ca*. 14 %, mainly supported by assays in real matrices using microcosms) they count for more than three quarters of the literature reviewed. Interestingly enough, *Pseudomonas* spp. are represented at more than 75 % by *P. aeruginosa* strains; *P. putida* strains counting for, comparatively, only 19 %. On the other hand, the use of *Vibrio fischeri* (5 %) and *Salmonella* spp. (4 %) may be noticed as well as a significant “Miscellaneous” section (10 %) attesting overall to the intrinsic diversity of bacteria.

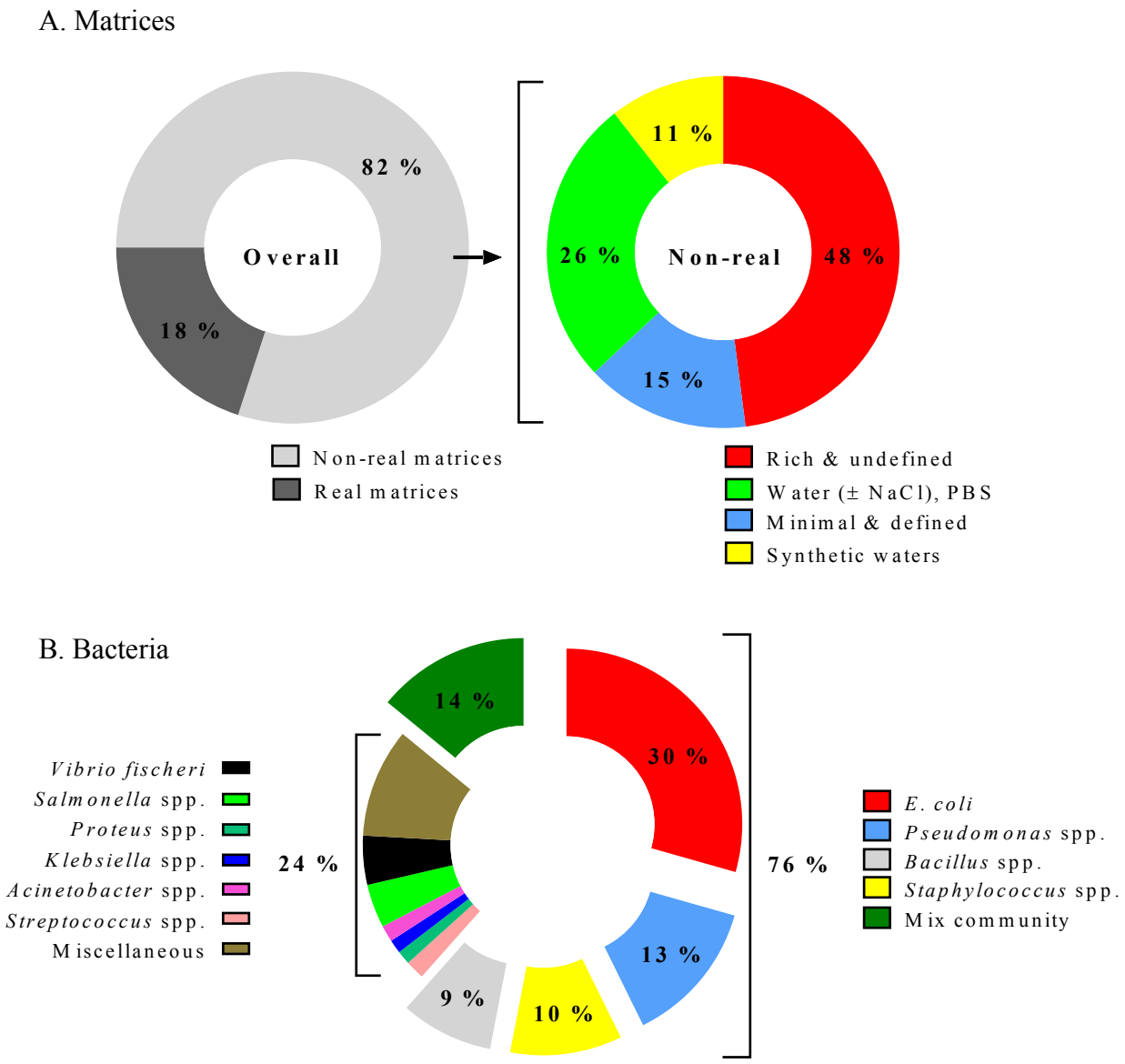


**Fig. 1.7: Deciphering the matrices of exposure and the bacterial species commonly used for NP testing.** The outputs from the performed literature review on bacteria based nanoecotoxicology considering 250+ publications with overviews of used matrices (in A) and bacteria (in B) are shown above, regardless of the methodology (*e.g.* planktonic, biofilm, microcosm).

### *1.1.4.2.2 Planktonic based studies*

Considering the planktonic case, *E. coli* were used in more than half of the publications considered here [50, 52-55, 59, 60, 62, 63, 74, 102, 104, 105, 108, 110, 111, 115-117, 119-121, 124, 131, 137-139, 144, 145, 147, 148, 152, 155, 156, 158, 160, 162, 163, 168-172,

174, 176, 178-182, 187-190, 192, 196-200, 202-204, 206-208, 210-214, 216-218, 220-222, 224, 225, 230-232, 235, 236, 238, 240-242, 244-247, 250-261, 263-265, 267] and finally represents *ca*. 40 % of the used bacterial models, followed by *Pseudomonas* spp. (12 %, which *ca*. 17 % of *P. putida*), *Staphylococcus* spp. (10 %) and *Bacillus* spp. (9 %). Interestingly, about a quarter of the planktonic literature are clearly presented as more related to health sciences [111, 112, 138, 143, 148, 149, 152, 159-162, 169, 171, 172, 176, 180, 181, 186-188, 196, 202, 203, 213, 217, 221, 224, 225, 237, 238, 242, 247, 249, 251, 253, 256, 257, 260, 261, 263, 265, 266, 268, 269] than environmental sciences; nonetheless the same bacteria are being used in both contexts.

As shown in Fig. 1.8 A, the testing of Ag, $TiO_2$, ZnO and CuO NPs represent two thirds of the available information. A myriad of different NPs are then represented in the "Miscellaneous" section (*e.g*. Au, MgO, $Al_xO_y$, $Fe_xO_y$, $CeSO_2$, $SiO_2$, $In_2O_3$, etc.; each representing less than 5 % of the literature) attesting to the overwhelming sweep of the NP testing task.

From a methods viewpoint (Fig. 1.8 B), the use of plating approaches (*i.e*. based on colony forming units (CFU) counting and disc or well diffusion principles) and of absorbance/transmittance means (*i.e*. turbidity or colour forming monitoring by naked eye or spectrophotometric readers) overlook all the others being used respectively 103 and 78 times. Interestingly, those approaches are generally the ones proposed as "standards" (especially the disc/well diffusion method) in NP biosynthesis related (*e.g*. [348-352]) or clinical orientated literature (*e.g*. [112, 138, 143, 148, 149, 152, 161]). They are also referred as particularly inaccurate for the plating case and non-suitable with colour or complex materials for the optical density (OD) monitoring case [358, 359]. In addition, rarely performed in real matrices (*ca*. 8 % of the available data) the actual relevance of the above might be questioned.

Some alternative applications are emerging such as the use of flow cytometry, but those remain scarce despite being promising [118, 158, 178-181, 190, 203, 226, 253, 257]. Assays with some natural bioluminescent bacteria such as *Vibrio fischeri* (mainly used as proposed by Microtox) have been proposed [113, 114, 135, 140, 142, 150, 165, 175, 177,

183, 195, 215, 228, 229, 233, 236, 243, 248] but dramatically suffered from being generally performed in water supplemented with NaCl at 2 - 22 % (w/v). The use of light-emitting GMB (based on bespoke *E. coli* at 75 %) has been reported too [52, 61, 66, 104, 124, 141, 144, 145, 147, 182, 185, 200, 203, 204, 207, 219, 222, 227, 235, 236, 238, 258, 360] but not quite as extensively as observed in ecotoxicology (Appendix A, Table S1.1).

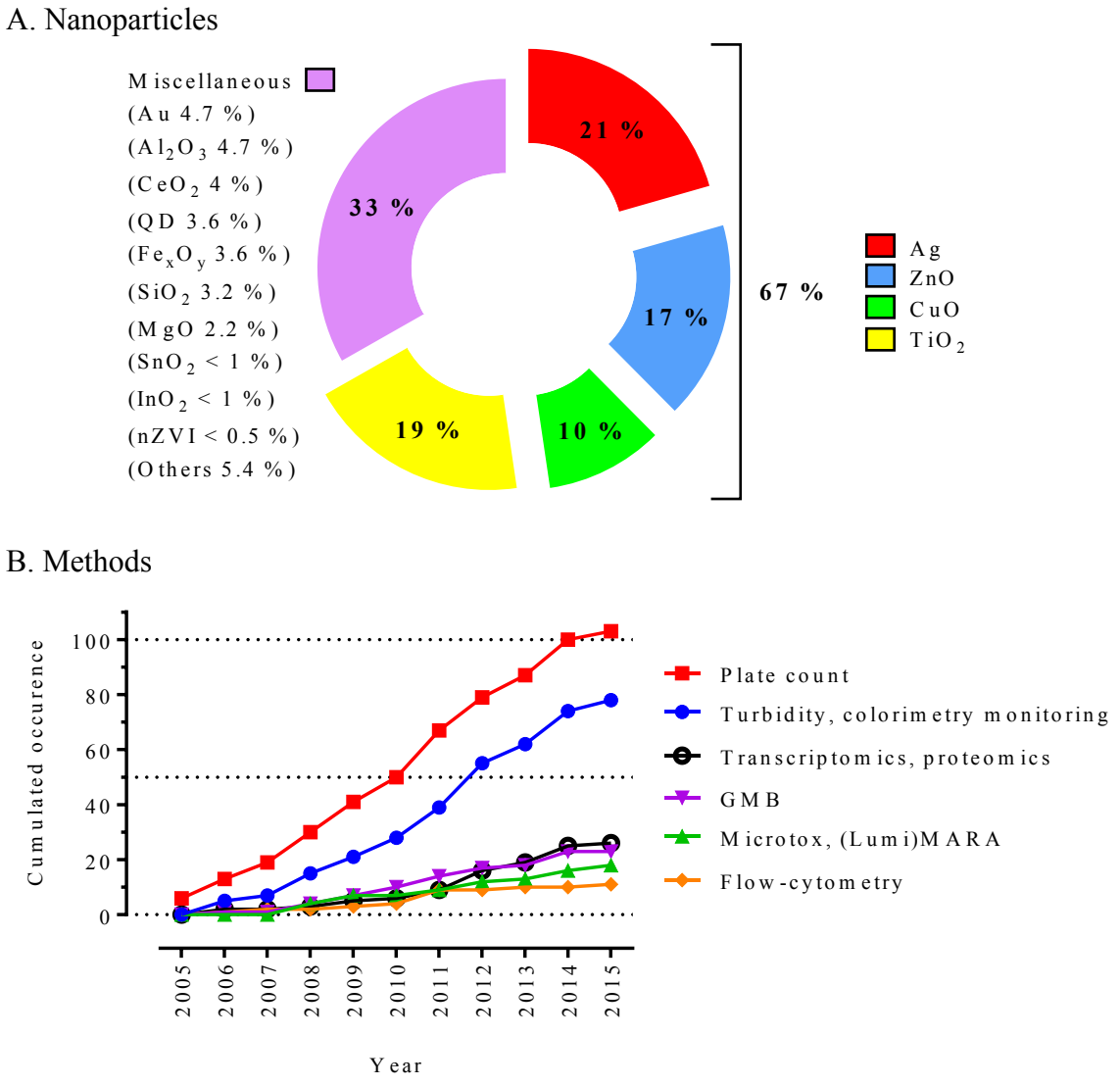


**Fig. 1.8: Insights into the toxicity testing of NPs using planktonic based assays.** The outputs from the performed nanoecotoxicological literature review dedicated to the bacterial planktonic case considering 170+ publications with overviews of tested NPs (in A) and used methods (in B) are shown.

The aforementioned planktonic based methods used for the toxicity assessment of NPs are now commonly associated with characterisation techniques such as transmission electron microscopy (TEM), atomic force microscopy (AFM), Fourier transform infrared spectroscopy (FTIR) and X-ray photoelectron spectroscopy (XPS), or more recently by transcriptomic and proteomic techniques (*e.g*. [104, 108, 111, 112, 116, 124, 132, 133, 139, 145, 154, 155, 163, 164, 166, 167, 283]). The use of fluorescent viability markers, the monitoring of utilised substrates (*e.g*. gas, ATP, carbon sources) or expressed enzymes (*e.g*. from the ROS pathway) are also being increasingly reported.

Interestingly, only a handful of planktonic studies (*ca*. 9 %) clearly questioned the NP ageing or the potential recovery of bacteria [53, 118, 129, 136, 140, 143, 157, 166, 175, 194, 195, 225, 229, 234, 239, 250].

#### *1.1.4.2.3 Biofilm based studies*

Focussing on the biofilms [71, 270-315], Ag, $TiO_2$, ZnO, CuO and Au NPs were mainly tested (Fig. 1.9 A) using mono-species biofilms with *Pseudomonas* spp. (*ca*. 23 %, which about a quarter is using *P. putida*), *Staphylococcus* spp. (*ca*. 16 %), *E. coli* (*ca*. 11 %) and *Bacillus* spp. (*ca*. 8 %) especially. The tested materials and used models are fundamentally the same than with the planktonic approaches even if the rankings may differ between the two. Interestingly, multi-species biofilms (*i.e*. based on mix communities) were also reported (*ca*. 11 %).

As similarly stressed above, some species such as *P. aeruginosa* may be alternatively used in ecotoxicological (*e.g*. [71, 282, 291, 296-298]) or toxicological (*e.g*. [294, 300, 301, 303, 311]) contexts. Overall, slightly more than 40 % of the biofilm literature identified here is clearly positioned in a health (or clinical) related context [270-273, 275, 281, 284-286, 289, 291, 294, 300, 301, 303, 305, 309, 311, 313, 315] while being relevant for environmental scientists too. Interestingly and regardless of the materials, only about 50 % [271-273, 275, 276, 279-284, 286, 287, 289, 291, 293, 295, 297, 298, 305, 308-310, 312] of the biofilm literature actually compare the toxicity information with a planktonic counterpart.

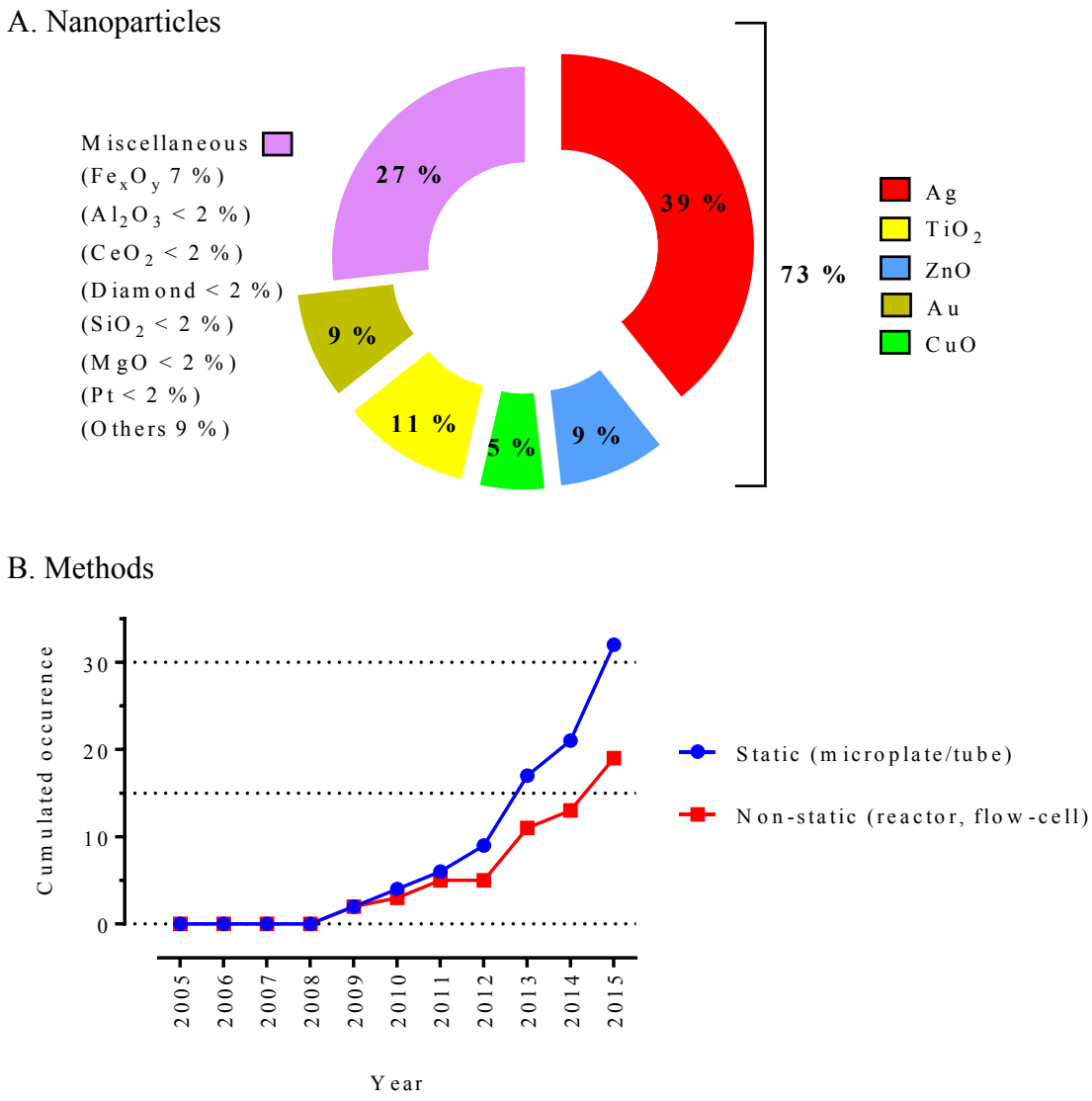


**Fig. 1.9: Insights into the toxicity testing of NPs using biofilm based assays.** The outputs from the performed nanoecotoxicological literature review dedicated to the bacterial biofilm case considering 45+ publications with overviews of tested NPs (in A) and used methods (in B) are shown.

From a methodological standpoint (Fig. 1.9 B), the biofilms can be separated in two main groups which are the static and the non-static. Static biofilms are established in microtiter plate or microtubes, on beads, slides or membranes in the absence of flow [271-276, 279-281, 283, 286, 287, 289, 291-294, 298-301, 303-305, 307, 309-311, 313, 315]. Non-static biofilms are established in reactors (*e.g.* rotating, CDC and flow-cell reactors) and/or on slides (*i.e.* generally immerged within a matrix in recipients or in natural environments)

under controlled or not turbulent or laminar hydrodynamic conditions [71, 270, 277, 278, 282, 284, 285, 288, 290, 295-297, 299, 302, 306, 308, 312, 314]. The use of non-static biofilms is often encouraged as leading to mature (and fully hydrated) structures "free" from planktonic cells, being therefore overall more relevant that the static ones [361-363]. However, non-static biofilm based studies represent less than 40 % of the reviewed literature. Interestingly, not half of those latter actually performed the exposure to the NPs under the flow conditions too; in a majority of cases biofilms are first sampled (*i.e.* harvested) before being exposed to NPs in a "static" manner. The toxicity testing of NPs to mature biofilms under flow conditions appears therefore very limited still.

From a characterisation viewpoint, the analysis of biofilms in microtiter plate is mainly performed using a crystal-violet based approach while slides are generally treated with viability stains associated with, respectively, spectrophotometric or microscopic supports. The plate count from disrupted biofilms [71, 282, 284-286, 291, 292, 294, 297, 299, 301, 302, 308, 310, 311] or the monitoring of metabolic parameters [276-279, 282, 283, 288-290, 292, 295, 310, 313] are not common practices (each in *ca*. 30 % of the listed biofilm papers) but are reported. Approaches based on flow-cell systems generally required fluorescent staining coupled with microscopy such as confocal laser scanning microscopy (CLSM) in order to image through the biofilm structure (*e.g.* [272, 274, 282, 289, 294, 306, 309, 314]). Here as well, inputs from proteomics and transcriptomics are emerging [276, 277, 280, 282-284, 295].

#### *1.1.4.2.4 Microcosm based studies*

Finally looking at microcosm related papers [316-347], unsurprisingly about 95 % used real matrices. Interestingly those matrices were mainly soils, sands and sediments; river, estuarine or stream waters were scarce comparatively [318, 331, 333, 343, 345-347]. In addition to the matrix, intrinsically with the idea of microcosm comes the notion of long term experiments (from days to months) and of mix microbial communities as both observed here for most of the papers. Due to the complexity of the exposed microbial population, molecular biology based characterisation means such as sequencing, terminal restriction fragment length polymorphism (T-RFLP) and fluorescence *in situ* hybridisation

(FISH) were generally deployed (*ca*. 70 %) as support for global metabolic based analyses (*ca*. 80 %) *via* leucine incorporation, protease activity, C or N use and gas production monitoring techniques for example.

### 1.1.5 Knowledge gaps

In light of the above literature review (§ 1.1.4.2), some fields of application are clearly underexploited using bacteria. The use of environmental strains such as *P. putida*, of complex materials such as biofilms and of real matrices of exposure such as wastewaters should be promoted to support the generation of more relevant data. Similarly, the development of some approaches such as the use of bespoke GMB within planktonic and the use of hydrodynamic conditions within biofilm, both in real-time, should be encouraged. The further development of microcosm based studies was also identified as a potentially relevant source of information but was not pursued herein.

In addition and surprisingly, despite a consensus about the importance of NP ageing in regards to toxicity; this later is only scarcely considered. Similarly, the investigation of the potential recovery of the model microorganisms *post* exposure to NPs is not common information in spite of being potentially crucial. Consequently, the consideration of those (ageing of NPs and recovery of bacteria) when performing planktonic or biofilm based assays would further support novelty.

Interestingly, despite the fact that NPs are widely used in the sensor sector [16], the use of biosensor technologies (defined by Turner *et al*. (1989) [364] as analytical approaches incorporating a biologically-derived sensing element intimately associated with a physico-chemical transducer designed to translate biochemical reactions into electrical signals) such as microcantilever (µCT) or surface plasmon resonance imaging (SPRi) for performing toxicity testing of NPs is not reported yet. Any implementation of biosensor technologies using bacteria could therefore be valued as original proof of concept for NP testing applications.

#### 1.1.5.1 Switch-on/off bespoke GMB

Switch-on/off methods of monitoring bacterial growth are based on light emitting bacteria (such as bespoke GMB) expressing an optically monitorable signal (*e.g.* luminescence, fluorescence). Regardless of the signal type, the general principle is based on the monitoring of the emitted signal over time when the GMB is exposed to various concentrations of potential toxicants [90].

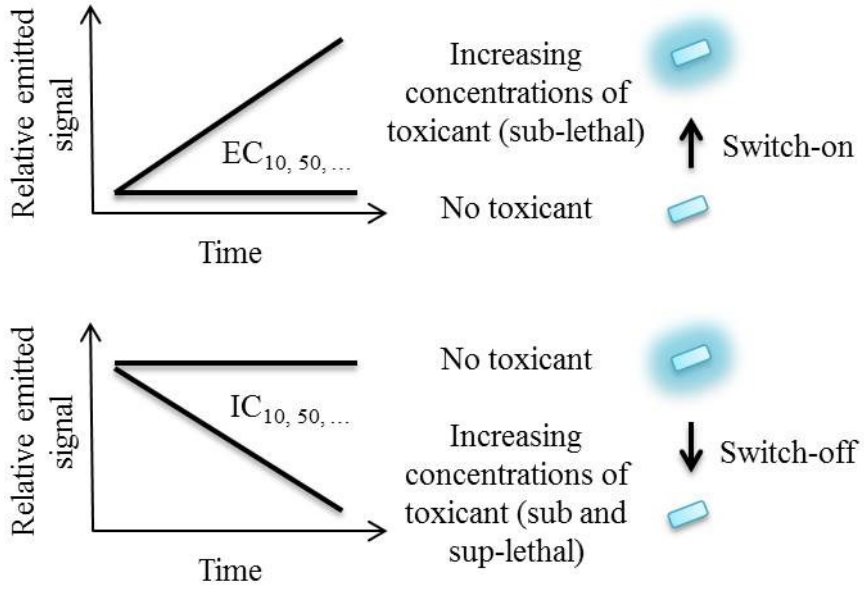


**Fig. 1.10: Switch-on/off based method.** Adapted from van der Meer and Belkin (2010) [90].

Switch-on bioreporters are inducible. They are genetically engineered to emit a signal under particular conditions of stress (*e.g.* membrane, DNA, protein or oxidative damages) regardless of the identity of the toxicant, or under the presence of a targeted compound (*e.g.* heavy metals, mono and poly-aromatic hydrocarbons). The presence/impact of toxicants is therefore characterised by an increase over time of the emitted signal (corresponding to the activation of selected signalling pathways) when compared to a non-exposed control (Fig. 1.10, top scheme).

Conversely, switch-off bioreporters are genetically designed to bear reporter genes under a constitutive control. The presence/impact of toxicants is therefore characterised by a decrease of the emitted signal over time (corresponding to bacterial growth inhibition

and/or bacterial death) when compared to a non-exposed control (Fig. 1.10, bottom scheme).

Consequently, switch-on systems are either unspecific or specific and may inform on the presence/absence of a targeted toxicant as well as the way by which it may be toxic. Such bioreporters are operated at the sub-lethal level. Conversely, switch-off bioreporters are unspecific and provide information on the relative toxicity of the tested toxicant. Switch-off systems can lead to $IC_{50}$ values (*i.e*. defined as the concentration of toxicant inhibiting half of the exposed microbial reporting population) and therefore inform on the acute toxicity of tested toxicants.

Overall 23 studies assessing antibacterial properties of NPs (*ca*. 13 % of the aforementioned planktonic literature) were identified as using switch-on/off GMB bioreporters. As discussed by van der Meer and Belkin (2010) [90] and Xu *et al.* (2013) [87], and also observed here in the large majority of cases, *lux* based systems are generally preferred because luminescence offers better kinetics overall (*i.e*. quicker response, shorter life time) than fluorescence. More specifically, a few different stress based switch-on GMB were reported [66, 104, 124, 145, 147, 182, 204, 219, 222, 227, 236, 238, 360]. Current limitation of the switch-on approaches relies on the absence of clearly understood mechanism(s) of identified specific pathway(s) for NP toxicity, limiting the development of "NP specific GMB". Alternatively, switch-off GMB were proposed for acute testing of diverse NPs along with $IC_{50}$ values after, generally, 1 - 2 h of exposure [144, 200, 203, 235, 258, 365, 366]. The development of arrays has been proposed [114, 182]. This literature attests to the potential of light-emitting GMB based tools for NP testing; however applications have been almost exclusively based on *E. coli* bioreporters (*ca*. 90 % of the cases) and restricted to NP testing in microbiological growth media.

Recently, the *P. putida* BS566 lux::CDABE (hereafter referred to as *P. putida* BS566 *lux*) GMB has been proposed but only employed for Ag NP testing in LB [185]. *P. putida* BS566 was isolated from a coke WWTP then modified by transposon (Tn5) mutagenesis to constitutively express the full *lux* operon from *Photorhabdus luminescens* along with a kanamycin resistance gene [367]. The workability of *P. putida* BS566 *lux* for toxicity testing in environmental matrices such as wastewaters was suggested [185, 367], but not

yet investigated. Building on those preliminary studies, additional screening assays with *P. putida* BS566 *lux* using various NPs in different matrices (*e.g*. artificial and real) would extend the scope of applicability of the methodology and substantiate further the nanoecotoxicological related knowledge.

#### 1.1.5.2 Mono/multi-species biofilms in reactors

Despite their relevance, only a handful of nanoecotoxicological studies have been carried out with fully hydrated mature biofilms under hydrodynamic conditions using reactors without sampling *ante* exposure [71, 277, 278, 282, 295, 296, 299, 314]. Unlike most reactors, the flow-cell systems present the additional advantages of real time and non-invasive morphological studies allowed by the CLSM compatibility of the flow-cells themselves [362, 363]. As being non-destructive, such approach could support the temporal assessment of the toxicity of NPs, questioning for example the potential biofilm recovery *post* exposure. Although not quite reported yet, functional studies based on the comparative analyses of influent and effluent samples could be performed. Considering different media and C sources or scenarios of exposure (*e.g*. flow rates, single/multiple pulses of toxicants, mono/multi-species biofilms), a high potential of bespoke assay development is associated with the use of flow-cell reactors (Fig. 1.11).

The application of flow-cell reactors has been reported in ecotoxicology for the testing of silver sulfadiazine and solvent styrene on *Pseudomonas* spp. biofilms [368, 369]. Examples in nanoecotoxicology are particularly scarce at the present time. Fabrega *et al*. (2009) [314] investigated the interactions (accumulation and uptake of NPs) between Ag NPs and *P. putida* biofilms. Ronen *et al*. (2013) [299] reported the higher resilience of non-static *P. putida* biofilms to ZnO NPs compared to static biofilms. Maurer Jones *et al*. (2013) [295] discussed the impact of $TiO_2$ NPs to flavin secretion by *Shewanella oneidensis* biofilms. More recently, this literature was substantiated further by the study of Mohanty *et al*. (2015) [282] who reported impacts of metal NPs to structure and function of *P. aeruginosa* biofilms.

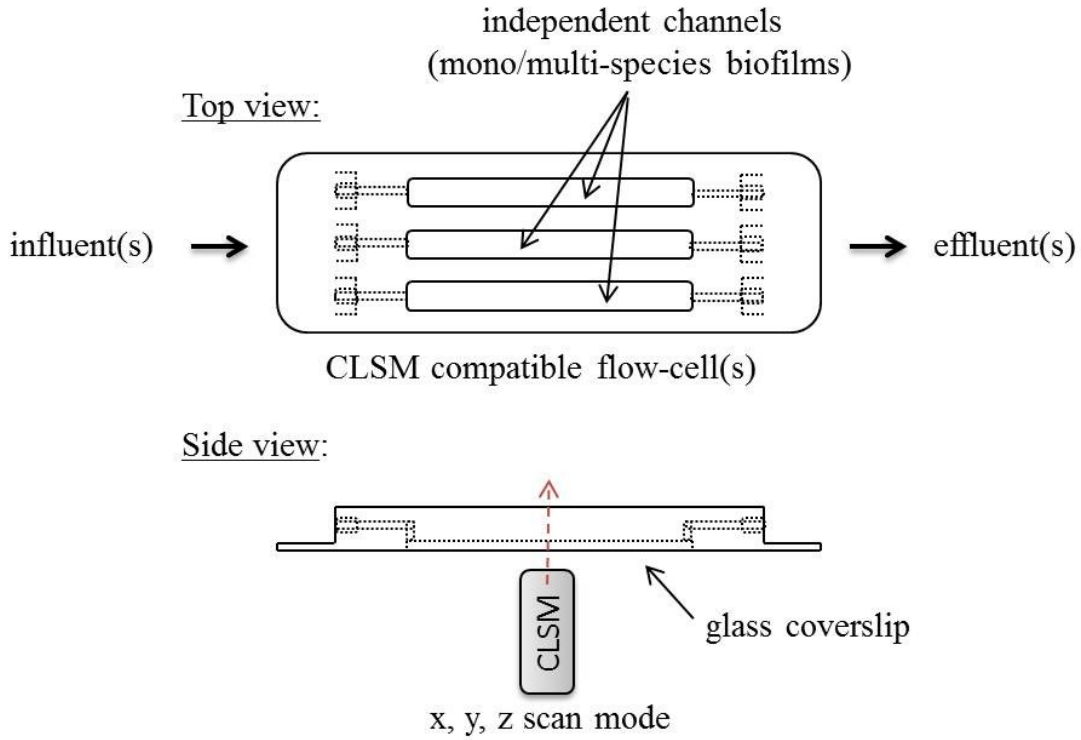


**Fig. 1.11: CLSM compatible flow-cell based reactor principle.** Adapted from Crusz *et al*. (2012) [362].

Building on those pioneer examples [295, 299, 314], the assessment of the temporal impact of NPs on non-static mono-species biofilm (*e.g. P. putida* based) morphology, viability and activity using flow-cell reactors could be performed in first intention. Furthermore, the use of multi-species biofilms (*e.g*. wastewater based) has been limited in nanoecotoxicology and was not reported yet with flow-cell reactors. Both mono and multi-species biofilms based studies would therefore further enrich the nanoecotoxicological method portfolio as well as the general knowledge regarding the toxicity of NPs to relevant and complex biological structures.

#### 1.1.5.3 Biosensor technologies

Biosensors are used for numerous purposes including disease diagnostic, drug discovery and environmental monitoring [89]. Microcantilever (μCT) and surface plasmon resonance imaging (SPRi) are examples of prolific biosensor related technologies (*i.e*. transducers) offering a wide range of applications and promises in life sciences [89, 370-373]. The main

advantages associated with the development and use of such technologies imply their label-free, high throughput, high sensitivity (*e.g.* work at single/few cells rather than population level) and potential portability. Frequent drawbacks imply their complexity, fragility and cost. In the absence of any biosensor based application using bacteria in nanoecotoxicology, the implementation of such approaches might lead to new ways of testing the toxicity of NPs.

#### *1.1.5.3.1 Microcantilever*

The biosensor related μCT technology derives from Atomic Force Microscopy (AFM) which is a widely used technique to characterise surfaces at the nano-scale. AFM is fundamentally based on the interactions (*i.e.* forces) monitoring between the thin needle of a suspended cantilever and the surface to be characterised [374].

Comparatively, biosensor related applications are based on the monitoring of mechanical events occurring at the surface of "free-standing" cantilevers in response to stimuli. Two main principles may then be considered as μCT can be operated in static or in dynamic mode where responses are transduced into bending changes or resonance frequency changes, respectively [371]. Static mode measurements are however generally preferred when performed in liquid environments [372, 373].

The mechanical bending of a static μCT (Fig. 1.12) has been shown to be proportional to the occurring changes (*i.e.* interactions or stresses) at its surface. Consequently, by quantifying the mechanical bending the primary changes on the μCT can be upraised. A classic readout mean for assessing this bending is the monitoring over time of the variation of the reflective angle of an incident laser beam onto the μCT tip (Fig. 1.12). This design may enable the interrogation of multiple μCTs used in parallel in a "comb-like" format leading to array based assays.

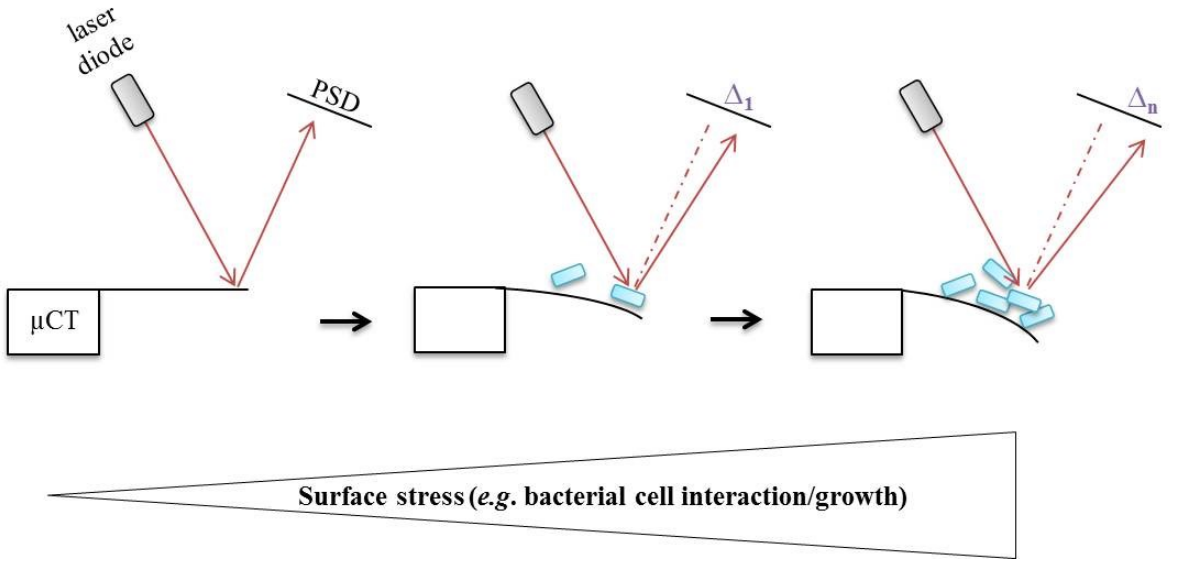


**Fig. 1.12: Static μCT principle.** The principle of the used static μCT based approach encompassing mainly a laser diode, the μCT and a position sensitive detector (PSD) is schematised. The modification of the μCT reflective angle in response to surface stresses such as the growth of bacteria results in a quantifiable variation (Δ) in position terms on the PSD. Adapted from Zhang *et al*. (2012) [372].

To date, the μCT biosensors have been essentially applied for real-time biomolecular interaction monitoring, heavy metal ion detection, as well as yeast cell proliferation monitoring [371, 372, 375-377]. Their application to bacterial systems has however been limited [378]. Their proof of workability in nanoecotoxicology has not been reported yet.

*1.1.5.3.2 Surface plasmon resonance imaging*

The SPR phenomenon was first described by Wood in 1902 but theorised by Fano about forty years later (in 1941) then experimented during the late seventies (1968) by Kretschmann and Otto [370, 379, 380]. A surface plasmon is an electro-magnetic wave propagating along the surface of a thin di-electric metal film (*e.g*. gold). Depending on the configuration (*i.e*. Kretschmann or Otto), the metal film may be intimately associated with (*i.e*. deposited onto), or not, a glass prism of high refractivity index (RI).

Regardless of the configuration, the optical excitation (*i.e*. resonance) of the surface plasmon can be achieved by a polarised and collimated light beam undergoing total internal

reflection at the metal film and medium (gas or liquid, low RI) interface. The angle at which the resonance occurs is extremely sensitive to changes in the RI of the medium adjacent to the metal surface. Modifications at this level can be quantified in resonance units or response units (RUs) or again in variation of reflectivity (ΔR, in % terms) *via* the monitoring of the variations in the reflected light intensity. By using metal films coated with probes of interest (*e.g.* DNA, antibodies, carbohydrates) the potency of interaction with possible partner molecules (*i.e.* defined as analytes, inducing very local changes of RI) can be evaluated.

In light of the above, SPRi is the application and characterisation of the SPR signals on the whole surface of a biochip (defined as the metal film coated support bearing the selected and grafted probes) *via* a video camera. This design enables the biochips to be prepared in a microarray format with each active site bearing probes (defined as spots or channels depending on the configuration) providing SPR information simultaneously (based on the analysis of generated grey scale images over time eventually). A schematic representation on the working principle of SPRi is presented in Fig. 1.13.

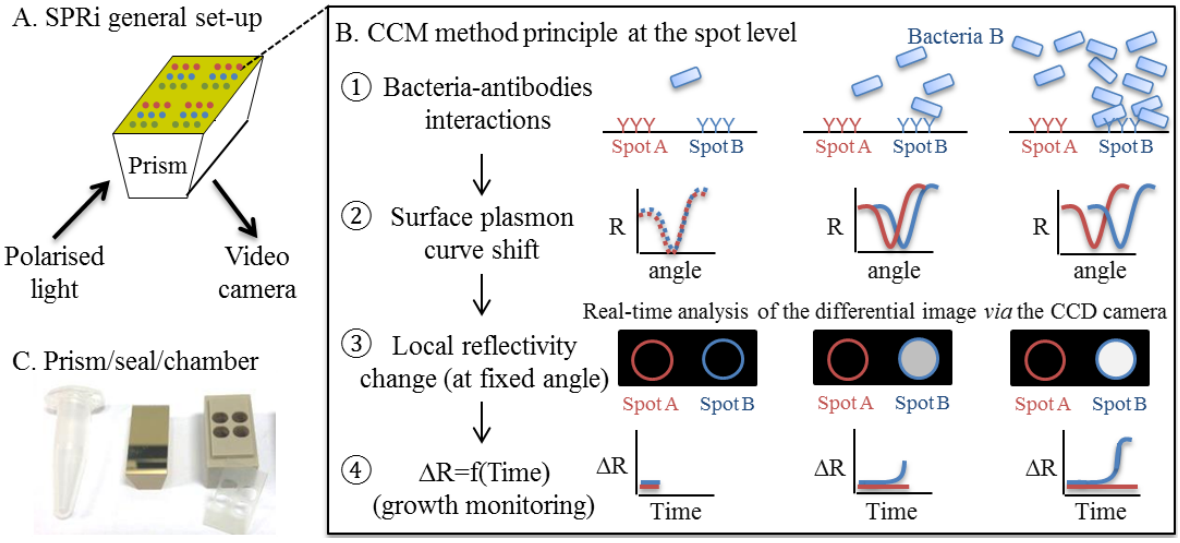


**Fig. 1.13: SPRi principle.** The working principle of SPRi (using a Kretschmann configuration) is schematised. In brief, the local variations (*i.e.* shifts) of the plasmon resonance in response to surface interactions (*e.g.* bacteria-antibodies) on a biochip (*e.g.* functionalised prism) result in modifying the reflectivity (ΔR, at the single spot level); ΔR which is assessed *via* the monitoring and quantification of the SPR images of difference over time. Adapted from Bouguelia *et al.* (2013) [381].

SPRi has already shown workability for biomolecular interaction assessment and analytes detection using a microarray format [382, 383]. SPRi has proven to be robust over the years *via* the emergence of various instruments, dedicated studies and companies worldwide [370, 384, 385]. The BIAcore (from GE Healthcare), the ProteOn (from Bio-Rad) and the SPRi-Plex/Lab (from Horiba Scientific) series can be proposed as examples of commercialised apparatus basically based on Otto (*i.e*. where prism and metal are close but independent) or Kretschmann (*i.e*. where the metal layer is deposed onto the prism) configurations.

SPRi applications with bacteria have emerged recently [381, 383, 386, 387]. The notion of real-time monitoring of the bacterial growth by SPRi was first reported by Bouguelia *et al*. (2013) [381] proposing a culture-capture-measure (CCM) method using the advantages of specific interactions between monoclonal antibodies microarrays and bacteria (*e.g. S. enterica*, *E. coli*). Additional applications followed using the same method [386, 387]. A company, namely Prestodiag (Paris, France), exploits a similar approach for detecting pathogenic bacteria within complex food related matrices. Concomitantly, Abadian *et al*. (2014) [388] reported the use of SPRi for the monitoring of *E. coli* and *P. aeruginosa* biofilm attachment, formation and removal. The use of SPRi with bacteria has been initiated in ecotoxicology for the testing of antibiotics [388] and for the impact assessment of thermal stresses [387]. However, no proof of workability in nanoecotoxicology has yet been reported.

#### *1.1.5.3.3 Implementation in nanoecotoxicology*

Interestingly, the term of "biosensors" is frequently used in the literature to describe "bioreporter microorganisms" too, especially GMB [89]. Consequently, despite the terminology "biosensors" indeed exists in nanoecotoxicology it generally does not involve technology (*i.e*. the associated transducer part). As such, examples of biosensor (as described by Turner *et al*. (1989) [364], also founder of the *Biosensors* peer review journal) related applications in nanoecotoxicology are not yet available in the literature. However, recent applications of both µCT and SPRi for monitoring cell (yeast or bacteria) kinetics in real time were shown [377, 381]. In light of this, µCT and SPRi based assays were

hypothesised suitable for novel applications in nanoecotoxicology based on the real time monitoring of the impact of selected NPs to the bacterial growth.

## 1.2 Aims

As aforementioned, the putative toxic (antimicrobial) properties of anthropogenic NPs (especially widely used metal and metal oxide inorganic NPs) and related ions (when applicable) are of critical concern in nanoecotoxicology. Bacteria are relevant and widely used testing model microorganisms with numerous advantages but, despite a wealth of possible combinations, their applications to date could be largely summed-up as using planktonic *E. coli* testing in microbiological growth media using plating and OD monitoring. The applications proposing new GMB or non-static biofilms, testing toxicity of aged NPs, questioning the potential microbial recovery or implementing biosensor technologies were shown to be limited while certainly substantiating further the domain. Toxicity of NPs in real matrices is also still rarely performed because of the lack of suitable methodologies, the scarceness of original implementations, and the extent of the task.

The main aim of this work was therefore to explore and compare (when possible) new planktonic, biofilm and biosensor based bacterial assays for NP toxicity testing with an ecotoxicological prospective. It was hypothesised: (1) that bacterial bioreporters originally isolated from environmental matrices (*P. putida* BS566 *lux*) would be suitable for NP testing in wastewaters, (2) that dynamic and complex microbial structures such as mono (*P. putida* based) and multi (wastewater based) species bacterial biofilms in flow-cell systems would be valuable models in nanoecotoxicology, and (3) that implementation of biosensor technologies such as microcantilever and surface plasmon resonance imaging would be possible with bacteria (*P. putida*) and suitable for applications in NP testing.

In light of the above, the main following questions were identified and addressed in chapters 3, 4 and 5, respectively.

-What is the acute toxicity of commonly used NPs (Ag, ZnO, $TiO_2$, CuO) to *P. putida* BS566 *lux* planktonic bioreporter when comparatively tested in microbiological media (Luria Bertani and Artificial Wastewater) and real complex matrices (crude and final

wastewaters)? How does the NP ageing impact on toxicity? How do these results compare with and/or complete the planktonic based literature?

-What is the impact of, specifically, antimicrobial Ag (NPs and ions) to mono-species biofilms (*P. putida* based) and multi-species biofilms (real crude wastewater based) morphology (and composition when relevant), viability and activity in Artificial Wastewater under hydrodynamic (laminar) conditions? Are biofilms capable of recovery following a single pulse exposure? How do these results compare with and/or complete the above and the biofilm based literature?

-How suitable are microcantilever and surface plasmon resonance imaging biosensor technologies for assessing NP toxicity to bacteria (*P. putida*)? Are both technologies equally ready for such implementation? How does it compare with and/or complete the above and the literature?

The testing of widely used and well characterised representative inorganic NPs from the Organisation for Economic Co-operation and Development (OECD) is prioritised herein. Relevant additional physico-chemical characterisation of tested NPs is proposed alongside toxicity data in each result chapter. The outcomes of this work will help fill a current knowledge and methodological gap in nanoecotoxicology providing relevant data and methodologies to assess NP toxicity in a bacterial context. In light of this work, further applications beyond nanoecotoxicology (*e.g*. nanotoxicology, nanomedicine, food science) may also be anticipated as well as the development of other original bacterial models and the further implementation of biosensor technologies (*e.g*. SPRi, μCTs, optical fibres, microfluidics).

# CHAPTER 2: Material and Methods

This chapter will present or reference the technical information related to the operated experimentations in this project. First are detailed the used material *e.g*. the "Bacteria", "Toxicants" and "Media". Then are reported the procedures for reproducing the "Planktonic", "Biofilm" and "Biosensor" based assays performed. The means by which the "Characterisation" of the NPs was performed are closing the chapter.

## 2.1 Material

### 2.1.1 Bacteria

Herein, the *Pseudomonas putida* BS566 lux::CDABE GMB bioreporter (originally isolated from wastewaters, hereafter referred to as *P. putida* BS566 *lux*) was used as the main model microorganism for both the planktonic and the biofilm based assays. For the works performed in collaborative laboratories (at HWU or oversea at CEA), the use of non-GMB models such as *P. putida* KT2440 was preferred. The *P. putida* strains were kindly donated by Emeritus Prof Nick Christofi and Prof Soeren Molin, respectively. In the case of the SPRi based assays, specifically, validated bacterial models from the host laboratory such as *Salmonella enterica* subspecies *enterica* serovar Enteritidis (hereafter referred to as *S.* Enteritidis) from the Scientific Institute of Hygiene and Analysis (ISHA, Massy, France) and *Staphylococcus epidermidis* ATCC 12228 (hereafter referred to as *S. epidermidis*) were also considered. *S.* Enteritidis is a biosafety level 2 microorganism; all experiments were performed in a dedicated laboratory accordingly equipped.

### 2.1.2 Toxicants

#### 2.1.2.1 Nanoparticles

The tested NPs, along with related information available in the literature from previous characterisation [389-391], are listed in Table 2.1. Silver (Ag NM-300K, reference JRCNM03000a), zinc oxide (ZnO NM-110, reference JRCNM01100a) and titanium dioxide ($TiO_2$ NM-104, reference JRCNM01040a) representative NPs from the Organisation for Economic Co-operation and Development (OECD) were obtained from

the European Commission's Joint Research Centre (Ispra, Italy) and characterised previously [389-391]. Copper oxide (CuO) NPs were kindly donated by Zuzanna Gajda-Meissner (PhD student, HWU, "NanoSolutions FP7" European Project) and supplied originally by PlasmaChem. Polystyrene NPs (Polybead® Carboxylate Microspheres reference 15913-10) were purchased from Polysciences.

**Table 2.1: Used nanoparticles related information from the literature** [389-391]**.**

| Product | Appearance | Primary particle size (nm) | Mean particle size (nm) | Specific surface area ($m^2$ $g^{-1}$) | Miscellaneous |
|---|---|---|---|---|---|
| **Ag NM-300K** | Suspension (brown) | 15 | 15 | N/A | Uncoated In dispersant[1] |
| **ZnO NM-110** | Powder (white) | 42 | 150 | 13 | Uncoated |
| **$TiO_2$ NM-104** | Powder (white) | 20 | 67 | 60 | Rutile Hydrophilic |
| **CuO** | Powder (white) | 15 | N/A | 55 | COOH-coated |
| **Polystyrene** | Suspension (white) | N/A | 50 | N/A | COOH-coated In dispersant[2] |

N/A - not available

[1] in suspension at 10 % (w/v) in 4 % (v/v) each of Polyoxyethylene Glycerol Trioleate and Polyoxyethylene (20) Sorbitan mono-Laurat (Tween 20) (supplier information)

[2] in suspension at 2.5 % (w/v) in deionised water with 0.1 % (v/v) sodium dodecyl sulphate (supplier information)

#### 2.1.2.2 Others

Silver nitrate ($AgNO_3$), zinc sulphate ($ZnSO_4$), copper chloride ($CuCl_2$) and copper sulphate ($CuSO_4$) salts were purchased from Fisher Scientific and used as sources of ions. As for the above NPs, all reported concentrations are in Ag (*i.e.* mg Ag $L^{-1}$), Zn (*i.e.* mg Zn $L^{-1}$) or Cu (*i.e.* mg Cu $L^{-1}$) final terms. Virkon® 1 % (w/v) was from DuPont; the kanamycin antibiotic was obtained from Sigma-Aldrich.

### 2.1.3 Media

#### 2.1.3.1 Laboratory growth media

Both undefined Luria Bertani (10 g $L^{-1}$ of tryptone, 5 g $L^{-1}$ of yeast extract, 5 g $L^{-1}$ of NaCl, pH 7, ionic strength *ca.* 80 mM) and defined Artificial Wastewater (2 g $L^{-1}$ $(NH_4)_2SO_4$, 6 g $L^{-1}$ $Na_2HPO_4$, 3 g $L^{-1}$ $KH_2PO_4$, 3 g $L^{-1}$ NaCl, 0.1 mM $CaCl_2$, 1 mM $MgCl_2$, 3 mM $FeCl_3$, pH 7, ionic strength *ca.* 300 mM) laboratory growth media (hereafter referred to as LB and AW, respectively) were freshly prepared prior to each experiment. All chemicals were obtained from Fisher Scientific. MilliQ water (18 MΩ $cm^{-1}$) was used for preparing the media. Typical sterilisation procedure was 121 °C for 15 min.

The AW consisted of AB mineral medium, as being comparable in composition to synthetic wastewaters described previously [392, 393], supplemented with a sole carbon source (*e.g.* D-glucose, D-fructose or D-sucrose at 0.5 % w/v) [394].

#### 2.1.3.2 Real matrices

Real crude wastewater (CW, non-treated, collected between the primary bar screen and the first clarifier) and final wastewater (FW, treated, collected after the last clarifier) samples were obtained from four WWTPs in the central belt of Scotland (East Calder, Whitburn, Seafield and Newbridge, respectively referred herein as site 1, 2, 3 and 4). WWTPs treated domestic wastewaters (*i.e.* with low COD loading *ca.* 500 mg $L^{-1}$) for population equivalent of approximatively 100 000, 15 000, 850 000 and 75 000 people, respectively. All samples were collected between February and July 2014 in sterile plastic containers using an auto-sampler, transported and stored at 4 °C, and finally used within 24 h following collection. All samples were supplemented with 0.5 % D-glucose (w/v) prior to use. The wastewater samples along with specific physico-chemical parameters were obtained *via* collaboration with Scottish Water (UK) thanks to the kind support of Craig Milne and Simon Gillespie.

## 2.2 Methods

### 2.2.1 Bacteria culture and storage

Bacteria were cultured on LB agar plates (for *S.* Enteritidis and *S. epidermidis*) or on *Pseudomonas* isolation agar (PIA, from Sigma) plates (for *P. putida* KT2440) supplemented with kanamycin sulphate at 100 mg $L^{-1}$ (for *P. putida* BS566 *lux*). Optimum temperatures of incubation were 37 °C and 28 °C, respectively.

Aliquots of the strains were prepared from clone colonies in 50 % glycerol (v/v) in 0.85 % NaCl (w/v) and stored at -80 °C.

### 2.2.2 Planktonic based assays

#### 2.2.2.1 General set-up: the *P. putida* BS566 *lux* bioreporter

The acute toxicity testing of the NPs was performed in LB, AW, CWs and FWs to the constitutively luminescent *P. putida* BS566 *lux* bioreporter using the principle of a switch-off planktonic based method (§ 1.1.5.1) in a 96-well microtiter plate format as previously reported [185] following the three-step based procedure schematised in Fig. 2.1.

#### 2.2.2.2 Testing pristine NPs in laboratory growth media

Prior to the experiments, the *P. putida* BS566 *lux* bioreporter was freshly plated on PIA then pre-cultured overnight at 28 ± 2 °C in LB or in AW medium at 140 rpm. The pre-cultured bioreporter was then diluted for final used at $10^8$ CFU $mL^{-1}$ *per* well as previously reported with same and different bioreporters [185, 200, 258, 366].

Stock suspensions of NPs were freshly prepared in LB or AW medium, sonicated twice 8 min (Kerry ultrasonic water bath, 38 ± 10 KHz) [390] and serially diluted to obtain final tested concentrations of 0, 0.781, 1.562, 3.125, 6.25, 12.5, 25, 50, 100 and 200 mg $L^{-1}$. The NPs were characterised in both LB and AW after spiking following the method described in § 2.2.5. Ag, Zn and Cu ions (applied as $AgNO_3$, $ZnSO_4$, $CuCl_2$ and $CuSO_4$ salts) were similarly prepared for final testing ranging from 0 to 25 mg $L^{-1}$ for Ag and from 0 to 200 mg $L^{-1}$ for Zn and Cu, respectively.

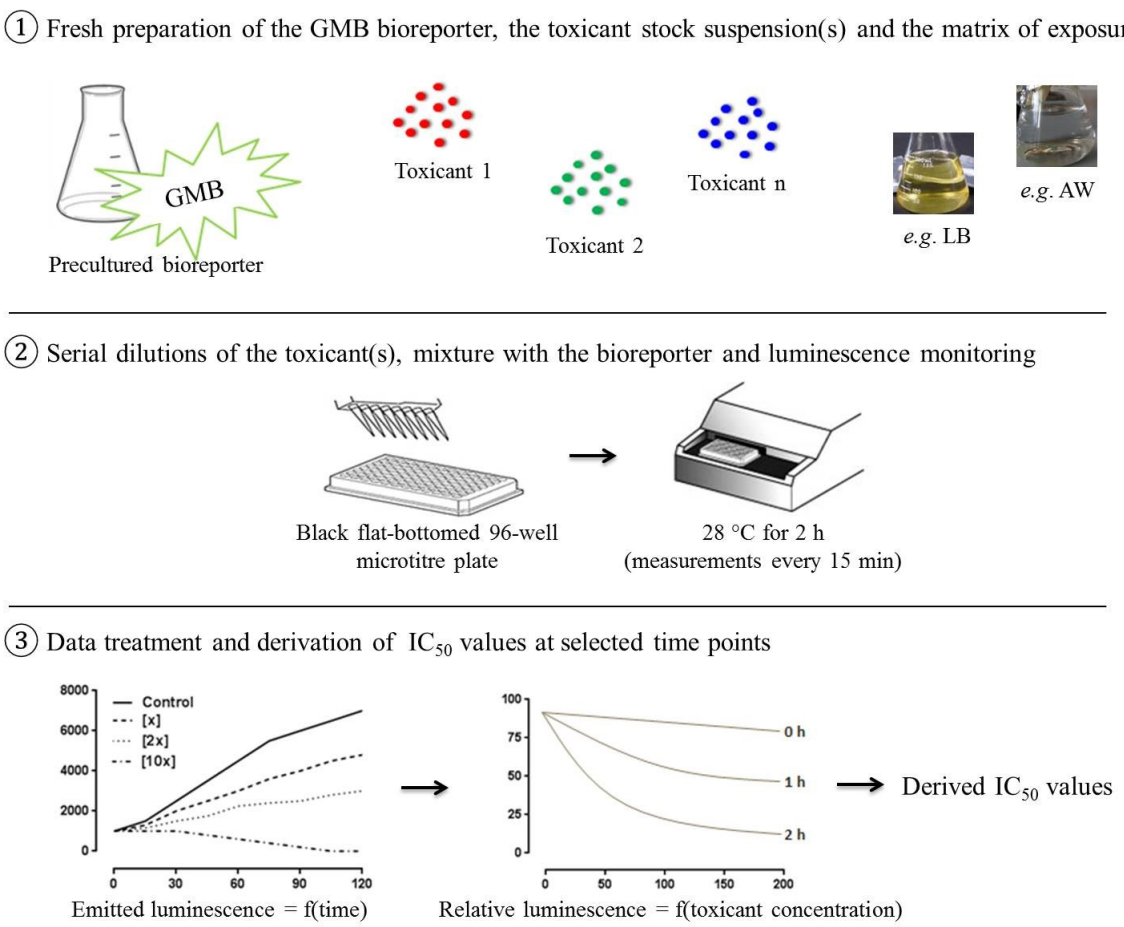


**Fig. 2.1: Schematic of the three-step based switch-off planktonic method.** As shown above, first both the GMB bioreporter and the toxicants (*i.e*. NPs) were freshly prepared in the selected medium; second the actual dilution of the toxicants in the microtiter plate followed by the bioreporter addition then the incubation within a temperature controlled luminometer were performed; third the monitoring of the emitted luminescence over time, eventually source of $IC_{50}$ values, was undertaken.

Assays were performed in 100 % LB or 100 % AW medium with final NP and bioreporter concentrations of 0 - 200 mg $L^{-1}$ and $10^8$ CFU $mL^{-1}$, respectively, in a final volume of 100 µL *per* well using 96-well flat bottomed black microtitre plates (Greiner bio-one). The microtitre plates were incubated at 28 ± 2 °C within a temperature controlled luminometer (SpectraMax M5 reader, Molecular Devices) and the emitted luminescence from *P. putida* BS566 *lux* monitored in a kinetic mode with measurements taken every 15 min for 120 min. Experiments included the test of ten different concentrations with two toxicants in one medium (or alternatively with one toxicant in two media) and four replicates *per* condition.

All the experiments were replicated four times (*i.e*. on different days) using fresh inoculum and media. An example of a typically used template is shown in Table 2.2.

Controls included wells with the bioreporter but without toxicant (*i.e*. reference, control or non-exposed condition), wells with the toxicant (at maximum concentration) but without the bioreporter (*i.e*. control of the emitted signal from the tested toxicant *per se*) and wells with the medium of exposure (*i.e*. control of the emitted signal from the medium *per se*). For the Ag NM-300K NP case, wells with the dispersant sole and with the dispersant with the bioreporter were also considered in order to verify the emitted signal from, as well as the potential toxicity of, the dispersant *per se,* respectively.

**Table 2.2: Example of template for the planktonic based assays in microtiter plates.**

| | ($mg\ L^{-1}$) | 0 | 0.78 | 1.56 | 3.12 | 6.25 | 12.5 | 25 | 50 | 100 | 200 | 200 | 0 |
|---|---|---|---|---|---|---|---|---|---|---|---|---|---|
| | | 1 | 2 | 3 | 4 | 5 | 6 | 7 | 8 | 9 | 10 | 11 | 12 |
| Medium 1 | A | Non exposed control | ← Serial diluted Ag NPs from 200 $mg\ L^{-1}$ (in presence of the bioreporter) | | | | | | | | | NPs alone | Medium alone |
| | B | | | | | | | | | | | | |
| | C | | | | | | | | | | | | |
| | D | | | | | | | | | | | | |
| Medium 2 | E | Non exposed control | ← Serial diluted Ag NPs from 200 $mg\ L^{-1}$ (in presence of the bioreporter) | | | | | | | | | NPs alone | Medium alone |
| | F | | | | | | | | | | | | |
| | G | | | | | | | | | | | | |
| | H | | | | | | | | | | | | |

The results were analysed at selected time points (0, 1 and 2 h) as described in § 2.2.2.5.1. The time point of 0 h corresponds to the first measure registered in a 5 min time window after exposure of the bioreporters to the toxicants (NPs or salts). The impact of tested toxicants was then characterised by calculating $IC_{50}$ values, as described in § 2.2.2.5.2, when applicable.

#### 2.2.2.3 Testing pristine NPs in real matrices

Assays in real wastewaters were conducted (and analysed) similarly to the aforementioned assays in laboratory growth media except that the *P. putida* BS566 *lux* bioreporter was

prepared exclusively in AW medium and the suspensions of NPs were prepared directly in freshly collected CW and FW samples (Fig. 2.2).

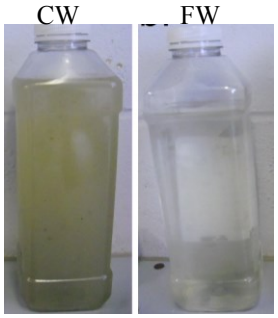


**Fig. 2.2: Pictures of the collected real wastewater samples.** The crude (picture on the left) and the final (picture on the right) wastewater samples (CW and FW, respectively) used as matrices of exposure are shown above.

The toxicity assays were therefore conducted using 90 % CW or FW (spiked with NPs) and 10 % AW (containing the bioreporter) with final toxicant and bioreporter concentrations of 0 - 200 mg $L^{-1}$ (0, 0.781, 1.562, 3.125, 6.25, 12.5, 25, 50, 100 and 200 mg $L^{-1}$) and $10^8$ CFU $mL^{-1}$ still, respectively.

The tested NPs were characterised in both CW and FW samples after spiking as described in § 2.2.5.

In addition, the biochemical oxygen demand (BOD), chemical oxygen demand (COD), total suspended solid (TSS), ammonia, chloride, sulphide, pH and biomass loadings of all the used wastewater samples were characterised before spiking with the NPs. The former four parameters were provided by Scottish Water; the others were measured at HWU. The BOD was determined after 5 days ± 4 h incubation at 20 ± 1 °C by a ROHASYS BOD robot fitted with WTW Oxi 340i meters and corresponding CellOx 325 oxygen probes. The COD was determined by Hach-Lange test kits LCK314 or LCK114 (depending on the concentration range) read using a DR3800 spectrophotometer. The TSS was determined by gravimetric analysis. The ammonia loading was determined spectrophotometrically by a KONE auto-analyser using the salicylate method (*e.g.* Hach-Lange test methods 8155). The indigenous microbial population was quantified *via* total plate counts (performed on

vegitone plate count agar with serial dilutions till $10^{-7}$ in NaCl 0.85 % w/v) after 48 h of incubation at 37 °C. The pH was measured with a HI 8424 pH meter (Hanna instruments). The concentrations of chloride and sulphide were measured using a DR2000 spectrophotometer following the Hach-Lange test methods 8113 and 8131 based on mercuric thiocyanate and methylene blue methods, respectively.

The information regarding both the characteristics of used wastewater samples and the eventual toxicity of freshly added NPs was used for multivariate analysis as described in § 2.2.2.5.3.

#### 2.2.2.4 Testing aged NPs

The assessment of the ageing impact on the eventual toxicity of NPs was piloted in wastewaters. The spiked stock suspensions of NPs (in CW, FW and AW) along with the original samples or medium (non-spiked) were stored at 4 °C for 8 weeks and used for acute toxicity testing as previously described (§ 2.2.2.3) in weeks 0, 1, 2, 4 and 8. In addition, the NPs were characterised in all samples alongside ageing (§ 2.2.5).

#### 2.2.2.5 Data analysis

##### *2.2.2.5.1 Luminometer data*

The data arbitrarily expressed in Relative Light Units (RLU) against time (min) by the luminometer were transformed to percent Relative Luminescence (%RLU, by normalisation against the control condition) then plotted against the toxicant concentrations (mg $L^{-1}$) for selected time points. All presented plots are means ± standard error of the mean (SEM) across four independent experiments considering, each, four replicates *per* tested condition (Table 2.2).

##### *2.2.2.5.2 Calculation of the $IC_{50}$ values*

The $IC_{50}$ values (mg $L^{-1}$) were calculated at selected time points by fitting a four parameter dose-response model to the logarithm of the concentration by weighted least squares using Prism software (GraphPad). All proposed $IC_{50}$ values were derived from four independent experiments considering, each, four replicates *per* tested condition.

#### 2.2.2.5.3 Multivariate analysis

The multivariate analysis was performed using Canoco5 software. Based on the real wastewater characterised parameters (*e.g*. BOD, COD, TSS, ammonia, chloride, sulphide, pH and total *i.e*. heterotroph plate count) used as environmental variables, a canonical correlation analysis was performed considering the calculated $IC_{50}$ values as explanatory variables. A total of thirty-two independent samples were considered (*i.e*. four independent samplings were performed with both CW and FW samples across four different WWTPs). The data were presented using a two axis based ordinary diagram.

## 2.2.3 Biofilm based assays

The acute toxicity testing of NPs was also performed with complex biological structures such as mono-species (using *P. putida* BS566 *lux*) and multi-species (using crude wastewater samples) biofilms in AW using confocal laser scanning microscopy (CLSM) compatible flow-cell based reactors [362, 363].

### 2.2.3.1 General set-up: the flow-cell reactor

As shown in Fig. 2.3 and 2.4, the biofilm reactor consisted of several (*i.e*. up to four) CLSM compatible inverted Perspex flow-cells containing three channels (1 x 4 x 40 mm each) independently connected to influent and effluent containers with silicon tubings (Versilic).

Each flow-cell was prepared by sealing a glass coverslip (24 x 50 mm, 0.13 mm thick) as previously described [362]. The flow rate was supported by a 205U multi-channel cassette peristaltic pump (Watson Marlow Ltd, Falmouth, UK) positioned downstream of the flow-cells in order to prevent the impact of the bubbles generated by the pump itself. In addition, bubble traps were placed upstream of the flow-cells to limit the impact of bubbles potentially carried by the flow from the influent containers. Both the flow-cells and the bubble traps (Fig. 2.4) were purchased from DTU Systems Biology (Lyngby, Denmark).

The set-up reactor was first cleaned with Virkon® 1 % (w/v) then extensively washed with sterile deionised water at 15 mL $h^{-1}$ *per* channel. The reactor was finally filled with sterile AW and left to stabilise overnight.

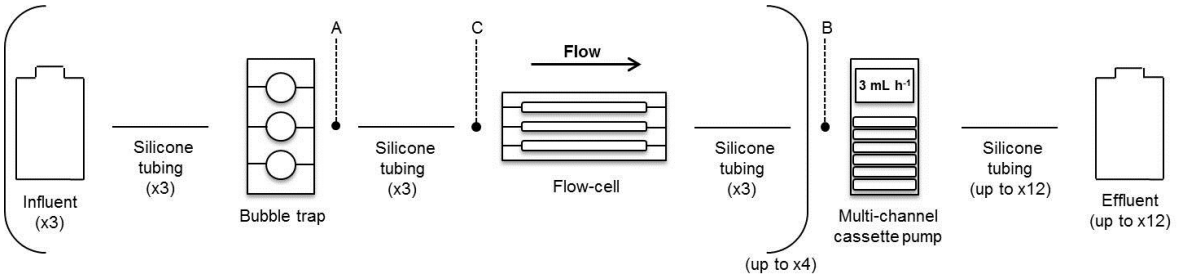


**Fig. 2.3: Schematic of the flow-cell reactor based method.** A, B and C refer to key actions during the inoculation process: clamp off in A, dis-connect in B then inoculate in C.

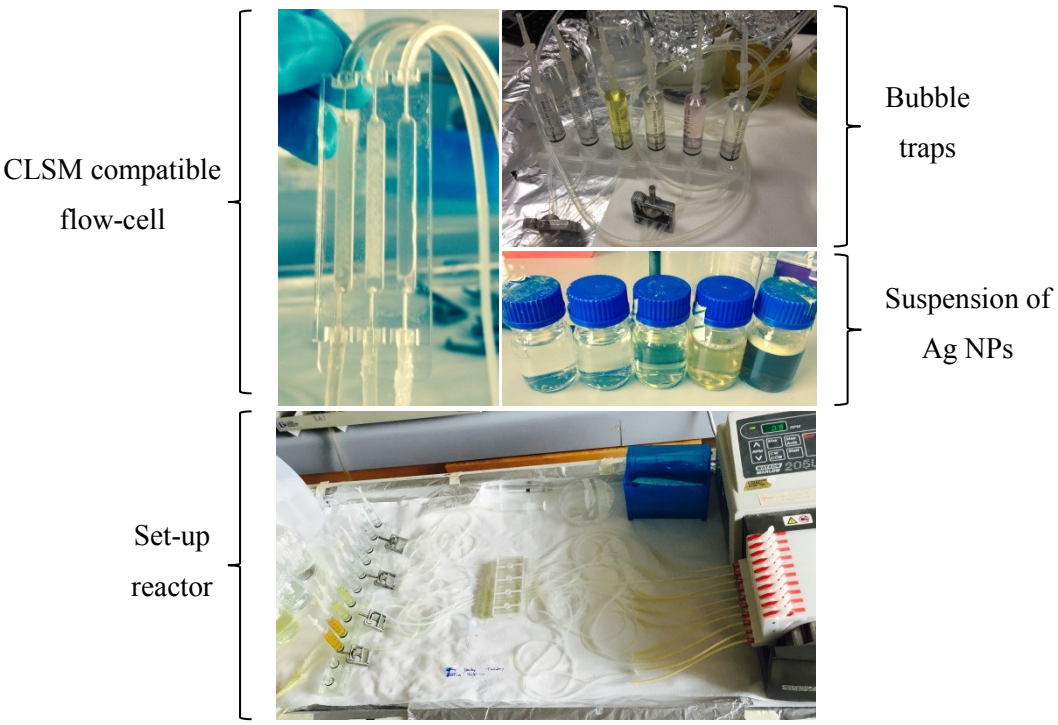


**Fig. 2.4: Pictures of the material related to the biofilm based assays.**

The inoculum (*P. putida* BS566 *lux* or crude wastewater samples) was prepared in AW as described previously (§ 2.2.2.2) then diluted in order to reach a final concentration of $10^7$ CFU $mL^{-1}$ corresponding to a dilution *ca*. 1:100e after pre-culture.

Each channel (presenting a volume of 160 µL according to the manufacturer) was then independently inoculated using 200 µL of the freshly prepared inoculum. The incubation

procedure involved: clamping off the tubing upstream of each flow-cell (Fig. 2.3, position A), disconnecting the tubing downstream of the flow-cells (Fig. 2.3, position B) and injecting the inoculum (using a 1 mL syringe equipped with a < 1 mm diameter needle, both sterile) directly within the flow-cells (Fig. 2.3, position C).The procedure was adapted from Weiss Nielsen *et al*. (2011) [363] considering here that the pump was placed downstream of the flow-cells.

After inoculation, the tubings were re-connected and dis-clamped, the holes were sealed then the flow-cells were incubated 1 h (*i.e*. flow off and glass coverslip on bottom, in order to help the deposition of bacteria on the glass surface). The culture was finally undertaken (*i.e*. glass coverslip on top, in order to help the development of mature structures by limiting the presence of planktonic bacteria) for 48 h in AW with a consistent flow rate of 3 mL $h^{-1}$ *per* channel at room temperature. Different scenarios of exposure (and recovery) were thereafter considered depending on the study (§ 2.2.3.3 and § 2.2.3.4).

#### 2.2.3.2 Confocal laser scanning microscopy

The biofilms were characterised using a Leica Microsystems TCS SP2 inverted CLSM with a HCX APO CS 63x 1.4 oil immersion lens after staining with dedicated fluorescent dyes (Table 2.3). All dyes were from Life Technologies, stored at -20 °C and used following the manufacturer's recommendations.

The biofilm analysis was performed across the whole thickness of the specimens by scanning along the z-axis at consistent intervals to constitute a stack of parallel images hereafter referred to as z-stack. The data acquisition was consistently performed in a xyz scale (in z-wide) using a unidirectional scanning at a frequency of 400 Hz without image averaging.

Syto®9 (green), propidium iodide (PI, red) and hexidium iodide (HI, red) stains were excited with a laser source at 488 nm. Green and red emissions were simultaneously monitored *via* distinct photomultipliers (PMT) set at 510 - 530 nm and 610 - 630 nm, respectively. In case of the FilmTracerTM Live/Dead® Biofilm Viability Kit, green and red correspond to live and dead bacteria, respectively. For the LIVE BacLightTM Bacterial Gram Stain Kit, green and red correspond respectively to Gram- and Gram+ bacteria. The

Concanavalin A dye was used as follows (*i.e*. laser source: 543 nm; PMT: 570 - 590 nm) and was artificially converts to a purple signal in order to facilitate the imaging when used concomitantly with the other dyes. In the absence of light source *ca*. 355 nm, blue based staining could not be used here.

**Table 2.3: Fluorescent dyes related information.**

| Product | Excitation/Emission (nm) | Final concentration | Incubation time (min) |
|---|---|---|---|
| **FilmTracer™ Live/Dead® Biofilm Viability Kit** | Syto®9: 485/520<br>PI*: 485/620 | 10 µM<br>60 µM | 10-15 |
| **LIVE *Bac*Light™ Bacterial Gram Stain Kit** | Syto®9: 485/520<br>HI*: 485/620 | 10 µM<br>14 µM | 10-15 |
| **Concanavalin A, TetraMethylRhodamine Conjugate** | TMR*: 555/580 | 50 - 200 µg $mL^{-1}$ | 10-15 |

* PI = Propidium Iodide, HI = Hexidium Iodide, TMR = TetraMethylRhodamine

A total of seven z-stacks (characterised by 100 images at 512 x 512 in resolution in a consistent 100 µm thickness window) were randomly registered *per* condition (*i.e*. *per* channel) for each time point in all experiments. The recorded z-stacks were further analysed as explained in § 2.2.3.5.1.

Consequently, at selected time points (§ 2.2.3.3 and 2.2.3.4), the biofilms were stained by careful injection of dyes mixture (prepared in AW) in each channel then imaged directly within the flow-cells in a non-destructive manner.

#### 2.2.3.3 *P. putida* based mono-species biofilms

The *P. putida* BS566 *lux* bioreporter was used as a model bacterium for establishing mono-species biofilms. As aforementioned, bacteria ware pre-cultured overnight in AW (supplemented with 0.5 % w/v of D-glucose) then used as inoculum at $10^7$ CFU $mL^{-1}$ (*ca*. 1:100e dilution).

Being empirically the most toxic of the selected toxicants here, the case of Ag was prioritised when exploring the toxicity testing with biofilms. Stock suspensions of Ag NPs at 100 mg $L^{-1}$ were freshly prepared in AW prior to each experiment, sonicated as previously mentioned, then serially diluted to give final concentrations of 0, 0.01, 0.1, 1, 10 and 100 mg $L^{-1}$. Ag ions (applied as $AgNO_3$) were similarly used at final concentrations of 0, 0.001, 0.01, 0.1, 1 and 10 mg $L^{-1}$. Virkon® 1 % (w/v) was tested as toxicant positive control.

Typical experiments involved two flow-cells (*i.e*. six independent channels or conditions) in order to maintain manageable CLSM analysis times and to limit the manipulation of the flow-cells (*i.e*. to preserve the biofilms and prevent formation of bubbles). Ag NPs and Ag ions were therefore tested separately. The toxicants were applied onto 48 h old biofilms for 24 h with a consistent flow rate of 3 mL $h^{-1}$ *per* channel. After exposure, the upstream tubings were purged and the system filled with fresh AW (*i.e.* free from any toxicant). Thereafter, the biofilms were cultured for an additional 24 h in order to initiate and assess their potential recovery *post* exposure.

In light of this scenario, schematised in Fig. 2.5, three time points were defined: 48 h (*i.e*. *ante* exposure), 72 h (*i.e. post* exposure) and 96 h (*i.e. post* recovery) respectively addressing control, impact and potential recovery related information. At each time point both the morphology and the microbial activity of the biofilms were characterised by, respectively, performing CLSM analysis using a live/dead staining and quantifying the utilisation of D-glucose (*i.e*. the sole carbon source).

For the CLSM assays, 7 z-stacks were randomly registered *per* condition at 48, 72 and 96 h in all replicated experiments (up to n = 5). From a qualitative standpoint, the z-stacks were processed using the Leica Application Suite Advanced Fluorescence Lite (LAS AF)

software. From a quantitative standpoint (*e.g.* determination of the biofilm total biomass, thickness, roughness and surface area) data were analysed using Matlab software along with the COMSTAT program (§ 2.2.3.5.1).

Regarding the C source utilisation, the amount of D-glucose (Glc) was quantified in both influent and effluent collected samples at 48, 72 and 96 h (after filtration at 0.2 µm) following the phenol-sulphuric acid assay based protocol described elsewhere [395]. The method is based on the absorbance at 490 nm of a coloured aromatic product formed by the stoichiometric reaction between phenol and Glc. The Glc loading is finally determined spectrophotometrically by comparison with a Glc based calibration curve (Appendix B, Fig. S2.1). The Glc removal (or utilisation, in % terms) was defined as the ratio between determined loadings in both types of sample for each time point. Similar analyses were performed in cases where alternative carbohydrate based C sources (*e.g.* D-fructose and D-sucrose) were tested.

In addition to the above, the collected samples were also used for the characterisation of tested NPs when applicable (§ 2.2.5).

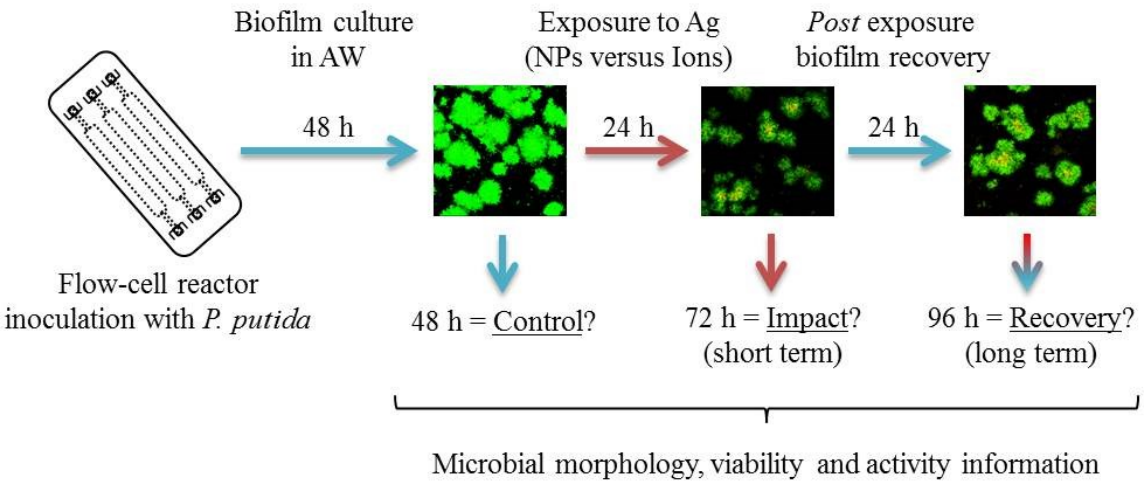


**Fig. 2.5: Schematic of the followed scenario using the *P. putida* based mono-species biofilms.**

2.2.3.4 Real wastewater based multi-species biofilms

Samples of real crude wastewater (CW from site 3) were used for establishing multi-species biofilms. Wastewater samples were pre-cultured in AW (supplemented with 0.05 % w/v of D-glucose) then used *ca*. 1:100 dilution for inoculating the flow-cells as mentioned previously (§ 2.2.3.3).

The multi-species biofilms were cultured for 48 h then exposed to toxicants for 24 h under flow conditions (*i.e*. 3 mL $h^{-1}$ *per* channel in AW). The case of Ag was here as well prioritised. No recovery was assessed *post* exposure due to a specific need of channels for performing additional (and destructive) analyses. More specifically, the biofilms were characterised at both 48 and 72 h using: CLSM (*i.e*. morphology and Gram+/- related information), DNA extraction and sequencing (*i.e*. composition related information) and quantification of D-glucose, ammonia and phosphorus removal (*i.e*. microbial activity information). The experimental design is schematised in Fig. 2.6.

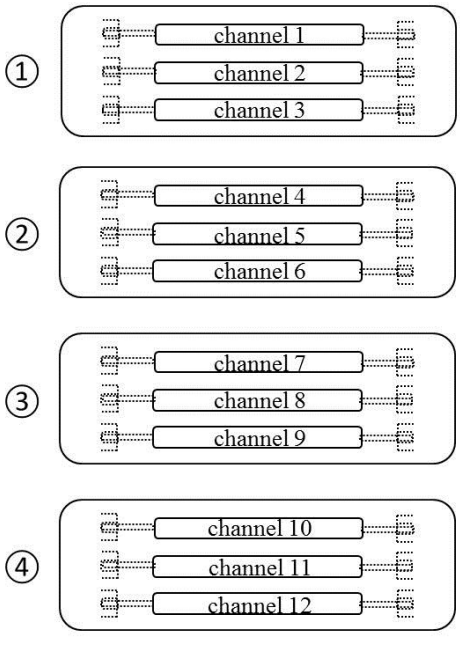


| Exposed to (for 24 h) | Stained (CLSM) | Harvested (NGS) | Microbial activity |
|---|---|---|---|
| 0 mg $L^{-1}$ | at 48 and 72 h | at 72 h | Using collected influent and effluent samples at both 48 and 72 h |
| 0 mg $L^{-1}$ | no | at 48 h | |
| 0 mg $L^{-1}$ | no | at 72 h | |
| 1 µg $L^{-1}$ Ag NPs | at 48 and 72 h | at 72 h | |
| 0 mg $L^{-1}$ | no | at 48 h | |
| 1 µg $L^{-1}$ Ag NPs | no | at 72 h | |
| 1 mg $L^{-1}$ Ag NPs | at 48 and 72 h | at 72 h | |
| 0 mg $L^{-1}$ | no | at 48 h | |
| 1 mg $L^{-1}$ Ag NPs | no | at 72 h | |
| 0 mg $L^{-1}$ | no | at 48 h | |
| 1 mg $L^{-1}$ Ag ions | no | at 72 h | |
| 1 mg $L^{-1}$ Ag ions | at 48 and 72 h | at 72 h | |

**Fig. 2.6: Schematic of the experimental design used with the multi-species biofilms.**

#### 2.2.3.4.1 Morphology

The CLSM analysis was performed using the Gram+/- and the extracellular matrix (*i.e*. Con A) related dyes (§ 2.2.3.2). Both simultaneous and sequential uses of the dyes were tested. The output data were treated as previously proposed (§ 2.2.3.3) and further detailed in § 2.2.3.5.1.

#### 2.2.3.4.2 Composition

Genomic DNA (gDNA) extraction was performed using Qiagen mini DNA extraction kits (based on fast spin-columns embedding DNA binding silica-gel membranes) following the manufacturer's recommendations for work with Gram+ bacteria. This version of the protocol was recommended as including a pre-enzymatic digestion with lysozyme likely to help obtaining a representative extraction from complex materials such as multi-species biofilms. The sole modification implied the elution volumes which were reduced at 100 µL and used three times consecutively (*per* column) in order to obtain highly concentrated extracts.

The extracted gDNA from the biofilms was quantified (*e.g*. concentration, $Abs_{260/280}$ and $Abs_{260/230}$) using a NanoDrop 2000c spectrophotometer (Thermo Fisher Scientific Inc.) then sent for sequencing (*i.e.* using the 454 method on a MiSeq platform from Illumina). The MiSeq principle is based on the solid phase polymerase chain reaction (PCR) process and the "sequencing on synthesis" method as described elsewhere [396, 397]. Necessary storage was performed at 4 °C in the Qiagen elution buffer. No RNase treatment was applied. Both the sequencing and the data analysis were supported by collaborators at Warwick University (§ 2.2.3.5.3).

For each sample, 15 ng DNA was used to amplify approximately 252 bp of the 16S rRNA gene using the 515f-806r region of the 16S rRNA gene [398] with Nextera XT Index Kit v2 adapters (Illumina) and 50 °C annealing. The libraries were sequenced using the MiSeq Reagent Kit v3 600-cycle (Illumina). Following sequencing 748 144 sequences were assembled. Trimmomatic v0.35 was used to remove low quality bases from the sequence end [399]. Paired-ends reads were then assembled by aligning the forward and reverse reads, trimming primers and quality filtering using USEARCH and UPARSE software

[400, 401] (version 8.1.1861). This resulted in 409 529 paired end reads. Unique sequences were sorted by abundance; singletons in the data set were discarded. Sequences were clustered, followed by chimera filtering using the Greengene database as reference [402]. To obtain the number of reads of each OTU, reads were mapped back to OTUs with a minimum identity of 97 %. Taxonomy was assigned using Quantitative Insights into Microbial Ecology (QIIME 1.8) [398] and the Greengenes database [402]. To compare samples on an equal basis all samples were rarefied to even sampling depths of 17 000 prior to statistical analysis.

*2.2.3.4.3 Activity*

The Glc, ammonia ($NH_3$-N) and phosphorus ($PO_4^{3-}$) loadings were quantified in both influents and effluents collected samples at 48 and 72 h (after filtration at 0.2 µm) following the phenol-sulphuric acid (as previously mentioned in § 2.2.3.3), salicylate (Hach-Lange method reference 8155 using powder pillows) and ascorbic acid (USEPA PhosVer 3®, Hach-Lange method reference 8048 using powder pillows) colorimetric based assays, respectively. All readings were performed using a DR1900 spectrophotometer (Hach-Lange). Methods for ammonia and phosphorus determination are recommended for water and wastewater applications and implied the use of the pre-registered calibration curves (within the DR1900 spectrophotometer) from the manufacturer. All the obtained data were treated according to the method described in § 2.2.3.5.2.

The characterisation of Ag NPs in all collected samples was performed as described elsewhere (§ 2.2.5).

2.2.3.5 Data analysis

*2.2.3.5.1 Morphology*

The COMSTAT based analysis of both mono and multi-species biofilms was performed from the registered CLSM z-stacks using Matlab software (R2013b, MathWorks, USA) following a previously reported methodology for, specifically, characterising the structure of biofilms [403].

The COMSTAT scripts are freely available and allow the determination of key descriptive parameters of biofilms such as the total biomass ($\mu m^3\ \mu m^{-2}$), the thickness (μm), the roughness coefficient (dimensionless) and the surface area ($\mu m^2$). Regarding the terminology, the total biomass (which also refers to the bio-volume of the biofilms) corresponds to the number of biomass pixels in all the images of a stack multiplied by the voxel size and divided by the substratum area of the image stack. The maximum thickness function locates the highest biomass pixel from the bottom layer over a given location, ignoring pores and voids inside the biofilm, in contrast with the mean thickness function which provides a measure of the global spatial size of the biofilm within a given stack. The roughness coefficient assesses how much the thickness of the biofilms varies and therefore informs about the biofilm heterogeneity. The surface area represents the summation of all biomass voxel surfaces exposed to the flow.

The aforementioned parameters are impacted by the selected threshold used by the program to exclude or include more or less of the background pixels. In order to limit bias between results the same threshold was used for all the stacks from a same experiment. This threshold may vary across experiments though.

In order to evaluate the relative evolution (in % terms) of each parameter between selected time points (defined by the scenario) *per* tested condition, the determined total biomass, thickness, roughness and surface area data were processed according to equation 2.1:

$$\text{Relative evolution} = (\text{results at y} - \text{results at x}) / (\text{results at x}) \qquad \textit{eq. 2.1}$$

where x, y are 48 and 72 h, or 72 and 96 h, respectively.

In case of the Gram+/- dye, specifically, the relative ratio of both type of bacteria was calculated from the total biomass information (as aforementioned) but using data from both PMT independently.

#### *2.2.3.5.2 Microbial activity*

The microbial activity was herein associated with the capability of biofilms to remove (or utilise) particular sources available in their environment. The removal information (in %

terms) was calculated between influent and effluent collected samples according to equation 2.2 at selected time points (defined by the scenario) *per* tested condition.

Removal = | (results in effluent - results in influent) / (results in influent) | *eq. 2.2*

The data related to the removal of D-glucose, D-fructose, D-sucrose, ammonia and phosphorus were similarly treated regardless of the study (*i.e*. mono-species or multi-species biofilms).

*2.2.3.5.3 Composition*

The composition of the established CW based multi-species biofilms was determined by the MiSeq based NGS of the extracted gDNA *ante* and *post* exposure to the toxicants. The data were analysed by Dr Sally Hilton (Warwick University, UK) using a dedicated Quiime pipeline with the highest detailed (*i.e*. L6) data obtained.

2.2.4 Biosensor based assays

2.2.4.1 A collaborative context

The acute toxicity testing of NPs was assessed using biosensor technologies *via* the pilot implementation of μCT and SPRi based methods with bacteria. As requiring specific materials and expertise, this part of the project was realised in collaboration with experts from each domain. The μCT based assays were performed with Dr Will Shu and co-workers in the Institute of Biological Chemistry, Biophysics & Bioengineering at HWU. The SPRi based assays were operated with Dr Thierry Livache and co-workers in the Institute for Nanoscience and Cryogenics at CEA-Grenoble (France). Both short term collaborations focussed on the novel application (*i.e*. the NP toxicity testing on bacteria) of already developed techniques from the host laboratories.

2.2.4.2 The microcantilever technology

*2.2.4.2.1 General set-up*

The microcantilever based assays were performed using static μCTs as described elsewhere [377] coupled with a laser based optical readout technique (§ 1.1.5.3.1). The general set-up is presented in Fig. 2.7 A and B.

The µCTs (rectangular in shape, 100 x 1000 µm in dimension, Fig. 2.7 D) were laser cut from polyimide sheets after being coated with chromium (5 nm) then gold (40 nm) on one side, as previously described [377]. The fabrication was fully supported by the host laboratory and the µCTs were delivered ready to use.

For each experiment, new µCTs were manually fixed with a small nylon screw inside the in-house developed flow-chamber (made of PEEK, PolyEther-Ether-Ketone, known as a biocompatible and solvent resistant material) which was then hermetically closed by a transparent lid (*i.e.* due to a round sapphire glass embedded) pressurised onto a rubber-O-ring seal with four external metallic screws (Fig. 2.7 C). The flow-chamber was place onto a Peltier device (33.4 W, ΔT of 67 °C, RS Components) for the temperature control, appropriately fixed onto an optical table and connected to influent and effluent containers *via* microfluidics. The laser beam (from a 5 mW laser diode, 532 nm, Thorlabs) was focussed on the free extremity of one µCT using a video camera (Fig. 2.7 D).

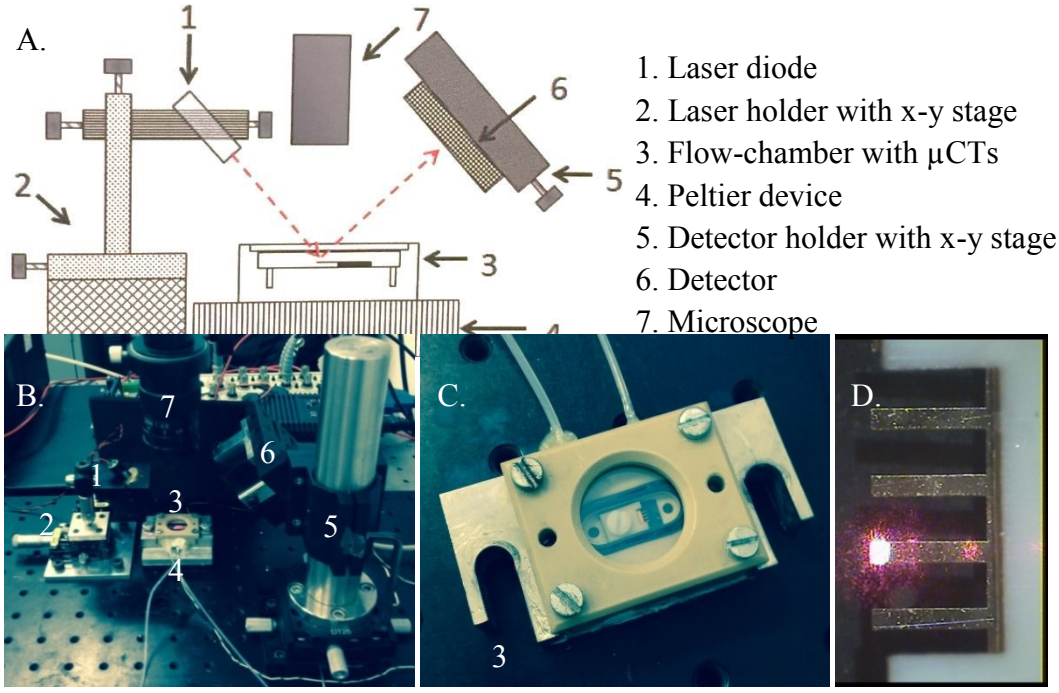


**Fig. 2.7: Microcantilever set-up and related materials.** Are shown in A and B a schematic and a picture of the used system, respectively; in C the µCT holder flow-chamber and in D the actual µCTs as well as the laser position.

The reflected beam by the gold surface of the μCT (*i.e*. which basically acts as a mirror) was aligned with the centre of a position sensitive detector (PSD) and the mechanical bending (*i.e*. surface changes) was then assessed over time by monitoring the optical variations of the reflected signal *via* the PSD (§ 1.1.5.3.1).

The whole system was controlled with an in-house developed LabVIEW program along with a dedicated data acquisition card and a proportional-integral-derivative (PID) controller which principles were detailed elsewhere [377]. The flow rate was ensured by a 50 mL push syringe pump (Cole-Parmer) at 100 μL $min^{-1}$. For both the user and the system protection, all assays were operated under a black protective box.

*2.2.4.2.2 Assays*

Assays were piloted in the host laboratory with *P. putida* KT2440 (non-GMB, § 2.1.1). The model bacterium was prepared as previously described (§ 2.2.2.2). All the assays were piloted in LB. A consistent temperature of 28 °C was applied during both the preparation of the bacterium and the assays.

Different assays were performed: first, to confirm the response of the system to a controlled stress (*i.e*. based on variations of the temperature) without bacteria; and second, to assess the bacterial growth (*i.e*. at constant temperature) in the presence/absence of the toxicants. Regardless of the type of assay, the system was set-up as described above then first cleaned with Virkon® 1 % (w/v). After being washed extensively with sterile deionised water, the system was full up with LB and left to stabilise for 2 to 4 h at fixed temperature (*e.g*. 28 °C). The laser alignment was refined at the beginning of the stabilisation period. In the absence of evident drifting signal over time, the experiments were then initiated.

The impact of temperature was performed by first applying a fixed temperature over a long period of time and second by applying pulses of increasing temperatures over short periods of time. Assays with bacteria were first performed in the absence of toxicant by the injection within the system of freshly prepared bacterial suspension at $10^7$ CFU $mL^{-1}$. After incubation for 1 h without flow (*i.e*. similarly to the methodology used for the biofilm based assays), the culture was performed and monitored for up to 16 h (overnight) under constant flow and temperature conditions. Assays in the presence of toxicants were

similarly designed except the bacterial suspension was appropriately mixed with a selected concentration of NPs before injection. Due to the system configuration, only one concentration could be tested at a time.

#### 2.2.4.3 The surface plasmon resonance imaging technology

##### *2.2.4.3.1 General set-up*

The SPRi based assays were performed using a SPRi PlexII apparatus (Horiba Scientific, Fig. 2.8 A) in a Kretschmann configuration as previously described [381] (§ 1.1.5.3.2). Pictures of the SPRi system are shown in Fig. 2.8 A and B.

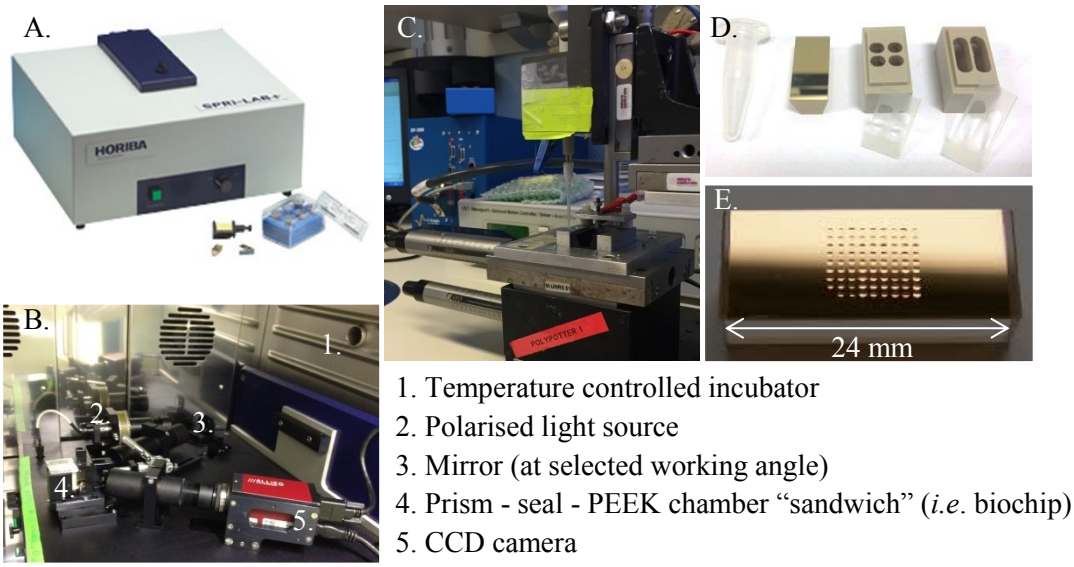


**Fig. 2.8: Surface plasmon resonance imaging set-up and related materials.** Are shown above: in A the commercial apparatus used, in B the apparatus core housed in a temperature controlled incubator, in C the house-developed electrochemical based spotter used for the prism functionalisation process, in D examples of PEEK chamber and related silicon seals used alongside a typical gold coated prism which is also presented in E once spotted (*i.e.* a random array pattern is shown).

High reflexion index glass prisms (n = 1.717 at λ = 633 nm), coated with chromium (5 nm) then gold (40 nm) were purchased from Horiba Scientific and used as support (Fig. 2.8 D and E). The gold surface of the prisms was grafted with bespoke series of spots embedding the probes of interest (*i.e.* bacterial strain specific antibodies as well as negative control

antibodies). For functionalisation purposes, the antibodies were first pyrrolylated following the procedure reported elsewhere [381, 404]. Pyrrolylated-antibodies were then immobilised as spots (*ca*. 500 µm in diameter with a pitch of 1 mm in both x and y axes) onto the prism gold surface by electrochemical directed pyrrole based polymerisation using a dedicated spotter (Fig. 2.8 C) following a method previously described [404]. The used spot template (*i.e*. including the type of used antibodies) was variable and defined by the experimental needs (and materials such as the PEEK chamber considered).

Both two and four chamber based assays were performed using corresponding in-house designed chambers (Fig. 2.8 D) positioned on top of the accordingly functionalised prisms. Dedicated seals were used between the prism and the PEEK to support the pressure later applied on the constituted "sandwich" (*i.e*. defined as the functionalised prism with seal and PEEK chamber, hereafter referred to as biochip) in order to form the final working chambers. The biochip was positioned inside the apparatus following manufacturer's recommendations. Sterile adhesive breathe seal was used to close the top of the biochip. The apparatus itself was placed in a temperature controlled incubator set appropriately to the used bacterium.

A charge coupled device (CCD) camera aligned with a polarised light source was used to monitor the local evolutions in reflectivity due to occurring modifications of the surface resonance conditions in response to "weight" changes within each spots (*i.e*. because of the probe-target interactions) over the whole surface of the biochip (Fig. 2.8 B).

The system was used in a static mode (*i.e*. without flow). The system supports the analysis of one biochip at a time. Both the seals and the prisms were originally sterile and disposable. The PEEK chambers were re-usable after extensive cleaning *via* two consecutive cycles of disinfection (with Phargogermyl from Dutcher then high concentrated sodium hypochlorite solution) and washing (with milliQ water).

#### *2.2.4.3.2 Assays*

Assays were piloted in the host laboratory with *P. putida* KT2440 (non-GMB, § 2.1.1). Both Ab38825 (polyclonal, specific for *P. putida*) and Ab68538 (polyclonal, specific for *P. aeruginosa* with known cross reaction for *P. putida*) antibodies (from Abcam) were tested.

A temperature of 28 °C was applied during both the preparation of the bacterium and the realisation of the assays.

Additional bacteria, already validated for use with SPRi by the host laboratory, were also considered on site: *S.* Enteritidis *and S. epidermidis* (§ 2.1.1) in combination with the antibodies SE103 (monoclonal, specific for *S.* Enteritidis, kindly provided by Dr H. Volland, CEA-Saclay, France) and KPL (polyclonal, specific for *S. aureus* with known cross reaction for *S. epidermidis,* from KPL reference 01-90-05), respectively. A temperature of 37 °C was applied during both the preparation of the bacteria and the realisation of the assays. As previously proposed [381], the keyhole limpet hemocyanin (KLH) monoclonal antibody (kindly sourced by Dr L. Bellanger, CEA-Marcoule, France) was used as a negative control.

Prior to the inoculation of the SPRi system, the bacteria were pre-cultured overnight as previously described (§ 2.2.2.2) then freshly prepared *ca*. $10^5$ CFU $mL^{-1}$ before being mixed with the toxicants [381]. As metal NPs may exhibit optical properties (*e.g*. absorbance and SPR signal) potentially interfering with the analysis, both metal (*e.g*. Ag, ZnO and $TiO_2$ NPs and related ions when applicable) and non-metal (*e.g*. polystyrene NPs) based antimicrobial toxicants were tested (§ 2.1.2). The tested concentrations of used toxicants are summarised in Table 2.4.

**Table 2.4: Summary of the used concentrations of tested toxicants using SPRi.**

| Product | Concentration (mg $L^{-1}$) |
|---|---|
| Ag NM-300K NPs (Ag ions) | up to 50 (up to 10) |
| ZnO NM-110 NPs (Zn ions) | up to 200 (up to 100) |
| $TiO_2$ NM-104 NPs | up to 200 |
| Polystyrene NPs | up to 10 |

The prisms were prepared the day of their use (or the day before) and stored in sterile PBS at 4 °C until utilisation. Precautions were taken to never dry the surface of the functionalised prisms in order to preserve the structure and function of the grafted antibodies.

The assembled biochip positioned inside the apparatus, all the chambers were emptied (from PBS) then immediately inoculated with 200 µL of bacteria-toxicants mixture. The experimental settings were performed (*e.g*. spot definition, plasmon curves registration and working angle selection) in a *ca*. 20 min time window following inoculation. The monitoring was then initiated and operated up to *ca*. 16 h (in the obscurity and at controlled temperature). All the assays were piloted entirely in LB.

#### 2.2.4.4 Data analysis

Regarding the µCT based assays, the output data were proposed by default, and here presented, as the variation of the PSD potential (in mV) over time.

For the SPRi based assays, the generated data were proposed by default as the variation of the reflectivity over time (hereafter referred to as ΔR, in % terms) when compared to the original image of reference for all the spots defined. As being a classical way of representing the SPRi data this format was conserved. For additional comparative purposes the detection times ($T_D$, in h terms) of the apparent growth curves were determined using Prism software (GraphPad) *via* the peak of the derivative curves as reported elsewhere [386]. Generation times ($T_G$, in min terms) were derived from the linear part of exponential based bacterial growth plots additionally obtained using a classical plating method.

### 2.2.5 Nanoparticle characterisation

#### 2.2.5.1 A bespoke approach

The hydrodynamic size (z-average), zeta potential, polydispersity index (PdI), UV-Visible spectrum, concentration and dissolution rate of used NPs were characterised by combined UV-Visible (UV-Vis), Dynamic Light Scattering (DLS) and Atomic Absorption Spectroscopy (AAS) based methods in the media of exposure when applicable. Bespoke analyses were performed depending on the aim addressed and varying across the toxicity

assays performed as well as the scenarios of exposure applied. The following information will therefore focus on the general principle and realisation of the used techniques regardless of the time point or the context of their application.

#### 2.2.5.2 UV-Visible spectroscopy

The UV-Vis assays were conducted in clear disposable cuvettes (semi micro 1.5 mL, Kartell) using an Evolution 600 spectrophotometer (Thermo Fisher Scientific) between 300 and 800 nm in a scan mode with measures taken every 1 nm at a speed of 240 nm $min^{-1}$.

#### 2.2.5.3 Dynamic Light Scattering

The DLS assays were operated in dedicated clear disposable capillary cuvettes (DTS1070, bearing electrodes) using a Nano Zetasizer (Malvern, compatible with both z-average and zeta potential determination) equipped with a 633 nm laser set at a scattering angle of 173°. The z-average measurements were performed prior to the zeta potential ones. Four replicates were registered *per* measurement. All the analyses were performed at 20 °C. All the experiments were performed using the Zetasizer software (Malvern) and so were the data processed. An example of DLS output results is shown in Appendix B (Fig. S2.2).

#### 2.2.5.4 Atomic Absorption Spectroscopy

The AAS assays were conducted with an AAnalyst 200 Spectrometer (Perkin Elmer) equipped with an air/acetylene burner head (*i.e*. flame) after calibration with pure single element standards at concentrations of 0.156, 0.312, 0.625, 1.25, 2.5 and 5 mg $L^{-1}$ following manufacturer's instructions. Ag and Zn elements were considered, using dedicated lamps specific to each element (Lumina Hollow Cathode, diameter 50 mm). An example of calibration curve for Ag is shown in Appendix B (Fig. S2.3). The apparatus was not equipped for analysing Ti (*i.e*. using an acetylene/nitrous oxide burner head).

The dissolution rates were evaluated *via* the quantification of the released ion concentration from the NPs. The suspensions of NPs were pelleted by ultracentrifugation (Avanti Centrifuge J-26XP, Beckman Coulter) at 4 °C in 15 mL open-top polycarbonate tubes at 20 000 rpm (*ca*. 50 000 x g, JA-25.15 rotor, Beckman Coulter) for 30 min as described elsewhere [38, 199]. An example of obtained pellets with the Ag NPs is shown in Appendix

B (Fig. S2.4). Half of the supernatants were carefully collected and used for AAS analysis. Dissolution rates were calculated as ratios (in % terms) between the AAS measured concentration of released element from the NPs and the original prepared concentration of NPs.

### 2.2.6 Statistical analysis

The statistical means used herein are noted along with the corresponding figures. All the analyses were performed using Prism software (GraphPad).

# CHAPTER 3: Results - Planktonic based assays

Since the widespread application of products of nanotechnology the general knowledge about the toxicity of various NPs to a range of environmental model microorganisms has grown dramatically (§ 1.1.2 and 1.1.4) although specific knowledge relating to NP fate in different environments, and related exposure and hazard, are still missing. As reported in the literature [33, 72, 405] and stressed in the introduction (§ 1.1.2.2 and 1.1.2.3), the current assessment of NP toxicity in real matrices such as wastewaters remains limited in part due to a lack of suitable methodologies for testing [75]. The use of bacteria as environmental bioreporters has shown to be a suitable approach in ecotoxicology for applications with real matrices (§ 1.1.3.2). The development of bespoke genetically modified bioreporters (GMB) using environmentally relevant model bacteria (*e.g*. *P. putida* and *B. subtilis*), directly extracted from matrices of interest [90], extends the scope of possibilities already demonstrated by numerous *Escherichia coli* based GMB reports [84]. However, the use of, specifically, bespoke GMB remains scarce for NP testing (§ 1.1.4.2.2 and 1.1.5.1) and examples of applications using real matrices are not reported yet. There are therefore underexploited avenues using bacterial GMB in nanoecotoxicology [406].

Consequently here, the potential workability of *P. putida* BS566 *lux* (originally isolated from wastewaters) as planktonic switch-off GMB is investigated in different media. Intrinsically high throughput and easy to standardise, the microtiter plate format is used. Firstly, the acute toxicity of widely used Ag, ZnO, CuO and $TiO_2$ inorganic NPs in undefined rich (Luria Bertani, LB) and defined minimal (Artificial Wastewater, AW) laboratory growth media is assessed; questioning rankings of toxicity to *P. putida* BS566 *lux* and potential impacts of different laboratory matrices of exposure. Secondly, the comparative study using crude and final real wastewater samples (CWs and FWs, respectively, collected from four different WWTPs then spiked with NPs) as matrices of exposure is reported; in which the overall workability of the method in such complex matrices as well as the potential impacts of both the wastewater type and the site of sampling are investigated. In addition, a pilot study assessing the impact of ageing on NP toxicity in AW, CW and FW is finally reported.

## 3.1 Pristine NPs in laboratory matrices

### 3.1.1 Screening of toxicity

Light output evolutions over time by the *P. putida* BS566 *lux* bioreporter when exposed to a range of concentrations of Ag, ZnO, CuO and $TiO_2$ NPs (from 0 to 200 mg $L^{-1}$) in LB or in AW are shown in Fig. 3.1. The derived $IC_{50}$ values are presented in Table 3.1.

Ag NPs exhibited dose dependent toxicity from 0 h (*i.e.* this corresponds to the first measure registered in a 5 min time window after exposure of the bacterial bioreporters to the NPs) between 12.5 and 200 mg $L^{-1}$ in LB (Fig. 3.1 A, blue curve). At 1 h, the toxicity was displayed at lower concentrations (*i.e.* below 12.5 mg $L^{-1}$) (Fig. 3.1 C). Consistent results were then observed at 2 h (Fig. 3.1 E). Similar results were obtained overall with Ag NPs in AW (Fig. 3.1 B, D and F).

Based on the derived $IC_{50}$ values (Table 3.1), there was no significant difference in toxicity between 15 min and 2 h of exposure in either medium. In addition, no cellular recovery phenomenon over time was observed (*i.e.* emitted luminescence due to regrowth of the bacterial bioreporter population). As the tested Ag NPs were supplied in suspension with a dispersant (Table 2.1), the potential impact of the sole dispersant was tested; no related toxic effects to *P. putida* BS566 *lux* were observed (Appendix C, Fig. S3.1).

In summary, toxic effects of Ag NPs were found to be similar in LB and AW and were characterised by $IC_{50}$ values at 1 h of 3.8 ± 0.1 mg $L^{-1}$ and 5 ± 0.7 mg $L^{-1}$, respectively. Comparatively, the toxicity of Ag ions (applied as $AgNO_3$) in both LB and AW is shown in Fig. 3.2 (blue curves). Corresponding $IC_{50}$ values of 0.39 ± 0.05 mg $L^{-1}$ and 0.36 ± 0.03 mg $L^{-1}$ were derived at 1 h in LB and AW, respectively.

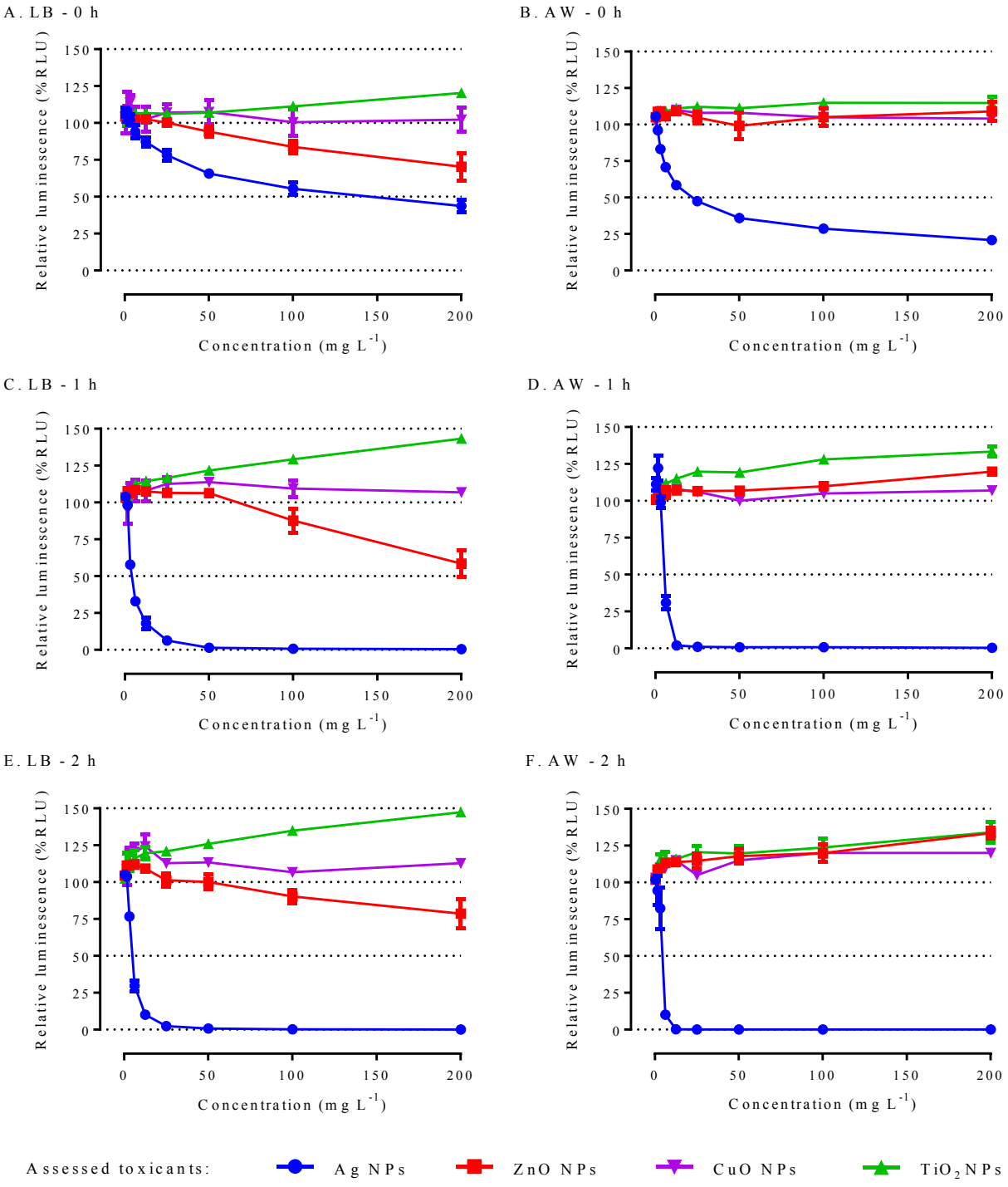


**Fig. 3.1: Toxicity of Ag, ZnO, CuO and $TiO_2$ NPs on *P. putida* BS566 *lux* in LB and AW.** The relative luminescence output evolutions by the bacterial bioreporter when challenged with 0 - 200 mg $L^{-1}$ of Ag (blue circles), ZnO (red squares), CuO (purple inverted triangles) and $TiO_2$ (green triangles) NPs in Luria-Bertani (A, C and E) or in Artificial Wastewater (B, D and F) for selected time points (0, 1 and 2 h, respectively) are presented. Data are mean ± SEM (n = 3).

The relative luminescence evolution patterns following the exposure to Zn (Fig. 3.1, red curves) showed overall lower toxicity over time than was obtained for Ag. More specifically, ZnO NPs showed transient toxicity on *P. putida* BS566 *lux* in LB (*i.e*. due to bacterial recovery), characterised by $IC_{50}$ values evolving from 58.8 ± 6.1 mg $L^{-1}$ to 100.4 ± 2.3 mg $L^{-1}$ for the first hour of exposure (Table 3.1). No $IC_{50}$ could be derived at 2 h. ZnO NPs were therefore as toxic as Ag NPs at the first time point (0 h) in LB before the toxicity patterns diverged. In AW, no toxicity was monitorable, so no $IC_{50}$ could be derived.

Consequently, toxic effects of tested ZnO NPs occurred exclusively and transiently in LB for the first hour of exposure along with cellular recovery over time as suggested by the relative luminescence reduction plots (Fig. 3.1, red curves) and supported by the derived $IC_{50}$ values (Table 3.1). Comparatively, $IC_{50}$ values for Zn ions (applied as $ZnSO_4$, Fig. 3.2, red curves) evolved from 46.9 ± 6.6 mg $L^{-1}$ to 73.3 ± 8.3 mg $L^{-1}$ in LB during the first hour of exposure and were not derived in AW as no toxicity was observed.

**Table 3.1: Calculated $IC_{50}$ on *P. putida* BS566 *lux* in LB and AW.**

| | | $IC_{50}$ (mg $L^{-1}$) | | | | | |
|---|---|---|---|---|---|---|---|
| | | **0 min** | **15 min** | **30 min** | **60 min** | **90 min** | **120 min** |
| **Ag NPs** | LB | 62.8 (±16.2)[c] | 9.3 (±1.3)[ab] | 4.8 (±0.3)[a] | 3.8 (±0.1)[a] | 4.0 (±0.1)[a] | 4.0 (±0.2)[a] |
| | AW | 32.0 (±4.9)[c] | 13.8 (±1.5)[b] | 6.4 (±0.4)[a] | 5.0 (±0.7)[a] | 4.4 (±0.9)[a] | 4.0 (±0.8)[a] |
| **ZnO NPs** | LB | 58.8 (±6.1)[c] | 79.8 (±1.3)[abc] | 88.5 (±1.3)[abc] | 100.4 (±2.3)[abc] | 100.4 (±0.3)[ac] | ND[ab] |
| | AW | ND[c] | | | | | |

Data are mean ± SEM (n = 3).

ND - $IC_{50}$ were not calculated due to non-observed toxicity (considered higher than 200 mg $L^{-1}$).

Statistical significant differences between results were tested *via* two-way ANOVA followed by Tukey test.

[a] Significantly different from the first time point ($p < 0.001$)

[b] Significantly different from the previous time point ($p < 0.05$)

[c] Significantly different from the other matrix ($p < 0.001$)

Regardless of the medium of exposure, testing at concentration up to 200 mg $L^{-1}$ resulted in no detectable toxicity over time for both CuO NPs (Fig. 3.1, purple curves) and $TiO_2$ NPs (Fig. 3.1, green curves). In the Cu case, no toxicity was observed either using the related ions, $CuCl_2$ (Fig. 3.2, purple curves) or $CuSO_4$ (data not shown). Due to absence of detected toxicity, no $IC_{50}$ could be derived.

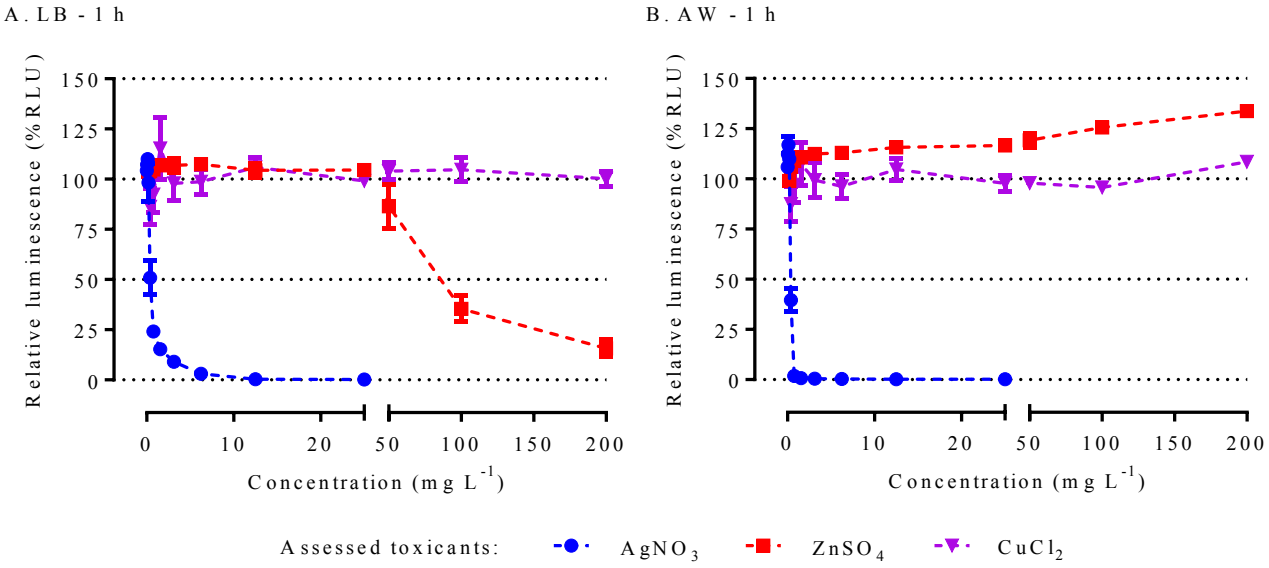


**Fig. 3.2: Toxicity of Ag, Zn and Cu ions on *P. putida* BS566 *lux* in LB and AW.** The relative luminescence output evolutions by the bacterial bioreporter when challenged with 0 - 25 mg $L^{-1}$ of Ag ions ($AgNO_3$, blue circles), 0 - 200 mg $L^{-1}$ of Zn ions ($ZnSO_4$, red squares) and 0 - 200 mg $L^{-1}$ Cu ions ($CuCl_2$, purple inverted triangles) in Luria-Bertani (A) or in Artificial Wastewater (B) for the selected time point of 1 h are presented. Data are mean ± SEM (n = 3).

### 3.1.2 Characterisation of NPs

Pristine (*i.e.* non-aged) nanoparticles were characterised in both LB and AW by UV-vis (Fig. 3.3), DLS (Fig. 3.4) and AAS (Fig. 3.5) when applicable.

As presented in Fig. 3.3 A, Ag NPs showed characteristic and comparable UV-vis spectra with a unique and narrow peak in both media. Peak positions were observed at 413.6 ± 0.6 nm and 415.2 ± 0.3 nm with absorbance intensities of 1.06 ± 0.04 a.u. and 0.89 ± 0.02 a.u. in AW and LB, respectively. DLS data showed mean hydrodynamic sizes of 140 ± 7 nm in LB and 40 ± 1 nm in AW, which were not found to be significantly different; and zeta

potentials of -16.6 ± 0.5 mV and -5.1 ± 0.2 mV in LB and AW which were found significantly different between media (Fig. 3.4). PDI of the Ag NP suspensions were consistently measured below 0.5 regardless of the medium. AAS analyses indicated low and time independent dissolution rates of used Ag NPs close to 4 % in LB and to 2 % in AW, which were not found to be significantly different (Fig. 3.5 A). Consequently, pristine Ag NPs showed better stabilisation in LB (higher absolute zeta potential and bigger z-average) than in AW but comparable behaviours overall in terms of polydispersity (DLS), agglomeration (UV-vis) and dissolution (AAS).

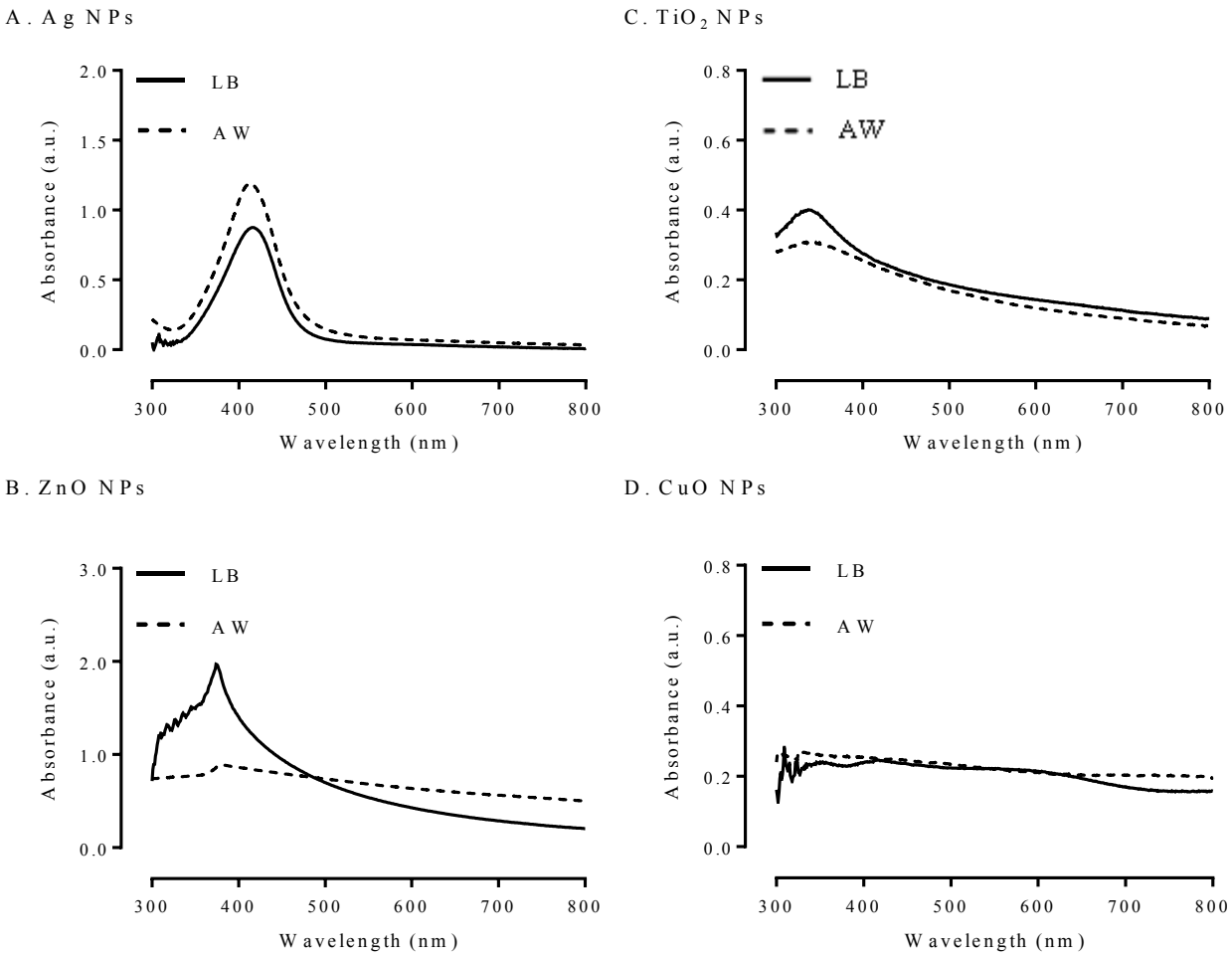


**Fig. 3.3: Ag, ZnO, $TiO_2$ and CuO NP characterisation by UV-visible spectrophotometry in LB and AW.** The specific absorption spectra (from 300 to 800 nm) of: 10 mg $L^{-1}$ Ag NPs (A), 200 mg $L^{-1}$ ZnO NPs (B), 10 mg $L^{-1}$ $TiO_2$ NPs (C) and 200 mg $L^{-1}$ CuO NPs in both used media (- Luria-Bertani and -- Artificial Wastewater, respectively) are shown. Spectra are representative examples of obtained results in replicated experiments.

As shown in Fig. 3.3 B, ZnO NPs exhibited characteristic (one peak close to 380 nm followed by a long tail) but non-comparable UV-vis spectra between matrices. Peak positions were observed at 374.8 ± 0.3 nm and 385.4 ± 4.5 nm with absorbance intensities of 2.0 ± 0.3 a.u. and 0.78 ± 0.8 a.u. in LB and AW, respectively. Significantly different mean hydrodynamic sizes (177 ± 4 nm in LB and 1537 ± 265 nm in AW) and zeta potentials (-12.2 ± 0.5 mV in LB and -28.2 ±1 mV in AW) were observed between media (Fig. 3.4). PDI of the ZnO NP suspensions were consistently measured *ca.* 0.6 regardless of the medium. AAS analyses indicated medium dependent and time independent dissolution rates of tested ZnO NPs close to 40 % in LB and to 2.5 % in AW (Fig. 3.5 B). Consequently, ZnO NPs exhibited non-comparable behaviours in LB and AW attesting overall to high aggregation/agglomeration and low dissociation in AW compared to LB.

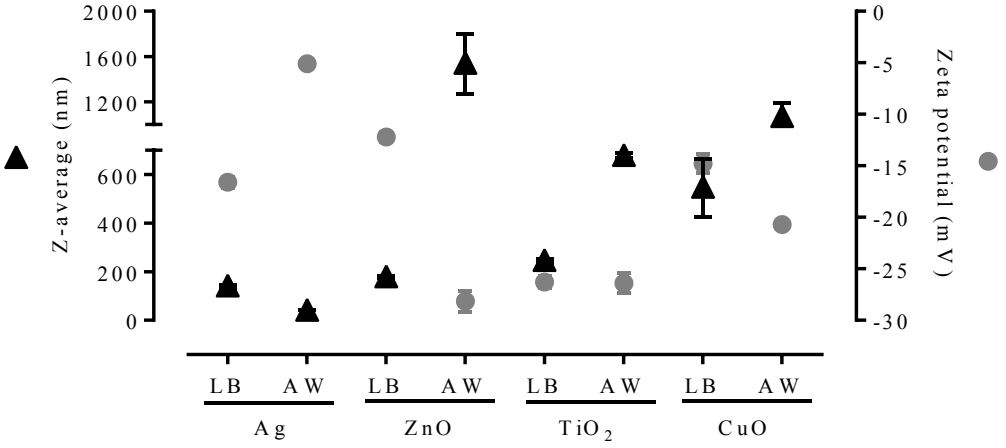


**Fig. 3.4: NP characterisation by DLS in LB and AW.** The mean hydrodynamic size (z-average) and the zeta potential values of 10 mg $L^{-1}$ Ag, ZnO, CuO and $TiO_2$ NPs in both media (Luria-Bertani and Artificial Wastewater) are presented. Data are mean ± SEM (n = 3). Statistical significant differences between results were tested *via* two-way ANOVA followed by Tukey test and reported in the text.

As shown in Fig. 3.3 C, $TiO_2$ NPs exhibited similar UV-vis spectra between media. Peak positions were observed at 325.1 ± 5.2 nm and 340.5 ± 6.8 nm with absorbance intensities of 0.38 ± 0.03 a.u. and 0.29 ± 0.02 a.u. in LB and AW, respectively. DLS data showed significantly different mean hydrodynamic sizes (244 ± 8 nm in LB and 677 ± 11 nm in AW) and comparable zeta potentials (-26.3 ± 0.6 mV in LB and -26.4 ± 1 mV in AW)

between media (Fig. 3.4). PDI of the $TiO_2$ NP suspensions were consistently measured *ca.* 0.3 regardless of the medium. No dissolution studies were carried out with $TiO_2$ NPs since it was not considered relevant (*i.e.* first $TiO_2$ NPs are essentially non-soluble in aqueous media and second the tested $TiO_2$ NPs did not exhibit detectable toxicity in our assays). Consequently, $TiO_2$ NPs showed non-comparable behaviours in LB and AW attesting especially to more aggregation in AW compared to LB.

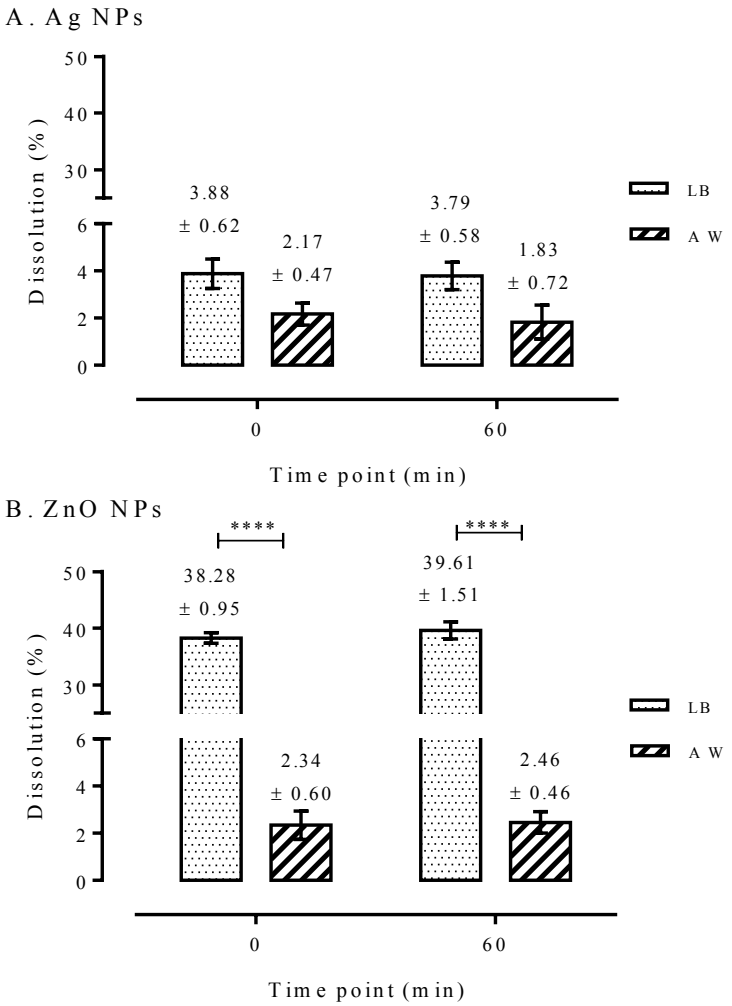


**Fig. 3.5: Ag and ZnO NP characterisation by AAS in LB and AW.** Dissolution rates (in mass % terms) of 50 mg $L^{-1}$ Ag NPs (A) and 200 mg $L^{-1}$ ZnO NPs (B) in Luria-Bertani and Artificial Wastewater after 0 or 1 h of incubation are presented. Mean $R^2$ ± standard error obtained for AAS instrument calibration between 0.156 mg $L^{-1}$ and 5 mg $L^{-1}$ were 0.9998 ± 0.0001, 0.9880 ± 0.0010 for Ag and Zn standard elements, respectively. Data are mean ± SEM (n = 3). Significantly different at ****$p < 0.0001$ *via* two-way ANOVA followed by Tukey test.

A shown in Fig. 3.3 D, no characteristic spectrum was obtained for the tested CuO NPs up to 200 mg $L^{-1}$ neither in LB nor in AW. Different mean hydrodynamic sizes (545.8 ± 119.1 nm in LB and 1067 ± 123.8 nm in AW) and zeta potentials (-14.8 ± 0.9 mV in LB and -20.7 ± 0.4 mV in AW) were observed between media (Fig. 3.4). PDI of the CuO NP suspensions were reported *ca.* 0.66 in both media. In the absence of evident toxicity of both the CuO NPs and the related ions, the dissolution rate of the NPs was not investigated. From a characterisation viewpoint, pristine CuO NPs have therefore been shown to aggregate more in AW than in LB.

## 3.2 Pristine NPs in real matrices

In the absence of toxicity of ZnO, CuO and $TiO_2$ NPs in AW, assays in real crude and final wastewaters (CWs and FWs) were prioritised with Ag NPs.

### 3.2.1 Screening of toxicity

Light output evolutions over time by the *P. putida* BS566 *lux* bioreporter when exposed to a range of concentrations of Ag NPs spiked in real CW and FW samples (*i.e.* from site 2) are shown in Fig. 3.6.

A dose-response toxicity pattern characterised by a decrease in the signal output with increasing concentrations of Ag NPs (up to 200 mg $L^{-1}$) was observed in both CW2 and FW2 samples. Greatest variability between replicated experiments occurred *ca.* 12.5 mg $L^{-1}$ of Ag NPs in CW2 and between 3.125 mg $L^{-1}$ and 6.25 mg $L^{-1}$ in FW2, lower doses being not toxic and higher doses being lethal at 1 h, respectively (Appendix C, Fig. S3.2). Regarding the assays performed with samples from the other sites, similar dose-response toxicity patterns were obtained overall (Appendix C, Fig. S3.2 to S3.5). Crude samples, especially CW1 and CW4, showed the highest variability amongst experiments in terms of toxicity.

In summary, Ag NPs were more toxic in FW than in CW samples. Results with the Ag NM-300K dispersant did not indicate any toxic effect to the *P. putida* BS566 *lux* bioreporter in the real matrices (Fig. 3.6). No background noise (*i.e.* luminescence) was registered from the wastewater samples in the absence of the luminescent bacterial

bioreporter (Fig. 3.6). In no case did the NP addition result in increased output signals, regardless of the presence or absence of the bacterial bioreporter.

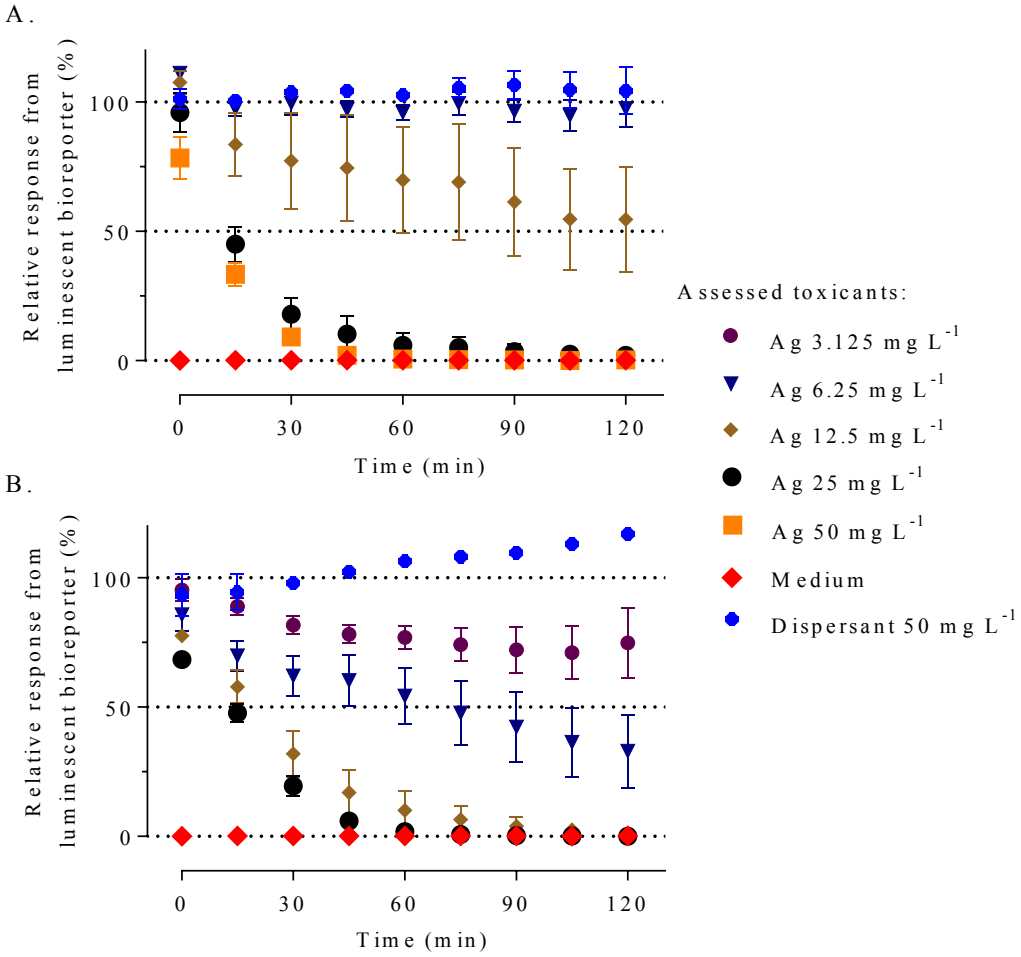


**Fig. 3.6: Comparative toxicity of Ag NPs on *P. putida* BS566 *lux* in real wastewaters.** Relative luminescence output evolutions over time by the bacterial bioreporter when challenged up to 200 mg $L^{-1}$ of Ag NPs in crude (A) and final (B) wastewaters from site 2 are shown. Four out of the nine used NP concentrations are plotted for better clarity (from 6.25 to 50 mg $L^{-1}$ in A and from 3.125 to 25 mg $L^{-1}$ in B); the entire graphics as well as results with samples from other sites are presented in Appendix C (Fig. S3.2 to S3.5). Background signal from used media and effect of Ag NP dispersant (at 50 mg $L^{-1}$) are also presented. Data are mean ± SEM (n = 4).

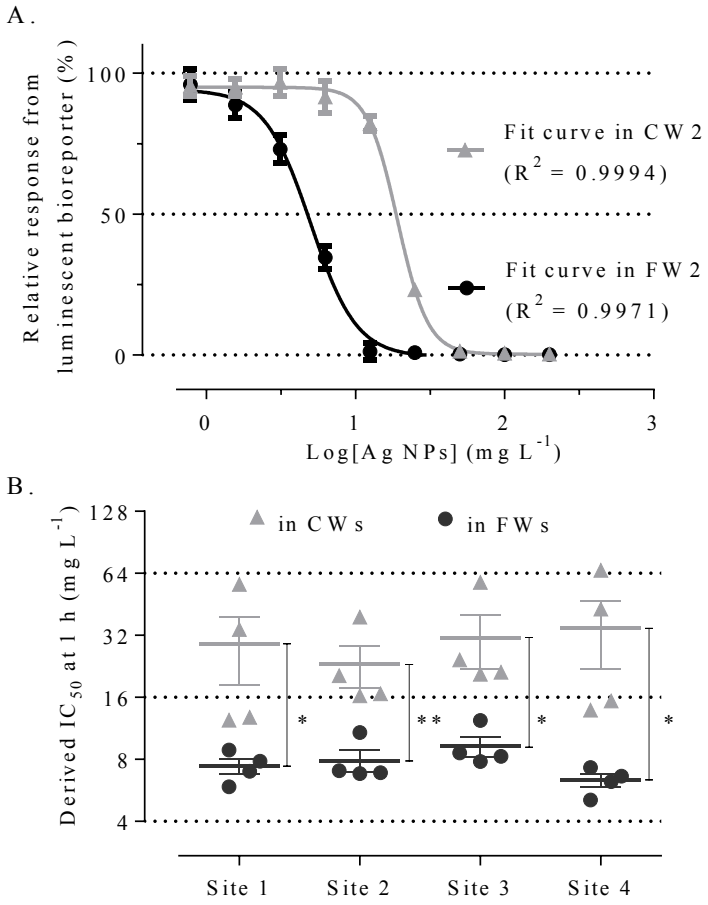


**Fig. 3.7: Derived $IC_{50}$ values in real wastewaters.** Toxicity results from light output reductions by *P. putida* BS566 *lux* when exposed to Ag NPs in crude and final wastewaters (CWs and FWs, respectively) from four different wastewater treatment plants (site 1 to 4) were plotted as (response) = f(log[Ag NPs]) for selected time points and $IC_{50}$ values were derived by fitting a four parameter dose-response model. Graphic A shows an example of (response) = f(log[Ag NPs]) treated information and obtained fits for one test with wastewaters from site 2 (including four replicates *per* condition). Average $R^2$ from fits for all derived $IC_{50}$ values is 0.9960 ± 0.0036 (mean ± SD). Graphic B shows the comparison of calculated $IC_{50}$ values at 1 h. Data are mean ± SEM (n = 4), significantly different by unpaired t-test with $p < 0.1$ (*) or $p < 0.05$ (**). Derived $IC_{50}$ at 0.5 and 2 h are presented in Appendix C (Fig. S3.6).

An example of generated fit curves for both types of wastewaters along with the derived $IC_{50}$ values at 1 h is presented in Fig. 3.7. As shown in Fig. 3.7 A, all proposed data were derived from good fits considering nine different doses *per* experiment and exhibiting a mean $R^2$ of 0.9960 ± 0.0036 amongst all treated data.

$IC_{50}$ values of 7.4 ± 0.6 mg $L^{-1}$, 7.9 ± 1 mg $L^{-1}$, 9.3 ± 1 mg $L^{-1}$ and 6.3 ± 0.5 mg $L^{-1}$ were calculated in FWs for sites 1 to 4, respectively, and were not found to be significantly different (Fig. 3.7 B). The mean relative standard error (RSE) of all derived $IC_{50}$ was inferior to 10 %.

In CWs, mean RSE was close to 30 % and the $IC_{50}$ values derived between 23.1 ± 5.4 mg $L^{-1}$ and 34 ± 12.5 mg $L^{-1}$ without being significantly different between sites either (Fig. 3.7 B). However, Ag NPs were found in all cases to have significantly lower toxicity in CWs than FWs. Comparable patterns were obtained at 0.5 h and 2 h time points (Appendix C, Fig. S3.6).

### 3.2.2 Characterisation of wastewaters

A comprehensive list of physico-chemical characteristic parameters including BOD, COD, BOD/COD ratio, TSS, pH, ammonia, chloride, sulphide and silver original loadings was considered alongside toxicity. Total plate counts were also used as a basic indicator of the indigenous bacterial population size. Data for all used CW and FW samples from the different sites are presented in Table 3.2.

CWs showed significantly higher BOD/COD ratios (from 0.4 to 0.46) than FWs (inferior to 0.18 for FW1, 2 and 3 and close to 0.28 for FW3) attesting to their respective high and low biodegradability. The concentration of TSS was generally found to be at least ten times higher in CWs than in FWs, although rather consistent between sites, as similarly observed for the ammonia load, except for FW samples from site 3. *Per* site, the pH was similar between samples (between 6.5 and 7), except for samples from site 3 which exhibited one unit of pH difference between CWs (at 6.45 ± 0.09) and FWs (at 7.56 ± 0.06). In all cases the original amount of silver was found below the lower detection limit of the AAS apparatus (< 0.1 mg $L^{-1}$). The total plate counts showed there were about $10^3$ - $10^4$ CFU $mL^{-1}$ in FWs and $10^6$ - $10^7$ CFU $mL^{-1}$ in CWs, regardless of the site.

Comparatively to the other WWTPs, site 3 had a significantly higher amount of chloride and sulphide for CWs and significantly higher amount of chloride, ammonia as well as higher BOD/COD ratio in addition to different pH readings for FWs. Samples from sites 1, 2 and 4 appeared generally comparable.

### 3.2.3 Multivariate analysis

Results from the multivariate analysis carried out with the aforementioned environmental parameters characterising the used wastewaters constrained with the derived $IC_{50}$ values at 1 h are presented in Fig. 3.8.

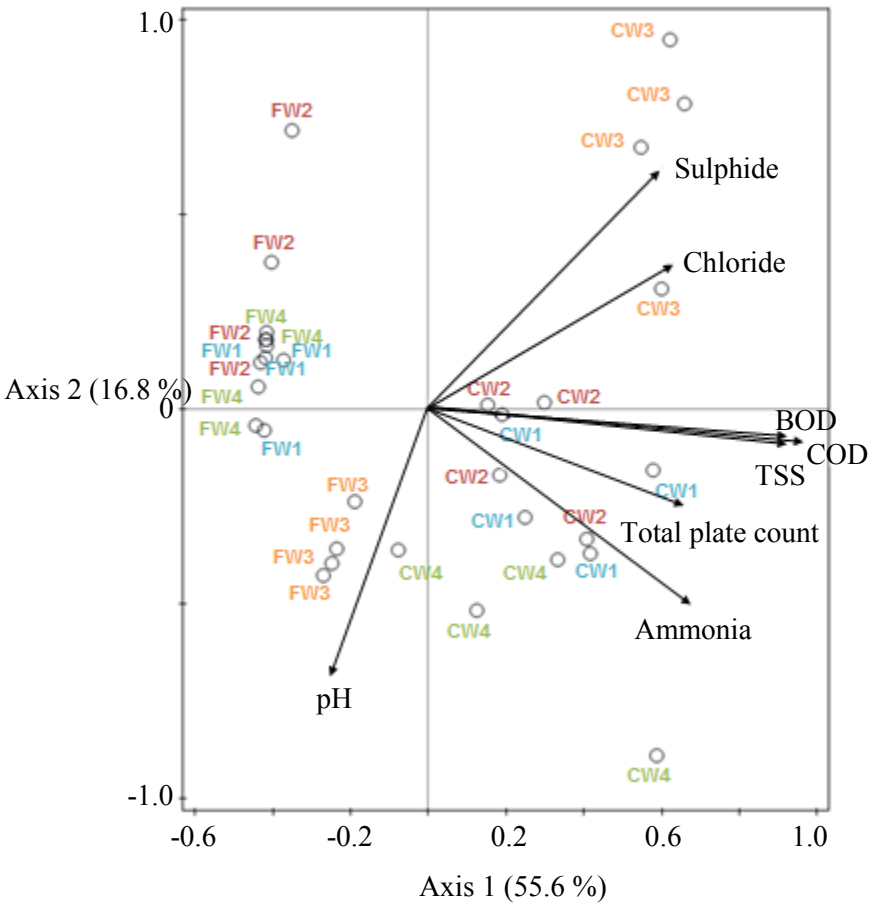


**Fig. 3.8: Multivariate analysis.** The ordination diagram of used thirty two wastewater samples (crude or final samples, CW or FW, respectively) from four different WWTPs (site 1 in blue, site 2 in red, site 3 in orange and site 4 in green) by canonical correlation analysis considering height biochemical parameters (BOD, COD, TSS, ammonia, pH, chloride, sulphide and total plate count) as environmental variables constrained with one explanatory variable (the derived $IC_{50}$ values at 1 h) is presented above.

**Table 3.2: Physico-chemical and microbiological parameters of used wastewaters.** Data are mean ± SEM (n = 4) before spiking with NPs.

| | Site 1 | | Site 2 | | Site 3 | | Site 4 | |
|---|---|---|---|---|---|---|---|---|
| | Crude | Final | Crude | Final | Crude | Final | Crude | Final |
| BOD (mg $L^{-1}$) | 181 ± 13.7 [a] | ≤ 3 | 163.7 ± 11.7 [a] | ≤ 3 | 166.4 ± 25.7 [a] | 16.8 ± 3.2 [b] | 133 ± 23.6 [a] | ≤ 3 |
| COD (mg $L^{-1}$) | 393.4 ± 30.9 [a] | 23.8 ± 3.1 | 407.2 ± 40.2 [a] | 22 ± 2.7 | 402.8 ± 51.3 [a] | 58.2 ± 4.9 [b] | 342.5 ± 70.5 [a] | 18.2 ± 1.1 |
| BOD/COD ratio | 0.46 ± 0.03 [a] | ≤ 0.15 | 0.41 ± 0.03 [a] | ≤ 0.16 | 0.41 ± 0.01 [a] | 0.28 ± 0.03 [b] | 0.40 ± 0.02 [a] | ≤ 0.18 |
| TSS (mg $L^{-1}$) | 203.6 ± 23.9 [a] | ≤ 10 | 235.8 ± 31.3 | N/A | 224.2 ± 29.4 [a] | 28.2 ± 2.7 | 179.7 ± 57.9 | N/A |
| Ammonia (mg $L^{-1}$) | 15.8 ± 1.1 [a] | 0.63 ± 0.19 | 17.5 ± 1.6 [a] | 0.43 ± 0.14 | 18 ± 2.2 | 20.5 ± 2.6 [b] | 32.6 ± 10.5 [a] | 0.125 ± 0.075 |
| pH | 6.8 ± 0.16 | 7 ± 0.08 | 6.59 ± 0.26 | 6.50 ± 0.2 | 6.45 ± 0.09 [a] | 7.56 ± 0.06 [b] | 7.12 ± 0.04 | 6.94 ± 0.12 |
| Total plate count (CFU $mL^{-1}$) | 9.2 ± 5.2 x $10^{6}$ [a] | 1.1 ± 0.7 x $10^{4}$ | 1.5 ± 0.3 x $10^{6}$ [a] | 3.3 ± 1.3 x $10^{3}$ | 4.1 ± 0.4 x $10^{6}$ [a] | 7.83 ± 1.9 x $10^{3}$ | 6.4 ± 2.8 x $10^{6}$ | 1.4 ± 0.9 x $10^{4}$ |
| Ag (mg $L^{-1}$) | < 0.1 [c] | < 0.1 [c] | < 0.1 [c] | < 0.1 [c] | < 0.1 [c] | < 0.1 [c] | < 0.1 [c] | < 0.1 [c] |
| Chloride (mg $L^{-1}$) | 119.6 ± 21.3 | 71.6 ± 12.9 | 95.8 ± 7.81 [a] | 47.5 ± 1.65 | 253.9 ± 37.9 [a, b] | 148.2 ± 29.8 [b] | 79 ± 8.2 [a] | 50.5 ± 1.7 |
| Sulphide (mg $L^{-1}$) | 0.166 ± 0.03 [a] | < 0.010 | 0.362 ± 0.088 [a] | < 0.010 | 3.681 ± 1.2 [a, b] | < 0.010 | 0.272 ± 0.09 [a] | < 0.010 |

N/A corresponds to incomplete series of data.

Symbols < indicate that parameter was consistently below the lower detection limit of the method or of the apparatus.

[a] Data are significantly different between crude and final samples for the considered site (unpaired t-test, $p < 0.05$).

[b] Considered information is significantly different to results with the same type of samples (Crude or Final) from all other sites (unpaired t-test, $p < 0.05$).

[c] Tested with acidification (in 5 % v/v final nitric acid) and without acidification.

Overall 72.4 % of the total variability was addressed by a two-way representation. Samples were separated in two groups (FWs and CWs) along axis 1 by mainly the BOD, COD and TSS parameters which were highly related. In addition, sulphide, chloride, total plate count and ammonia information supported this separation along both axes 1 and 2; these were also closely related.

The highest variability was associated with the CWs as they were represented as generally more spread out than the FWs. Both FW3 and CW3 samples occurred isolated from the other FWs and CWs, respectively, and were mainly characterised by different sulphide, chloride and pH related data as previously mentioned. The analysis with derived $IC_{50}$ at 0.5 h or 2 h led to comparable results as global toxicity patterns were similar at those time points (data not shown).

### 3.2.4 Characterisation of NPs

Ag NPs were characterised in wastewaters by DLS and UV-vis. Corresponding hydrodynamic sizes, zeta potentials and absorbance spectra are presented in Fig. 3.9.

Ag NPs showed consistent hydrodynamic sizes and zeta potentials in FWs between 53 ± 2.1 nm and 58.7 ± 2.7 nm and between -16.6 ± 1.1 mV and -19.7 ± 0.5 mV, respectively. In CWs consistent zeta potentials were obtained between -20.9 ± 0.9 mV and -23.5 ± 1.1 mV, but variable hydrodynamic sizes between 71.3 ± 2.1 nm and 233.3 ± 16.9 nm were measured. Hydrodynamic size and zeta potential were both found significantly different between FWs and CWs, regardless of the site. Registered spectra of absorbance were found similar between all samples and characterised by a single peak at 413.2 ± 0.8 nm in FWs and at 413.5 ± 1 nm in CWs for an average absorbance of 1.39 ± 0.12 a.u. and 1.40 ± 0.2 a.u. respectively, attesting to the consistent and comparable non-aggregated status and nano-size range of all freshly prepared and used Ag NP suspensions. Comparable low dissolution rates *ca*. 3 % were equally obtained in both CWs and FWs.

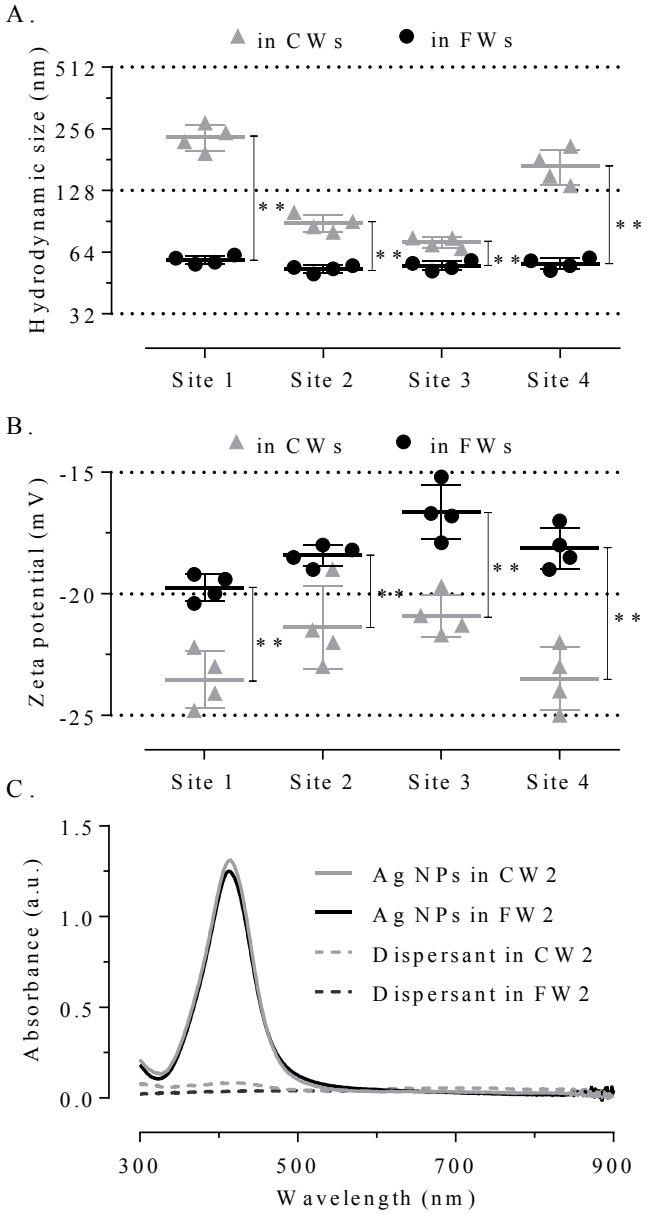


**Fig. 3.9: Ag NP characterisation in real wastewaters.** Ag NPs at 10 mg $L^{-1}$ in crude and final wastewaters (CWs and FWs) were characterised by DLS and UV-vis. Graphics A and B show the hydrodynamic size and the zeta potential information, respectively. Data are mean ± SD, significantly different by unpaired t-test with $p < 0.05$ (**). Graphic C shows an example of typical spectra of absorbance (between 300 to 900 nm) obtained for spiked CWs and FWs from site 2.

## 3.3 Aged NPs in AW, CWs and FWs

In addition to the aforementioned studies operated with pristine Ag NPs, assays with aged Ag NPs were piloted in both artificial (AW) and real (CW and FW) wastewaters. As site 3 presented particular characteristics compared to the other sites, especially a high content of chloride and sulphide, in addition to be the largest WWTP of the four (*i.e.* treating wastewaters for a population equivalent of approximatively 850 000 people), preliminary assays were performed with CW3 and FW3 samples.

### 3.3.1 Screening of toxicity

Effects of ageing in wastewaters (CW, FW, AW) on the eventual Ag NP toxicity to the *P. putida* BS566 *lux* bioreporter are presented in Fig. 3.10. Ag NPs showed a consistent toxicity pattern following ageing for 4 weeks in FW3 (*i.e.* $IC_{50}$ at 1 h close to 7.8, 7.8, 6.9 and 6 mg $L^{-1}$ at week 0, 1, 2 and 4 respectively) before becoming less toxic in week 8 (*i.e.* $IC_{50}$ at 1 h close to 12.6 mg $L^{-1}$). Overall, comparable stable patterns were obtained in AW ($IC_{50}$ at 1 h oscillating between 3 and 6 mg $L^{-1}$ regardless of ageing). In CW3 though, effects from ageing were visible from week 1 where $IC_{50}$ values were twice the values derived with non-aged materials; then $IC_{50}$ almost doubled again by the end of week 8.

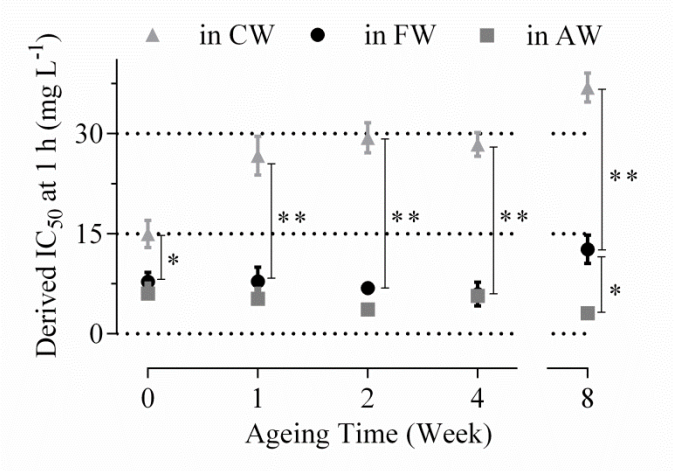


**Fig. 3.10: Effect of ageing on Ag NP toxicity.** The derived $IC_{50}$ values at 1 h obtained from the *P. putida* BS566 *lux* based planktonic assays performed with aged Ag NPs (from 0 to 200 mg $L^{-1}$) in artificial (AW) and real (CW and FW from site 3) wastewaters after respectively 0, 1, 2, 4 and 8 weeks of ageing are shown above. Data are mean ± SEM (n = 3), significant differences are represented as $p < 0.1$ (*) or $p < 0.05$ (**) following analysis with unpaired t-tests.

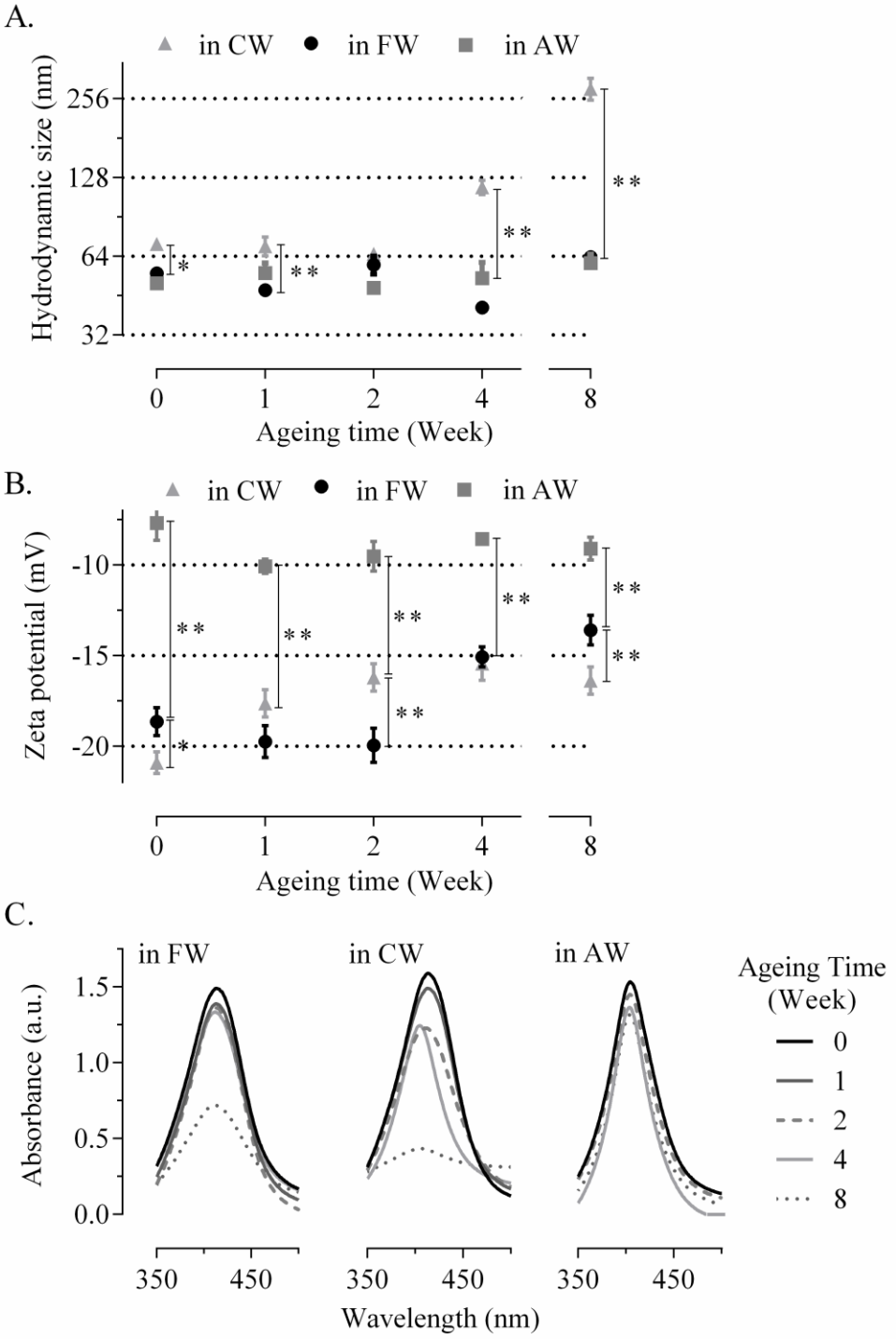


**Fig. 3.11: Effect of ageing on Ag NP characteristics.** The evolution over ageing (up to 8 weeks) of the hydrodynamic size (A), zeta potential (B) and absorbance spectrum (C) of Ag NPs in artificial (AW) and real wastewaters (CW and FW from site 3) is presented above. All characterisation assays were performed with Ag NPs at 10 mg $L^{-1}$. Data are mean ± SEM (n = 3), significant differences are represented as $p < 0.1$ (*) or $p < 0.05$ (**) following analysis with unpaired t-tests.

3.3.2 Characterisation of NPs

Aged NPs were characterised in CW, FW and AW by UV-vis, DLS and AAS; results are presented in Fig. 3.11.

Increase in hydrodynamic size and the decrease of the absolute zeta potential values, especially in CW, were observed with ageing (Fig. 3.11 A and B). Modified absorbance spectra were in addition obtained through the weeks, mainly exhibiting lower amplitude compared to non-aged materials. No clear peak were finally characterised in week 8 (Fig. 3.11 C). A decrease in the dissolution rates especially in CWs (from *ca*. 3 % in week 0 to 1 % in week 1 then below 1 % in week 8) was also observed with ageing. Comparatively, behaviours of NPs remained rather stable in both AW and FW despite of ageing.

## 3.4 Discussion

3.4.1 Pristine NPs in laboratory matrices

3.4.1.1 The big picture

Overall data presented herein demonstrated higher toxicity of Ag NPs, followed by ZnO NPs and $TiO_2$ NPs with derived $IC_{50}$ values at 1 h close to 5 mg $L^{-1}$ in both LB and AW for Ag NPs, from 60 mg $L^{-1}$ to 100 mg $L^{-1}$ in LB exclusively for ZnO NPs, and higher than 200 mg $L^{-1}$ in both LB and AW for $TiO_2$ NPs. In addition, $IC_{50}$ values of 0.3 - 0.4 mg $L^{-1}$ for Ag ions in both matrices and between 50 and 70 mg $L^{-1}$ for Zn ions in LB were also identified. Consequently, different NPs presented different toxicity to *P. putida* BS566 *lux* and, when applicable, the ions were found more toxic than their NPs counterparts. In addition, the toxicity of NPs was shown to be possibly influenced by the matrix of exposure.

Bondarenko *et al*. (2013) [99] discussed median $IC_{50}$ to bacteria of 7.1 mg $L^{-1}$ for Ag NPs, 3.3 mg $L^{-1}$ for Ag ions, 500 mg $L^{-1}$ for ZnO NPs and 30 mg $L^{-1}$ for ZnO ions. Similarly, Chernousova and Epple (2013) [31] reported the mode of Ag NP and ion toxicity values on prokaryotes in the range 1 - 10 mg $L^{-1}$ and 0.1 - 1 mg $L^{-1}$, respectively; whereas toxicity of $TiO_2$ NPs was generally reported above 200 mg $L^{-1}$ when observed [43, 98]. Consequently, results presented here with *P. putida* BS566 *lux* bioreporter appear most of all directly in line with discussed nanoecotoxicological trends on various bacteria. Interestingly, both

CuO NPs and Cu salts were not toxic to *P. putida* BS566 *lux* up to 200 mg $L^{-1}$ whereas detrimental impacts *ca*. 200 mg $L^{-1}$ for CuO NPs and 32 mg $L^{-1}$ for Cu ions were already reported on bacteria [99]. Consequently, the used bioreporter herein may be more resilient to copper than previously reported bacterial strains.

#### 3.4.1.2 Toxicity of Ag NPs (and ions) to *P. putida* BS566 *lux*

Regarding Ag NM-300K NPs, results indicated comparable toxicity patterns in both LB and AW with main effects occurring during the very first stages of exposure. Although Ag NPs appeared toxic at slightly lower doses in AW (*i.e*. lower $IC_{50}$ at 0 h, time point corresponding to the first measure registered in a 5 min time window after exposure of bacterial bioreporters to the NPs) compared to LB, consistent $IC_{50}$ values *ca*. 4 - 5 mg $L^{-1}$ were derived over time in both matrices.

Low dissolution rates were consistently observed over time and matrices for Ag NM-300K NPs, as also described elsewhere [390, 391]. Mean hydrodynamic sizes were not found significantly different between matrices but suspensions of Ag NPs were shown to be less stable in AW compared to LB based on the zeta potential values. The UV-vis spectra showed narrow and specific peaks close to 413 nm, further attesting to the actual nano-size of tested Ag NPs in both matrices. Observed low agglomeration as well as consistent low dissolution and toxicity indicated that although ionic strength of AW was almost four times that of LB (*ca*. 300 and 80 mM, respectively, at pH 7), it was not instrumental in determining hazard over the full time period. The characterised differences in terms of zeta potential of NPs are besides likely to be supported by the different protein-free/rich properties of each matrix.

Dams *et al*. (2011) [185] first reported on *P. putida* BS566 *lux* bioreporter higher toxicity of nano Ag (*ca*. 80 - 90 mg $L^{-1}$ at 1 h) compared to micro Ag (*ca*. 500 - 700 mg $L^{-1}$ at 1 h) in LB. They did not discuss potential dissolution of NPs but they reported ionic silver (applied as silver nitrate) based $IC_{50}$ values from 0.44 to 0.18 mg $L^{-1}$ between 0.5 and 1.5 h of exposure. Considering in our case at 1 h a dissolution rate of ~ 4 % (in mass terms) and an $IC_{50}$ of ~ 4 mg $L^{-1}$ for Ag NM-300K in LB, an ion based $IC_{50}$ around 0.16 mg $L^{-1}$ may be estimated. Herein assays with Ag ions (also applied as silver nitrate) led to $IC_{50}$ values at 1

h between 0.3 and 0.4 mg $L^{-1}$ in both matrices. In addition, the toxicity of Ag NM-300K NPs was recently reported to be in the range 10 - 100 mg $L^{-1}$ in LB with different *Salmonella* spp. [407]. These authors concluded similarly that dose-dependent effects occurred in the early stages of exposure for both NPs and ions with, again, one order of magnitude of difference in the dose metric of both tested materials. Consequently, herein results are directly comparable to previously published data [185] and emphasise the relative sensibility of *P. putida* compared to other bacteria (*e.g*. *Salmonella* spp.) [247, 407, 408], the recurrent greater toxicity of Ag ions compared to Ag NPs, and the impact of the NP size as the smallest NPs occurred to be the most toxic eventually (*i.e*. Ag NM-300K NPs with primary size < 15 nm were found more toxic than the Ag NPs *ca*. 35 nm tested by Dams and co-workers [185]).

The use of *P. putida* is scarce in nanoecotoxicology (§ 1.1.4.2), limiting the possibility for intra-species comparisons. Hachicho *et al*. (2014) [130] reported $IC_{50}$ values *ca*. 250 mg $L^{-1}$ for Ag NPs and 0.175 mg $L^{-1}$ for Ag ions on *P. putida* mt-2. Gajjar *et al*. (2009) [219] discussed impacts of Ag NPs *ca*. 1 mg $L^{-1}$ on a modified KT2440 and between 0.1 - 0.2 mg $L^{-1}$ for the ionic counterparts. Jin and co-workers (2010) [209] also discussed $IC_{50}$ values of Ag NPs orders of magnitude higher than results with Ag ions on *P. putida* (depending on the matrix of exposure composition). Regardless of the methodology, overall studies emphasised that Ag ions are more toxic than Ag NPs and that the effective antibacterial dose of the ions is relatively consistent across studies and *P. putida* strains whereas the NPs, conversely, exhibit evident versatility in terms of antibacterial efficacy.

In light of the above, in the case of the *P. putida* BS566 *lux* bioreporter the observed Ag NM-300K toxicity is therefore likely to be driven (mainly) by ion release, even at low dissolution rates, linked to the size of NPs (both found consistent in the different matrices) as described elsewhere [31, 234, 366, 390, 391, 407].

#### 3.4.1.3 Toxicity of ZnO NPs (and ions) to *P. putida* BS566 *lux*

For ZnO NM-110 NPs, results indicated different toxicity patterns in both matrices. In LB ZnO NM-110 exhibited transient toxicity to *P. putida* BS566 *lux*, whereas, in AW no toxicity was observed. ZnO NPs are widely described to have high dissolution rates and to

exhibit a toxicity mostly ion based [107, 168, 199]. Consequently, the detection of ZnO NM-110 toxicity in LB (*i.e*. $IC_{50}$ between 60 and 100 mg $L^{-1}$ during the first hour of exposure) might be at least partly associated to high dissolution rates (close to 40 %, in mass terms) observed in this medium, whereas in contrast the absence of toxicity in AW is likely to be linked to low dissolution rates (calculated *ca*. 2.5 %).

Dissolution of ZnO NPs is known as highly influenced by agglomeration, which tends to occur particularly in real waters and more generally under increasing ionic strength conditions [56, 199]. Data from DLS and UV-vis analyses confirmed NP agglomeration in AW (*e.g*. higher z-average, higher absolute zeta potential, and loss of absorbance spectrum). Consequently, the different fate of ZnO NM-110 NPs leading to dissolution in LB and aggregation in AW, which governed their ion based antibacterial activity, is likely to be supported by the higher ionic strength of AW compared to LB.

There is no existing data with ZnO NPs or related ions on *P. putida* BS566 *lux*. Gajjar *et al*. (2009) [219] discussed impacts of ZnO NPs *ca*. 10 mg $L^{-1}$ on a modified *P. putida* KT2440 and *ca*. 1 mg $L^{-1}$ or below for the ionic counterparts. Interestingly, they reported major hormesis effects and described ZnO NPs (and related ions) as bacteriostatic agents as never leading to the complete loss in culturability of the tested *P. putida*. Herein, hormesis effects were rarely observed however the discussed transient toxicity patterns of ZnO NPs (and related ions) may corroborate the bacteriostatic results described by those authors. Their model being more susceptible to toxicants than ours, they potentially suffered from exacerbated hormesis patterns compared to *P. putida* BS566 *lux*. The Zn ion toxicity on other bacteria species is otherwise reported in the range of 10 - 100 mg $L^{-1}$ in laboratory media depending on NP type and size, matrix of exposure and method of assessment [43, 99, 168, 188, 199, 207, 237]. Considering here a dissolution rate of 40 % and $IC_{50}$ values between 60 and 100 mg $L^{-1}$ in LB, an ion based $IC_{50}$ around 25 - 40 mg $L^{-1}$ might be estimated. Our own assays with Zn ions (applied as zinc sulphate) led to transient toxicity (with $IC_{50}$ values evolving from about 50 to 70 mg $L^{-1}$) during the first hour of exposure in LB and to no toxicity in AW.

Consequently, the observed ZnO NM-110 toxicity to *P. putida* BS566 *lux* is likely to be driven by the released Zn ions. The transient toxicity in LB and the absence of toxicity in

AW may be associated with readily occurring Zn ion complexation (with anions such as $SO_4^{2-}$, $Cl^-$ and $PO_4^{3-}$) and/or precipitation, in addition to, Zn NP aggregation/precipitation in the different matrices as discussed elsewhere [107, 168, 199].

#### 3.4.1.4 Toxicity of $TiO_2$ NPs to *P. putida* BS566 *lux*

Results indicated similar and non-detectable toxicity despite non-comparable NP fates in both matrices for $TiO_2$ NM-104 NPs. $TiO_2$ NPs are however widely described to be toxic at very high doses (up to the g $L^{-1}$) by the triggering of cellular oxidative stress pathways *via* their catalytic properties especially after photo-activation rather than by any ion based mechanisms [56, 98, 168, 200, 207]. Non-detectable toxicity of $TiO_2$ NM-104 here might be therefore mainly explained by the concentrations used (up to 200 mg $L^{-1}$) and the absence of photo-activation of materials. However, increasing concentrations or pre-activating materials, even if leading to monitorable toxicities, would not have been more relevant thus was not explored. A $TiO_2$ dose-dependent increase in the output signal could be discussed, however as this occurs similarly from the first time point in both matrices this is likely to be associated with the intrinsic optical properties of $TiO_2$ (rutile form especially) to scatter and reflect light, as discussed elsewhere [409]. This was confirmed with experiments using a luciferase based reaction with increasing concentrations of $TiO_2$ NM-104 (without bioreporters) as well as commonly reported in the laboratory by scientists working with chlorophyll based outputs with other model microorganisms (testing the same NPs).

Once again here, there is no existing data with $TiO_2$ NPs on *P. putida* BS566 *lux*. Picado *et al*. (2015) [113] recently reported toxicity of $TiO_2$ NPs (Aeroxide® P25, primary size 21 nm) on several models from different trophic levels including a *P. putida*; with $IC_{50}$ values *ca*. 10 mg $L^{-1}$ after 16 h of exposure. However, due to the methodology used (ISO 10712:1995 which describes itself as non-suitable with colour samples and undissolved substances, as $TiO_2$ NPs may be) the direct comparison seems inappropriate. Nonetheless here, not observing evident patterns *via* the *P. putida* BS566 *lux* bioreporter does not necessarily mean there was no stress based pathways triggered inside the cells. It does mean, however, this bioreporter (as all bioreporters) presented limitations when used on its own.

#### 3.4.1.5 Toxicity of CuO NPs (and ions) to *P. putida* BS566 *lux*

Originally isolated from a coke rich WWTP the BS566 strain may have developed resistance to some metals (personal communication with Emeritus Prof Nick Christofi), such as for Cu. Besides, other *P. putida* such as KT2440 or W619 (which are fully sequenced) are known to bear Cu resistance genes in their genome [410]. It is therefore plausible that *P. putida* BS566 carries expressible Cu resistance genes although this is not yet reported for this strain; eventually promoting its resilience to Cu as shown here. In light of this, the behaviour of the tested CuO NPs *per se*, shown to be variable between LB and AW matrices, is finally of little importance here as essentially none of the two tested copper salts did lead to a toxicity pattern. There is no existing data with CuO NPs on *P. putida* BS566 *lux*. Interestingly, Gajjar *et al*. (2009) [219] reported CuO NPs toxicity on their modified KT2440 model without mentioning any possible resistance to Cu; emphasising that presence of a specific genetic material (*e.g*. resistance genes) is not synonym of expression.

### 3.4.2 Pristine NPs in real matrices

#### 3.4.2.1 The big picture

The toxicity of Ag NPs is commonly attributed to the released ions [31, 47]. $IC_{50}$ values at 1 h of exposure close to 5 mg $L^{-1}$ for pristine Ag NM-300K NPs and 0.4 mg $L^{-1}$ for Ag ions in AW simulating effluent using *P. putida* BS566 *lux* were previously discussed (§ 3.4.1). The toxicity of Ag NM-300K NPs was shown to be mainly driven by the released ions, corroborating previous literature [407]. The further results (*i.e*. $IC_{50}$ values at 1 h) obtained in FWs between 6 and 9 mg $L^{-1}$ appear most of all directly comparable to those already discussed in AW using the same method and material; they are consequently likely to be explained by the same impact of the released Ag ions.

The pristine Ag NPs were less toxic in CW than FW, with $IC_{50}$ values at 1 h of exposure up to *ca*. 50 mg $L^{-1}$. This was associated with higher BOD, COD, TSS, total plate count, ammonia, chloride, sulphide loadings in CWs, attesting overall to the higher "complexity" of CWs compared to FWs. The dynamics of impact (*i.e*. kinetics) of these multiple

parameters onto the NPs remains uncertain here, even if increasing concentrations of BOD, COD, chloride and sulphide have already been shown (independently) to diminish the antimicrobial properties of Ag NPs *via* especially aggregation/agglomeration and complexation phenomena. No evident aggregation of the freshly added NPs to the wastewaters was visible by UV-vis. No different dissolution rates of pristine NPs were evaluated in both matrices. However, significantly different hydrodynamic size and zeta potential values were measured in CWs compared to results in FWs, attesting to matrix driven effects on the NPs (*i.e*. complexation) in CWs. Aggregated (*i.e*. complexed) NPs have been shown to display lower ion release and diminished bioavailability in complex matrices [51, 68, 411]. Ions themselves were shown to be susceptible to complexation in wastewaters [32, 412]. Altogether, the reported data therefore support the hypothesis that aggregation/agglomeration and complexation of Ag NPs and related ions led to attenuated toxicity of Ag NM-300K to *P. putida* bioreporter in the most complex matrices, the CWs.

The acute toxicity (*i.e*. $IC_{50}$ values) of pristine Ag NPs to bacteria was reported in the mg $L^{-1}$ range in laboratory media [31, 99]. Comparatively, similar and attenuated toxicity of Ag NM-300K NPs were therefore reported here in FWs and CWs. Interestingly, both the microbial resilience [338, 413] and sensitivity [308, 414] were reported before in influent wastewaters testing Ag NPs, respectively below and above 5 mg $L^{-1}$. The present work therefore further supports those previous studies.

Consequently, whilst demonstrating the workability of the proposed method for performing acute testing in real wastewaters the work highlights further the importance of the nature of the matrix of exposure.

#### 3.4.2.2 CWs versus FWs characteristics

The behaviour of Ag NPs has already been shown to be influenced by pH, ionic strength, salinity and presence of chloride or sulphide when studied separately in artificial conditions [49, 57, 412, 415]. Considering FWs and CWs collectively (*i.e*. regardless of the site); *ca*. 75 % of the observed variability was explained by the performed multivariate analysis (*i.e*. based on a canonical correlation using key wastewater parameters constrained by the

calculated $IC_{50}$ of spiked NPs). This would therefore point to synergistic effects from the matrix characteristics on the eventual Ag NP toxicity displayed.

On a wastewater type basis, the direct influence of the site or of key physico-chemical parameters to the eventual Ag NP toxicity cannot be drawn. One may incriminate the dose metric (up to 200 mg $L^{-1}$) which possibly exhausted the available sulphide and chloride limiting their potential impact. However, Kaegi *et al*. (2013) [416] demonstrated that Ag NPs were only sulfidised at 15 % within 5 h in wastewaters, as also proposed elsewhere [411]. In addition, the sulphidisation of Ag NPs was shown limited due to oxic conditions [417]. Consequently, in the absence of ageing the actual impact of such sulphidisation is uncertain here when considering data registered after only 1 h of exposure under oxic conditions. Meanwhile, although differences were evident between samples from the different sites they were probably too low overall to obtain conclusive assessment of the direct effects of matrix parameters, even synergistically. Studies in the literature discussing such aspects (*i.e*. separately) have generally deployed concentrations or conditions which ranged several orders of magnitude therefore exacerbating, potentially, the effects observed when compared to conditions offered by real samples [49, 57, 412, 415]. Finally, the dispersant in which Ag NM-300K NPs are prepared may further enhance their stability [136, 142], and therefore decrease (*i.e*. in some degrees) their susceptibility to environmental variations such as proposed by the tested FW and CW matrices.

Consequently, the above emphasised further the intricate physico-chemical parameters involved in determining NP toxicity considering the intrinsic properties of both the matrices and the NPs.

### 3.4.3 Aged NPs in AW, CWs and FWs

The ageing impact in wastewaters on the eventual antibacterial properties of Ag NM-300K NPs was also reported. Interestingly, Ag NPs showed consistent toxicity patterns in FWs despite ageing. Comparable behaviours were obtained in AW. In both cases, this was related to steady hydrodynamic sizes and dissolution rates. Conversely in CWs, the increase in hydrodynamic size and zeta potential as well as the loss of typical spectra of absorbance

and the decrease in dissolution (*i.e.* traducing exacerbated aggregation and complexation phenomena), then eventually in NP toxicity, were characterised with ageing.

Although reports on the speciation of Ag NPs are abundant [56, 412, 416, 418-420], very little information exists on actual toxicity of aged Ag NPs, especially in real matrices. Ag NPs discharged to the wastewater stream were shown to be sulphidised to varying degrees and to be largely aggregated with biomass and biosolids, potentially reducing there toxicity [56, 411, 416, 418-421]. Here, the toxicity based results reported in CWs with aged Ag NPs further corroborate these recent reports. However, our results in FWs suggest that attention should be given to impact of Ag NPs on environments downstream of WWTPs, especially as NPs have been already shown capable of escaping WWTPs [239].

Consequently, whilst piloting ageing based assays we highlighted the divergent fate of the patterns of toxicity of Ag NPs in CWs and FWs (despite "conservative" conditions of ageing).

# CHAPTER 4: Results - Biofilm based assays

Biofilms are self-produced matrix enclosed mono or multi-species microbial communities that adhere to biological or non-biological interfaces [77] generally referred to as the main living form of bacteria in the environment [422]. Structurally organized, dynamic and complex ubiquitous biological systems, biofilms have in addition essential beneficial implications (*e.g*. facilitators within the natural environment or in the treatment of wastewaters) [77, 422]. Consequently, biofilm based assays represent a desirable source of information in nanoecotoxicology (§ 1.1.4.2.1). Despite their relevance, only a handful of nanoecotoxicological studies has been carried out using biofilms to date (§ 1.1.4.2.3). Assays performed under hydrodynamic conditions specifically (*i.e*. leading to fully hydrated, planktonic free and mature structures compared to the static approaches) are gradually emerging using diverse rotating biological contactor and reactors [288, 294, 297, 314]. Unlike most reactors, the flow-cell systems present the additional advantages of real time, non-invasive and non-destructive versatile studies [362, 363]. Consequently, a high potential of assay development is associated with the use of flow-cell reactors (§ 1.1.5.2). Applications of flow-cell reactors were reported in ecotoxicology for the testing of silver sulfphadiazine and solvent styrene on *Pseudomonas* spp. biofilms [368, 369]. Examples in nanoecotoxicology are particularly scarce at the present time with the sole contribution being the study by Fabrega *et al*. (2009) [314] where the interactions between Ag NPs and *P. putida* biofilms were investigated (*e.g*. accumulation and uptake of NPs).

Consequently, the present work builds on these pioneer examples [314, 368, 369] and aims to assess the temporal impact following a single pulse of NPs on non-static mono and multi-species biofilm morphology, viability and activity in AW using flow-cell reactors. *P. putida* BS566 *lux* is used for establishing the mono-species biofilms since *P. putida* are commonly proposed as an environmental bacterial model, are already reported in studies using flow-cell reactors [314, 368, 369], and are used in the planktonic based assays previously reported here (Chapter 3). Multi-species biofilms are established from real crude wastewater samples. In both cases, silver (Ag NPs and ions) is prioritised given that it is a well-known bactericidal agent [265], one of the most widely used NPs [15], and the sole having shown toxicity to *P. putida* in AW using planktonic based assays (§ 3.1).

## 4.1 *P. putida* based mono-species biofilms

The study was articulated around an original scenario of culture (for 48 h), exposure (for 24 h) and recovery (for 24 h) assessment (as detailed in the *Material and Methods,*§ 2.2.3.3), extending the pioneer study proposed by Fabrega *et al*. (2009) [314].

### 4.1.1 The *P. putida* control biofilms at 48 h

Representative examples of CLSM z-stack registered *ante* exposure to Ag NPs are presented in Fig. 4.1 (top row).

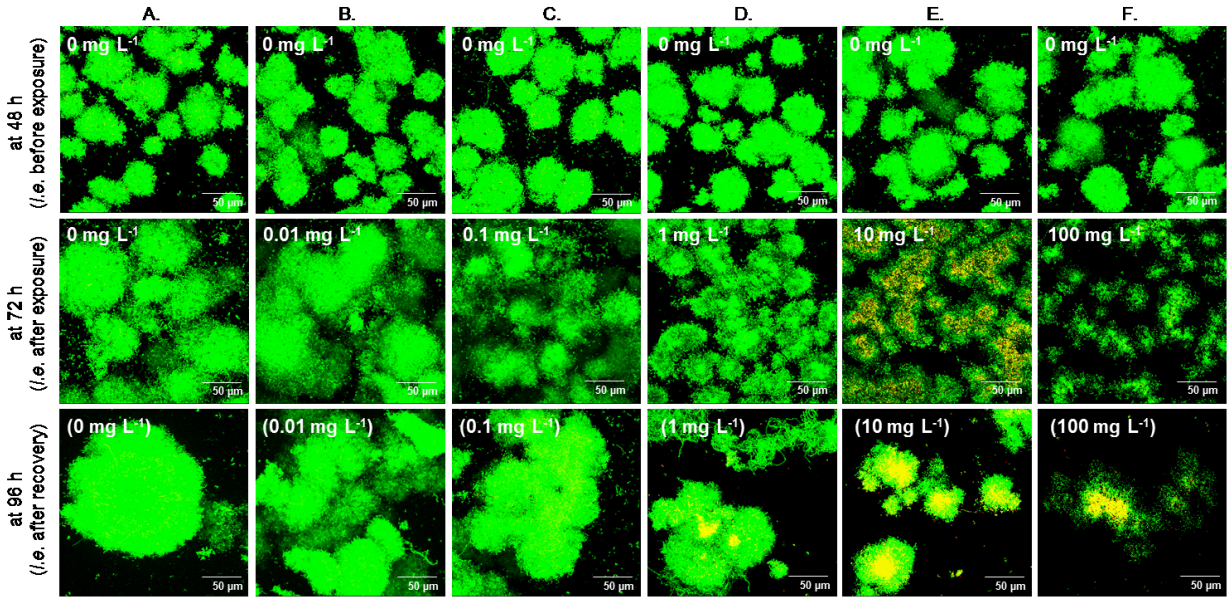


**Fig. 4.1: Qualitative characterisation of the biofilm morphology *ante* and *post* exposure to the Ag NPs.** *P. putida* biofilms were cultured for 48 h then exposed to Ag NPs at 0, 0.01, 0.1, 1, 10 and 100 mg $L^{-1}$ for 24 h (from A to F, respectively). Biofilms were analysed by CLSM after live (green) / dead (red) staining at 48 h (*i.e. ante* exposure, top row), 72 h (*i.e. post* exposure, middle row), and 96 h (*i.e.* 24 h *post* exposure, bottom row). Representative examples of maximised z-stack are shown above. Each image represents 1 out of 7 z-stacks randomly registered *per* condition for 1 experiment. Scale is 50 µm wide.

*P. putida* BS566 formed distinct and consistent microcolonies in D-glucose supplemented AW medium across channels. This was confirmed across experiments as well *via* the morphology related information obtained by the COMSTAT based analysis. Control biofilms at 48 h (considering 210 z-stacks in total, n = 5) were consistently characterised by

comparable biomass, maximum thickness, mean thickness, roughness and surface area of: 27.5 ± 2.6 $\mu m^3$ $\mu m^{-2}$, 94.4 ± 3 μm, 50.2 ± 2.8 μm, 0.48 ± 0.01 and 3.2 ± 0.1 $10^6$ $\mu m^2$ respectively. No red staining (*i.e*. dead cells) was observed. From a microbial activity standpoint (Fig. 4.2), *ca*. 70 % of the original D-glucose loading was consistently found in the effluents across channels and experiments.

4.1.2 The *P. putida* exposed biofilms at 72 h

Representative examples of CLSM z-stack registered at 72 h, *post* exposure to a single pulse of Ag NPs at 0, 0.01, 0.1, 1, 10 and 100 mg $L^{-1}$ for 24 h, are presented in Fig. 4.1 (middle row). Additional examples are provided in Appendix D (Fig. S4.1).

From a morphological viewpoint, larger and less discrete microcolonies were observed at 72 h than at 48 h for the control (Fig. 4.1, column A). Biofilms exposed to the Ag NPs at 0.01 mg $L^{-1}$ showed comparable development overall (Fig. 4.1, column B). However the biofilm development was visibly altered at 0.1 mg $L^{-1}$; dose dependent impacts of the Ag NPs were then observed with, finally, sparsely distributed residues of microcolonies characterised at 100 mg $L^{-1}$ (Fig. 4.1, columns C - E). Red staining was obtained (in 3 out of 5 experiments) at 10 mg $L^{-1}$ exclusively. The corresponding quantitative information from the COMSTAT analysis is shown in Fig. 4.3.

Overall results confirmed the dose dependent impact of the Ag NPs on biofilm morphology following a 24 h pulse. The trend was characterised by a decrease in total biomass, thickness, surface area and an increase in roughness with increasing concentrations of NPs. More specifically, non-exposed biofilms gained 56.8 ± 8.25 % of biomass in 24 h; meanwhile the 0.01 mg $L^{-1}$ exposed biofilms gained significantly less (26.75 ± 10.7 %) (*i.e*. determined *via* multiple t-tests using the Holm-Sidak method, reporting significance with $p$ value < 0.05). The altered evolution of both the roughness and the surface area related information was also observed at 0.01 mg $L^{-1}$ compared to the non-exposed biofilms. Impact on thickness was not evident at 0.01 mg $L^{-1}$ though. Comparatively at 0.1 mg $L^{-1}$ Ag NPs, evident impacts on biomass, roughness, surface area and mean thickness were observed compared to the control; according to the COMSTAT results *post* exposure biofilms were rather similar to biofilms characterised *ante* exposure. Concentrations of 1,

10 and 100 mg $L^{-1}$ led to consistent dose dependent results with detrimental effects at 100 mg $L^{-1}$ resulting in *ca*. 75 % of the biomass and *ca*. 50 % of the thickness and surface area being lost when compared to the respective biofilm characteristics before exposure. Similarly, the roughness was increased by more than 200 % whereas non-exposed biofilms had there roughness decreased by *ca*. 50 % for the same 24 h period.

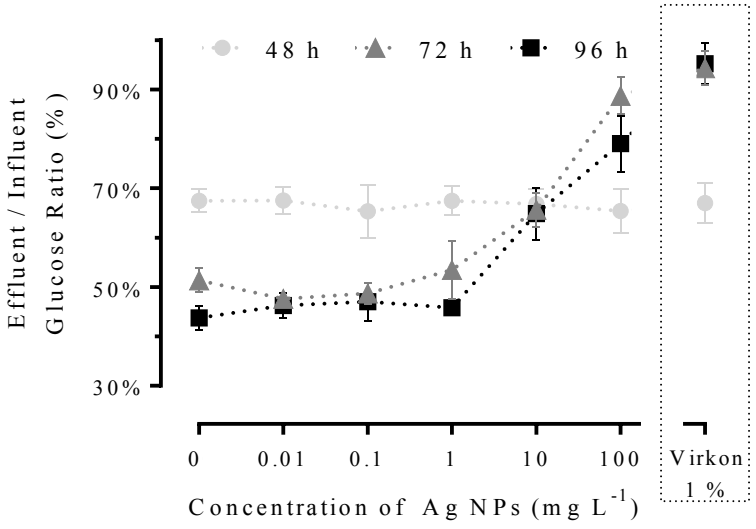


**Fig. 4.2: Quantitative characterisation of microbial activity (the Ag NP case).** Samples collected upstream (*i.e.* in influents) and downstream (*i.e.* in effluents) of the flow-cells at 48, 72 and 96 h were used for D-glucose quantification *via* the phenol - sulphuric acid assay. Presented data are mean ± SEM (n = 4) of the calculated D-glucose ratios between samples *per* condition. The detailed findings from the statistical analysis *via* multiple t-tests (corrected with the Holm-Sidak method) considering two parameters at a time are shown in Appendix D (Fig. S4.2).

Regarding the microbial activity, comparable amounts of D-glucose (*ca*. 50 % of the original loading) were found in effluents at 72 h *post* exposure to 0, 0.01 and 0.1 mg $L^{-1}$ Ag NPs (Fig. 4.2). Results were found significantly different (*i.e.* lower D-glucose ratios, increased activity) compared to results at 48 h ($p < 0.1$). Percentages of remaining D-glucose between 90 and 100 % were obtained *post* exposure to the Ag NPs at 100 mg $L^{-1}$ and Virkon® 1 %; results which were found significantly different from data at 48 h with the same channels ($p < 0.05$) and from data at 72 h with the other channels ($p < 0.05$). Results obtained *post* exposure to 10 mg $L^{-1}$ (*ca*. 70 % of the original loading) were not

significantly different ($p = 0.8$) to those obtained at 48 h. The intermediate concentration of 1 mg $L^{-1}$ showed the largest SEM of the 72 h data with D-glucose ratios varying between 45 % and 60 %; results which were found significantly different from data at 48 h ($p < 0.05$) but not from 0.1 mg $L^{-1}$ and 10 mg $L^{-1}$ related data at 72 h.

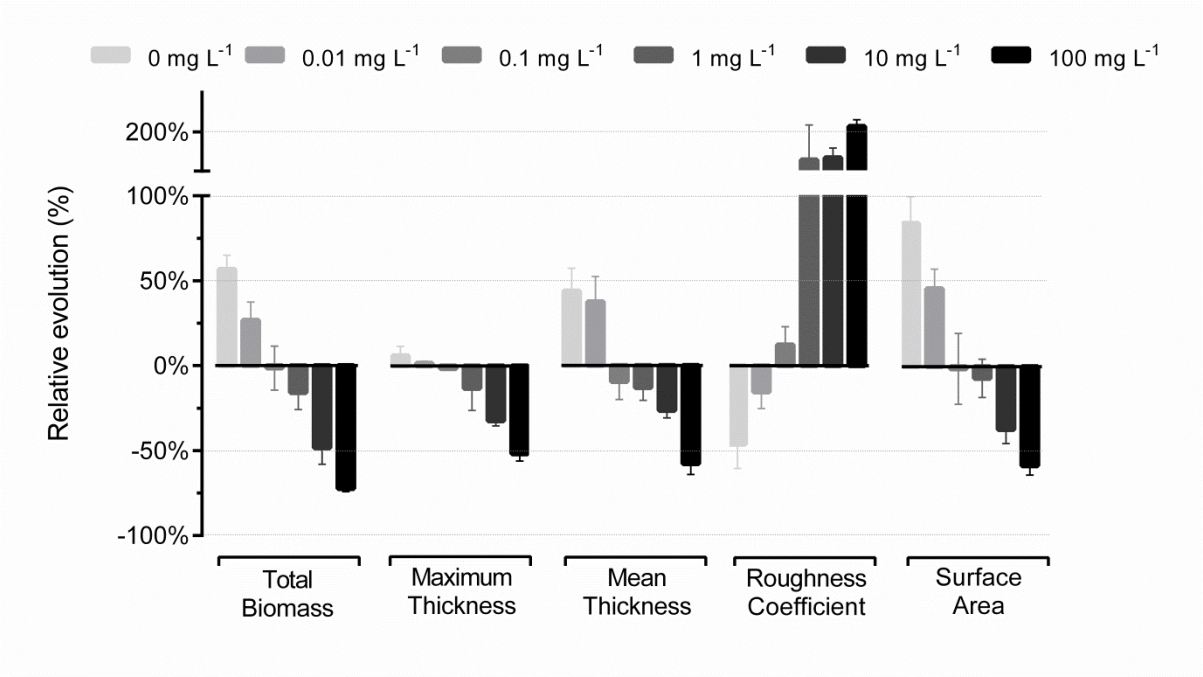


**Fig. 4.3: Quantitative characterisation of the biofilm morphology *post* exposure to the Ag NPs.** Histogram of the relative evolution (in % terms) of the descriptive biofilms parameters (*e.g.* total biomass, maximum thickness, mean thickness, roughness and surface area) *post* exposure for 24 h to the Ag NPs at 0, 0.01, 0.1, 1, 10 and 100 mg $L^{-1}$ is presented. Data, calculated *per* channel as (results at 72 h - results at 48 h) / (results at 48 h) after the COMSTAT analysis of the registered z-stacks, are mean ± SEM (n = 5). For each experiment 7 z-stacks were analysed *per* channel (*i.e*. *per* condition) at both time points.

Parallel experiments were performed with the Ag ions tested at 0, 0.001, 0.01, 0.1, 1 and 10 mg $L^{-1}$ (n = 3). Comparable dose dependent toxicity patterns were observed overall on morphology (Fig. 4.4) and activity (Fig. 4.5) but shifted by at least one order of magnitude, the Ag ions being more toxic than the tested Ag NPs. Red staining (*i.e*. dead cells) occurred consistently after exposure to 1 and 10 mg $L^{-1}$.

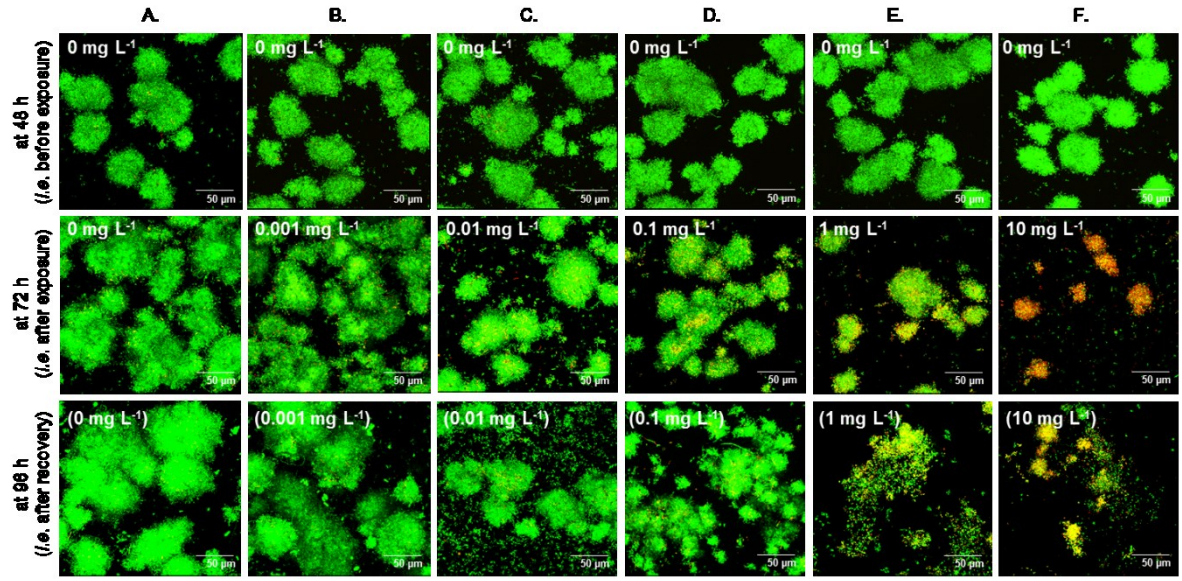


**Fig. 4.4: Biofilm morphology characterisation *ante* and *post* exposure to the Ag ions.** *P. putida* biofilms were cultured for 48 h then exposed to Ag ions (using $AgNO_3$ salts) at 0, 0.001, 0.01, 0.1, 1 and 10 mg $L^{-1}$ for 24 h (from A to F, respectively). Biofilms were analysed by CLSM after live (green) / dead (red) staining at 48 h (*i.e. ante* exposure, top row), 72 h (*i.e. post* exposure, middle row) and 96 h (*i.e.* 24 h *post* exposure, bottom row). Representative examples of maximised z-stack are shown. Each image represents 1 out of 7 z-stacks randomly registered *per* condition for 1 experiment (n = 3). Scale is 50 µm wide.

No biofilms were visible at 72 h after exposure to Virkon® 1 % as a positive control (data not shown). Exposure to the Ag NM-300K NP dispersant only has already been shown not to be toxic *per se* to *P. putida*.

### 4.1.3 The *P. putida* recovering biofilms at 96 h

Biofilms were left to recover for 24 h in AW medium *post* exposure. Examples of characteristic CLSM z-stack registered at 96 h for selected conditions (Ag NPs at 0, 0.01, 1 and 100 mg $L^{-1}$) along with the relative evolution (in % terms) of selected descriptive parameters (total biomass and mean thickness) are presented in Fig. 4.6. Additional examples of CLSM result at 96 h from replicated experiments are proposed in Fig. 4.1 (bottom row) and in Appendix D (Fig. S4.3).

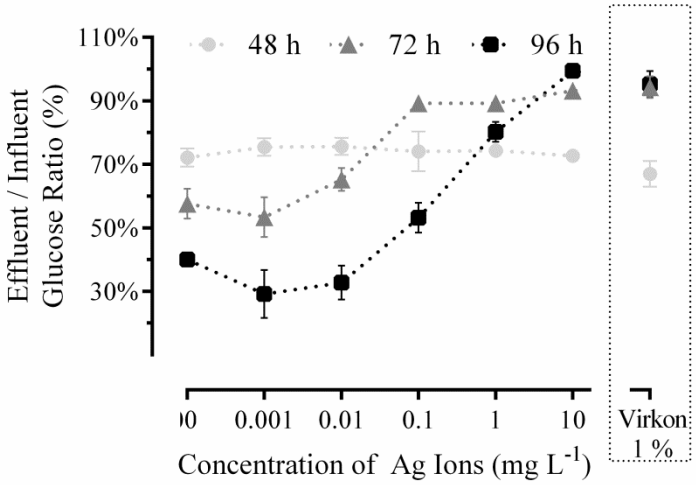


**Fig. 4.5: Quantitative characterisation of microbial activity (the Ag ion case).** Samples collected upstream (*i.e.* in influents) and downstream (*i.e.* in effluents) of the flow-cells at 48, 72 and 96 h were used for D-glucose quantification *via* the phenol - sulphuric acid assay. Presented data are mean ± SEM (n = 3) of the calculated D-glucose ratios between samples *per* condition. The detailed findings from the statistical analysis *via* multiple t-tests (corrected with the Holm-Sidak method) considering two parameters at a time are shown in Appendix D (Fig. S4.2).

From a morphological viewpoint, the non-exposed biofilms (Fig. 4.6, column A) were found to have developed, gaining more than 15 % in biomass and 6 % in mean thickness compared to results at 72 h. Comparatively, the exposed biofilms showed various patterns at 96 h as they were clearly recovering at 0.01 mg $L^{-1}$ Ag NPs (+23.3 ± 8.4 % in biomass and +35.5 ± 11.7 % in mean thickness, no dual staining; Fig. 4.6, column B) and hardly surviving at 100 mg $L^{-1}$ Ag NPs (+6.8 ± 3.8 % in biomass and -1.6 ± 20.9 % in mean thickness, dual staining; Fig. 4.6, column D). Very variable results across experiments were obtained at 1 mg $L^{-1}$ with evolutions in biomass and mean thickness up to +50 % and +20 % or down to -10 % and 0 %, respectively (Fig. 4.6, column C). Dual staining as well as possibly re-structuring microcolonies (*i.e.* presence of filaments) were also reported at 1 mg $L^{-1}$ Ag NPs. Tested 0.1 and 10 mg $L^{-1}$ concentrations led to similar dose dependent results (Appendix D, Fig. S4.4).

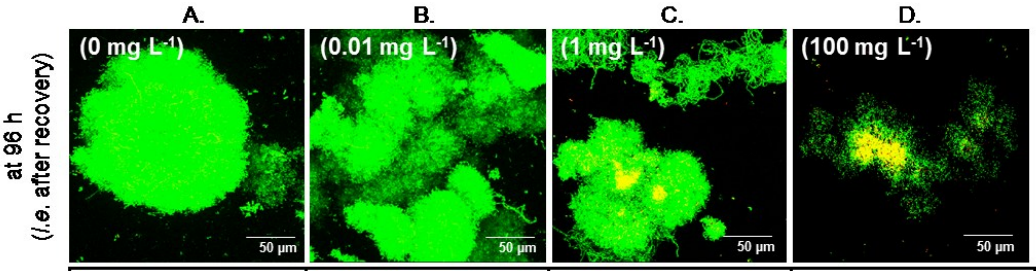


| | | | | |
|---|---|---|---|---|
| + 16.5 ± 1.2 % | + 23.3 ± 8.4 % | + 22.9 ± 30.0 % | + 6.8 ± 3.8 % | Total Biomass ($\mu m^3$ $\mu m^{-2}$) |
| + 6.1 ± 4 % | + 35.4 ± 11.7 % | + 9.7 ± 9.5 % | - 1.6 ± 20.9 % | Mean Thickness (µm) |

**Fig. 4.6: Biofilm morphology recovery assessment.** Representative examples of maximised z-stack registered at 96 h following the recovery period after exposure to 0 mg $L^{-1}$ (A), 0.01 mg $L^{-1}$ (B), 1 mg $L^{-1}$ (C) and 100 mg $L^{-1}$ (D) Ag NPs are shown. Each image represents 1 out of 7 z-stacks registered *per* condition for 1 experiment. Results following other tested concentrations of Ag NPs (0.1 and 10 mg $L^{-1}$) as well as additional examples of result for replicated experiments (n = 3) are presented in Appendix D (Fig. S4.4). Scale is 50 µm wide. The corresponding relative evolution (in % terms) in total biomass and mean thickness calculated between time points of 72 h and 96 h is also presented.

Regarding the microbial activity (Fig. 4.2), comparable D-glucose ratios close to 45 % were observed at 96 h from 0 mg $L^{-1}$ to 1 mg $L^{-1}$ tested NP concentrations. Significantly higher ratios *ca.* 70 % and 80 % (*i.e.* decreased microbial activity) were obtained for 10 and 100 mg $L^{-1}$ Ag NPs ($p < 0.05$). Overall results at 96 h were not found to be significantly different compared to ratios calculated at 72 h (Appendix D, Fig. S4.2) but they were found to be significantly different (up to 1 mg $L^{-1}$) compared to results obtained at 48 h ($p < 0.05$).

Experiments with Ag ions at 0, 0.001, 0.01, 0.1, 1 and 10 mg $L^{-1}$ led to more efficient recovery patterns (n = 3) (Fig. 4.4, bottom row; Fig. 4.5). Overall results at 96 h were found to be significantly different (up to 1 mg $L^{-1}$) from the ratios calculated at 72 h (Appendix D, Fig. S4.2). No biofilms were visible at 96 h *post* exposure to Virkon® 1 % (data not shown); D-glucose ratios were found consistently *ca*. 95 % of the original loading (Fig. 4.2).

4.1.4 Characterisation of Ag NPs within the experimental scenario

Ag NPs were characterised by DLS and UV-Vis after sampling upstream (*i.e.* in influents) and downstream (*i.e.* in effluents) of the flow-cells at 48, 72 and 96 h.

As shown in Fig. 4.7 A, UV-Vis spectra of the Ag NPs, characterised by a sole peak *ca.* 413 nm (0.9 a.u.), were comparable at the beginning and at the end of the 24 h exposure period upstream of the flow-cells. In the downstream samples: no peak was observed at 48 h, non-comparable profiles characterised by a sole peak *ca*. 415 nm (0.4 a.u.) were then obtained at 72 h. No specific peak was registered at 96 h regardless of the sample.

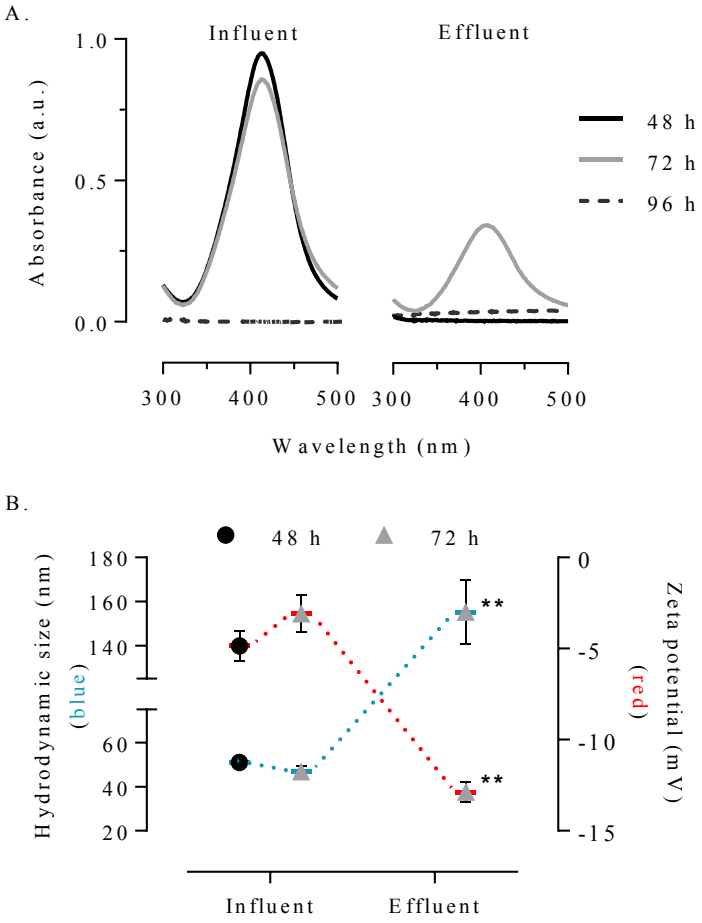


**Fig. 4.7: Ag NP characterisation.** Samples were collected upstream (*i.e.* in influents) and downstream (*i.e.* in effluents) of the flow-cells at 48, 72 and 96 h then characterised by DLS (A) and UV-Vis (B) when applicable. Data are mean ± SEM (n = 3) when tested at 10 mg $L^{-1}$ Ag NPs. Significantly different between samples *via* multiple t-tests corrected with Holm-Sidak with a *p* value < 0.05 (**).

As shown in Fig. 4.7 B, comparable hydrodynamic size and zeta potential data were obtained by DLS at both 48 and 72 h in upstream samples: 51 ± 1.4 nm and -4.8 ± 0.8 mV, 46.7 ± 2.8 nm and -3.1 ± 1 mV, respectively. In the downstream samples, hydrodynamic size and zeta potential results of 155.2 ± 14.6 nm and -12.9 ± 0.5 mV were respectively obtained at 72 h; 48 h samples were not suitable for DLS analysis (*i.e.* due to the absence of NPs). Results at 72 h were found to be significantly different between both types of sample. Mean polydispersity index (PDI) was 0.46 ± 0.02. Samples from 96 h were not suitable for DLS analyses either.

Ag concentrations (*i.e.* 1, 10 and 100 mg $L^{-1}$) were confirmed by AAS in upstream samples at both 48 and 72 h. The respective concentrations in the downstream samples were 68.9 ± 4.6 %, 50.5 ± 9.9 % and 89 ± 7.3 % of the concentrations measured in upstream samples when tested at 72 h. The concentration of Ag was below the lower detection limit of the apparatus (*i.e.* < 0.1 mg $L^{-1}$) when tested at 96 h regardless of the sample.

### 4.1.5 Testing the potential impact of different carbon sources

The biofilm morphology has already been shown influenced by the C source and so might be the extracellular matrix which has already been proposed as protective barrier to toxicants [78, 82, 83, 423].

Consequently, in addition to the aforementioned assays using D-glucose as the sole carbon source, the *P. putida* mono-species biofilms were comparatively cultured in AW medium supplemented with D-fructose. Corresponding examples of CLSM z-stack registered *ante* and *post* exposure to a single pulse of Ag NPs or Ag ions at 1 mg $L^{-1}$ are presented in Fig. 4.8. Additional examples of results (n = 4) are presented in Appendix D (Fig. S4.5).

The morphological characteristics of the *P. putida* biofilms developed on D-glucose or D-fructose as well as their resilience to the Ag NPs or ions were overall found to be comparable (based on the qualitative assessment of images, Fig 4.8 and Appendix D Fig. S4.5). Further, no different outcomes were obtained using D-sucrose as a carbon source either (data not shown). As shown in Fig. 4.9, the utilisation of the carbon source was affected in both, a time dependent manner (*i.e.* due to the biofilm development), and a toxicant dependent manner (*i.e.* the Ag ions exhibiting a higher impact than the Ag NPs).

However, the overall pattern was not different between the three tested carbon sources (*e.g.* D-glucose, D-fructose and D-sucrose).

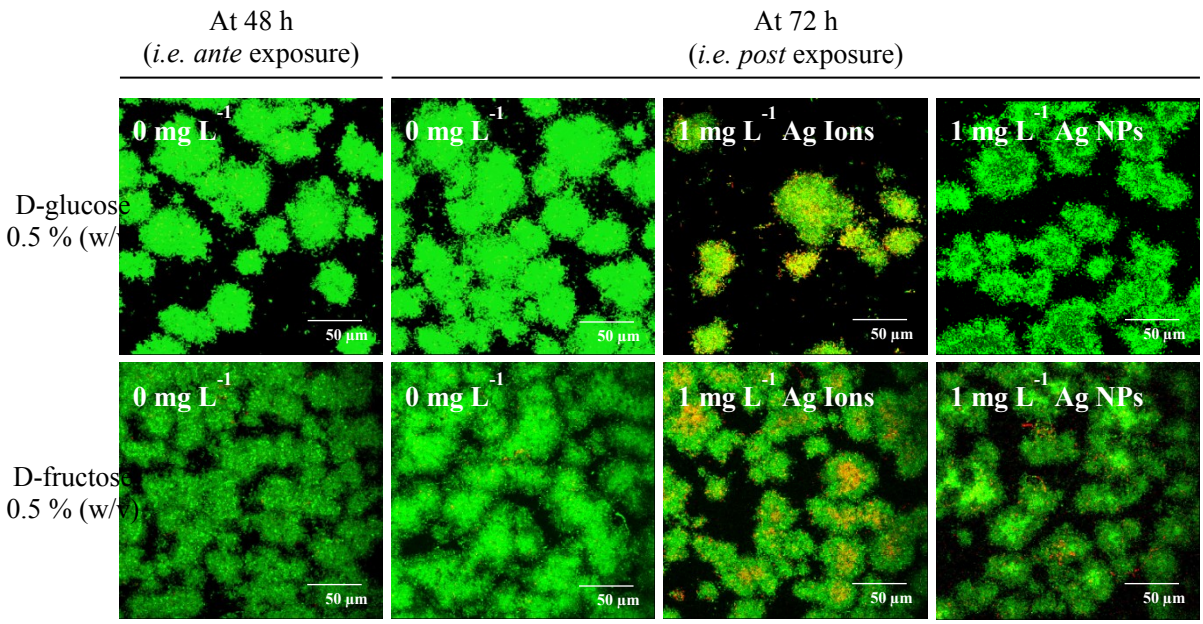


**Fig. 4.8: Impact of the carbon source.** *P. putida* mono-species biofilms were cultured for 48 h in D-glucose or D-fructose supplemented AW medium then exposed to 0 or 1 mg $L^{-1}$ Ag NPs and ions for 24 h. Biofilms were analysed by CLSM after live/dead staining at 48 h and at 72 h. Representative examples of maximised z-stack are shown. Each image represents 1 out of 7 z-stacks randomly registered *per* condition for 1 experiment. Scale is 50 µm wide.

Trials in characterising the potential differences in the biofilm extracellular polymeric matrix produced under the different conditions of culture using a ConA based fluorescent staining were not conclusive. As shown in Fig. 4.10 for D-glucose, no layer/matrix was apparent. In addition, signal overlaps between the live/dead (*i.e.* PI mainly) and the ConA stains were experienced (Fig. 4.10, arrows), however, no better outcomes were obtained using the ConA dye in higher concentration or on its own (*i.e.* without the live/dead dye). In the absence of clear impacts of the tested carbon sources and because the extracellular matrix based information were of little support, no further assays were undertaken with the mono-species biofilm format.

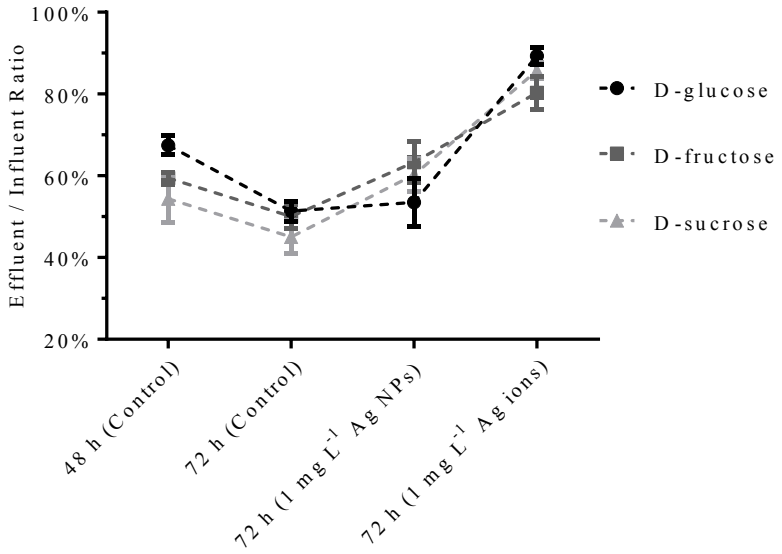


**Fig. 4.9: Utilisation of the carbon source.** Samples collected upstream and downstream of the flow-cells *ante* (at 48 h) and *post* (at 72 h) exposure to the Ag NPs or ions at 0 or 1 mg $L^{-1}$ were used for D-glucose, D-fructose and D-sucrose quantification *via* the phenol - sulphuric acid assay. Presented data are mean ± SEM (n = 3) of the calculated ratios between samples *per* condition.

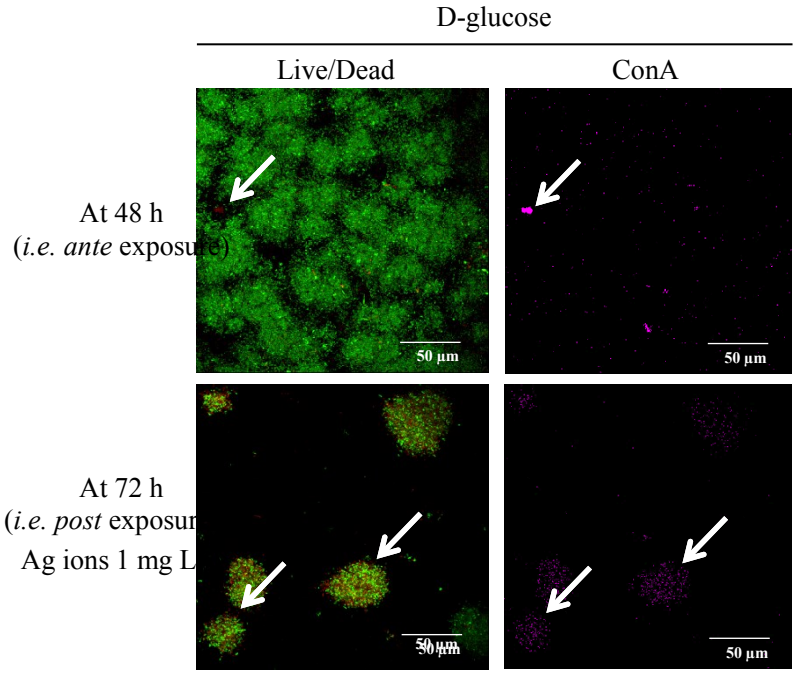


**Fig. 4.10: Visualisation of the biofilm extracellular polymeric matrix.** *P. putida* mono-species biofilms were cultured for 48 h in D-glucose supplemented AW medium before being exposed to the Ag NPs or ions for 24 h. Biofilms were analysed by CLSM after live/dead and ConA staining at 48 and at 72 h. Representative examples of maximised z-stack obtained with the Ag ions at 0 and 1 mg $L^{-1}$ are shown above. Arrows mark examples of signal overlap. Scale is 50 µm wide.

## 4.2 Multi-species biofilms

The *P. putida* BS566 *lux* used as a bioreporter in real wastewaters in the planktonic based assays (§ 3.2) and as model microorganisms for the mono-species biofilm based assays (§ 4.1) was originally isolated from a WWTP. The beneficial role of biofilms in the environment (*e.g.* treatment of wastewaters) is clear [76-78]. Consequently, the multi-species biofilm study was focused on the use of real wastewater samples (*i.e.* CW from site 3) as inoculum for the flow-cell reactors.

The study reports on the combined characterisations of the evolution of the biofilm morphology and produced extracellular matrix (using CLSM), of the established mix-community (using NGS), and of the microbial activity (monitoring the utilisation of key AW medium constituents such as C, N and P); assessing the global impact of both the Ag NPs and the Ag ions to multi-species biofilms under hydrodynamic conditions.

The pilot experiment was performed using a 12 channel based configuration (across four flow-cells) for which a template is shown in Appendix D (Table S4.1). The NGS was performed in collaboration with Warwick University (UK) thanks to the support of Prof Gary Bending and co-workers, especially Dr Sally Hilton who performed the NGS data analysis and proposed the following Fig. 4.15 and 4.16.

### 4.2.1 Morphological analysis

In line with the previous work on *P. putida*, the wastewater based multi-species biofilms were established in AW supplemented with D-glucose (0.05 %, w/v) for 48 h before being exposed to the Ag NPs (at 1 μg $L^{-1}$ and 1 mg $L^{-1}$) or the Ag ions (at 1 mg $L^{-1}$) for 24 h. The biofilm morphology was characterised using CLSM after simultaneous "Gram+/-" and "ConA" staining at 48 and 72 h. Examples of representative z-stack registered at both time points using the Gram+/- staining are shown in Fig. 4.11. The corresponding analysis of the biofilm biomass (or biovolume, as calculated using COMSTAT) along with the evolution of the Gram+/- ratio (in % terms) are shown in Fig. 4.12.

The multi-species biofilms rarely formed isolated microcolonies and were very heterogeneous in appearance. No clear recurrent structural patterns were found across

images. Whereas the control biofilms at 48 h were mainly composed by Gram- bacteria (green dye at more than 95 %, Fig. 4.11 and 4.12), the same non-exposed biofilms at 72 h showed more Gram+ bacteria comparatively (red dye *ca*. 40 %, Fig. 4.11 and 4.12). Consequently, while the overall biomass remained rather consistent and *ca*. 25$\mu m^3$ $\mu m^{-2}$, a clear modification of the microbial community occurred between 48 and 72 h in the absence of the toxicants.

Both a dose dependent effect (in the Ag NP case) and a material type effect (considering the Ag NPs versus the Ag ions) were suggested on the biofilm biomass evolution (Fig. 4.12). Impacts on the Gram+/- composition were also identified between the treated and non-treated biofilms at 72 h (Fig. 4.11 and 4.12).

Examples of representative z-stack registered at 48 h using the ConA staining are shown in Fig. 4.13. When compared to the Gram+/- staining it can be concluded that the registered signal under the ConA settings are not different from the red signal from the Gram+/- dye. Consequently, because of evident signal overlapping between PMTs, the extracellular matrix based dye was not more informative here than previously in the mono-species biofilm study.

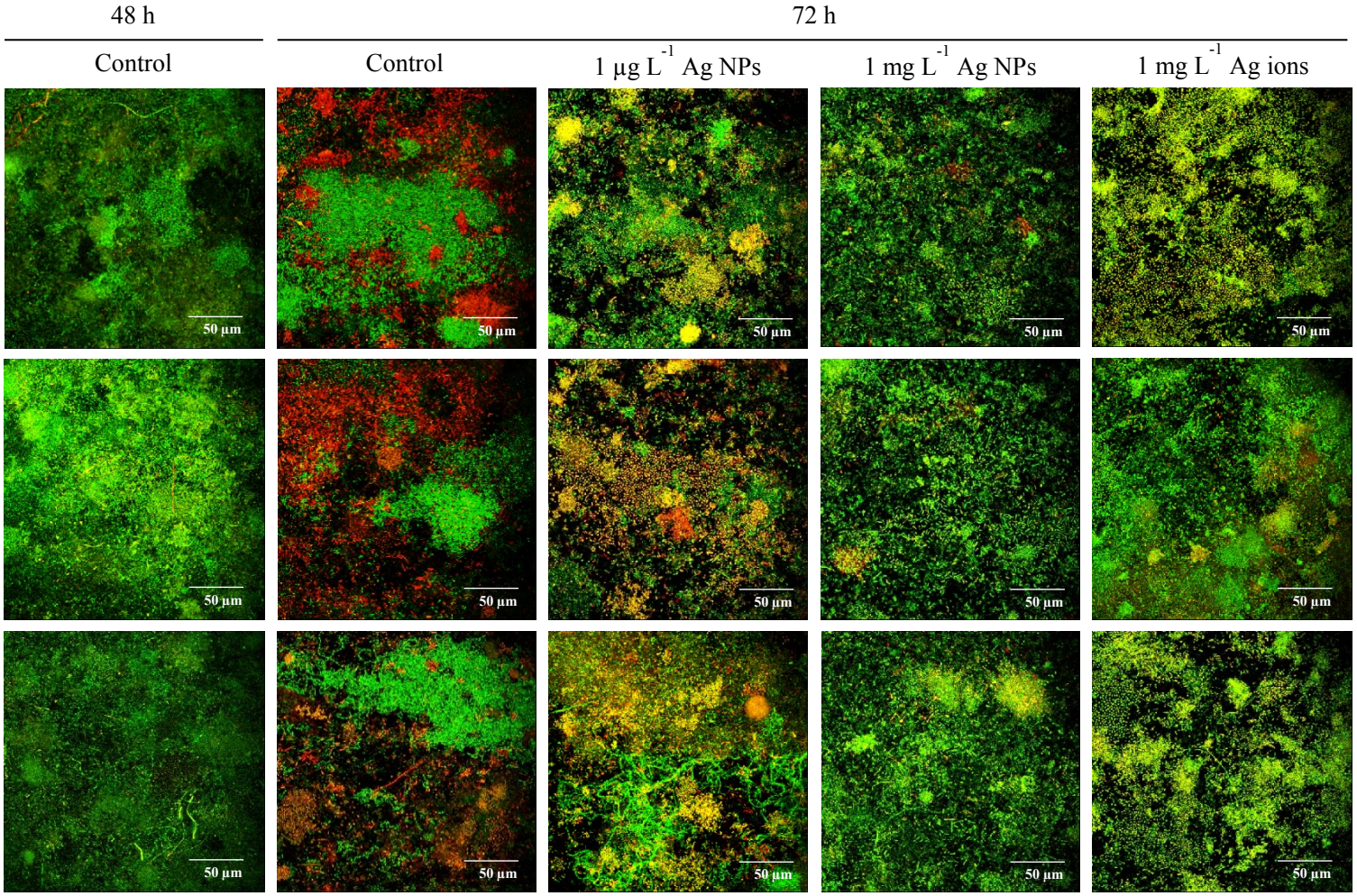


**Fig. 4.11**: **Multi-species biofilm morphology characterisation *ante* and *post* exposure to the Ag NPs and ions.** Representative replicated CLSM z-stacks obtained at 48 h (*i.e. ante* exposure) and at 72 h (*i.e. post* exposure to the Ag NPs at 1 µg $L^{-1}$ or 1 mg $L^{-1}$ and to the Ag ions at 1 mg $L^{-1}$) are shown. Biofilms were visualised using the Gram+/- dye (Gram+ in red, Gram- in green); CLSM settings were kept unchanged across analyses. Scale is 50 µm.

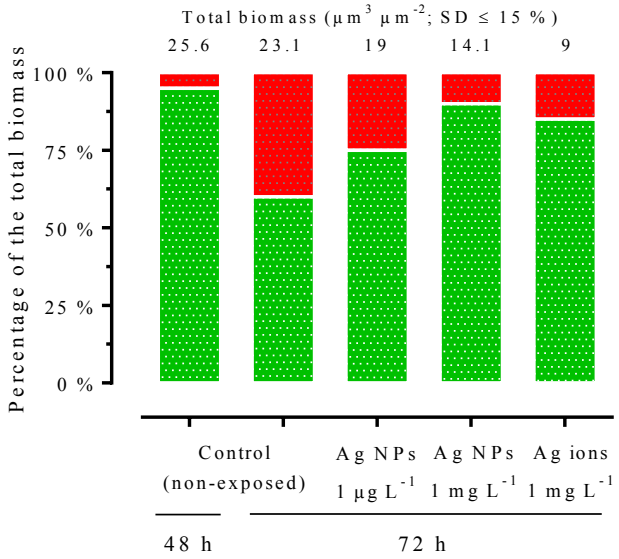


**Fig. 4.12: Quantitative assessment of the Gram+/- ratio evolution.** The histogram of the relative variation (in total biomass % terms) of the Gram+/- bacteria (Gram+ in red, Gram- in green) within the proposed scenario, as determined by COMSTAT analysis, is shown. Data are mean, SD < 15 %. For each condition, 7 z-stacks were analysed at 48 and 72 h.

### 4.2.2 Composition characterisation

Total gDNA of the biofilms was extracted in a kinetic manner accordingly to the template proposed in Appendix D (Table S4.1). DNA quality (*i.e.* as determined by spectrophotometry) *per* tested condition (from A to N) is also shown in Appendix D (Table S4.1). Two conditions (F and L) were excluded from the analysis as presenting unsatisfying quality ($Abs_{260/230}$ *ca.* 1.1). The extracted gDNA was sequenced by NGS using the 454 methodology. Six levels of OTU (Operational Taxonomic Unit) encompassing more than 17 000 sequences were obtained (hereafter referred to as L1 to L6, *i.e.* from the less to the most detailed level). The output results from the analysis at L1 are shown in Fig. 4.14.

The original wastewater sample used as inoculum was characterised by five main OTUs, namely Proteobacteria (65 %), Bacteroidetes (14 %), Actinobacteria (10 %) and Firmicutes (9 %). Those were completed by a sixth section simplified as “Others” considering fifteen other OTU (*e.g.* Acidobacteria, Armatimonadetes, Chlorobi, Chloroflexi, Cyanobacteria,

Fusobacteria, GNO2, Gemmatimonadetes, Nitrospirae, OD1, Planktomycetes, Spirochaetes, Synergistetes, Tenericutes, Verrucomicrobia and Thermi); overall counting for *ca*. 2 %.

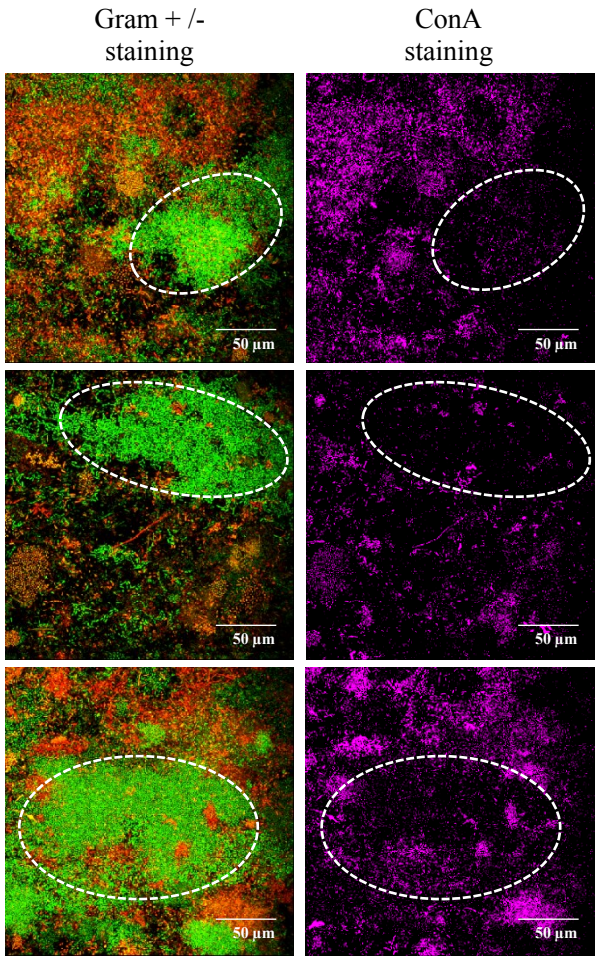


**Fig. 4.13: Gram+/- and ConA based characterisations of the multi-species biofilms.** Representative examples of CLSM z-stacks registered at 72 h after dual staining with the Gram+/- (on the left; Gram+ in red, Gram- in green) and ConA (on the right) dyes are shown. The same biofilms are presented *per* row of images. The white circles indicate examples of clearly varying areas between dyes. Scale is 50 µm.

The overnight pre-cultured sample in AW medium showed OTU selection (Proteobacteria 73 %, Bacteroidetes 22 %, Actinobacteria 3 %, Firmicutes 2 % and Others *ca*. 0 %). This trend was shown to be more exacerbated again when comparing with the sequencing data from the actually established biofilms at 48 h (Proteobacteria 98 %, Bacteroidetes 1 %, Actinobacteria with Firmicutes 1 % and Others *ca*. 0 %). Proteobacteria are Gram- bacteria,

consequently CLSM and NGS results closely related at 48 h (Fig. 4.12 and 4.14). The loss of diversity over time was confirmed at L6 (Fig. 4.15).

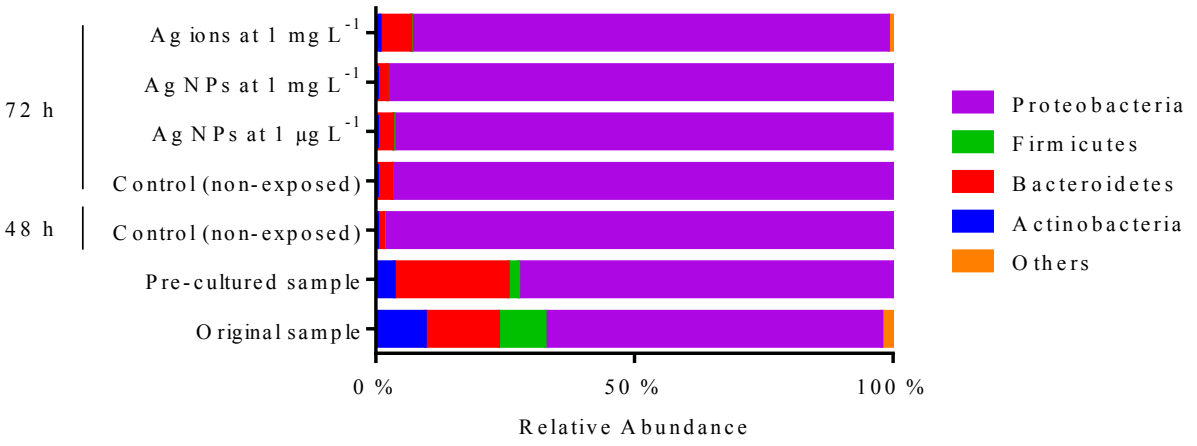


**Fig. 4.14: Histogram of the main OTUs identified at L1.** The simplified L1 results obtained by NGS within the scenario of culture and exposure of the multi-species biofilms in Artificial Wastewater are shown above (created from Dr S. Hilton's row data files). The "original sample" corresponds to the collected crude wastewater (CW) sample and the "pre-cultured sample" corresponds to the overnight cultured CW in Artificial Wastewater used as inoculum for the flow-cell system. Schematic of the experimental design is proposed in Fig. 2.6.

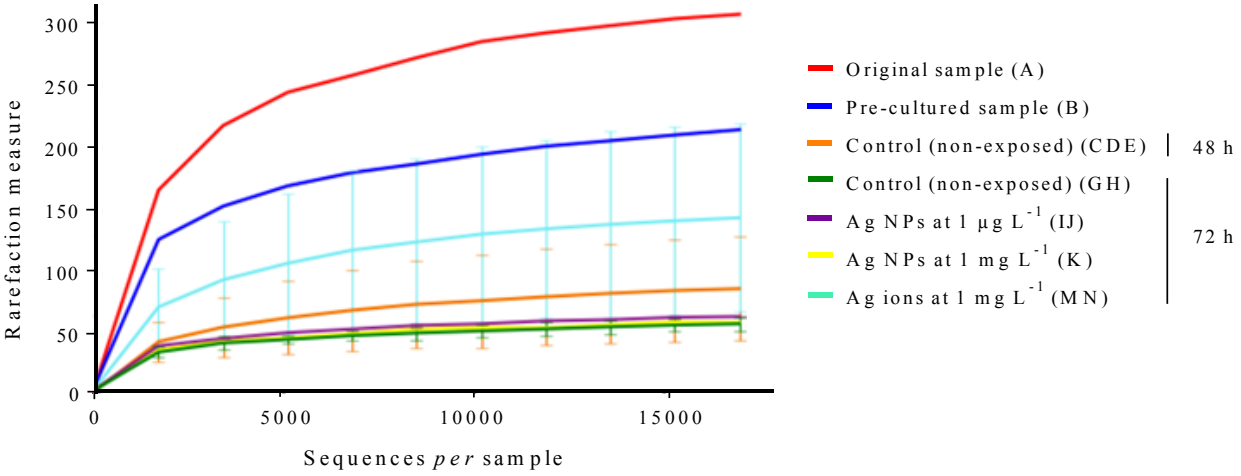


**Fig. 4.15: Diversity plot at L6.** In the above plot is presented the evolution of the diversity (or rarefaction) as determined at L6 considering all samples (from A to N, refer to Appendix D Table S4.1) within the proposed scenario. Adapted from Dr S. Hilton's report.

Interestingly, some new (but very minor, *i.e.* < 0.01 %) OTUs such as the Nitrospirae, the Armatimonadetes and the Planktomycetes were characterised following exposure to Ag ions. Those OTU were not characterised in the pre-cultured bacterial suspension used as inoculum and could therefore result from contaminations *via*, potentially, the Ag salt itself. As shown in Fig. 4.15, this tends to limit the rarefaction trend and to increase the variability of those results compared to the Ag NPs cases. Comparatively, no particular impact of the staining process (for the CLSM analysis) was observed on the OTU based outcomes.

As presented in Fig. 4.16, further analyses at L6 showed that the control biofilms at 48 and 72 h were different in OTU terms; however, no clear differences were characterised between the biofilms following the different treatments at 72 h. The latter result was confirmed by the analysis of the sole 72 h samples (data not shown). Consequently, the composition of the multi-species biofilms was not shown to be affected significantly by a 24 h exposure to the Ag NPs or ions at 1 mg $L^{-1}$ or below.

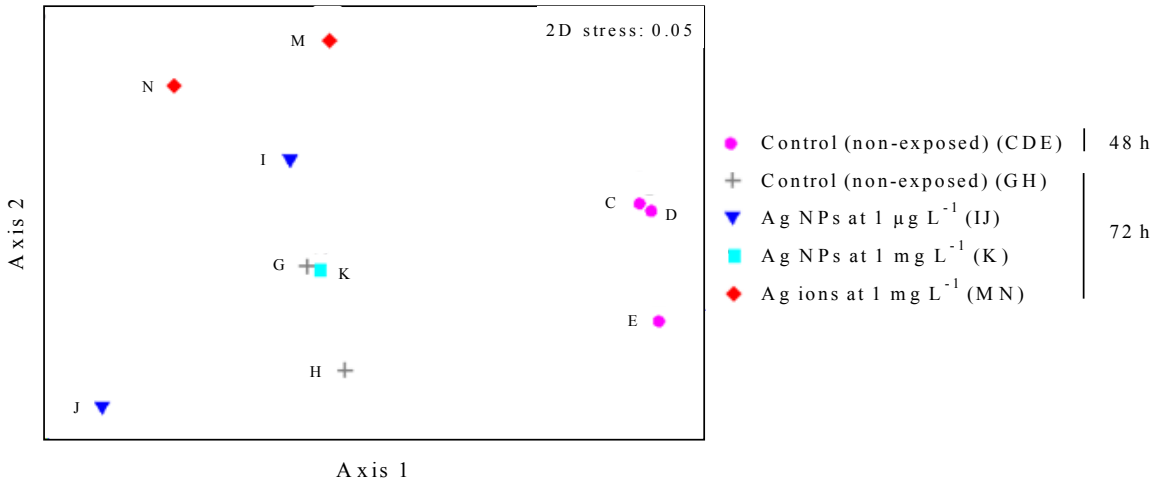


**Fig. 4.16: Similarity diagram at L6.** The NGS results of all biofilm samples (at 48 and 72 h) were coupled by replicates and tested for similarity using a Bray-Curtis based analysis. The excluded F and L replicates were confirmed as outliers using the same representation (data not shown). Adapted from Dr S. Hilton's report.

Overall results showed that Proteobacteria constituted the main OTU, regardless of the applied conditions or time points. Within the Proteobacteria, the analysis at L6 showed that

the Moraxellaceae (*e.g*. *Acinetobacter*), the Aeromonadaceae, the Pseudomonadaceae (*e.g*. *Pseudomonas*) and the Enterobacteriaceae were the main overall biofilm establishing bacterial families, representing 95 % of the total OTU abundance at this level. The four aforementioned families contributed for more than 80 % to the differences between 48 and 72 h samples. Then, apparent less abundant bacteria such as the Sphingobacteriaceae (*e.g*. Sphingobacterium) and the Flavobacteriaceae (*e.g*. Flavobacterium), both Bacteroidetes (Gram-), further contributed to the global variability between time points; Firmicutes and Actinobateria (both Gram+) finally showing very little contribution to the biofilm versatility. The OTU table (at L6) is presented in Appendix D (Table S4.2).

Despite some ratio mismatches, the NGS results showed overall rather coherent patterns compared to those obtained by CLSM using the Gram+/- dye as in both cases: the multi-species biofilms were shown to be driven by the Gram- bacteria (*e.g*. Proteobacteria and Bacteroidetes), the 48 and 72 h control biofilms were different, the actual impacts between different treatments (*e.g*. 1 µg $L^{-1}$ Ag NPs, 1 mg $L^{-1}$ Ag NPs, 1 mg $L^{-1}$ Ag ions) at 72 h were unclear.

Due to the cost of performing such analysis full sample plates are generally preferred; this considerably delayed the actual generation of the data here reported (*i.e*. gDNA sent in June 2015, data delivered in November 2015). Consequently, only one experiment could be performed.

### 4.2.3 Microbial activity monitoring

The monitoring of the C source utilisation (D-glucose based) previously reported with the mono-species biofilms was further applied here with the multi-species biofilms along with the additional analysis of both N and P *via* the ammonium and the phosphorus based quantification between effluent (*i.e*. downstream to the flow-cells) and influent (*i.e*. upstream to the flow-cells) samples. The output results presented as the biofilm removal activity (in % terms) within the proposed scenario of culture and exposure are shown in Fig. 4.17.

The C removal was shown to be consistently *ca*. 98 % of the original loading (0.05 % D-glucose, w/v), regardless of the tested condition. The P removal was, conversely, lower

than 10 % but it was not clearly impacted by any of the applied Ag treatments; so was the N removal case. This latter nevertheless showed to be increased between the control biofilms at 48 and 72 h.

Consequently, none of the three tested removal pathways were shown to be impacted significantly by a 24 h exposure to the Ag NPs or ions at 1 mg $L^{-1}$ or below in the tested regime based on D-glucose, ammonium and phosphorus measurements.

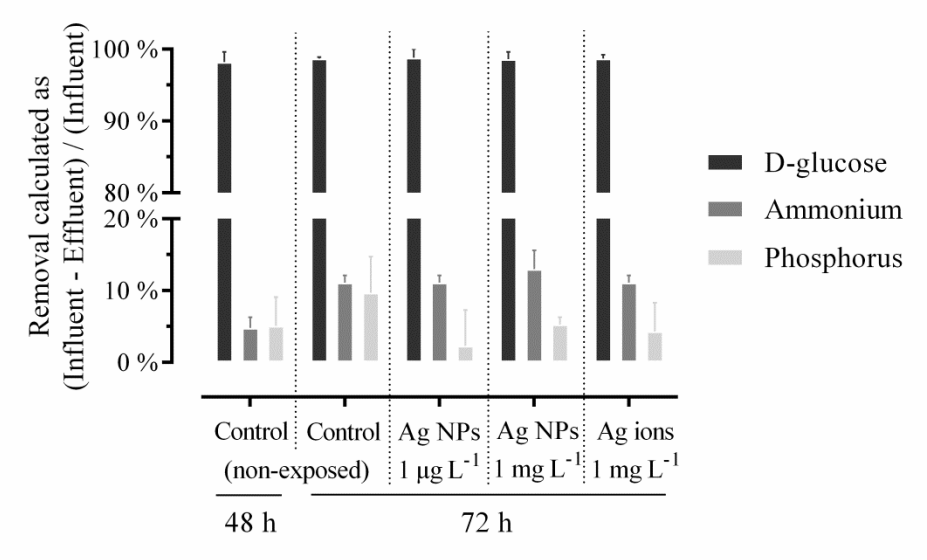


**Fig. 4.17: C, N and P removal activity of biofilms.** The evolution of the C (carbon, *via* D-glucose), N (ammonium) and P (phosphorus) removal activity of the multi-species biofilms as determined by their comparative quantification in influent and effluent samples taken from the flow-cell reactors at 48 and 72 h under the different conditions tested is presented above.

## 4.3 Discussion

### 4.3.1 *P. putida* based mono-species biofilms

#### 4.3.1.1 The big picture

The toxicity of Ag NPs to various static mono-species biofilms was reported in the literature [289, 293, 294, 298, 310, 424]. Overall conclusions emphasised that Ag NPs were harmless below 1 mg $L^{-1}$, inhibitory in the 1 - 10 mg $L^{-1}$ range and lethal above 100 mg $L^{-1}$.

Biofilms were as well consistently reported more resistant to NPs than the planktonic cell counterparts [289, 293, 294, 298, 310].

Considering non-static biofilms, there are too few studies using flow-cell reactors at the present time to draw conclusive trends. Pioneer works of Bjarnsholt *et al*. (2007) [368] showed toxic effects of Ag sulfadiazine *ca*. 10 mg $L^{-1}$ on mature *Pseudomonas* spp. biofilms under hydrodynamic conditions. Fabrega *et al*. (2009) [314] thereafter discussed the accumulation of Ag NPs onto and into *P. putida* biofilms and reported the absence of impact on viability up to 2 mg $L^{-1}$ using in-house built (mono-chambers) flow-cells. Herein, the viability of *P. putida* BS566 *lux* mono-species biofilms was not visibly affected *post* exposure to a single 24 h pulse of Ag NPs at 1 mg $L^{-1}$ and below using commercially available (multi-chambers) flow-cell reactors. However, the variable observation of dead cells reported herein (*i.e*. in 3 out of 5 experiments) at 10 mg $L^{-1}$ may inform about a transient state in the biofilm response to bactericidal (*i.e*. biofilm-cidal) doses of NPs. In light of this, the absence of visible dead cells at 100 mg $L^{-1}$ (certainly removed by the flow) *post* exposure is not a proof of unaltered viability but a testimony of biofilm temporal response as described with other chemicals [82, 425, 426].

In terms of morphology, the general trend of the biofilm response was characterised by a decrease in biofilm biomass, thickness and surface area coupled with an increase in roughness. The response was found to be dose dependent with impacts reported from 0.01 mg $L^{-1}$; therefore corroborating the sloughing phenomena reported *post* exposure to 0.02 - 2 mg $L^{-1}$ Ag NPs elsewhere [314]. In addition here, the microbial activity (*i.e*. monitored *via* the sole carbon source utilisation) was concomitantly shown to be time dependent (*i.e*. older and larger biofilms using more D-glucose in absence of NPs) as well as NP dose dependent (*i.e*. the utilisation of D-glucose being reduced *post* exposure to 10 mg $L^{-1}$ Ag NPs and above). Consequently, the dose dependent biofilm restructuring previously mentioned did not involve an evident loss in the biofilm activity with the lowest concentrations of NPs (*i.e*. 0.01 - 1 mg $L^{-1}$ range); instead the loss of activity was rather concomitant with the microbial death.

Despite being frequently reported, the direct comparison of the planktonic versus biofilm information may be rather inappropriate (*i.e*. the biofilm associated cells are differentiated

from the planktonic cells by reduced growth rate, up and down gene regulation, ability to show coordinated behaviour and generation of extracellular polymeric matrix) [79, 82]. As previously mentioned the toxicity of Ag NPs to planktonic bacteria was reported in the 1 - 10 mg $L^{-1}$ range and commonly associated with ions based effects [31, 47]. Ag NM-300K NPs, specifically, were shown to be toxic to planktonic *P. putida* BS566 *lux* in AW with $IC_{50}$ values *ca*. 5 mg $L^{-1}$ after 1 h of exposure (*i.e*. Ag ions were comparatively shown to be at least ten times more toxic). Considering the "worst case scenario" here, disperse microcolonies were visible *post* exposure to a single 24 h pulse of 100 mg $L^{-1}$ Ag NPs; the non-static *P. putida* based mono-species biofilms were therefore more tolerant to Ag NPs than the planktonic cells.

#### 4.3.1.2 Potential mode of action of Ag NPs

Toxicity of Ag NPs to bacteria was shown to be commonly associated with ion based effects on planktonic cultures. Such mechanisms were less discussed in case of biofilms. In addition, Ag cations were reported to complex with the negatively charged extracellular matrix (EPS) of biofilms, potentially diminishing their bioavailability for an eventual toxicity [427]. However here, Ag ions exhibited evident dose dependent toxic effects on non-static *P. putida* based mono-species biofilms. The occurrence of the live/dead dual staining was even visibly increased in the assays in the case of the Ag ions, attesting to a superior biofilm-cidal pressure overall (compared to NPs) as also stressed by Bjarnsholt *et al*. (2007) [368] with Ag sulfadiazine on mature biofilms. Fabrega *et al*. (2009) [314] did not report on the Ag ion toxicity, however correlative observations were discussed with $Zn^{2+}$ released ions from ZnO NPs elsewhere [288] still in flow-cell reactors. The tested Ag NM-300K NPs were not therefore a single case example and, as previously discussed with planktonic cultures, the Ag ions were essential to Ag NPs toxicity on biofilm cultures too.

Interest has been recently shown in investigating NP deposition onto and penetration into biofilms. Peulen and Wilkinson (2011) [307] reported that the relative self-diffusion coefficients of several NPs (including Ag NPs) were decreased exponentially with the square of the NP radius when tested with *Pseudomonas* spp. static biofilms. Choi *et al*. (2010) [310] showed that Ag NPs were able to penetrate *ca*. 40 μm in static biofilms in 1 h. Regarding the non-static biofilm literature, Miller *et al*. (2013) [296] showed that

distributions of NPs through the biofilms were consistent with diffusive transport and that uniform distributions through the thickness were achieved within a few hours. Interactions between NPs and biofilms were observed herein (*i.e.* impact on UV-vis spectra, loss in concentration as well as gain in size and negative charges in effluent samples) and discussed previously [314]. NP deposition onto and penetration into the biofilms during the 24 h exposure is therefore likely here.

The structure and function of *P. putida* biofilms as well as the composition and properties of their extracellular matrix were previously reported as impacted by the surrounding nutrients [423, 428]. Here, a "limited" barrier role of the produced matrix by *P. putida* BS566 *lux* due to the minimal conditions of growth in AW may be hypothesised, enhancing further the possible penetration and subsequent impacts of Ag NPs and/or (released) ions. Consequently, the toxicity of Ag NM-300K NPs is herein firstly reported on non-static *P. putida* mono-species biofilms and likely to be supported by combined effects of both NPs and ions. Interestingly, the dose dependent and sequential impact observed on biofilm morphology, viability and activity would support the hypothesis of a NP dose dependent bacteriostatic (biofilm-static) and bactericidal (biofilm-cidal) like response from the non-static biofilms, as only suggested before with static biofilms [289, 293, 294, 298, 310, 424]. This would also corroborate the notion of biofilm adaptive stress response already described with other toxicants such as disinfectants [82].

#### 4.3.1.3 Long term effects or possible biofilm recovery *post* exposure

The importance of information regarding the long term effects of NPs has been emphasised [72, 314]. Nevertheless, such results using biofilms are still to be reported in nanoecotoxicology. Herein, results from *P. putida* mono-species biofilms assessed 24 h *post* exposure to a single pulse of Ag NPs/ions showed overall recovering patterns on biofilm morphology and activity. In the absence of toxic pressure (*i.e.* the absence of NPs within the system during the recovery period was confirmed by AAS), biofilms were shown to restructure (*i.e.* presence of filaments and re-growth of microcolonies). The formation of filaments by *P. putida* was previously reported as an adaptive survival strategy in response to hostile conditions of growth [429, 430]. The formation of elongated bacteria was equally reported as a typical consequence of DNA damage or envelope stress [431].

Interestingly, variable results and potentially late effects were observed (at 96 h) *post* recovery *post* exposure to 1 mg $L^{-1}$ Ag NPs. Accordingly to the NP mode of action afore hypothesised, some intermediate or threshold concentrations of NPs may then constitute a particularly "grey area" where biofilms are highly versatile because literally in between two types of response and, in which case, the time becomes another critical factor on top of the dose.

### 4.3.2 Multi-species biofilms

Reports on non-static multi-species biofilms are limited in nanoecotoxicology. Fabrega *et al*. (2011) [306] reported significant impacts of Ag NPs at 2 mg $L^{-1}$ on marine biofilm volume and biomass without modification of their composition (based on T-RFLP profiles). Sheng and Liu (2011) [308] discussed tolerance of wastewater biofilms to Ag NPs up to 200 mg $L^{-1}$ and highlighted the protective role of the extracellular matrix. Gonzalez *et al*. (2015) [277] recently reported higher toxicity of Ag ions (compared to Ag NPs) to multi-species phototrophic biofilms in a rotating reactor. Here, the potential impact of Ag NPs (at 1 µg $L^{-1}$ and 1 mg $L^{-1}$) and Ag ions (at 1 mg $L^{-1}$) to mature wastewater based multi-species biofilms was investigated using flow-cell reactors in AW. In the absence of visible impact on viability at 1 mg $L^{-1}$ Ag NPs with the mono-species biofilms, the Gram+/- staining was thought to be more informative than the live/dead staining for applications with multi-species biofilms. In order to limit the artificial COD supported by the C source and potentially exacerbate the microbial activity related results, D-glucose was supplemented at a lower level (0.05 %, w/v) than the mono-species biofilm work. The extracellular matrix and the microbial composition as well as the removal of ammonium and phosphorus were in addition studied in case of the multi-species biofilms.

The original CW sample was pre-cultured in AW to promote microbial adaption to the medium and facilitate reproducibility between experiments (*i.e*. in terms, notably, of state of activity of the inoculum). It was demonstrated that such precautions led to evident selection of some microbial species. Selection process which also continued over time with established biofilms. Direct inoculation with non-pre-cultured wastewater sample could be considered in future assays; nonetheless, as not all bacteria can establish biofilms and as

some species may be better equipped or simply more abundant than others, some kind of selection is unavoidable.

Multi-species biofilms were shown overall more versatile (even in the absence of the toxicants) than the mono-species biofilms herein. Information on composition and activity did not show clear impact of NP or ions at tested concentrations. This emphasises the extreme complexity of such biological structures and the importance of working with or towards more realistic models. In order to propose more accurate analyse of such heterogeneous structures, more powerful package than COMSTAT 1 (such as IMARIS) may be necessary. COMSTAT 1 especially suffers from segmentation and thresholding weaknesses, possibly limiting its applicability to very complex specimen and numerous staining. Trials of image analyses are being initiated using IMARIS software (Bitplane) at the ESRIC platform (HWU) in order to inform on its beneficial input (or not) for potential next assays. Regardless of the package, the analysis of the extracellular matrix never was informative in our assays. Higher doses of dyes could have been tested again, but the approach suffered above all from the absence of a blue laser (*i.e*. for which numerous matrix dedicated dyes are available) on the used CLSM. Besides, the NGS results appeared overall promising and attested to the workability and relevance of the proposed methodology, however the lack of replicates obviously limited their global significance.

Consequently, more work is required here using multi-species biofilms. Nonetheless, the preliminary results, attesting to limited impact of Ag NPs at 1 mg $L^{-1}$ in AW based on composition (NGS) and activity (removal of D-glucose, ammonium and phosphorus), were found to be in line with the rare studies reporting on similar testing [277, 306, 308]. The suitability of CLSM compatible flow-cell reactors for testing of Ag NPs (and ions) to complex multi-species biofilms under hydrodynamic conditions is therefore already evident here.

# CHAPTER 5: Results - Biosensor based assays

Nanoecotoxicology is quickly growing but the toxicity testing of NPs remains overall a challenging task to complete [16, 44]. Although bacteria are widely used as model organisms (§ 1.1.4.2.1), methods based on plating and spectrophotometry have clear limitations. Plating is long to perform and lacks accuracy while spectrophotometry is rarely suitable for analyses in complex and/or coloured matrices [358, 359]. Approaches exploiting the advantages of luminescent genetically modified bioreporters (GMB) have emerged [147, 365] offering additional perspectives, but regulations and concerns on applicability about GMB limit their broad use and relevance [432]. In the meantime, due to an appealing portfolio of advantages (*e.g.* real-time, label-free, rapid, multiplex, GMB-free, using small volumes and generating little waste) and on-going refinements (*e.g.* increasingly operator friendly and compatible with various types of biological materials, matrices and configurations), applications of biosensors are expanding. Surface plasmon resonance imaging (SPRi) and microcantilever (μCT) are examples of widely used biosensor technologies for biomolecular interaction assessment and analyte detection using a microarray format [372, 373, 382, 383]. SPRi has proven to be robust over the years *via* the emergence of various instruments, dedicated studies and companies worldwide [370, 384, 385]; whilst μCT technology has been continuously developed since its implementation in AFM [371].

SPRi applications with bacteria have emerged recently [381, 386-388]. The notion of real-time monitoring of the bacterial growth by SPRi was first reported by Bouguelia *et al*. (2013) [381] proposing a culture-capture-measure (CCM) method using the advantages of specific interactions between monoclonal antibodies microarrays and bacteria (*e.g.* *Salmonella enterica* and *Escherichia coli*). Additional applications with various bacteria followed using the same method [386, 387]. Concomitantly, Abadian *et al*. (2014b) [388] reported the use of SPRi for the monitoring of *E. coli* and *Pseudomonas aeruginosa* biofilm attachment, formation and removal.

The use of SPRi with bacteria has been initiated in ecotoxicology for the testing of antibiotics [388] and for the impact assessment of thermal stresses [387]. However, no

proof of workability in nanoecotoxicology has yet been reported. In the meantime, the use of μCT with bacteria is limited and applications in ecotoxicology and nanoecotoxicology still have to be reported.

Consequently, in collaboration with experts from each field, it was hypothesized that μCT and SPRi could independently lead to original high throughput platforms for NP toxicity screening. However, not being actually in use in the host laboratory, the μCT based system was first appropriately set-up and calibrated. Then, in the presence of the bacteria only, despite the chamber became turbid over time no growth curve was registered *via* the system. Numerous trials were performed (considering different options of inoculation and culture) without being successful. In the absence of encouraging results (*i.e*. ability of monitoring the bacterial growth) using a single and non-functionalised μCT after several attempts, the short term collaboration was terminated. Assays in the presence of NPs were finally not considered. In light of the above, it was therefore decided not to report the corresponding results in the thesis core. Examples of result can be found in Appendix E (Fig. S5.1, S5.2 and S5.3). This chapter therefore reports exclusively the results from the SPRi based assays operated in collaboration with Dr Thierry Livache and co-workers at CEA-Grenoble (France). All experiments were designed, performed and analysed by the author of the thesis with the support of the host team.

## 5.1 Surface plasmon resonance imaging technology

Considering the work previously reported with *P. putida* BS566 *lux* using both planktonic and biofilm approaches, the SPRi technology was implemented first with *P. putida* KT2440 (the clearance for shipping/working with the GMB being refused). Because assays with such bacteria had never been performed by the host laboratory, the use of alternative validated models (*S*. Enteritidis, *S. epidermidis* and their related specific antibodies) was also anticipated.

### 5.1.1 *Pseudomonas putida*

The results from the SPRi based assays piloted with *P. putida* KT2440 (at $10^5$ CFU $mL^{-1}$, in LB medium at 28 °C) using two different specific antibodies (ab38825 and ab68538) in the absence of the toxicants in replicated experiments are shown in Fig. 5.1.

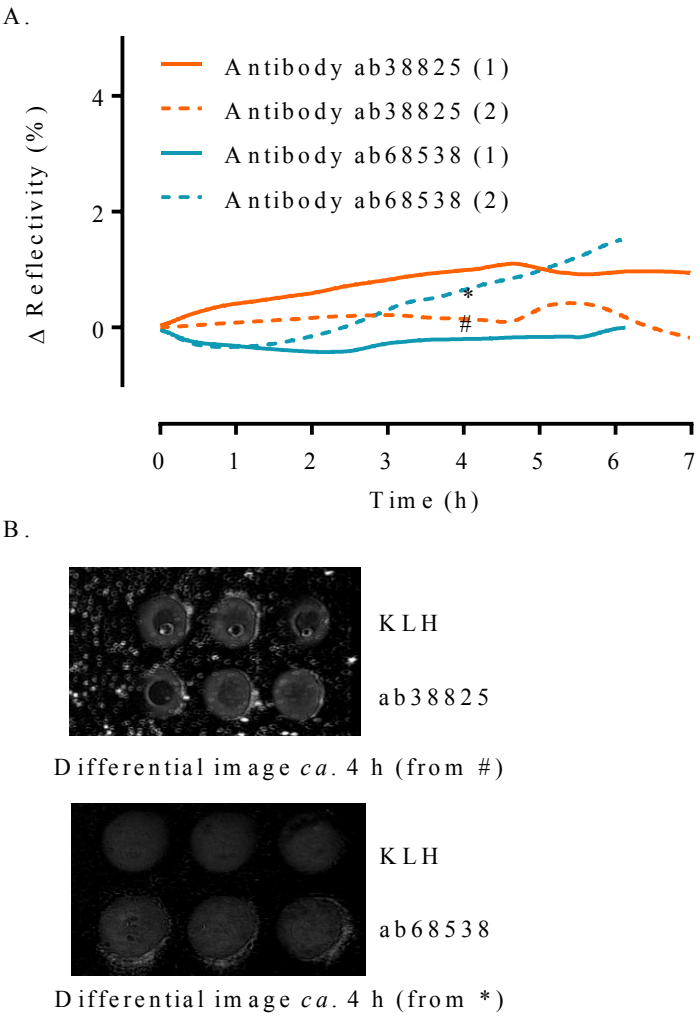


**Fig. 5.1: *P. putida* growth monitoring by SPRi in the absence of the NPs/ions.** The normalised variation of reflectivity over time from the *P. putida* specific antibody bearing spots obtained by SPRi is shown in A. The results with two different antibodies are reported, (ab38825 in orange) and (ab68538 in blue), from two independent trials (full and dash lines). Examples of registered differential images at 4 h with both antibodies are shown in B; KLH being a non-specific antibody used as control.

As shown in Fig. 5.1 A, overall no clear positive signals (*i.e.* growth curves) were obtained from the specific antibody bearing spots. As confirmed by the differential images proposed in Fig. 5.1 B, no clear bacterial deposition (*i.e.* surface interaction, marked by white "dots") was apparent on the ab38825 antibody. The ab68538 showed more specific behaviour as surrounding bacteria were visible and as the corresponding signal tends to mimic a growth curve; however this happened only once and occurred to be of very low amplitude to be really workable.

Consequently, none of the two tested (and only commercially available) specific antibodies for *P. putida* led to convincing interaction with the bacteria when used in SPRi in the absence of the NPs or ions. No typical growth curve was obtained despite the suspension extracted from the chambers was turbid at the end of the experiment and that the presence of bacteria within the chambers was visible on the recorded differential images (Fig. 5.1 B, white dots).

In the absence of evident interaction between bacteria-antibodies in several independent experiments (each using fresh batches of all materials), no further assays or developments were considered with *P. putida* within the short term collaboration. No toxicity testing of NPs could be performed. However, further assays were then performed with validated models by the host laboratory.

### 5.1.2 *Salmonella* Enteritidis

#### 5.1.2.1 Growth monitoring in the absence of the NPs/ions

The results obtained by SPRi for *S.* Enteritidis are shown in Fig. 5.2 A. The real-time growth monitoring of *S.* Enteritidis generated a typical exponential plot on the specific antibody (SE103) bearing spots. This was characterised by a detection time ($T_D$) derived at 4.6 ± 0.2 h with a starting bacterial inoculum concentration of 97 ± 7 CFU $mL^{-1}$ (mean ± SEM, n = 5). Overall, a low variability was obtained around the first inflection point of the growth curve, supporting the use of the derived detection times ($T_D$). Further details of the data processing are shown in Fig. 5.3, from which the quality of the spots, the specificity of interaction of *S.* Enteritidis with SE103 and the consistency of the generated data between the replicates were confirmed.

It can also be noticed that, with time (*i.e.* after 8 - 9 h of monitoring for the control case), the signal tends to occur on the spots bearing non-specific antibodies as exemplified by the differential image registered at 10 h (Fig. 5.3 A). This marks the saturation of the system when the bacterial population colonise completely the chamber and therefore interact with everything in a non-specific manner.

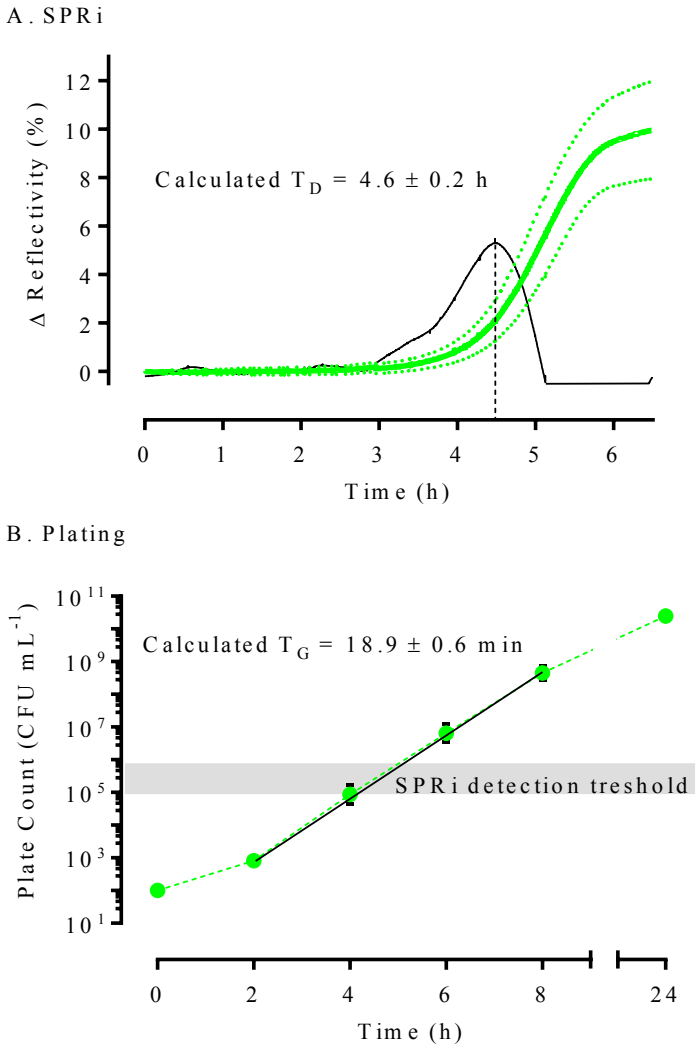


**Fig. 5.2: *S.* Enteritidis growth monitoring in the absence of the NPs/ions.** The normalised variation of reflectivity over time from the SE103 specific antibody bearing spots (*i.e.* the *S.* Enteritidis growth curve) obtained by SPRi is shown in A (—). The detection times ($T_D$) were obtained from the peak of the derivative curves (—). The output data (in CFU mL$^{-1}$ terms) from the *S.* Enteritidis growth monitoring obtained by plating are shown in B (●). The generation times ($T_G$) were calculated from the linear fit (—) on the exponential part of the curves. Data are mean ± SEM.

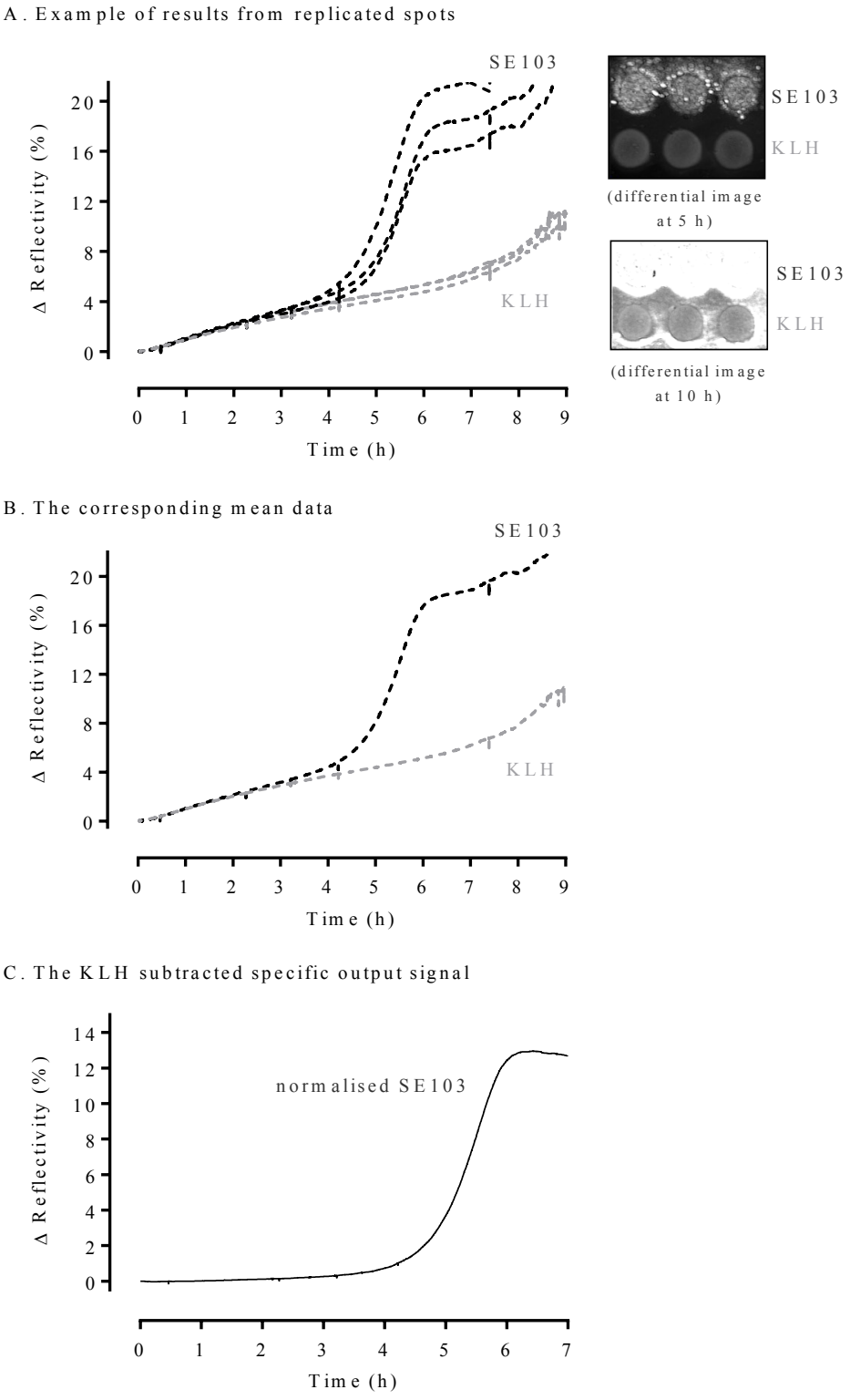


**Fig. 5.3: SPRi data processing.** Example of results from replicated specific (SE103) and non-specific (KLH) spots (*i.e.* from the same biochip) is shown in A along with a corresponding differential image. The corresponding averages of both signals are shown in B. The normalised SE103 specific sensorgram resulting from the subtraction of the KLH information is shown in C.

As characterised by plating (Fig. 5.2 B), *S.* Enteritidis exhibited a generation time ($T_G$) of 18.9 ± 0.6 min in the linear part of the growth curve. The SPRi detection threshold has already been shown to be in the $10^5$ - $10^6$ CFU $mL^{-1}$ range with bacteria [381, 387]. Starting from *ca*. $10^2$ CFU $mL^{-1}$, the $10^5$ - $10^6$ CFU $mL^{-1}$ range was expected to be reached after 4 to 5 h of growth; the plating information is therefore supporting the aforementioned SPRi results.

#### 5.1.2.2 Toxicity testing of the Ag ions

The impact of the Ag ions (tested at 0, 0.01, 0.1, 1 and 10 mg $L^{-1}$) on the growth of *S.* Enteritidis (starting at $10^2$ CFU $mL^{-1}$) in LB medium at 37 °C using the SPRi is shown in Fig. 5.4 A. The comparative results obtained *via* plating are presented in Fig. 5.4 B.

A dose dependent impact of the Ag ions on *S.* Enteritidis $T_D$ was observed using the SPRi (Fig. 5.4 A). More specifically, $T_D$ *ca*. 7.2 h were calculated at 1 mg $L^{-1}$ (*i.e*. delayed by *ca*. 2.6 h compared to the non-exposed control). Interestingly, the shape of the SPRi growth curves (*i.e*. the slope of the exponential parts) was not affected, which would suggest that early and temporal antimicrobial effects impacted the bacterial population. No clear impacts were detected at 0.01 and 0.1 mg $L^{-1}$. No growth was obtained at 10 mg $L^{-1}$.

As shown by plating (Fig. 5.4 B), the Ag ions were lethal at 10 mg $L^{-1}$ (*i.e*. clear impact from 2 h of exposure without recovery up to 24 h). A temporary impact was shown at 1 mg $L^{-1}$ characterised by a delayed growth with a detrimental effect during the first hours of exposure ($T_G$ ~ 260 min at 1 mg $L^{-1}$ versus 40 min at 0 mg $L^{-1}$ for the 0 - 2 h time window), followed by recovery over time. No difference from the control was visible at 24 h. A delay of two logs (in CFU $mL^{-1}$ terms) resulted at 4 and 6 h, compared to the control. No visible impact was observed at 0.01 and 0.1 mg $L^{-1}$.

Overall, the plate count supports the aforementioned shift in $T_D$ (but unchanged curve shapes) obtained by SPRi in the same condition of exposure (Fig. 5.4, arrows) as well as the hypothesis of a temporal antimicrobial effect of the Ag ions to explain the results obtained in the tested regime.

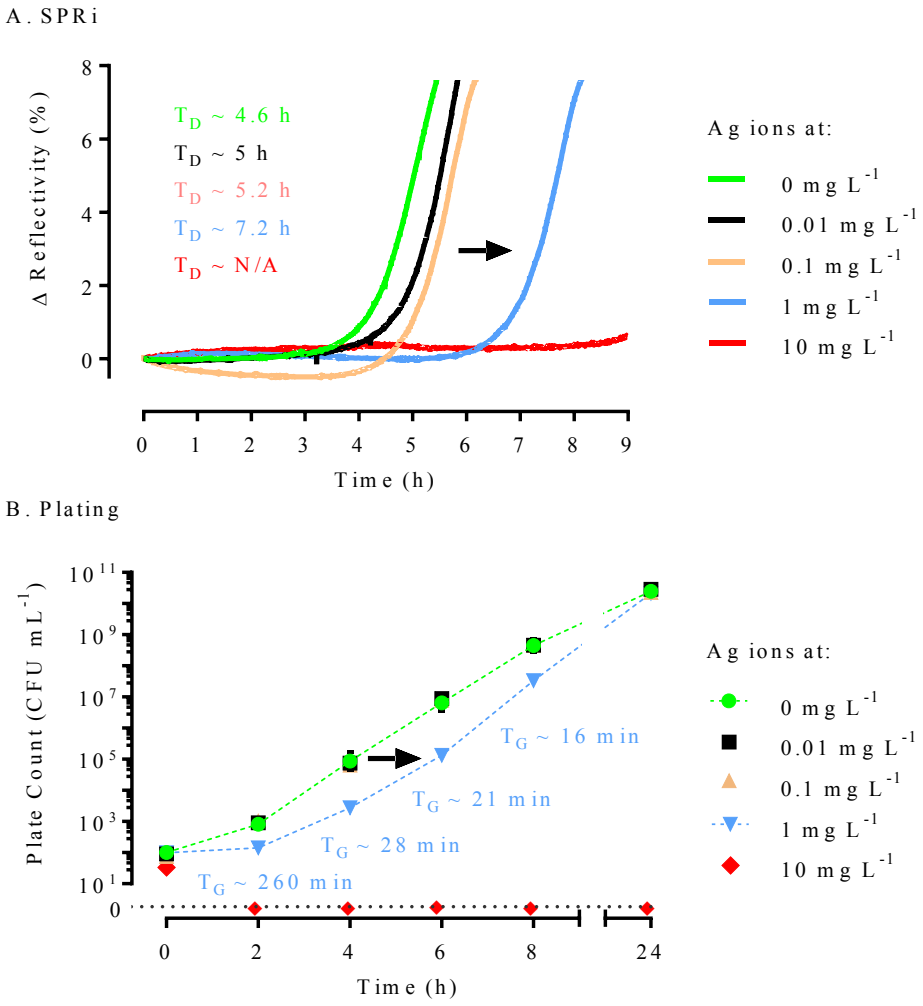


**Fig. 5.4: *S.* Enteritidis growth monitoring in the presence of the Ag ions.** The output data from the *S.* Enteritidis growth monitoring operated by SPRi (ΔR, in % terms) and by plating (in CFU $mL^{-1}$ terms) in the presence of 0, 0.01, 0.1, 1 and 10 mg $L^{-1}$Ag ions are shown in A and B, respectively. The corresponding detection times ($T_D$) are indicated in the SPRi case (*i.e.* N/A stands for non-applicable). The calculated times of generation ($T_G$) for the 1 mg $L^{-1}$ exposure condition are proposed for the plating case.

### 5.1.2.3 Toxicity testing of the Ag NPs

Comparatively, the Ag NPs (Fig. 5.5 A) were found to be ten times less toxic than the Ag ions. In accordance with the plating results (Fig. 5.5 B), exposure to 10 mg $L^{-1}$ Ag NPs led to shifted *S.* Enteritidis $T_D$ from 4.6 h to 7.5 h in SPRi whereas no visible effects were obtained at 0.1 and 1 mg $L^{-1}$ (Fig. 5.5 A). The shape of the SPRi growth curves was visibly affected (*i.e.* in a dose dependent manner) by the presence of the Ag NPs.

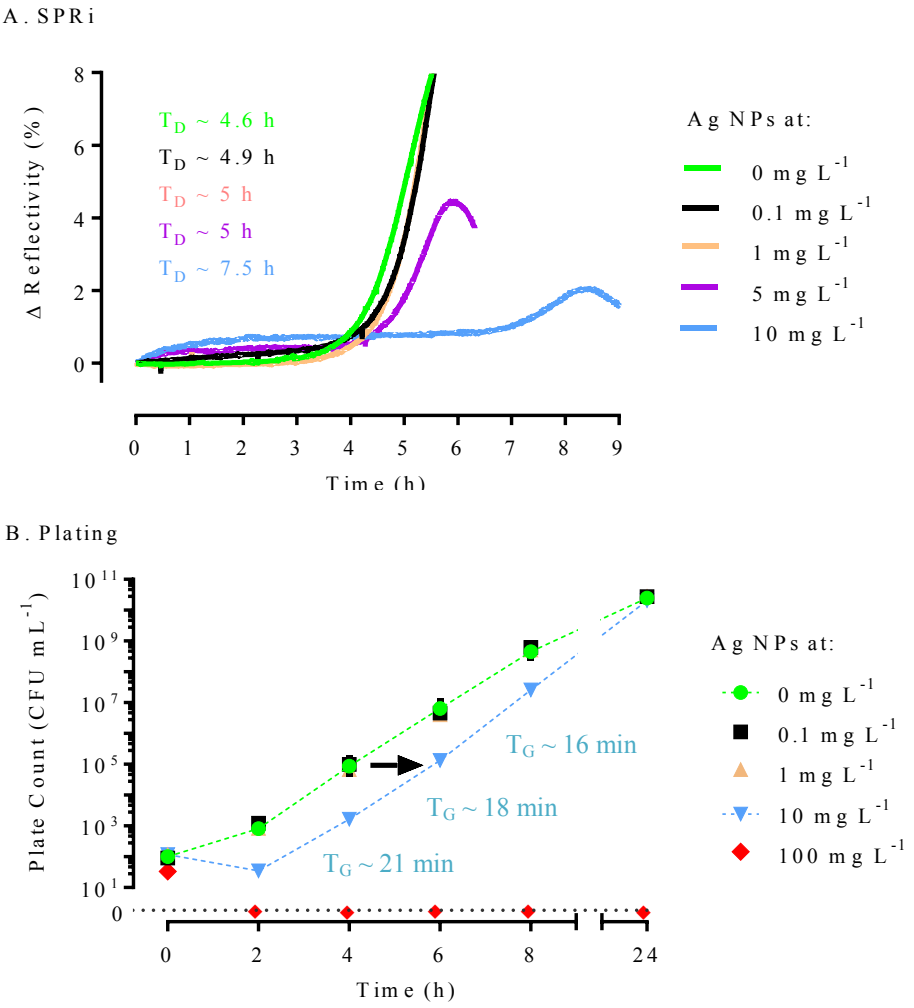


**Fig. 5.5: *S.* Enteritidis growth monitoring in the presence of the Ag NPs.** The output data from the *S.* Enteritidis growth monitoring operated by SPRi (ΔR, in % terms) in the presence of 0, 0.1, 1, 5 and 10 mg $L^{-1}$ Ag NPs are shown in A. The corresponding detection times ($T_D$) are indicated. Results obtained by plating are shown in B. The calculated times of generation ($T_G$) for the 10 mg $L^{-1}$ exposure condition are proposed too.

As presented in Fig. 5.6, this effect was limited by performing assays in inverted SPRi systems, even when using more concentrated bacterial inoculum (*i.e.* $10^5$ instead of $10^2$ CFU $mL^{-1}$). Using an alternative configuration of the SPRi system modified the testing conditions, therefore also slightly changing the $T_D$ eventually derived from the assays (*i.e.* 6 h for the control at $10^2$ CFU $mL^{-1}$, shifted at 7.5 h when exposed to the Ag NPs at 10 mg $L^{-1}$). Most importantly, the whole results demonstrated that the possible signal interference

due to the NPs *per se* was in any case a limitation for the direct data analysis (Fig. 5.5 A) or for further SPRi applications (Fig. 5.6).

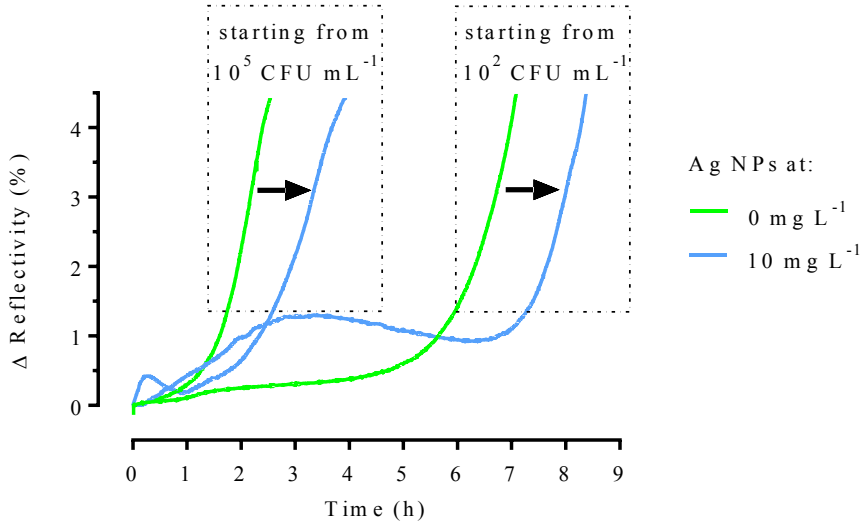


**Fig. 5.6: *S.* Enteritidis growth monitoring in the presence of the Ag NPs by inverted SPRi.** The normalised variation of reflectivity over time (from the SE103 specific antibody bearing spots) obtained by inverted SPRi in the presence of 0 and 10 mg $L^{-1}$ Ag NPs, starting from $10^5$ or $10^2$ CFU $mL^{-1}$, is shown above.

#### 5.1.2.4 Impact of the bacterial population size

As suggested in Fig. 5.6 with the Ag NPs, the original bacterial loading (in CFU $mL^{-1}$ terms) influenced greatly the output results: the largest population being detected first and being less altered by the exposure compared to the smallest population. This was further investigated using the Ag ions (*i.e.* as being overall an easier model material to handle than the NPs).

The impact of a selected effective concentration (*i.e.* 1 mg $L^{-1}$) of Ag ions was tested *via* SPRi on credential bacterial population sizes: $10^2$, $10^3$, $10^4$ and $10^5$ CFU $mL^{-1}$. As shown in Fig. 5.7, the non-exposed controls exhibited $T_D$ *ca.* 1.3, 2.2, 3.3 and 4.5 h (*i.e.* the largest population being detected first). When exposed to the Ag ions at 1 mg $L^{-1}$, the corresponding $T_D$ were obtained: 2.2, 3, 4.5 and 6.8 h, respectively. The amplitude of the characterised shifts was not different at $10^5$ and $10^4$, but slightly increased then at $10^3$ and $10^2$. In any case the slopes were visibly affected. Overall here, 1 mg $L^{-1}$ Ag ions "impacted"

*ca.* $10^1$ CFU $mL^{-1}$ of *S.* Enteritidis during the early stages of the exposure before life took over with more or less difficulties depending on the affected relative proportion (a fifth, a fourth, a third, or a half) of the population.

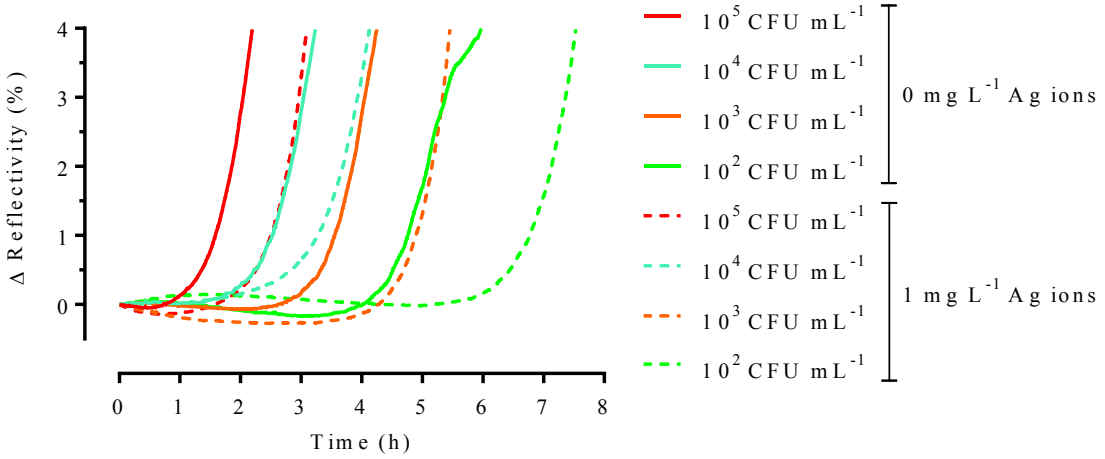


**Fig. 5.7: Impact of the *S.* Enteritidis population size on the toxicity testing outputs.** The normalised variation of reflectivity over time obtained by SPRi using *S.* Enteritidis at $10^5$ $10^4$ $10^3$ and $10^2$ CFU $mL^{-1}$ in the presence of the Ag ions at 0 and 1 mg $L^{-1}$ is shown.

### 5.1.2.5 Pilot assays with other NPs

Additional assays were performed with *S.* Enteritidis (at $10^5$ CFU $mL^{-1}$, in LB medium at 37 °C) testing the potential toxicity of ZnO NPs and related Zn ions (Fig. 5.8) and of $TiO_2$ NPs (Fig. 5.9).

Regarding the ZnO/Zn case, $T_D$ *ca.* 6 and 7.5 h were derived for *S.* Enteritidis exposed to the Zn ions at 100 mg $L^{-1}$ and to the ZnO NPs at 200 mg $L^{-1}$, respectively. Both the ions and the NPs therefore exhibited evident toxicity. The ZnO NPs however showed to generate interferences as previously mentioned with the Ag NPs.

Interestingly, Zn ions at 100 mg $L^{-1}$ temporarily impacted *S.* Enteritidis whereas 10 mg $L^{-1}$ of Ag ions were definitively lethal. Similarly, higher concentrations of ZnO NPs were applied to observe any toxicity when compared to the Ag NPs. Consequently, Ag (*i.e.* NPs and ions) was shown overall more toxic to *S.* Enteritidis than Zn (*i.e.* NPs and ions) using SPRi.

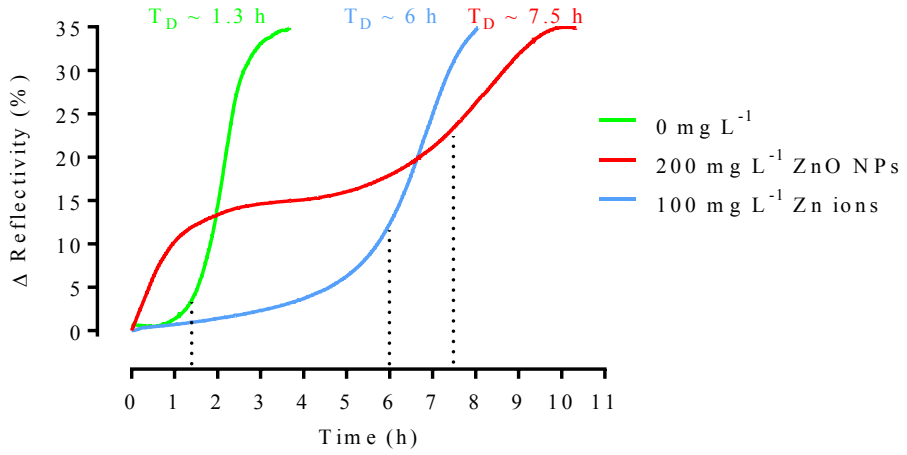


**Fig. 5.8: *S.* Enteritidis growth monitoring in the presence of the ZnO NPs and Zn ions by SPRi.** The normalised variation of reflectivity over time obtained by SPRi using *S.* Enteritidis at $10^5$ CFU $mL^{-1}$ in the presence of the ZnO NPs at 200 mg $L^{-1}$ and of the Zn ions at 100 mg $L^{-1}$ is shown.

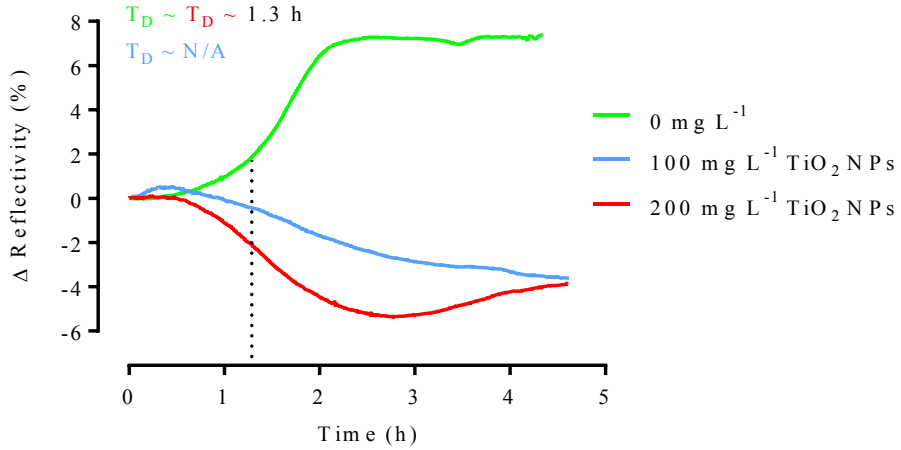


**Fig. 5.9: *S.* Enteritidis growth monitoring in the presence of the $TiO_2$ NPs by SPRi.** The normalised variation of reflectivity over time obtained by SPRi using *S.* Enteritidis at $10^5$ CFU $mL^{-1}$ in the presence of the $TiO_2$ NPs at 100 and 200 mg $L^{-1}$ is shown.

In the $TiO_2$ case, the NP exposed *S.* Enteritidis exhibited an atypical pattern with inverted output signals (*i.e.* possibly in a dose dependent manner) compared to the control and to what was observed so far using the SPRi. The atypical signal pattern was attributed to bacteria accessing the surface of the biochip through a “layer/film” of poorly suspended

and therefore depositing NPs. As such, by finally interacting with the specific antibodies over time the bacteria may "clean" from NPs those specific areas consequently reversely modifying the local refractivity index of those ones (*i.e*. which were previously dictated by the sole NPs in a dose dependent manner). The derived $T_D$ for the control and under the exposure to the $TiO_2$ NPs at 200 mg $L^{-1}$ were similar, the growth curves were almost symmetrical, the toxic effect of the $TiO_2$ NPs to *S*. Enteritidis appeared therefore very unlikely here. As such, the tested $TiO_2$ NPs were shown to be less toxic than both ZnO and Ag NPs using SPRi.

Toxic effects to *S*. Enteritidis as well as signal interferences were also observed using polystyrene NPs (data not shown). The NP based signal interferences were therefore not a specificity of the metal based NPs (*e.g*. Ag, ZnO and $TiO_2$).

### 5.1.3 *Staphylococcus epidermidis*

The processed data from the SPRi based assays with *S. epidermidis* (at $10^5$ CFU $mL^{-1}$, in LB medium at 37 °C) are shown in Fig. 5.10. Dose dependent effects were monitored with derived $T_D$ shifted from *ca*. 4 h for the control to *ca*. 6, 12 and 16 h with exposure to Ag ions at 1.25, 2.5 and 5 mg $L^{-1}$ respectively (Fig. 5.10 A). Similarly to the previously obtained results on *S.* Enteritidis, the slopes of the output signals were not significantly affected compared to the non-exposed control for *S. epidermidis*. No toxicity was observed at 0.1 mg $L^{-1}$ Ag ions; no growth was obtained at 10 mg $L^{-1}$ Ag ions (data not plotted).

Selected differential images are presented in Fig. 5.10 B demonstrating the spot quality, the dose (and consequently time) effect on the specific signal appearance, and the progressive saturation of the SPRi system (*i.e*. due to the bacteria colonisation leading to an out of range optical index saturating the apparatus, as mentioned previously with *S*. Enteritidis but clearly and timely exemplified here).

No toxic effects of the Ag NPs were observed up to 1 mg $L^{-1}$ then non-conclusive results were obtained due to interferences occurring above this concentration.

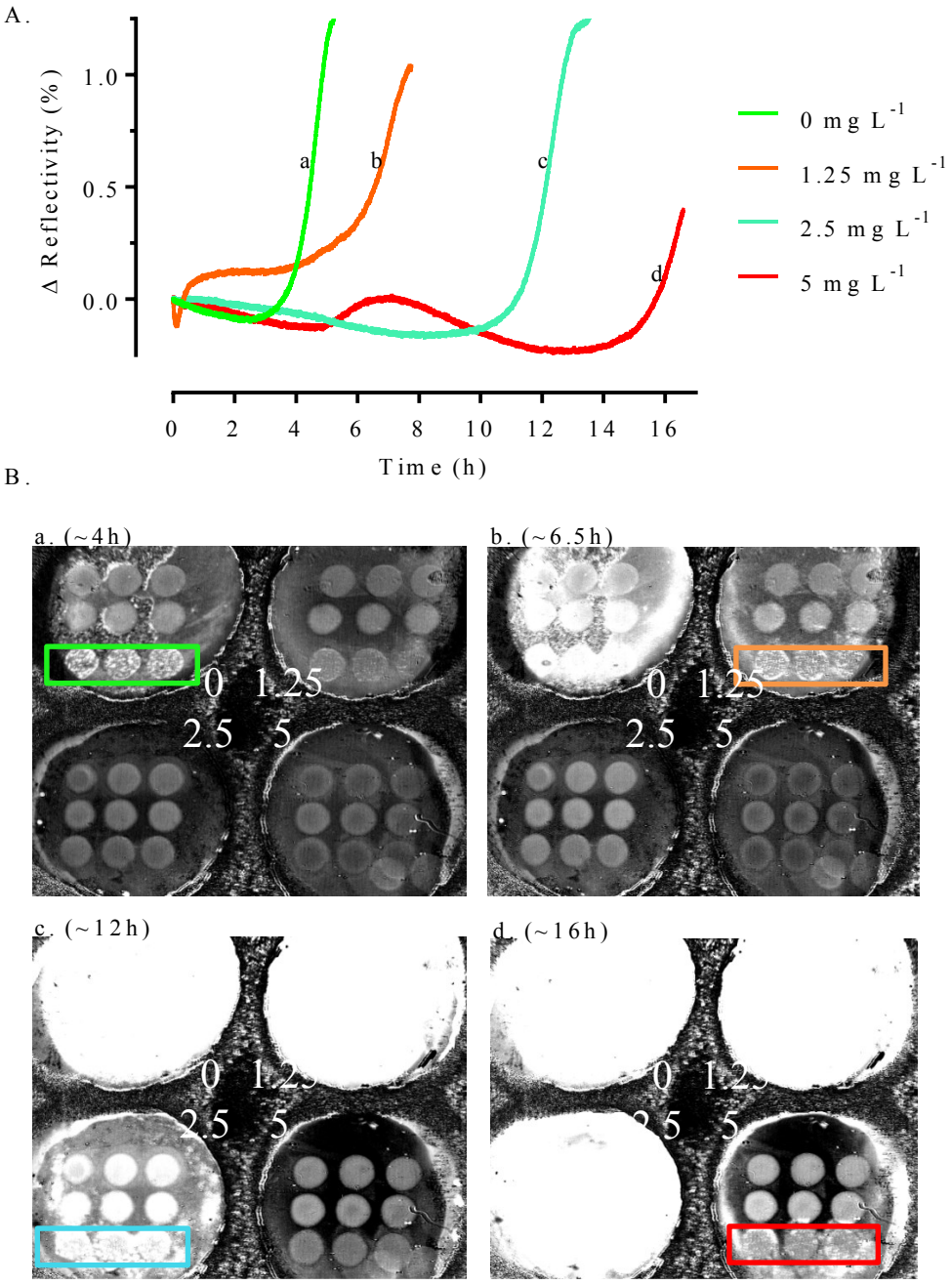


**Fig. 5.10: *S. epidermidis* growth monitoring by SPRi in the presence of the Ag ions.** The normalised variation of reflectivity over time from the *S. epidermidis* specific antibody (*i.e.* KPL) bearing spots obtained by SPRi in the presence of the Ag ions at 0, 1.25, 2.5 and 5 mg $L^{-1}$ is shown in A. Four examples of registered differential images over time of the whole biochip (encompassing four independent chambers with nine spots each) are shown in B. Each image (annotated from a to d) approximatively corresponds to a $T_D$ derived from A. The *S. epidermidis* specific spots were framed in B matching the coloured legend proposed in A; the non-framed spots are non-specific negative controls (*e.g.* KLH).

## 5.2 Discussion

### 5.2.1 The big picture

Overall, the proof of workability of SPRi for testing of Ag NPs and ions was reported on different bacteria (*S.* Enteritidis and *S. epidermidis*) in LB. Further assays would be necessary to propose, in addition, fully conclusive outputs testing ZnO (and related ions) and $TiO_2$ NPs. Preliminary data nonetheless attested to coherent trends in terms of toxicity with possible impact of ZnO and no effect of $TiO_2$ NPs, respectively. Being different from the working wavelength of the SPRi apparatus, the intrinsic SPR properties of tested NPs never were an issue. Signal interferences from NPs were nonetheless encountered and were attributed to an amplified sedimentation of NP-bacteria aggregates [35] occurring especially on the specific spots and eventually flattening the output SPRi signals. Such interferences were circumvented by using inverted SPRi systems. In the absence of reported studies using SPRi in nanoecotoxicology, no direct comparison could be performed.

### 5.2.2 *S.* Enteritidis

Looking at, especially, the growth monitoring of *S.* Enteritidis in the absence of the NPs, the reported information here corroborates results discussed elsewhere in buffered peptone water using the same bacterial model [381]. The toxicity of Ag ions and NPs was respectively reported from 2 and 20 mg $L^{-1}$ for *Salmonella* spp. elsewhere *via* plating [407]. The reported SPRi results (*i.e.* clear and comparable effects of Ag ions and NPs at 1 and 10 mg $L^{-1}$, respectively) appear most of all in line with the main trends in nanoecotoxicology and therefore attest to the relevance and suitability of the SPRi technique for the testing of NPs and related ions. The SPRi results were characterised by shifted signals in the presence of effective doses of NPs, attesting to early antibacterial effects of NPs (and ions) as previously reported herein using planktonic based approaches (*e.g.* plating with *S.* Enteritidis and bioreporting with *P. putida* BS566 *lux*). Similar observations (*e.g.* signal shifts and early effects of NPs) were reported elsewhere with various bacteria using OD monitoring [146, 433].

### 5.2.3 *S. epidermidis*

No comparable results were reported before using *S. epidermidis*. Result quality was found overall inferior with *S. epidermidis* compared to *S*. Enteritidis. This is essentially attributed to the strength of interaction bacteria-antibodies as high specificity gives high output signal and low background, so cleaner data overall; and conversely. In terms of toxicity, further assays would be necessary here to propose fully conclusive (and comparable) outputs testing both NPs and ions with *S. epidermidis*.

### 5.2.4 *P. putida*

In the used SPRi approach (*i.e*. CCM, patented) antibodies are critical. They may allow specific recognition and work in multi-species environments; however availability of specific enough antibodies is limited and sometimes rather expensive to consider larger applications. In addition, potential impacts of NPs to, directly, the antibodies (and their properties) may be questioned and shall be assessed in future work. Consequently, alternative approaches may be anticipated here as un-functionalised [388] or for example carbohydrate-functionalised [386] surfaces may also be suitable for work with bacteria.

*P. putida* was, unfortunately, the perfect example of the actual main limitation of SPRi using the CCM method as in the absence of a workable specific antibody the testing simply cannot be performed. Two commercialised antibodies were tested, unsuccessfully; no more options were then available except developing on purpose the needed antibody from the strain of interest. An option which was not coherent with the short collaboration terms, hence the aforementioned work on pre-validated models (*S*. Enteritidis and *S. epidermidis*) by the host laboratory.

# CHAPTER 6: General discussion

This chapter aims to highlight the novelty, relevance, advantages and limitations of the performed research.

## 6.1 Planktonic based assays

This work aimed to evaluate the suitability of the *P. putida* BS566 *lux* bioreporter based switch-off approach for the screening of NP toxicity in both artificial (*i.e.* laboratory) and real matrices. First, four commonly used inorganic NPs (Ag, ZnO, CuO and $TiO_2$) were tested in nutrient rich undefined laboratory medium (LB) and in minimal defined artificial wastewater simulating effluent (AW). Second, the NPs exhibiting toxicity in AW were further tested in real crude and final wastewater samples (CWs and FWs) and subjected to ageing. When applicable, ecotoxicity results were related to NP characterisation information as assessed by DLS, UV-vis and AAS in each matrix of exposure.

*P. putida* is a common model microorganism in environmental science (*e.g.* water and soil); its sensitivity to NPs was previously reported [113, 185, 209, 219] and its suitability for performing testing in real matrices was anticipated [367]. LB is a very common growth medium in microbiology, widely used in testing too despite being far from ideal (*i.e.* as being first undefined and second rich in proteins which may lead to capping of NPs). AW is comparable to various other synthetic wastewaters simulating effluent [392, 393] and presents the main advantages to be defined (can be easily modified if necessary), clear (limiting optical interferences) and protein-free (limiting potential interaction with NPs). CWs, exhibiting BOD and TSS loadings *ca*. 200 mg $L^{-1}$ were representative of medium urban influent wastewaters. The characteristics of used FWs were in compliance with the European directive 91/271/EEC. Samples from four different WWTPs were used across different seasons (February to July). The tested NPs (except for CuO) were representative materials from the European Commission (Ag NM-300K, ZnO NM-110, $TiO_2$ NM-104).

Complementing an extensive literature on *E. coli* (§ 1.1.4.2.1 and 1.1.4.2.2), the data on *P. putida* BS566 *lux* demonstrated: ranking of toxicity of tested NPs (Ag, ZnO and $TiO_2$) in LB (*i.e.* Ag being the most toxic), the higher toxicity of ions compared to NP counterparts

(when applicable), clear impact of the matrix of exposure on NP toxicity and characteristics using LB and AW then CW and FW (*i.e*. NPs were shown less toxic in real than artificial matrices and also found less toxic in CW than FW), and the importance of ageing (*i.e*. NPs were found susceptible to ageing in CW exclusively). No such assays using GMB were reported before in real wastewaters, neither were the tests of ageing. Consequently, the methodology presented here has shown to be a rapid and an inexpensive solution for high throughput toxicity testing assays of NPs in both artificial and real matrices, generating new data and offering new possibilities for acute testing. Additional work with various materials (*e.g.* type, size, shape) may be anticipated. The acute testing in FWs and CWs with $TiO_2$ NM-104 and ZnO NM-110 NPs did not result in clear toxicity patterns (data not shown). Complementary studies with the same bioreporter in different matrices or with other bioreporters in comparable matrices are of interest for the development of arrays of broader applicability. In times where the lack of appropriate, simple and standardised procedures is largely stressed in nanoecotoxicology [75], such methodology should be diligently taken into account for performing acute testing of pristine and aged NPs.

## 6.2 Biofilm based assays

This work aimed to assess the toxicity of selected NPs to mature (*i.e*. established and fully hydrated) biofilms under hydrodynamic conditions in AW. In light of the planktonic results in AW, the case of Ag NPs was prioritised with biofilms. First, the temporal impact of Ag NM-300K NPs (and related ions) on *P. putida* BS566 *lux* based mono-species biofilms was investigated using a flow-cell system. Biofilm morphology, viability and activity were upraised *ante* and *post* exposure to NPs as well as *post* recovery 24 h after exposure. Second, testing assays with multi-species biofilms were piloted using real wastewaters (CWs) as inoculum. Further biofilm characterisation using NGS was notably considered in the multi-species biofilm case. When applicable, ecotoxicity results were related to NP characterisation information as assessed by DLS, UV-vis and AAS within the scenario of exposure as well as compared to the aforementioned planktonic information.

Although well described and still improving [362, 363], macrofluidics systems as the flow-cell reactors used here may still appear difficult to assemble and perform. At the present

time, there are scarce applications in nanoecotoxicology with non-static mono-species biofilms in such systems and simply none with multi-species biofilms. In light of this, we first demonstrated the clear workability of flow-cell reactors for testing of NPs with both mono and multi-species biofilms; investigating scarcely studied mechanisms and proposing original information in the domain. Complementing an emerging area of research (§1.1.4.2.1 and 1.1.4.2.3), the data reported herein demonstrated: the higher resilience of *P. putida* mono-species biofilms compared to planktonic cultures, the possible recovery of biofilms *post*-exposure to NPs, the higher toxicity of ions compared to NP counterparts, a mode of action of NPs partly driven by the released ions, and the complexity but high relevance of developing further multi-species biofilm based assays. A plethora of short and long term as well as single and multiple pulse based scenarios of exposure with various NPs along with ageing and recovery assessment could be piloted from the information reported herein. In addition new free packages such as COMSTAT 2 (running with ImageJ), dedicated to the characterisation of biofilms and more friendly to use than previous versions (*e.g.* COMSTAT 1, used herein with Matlab), have been made available in 2015 by the DTU (Lyngby, Denmark); facilitating the analysis of registered z-stacks.

The biofilm activity assessment was piloted herein using a D-glucose based monitoring. As the sole carbon source of the system in AW, D-glucose utilisation appeared as a critical marker of the biofilm behaviour. Considering there is 1.07 mg of COD *per* mg of D-glucose [395], the theoretical COD removal activity may be estimated too. Being quicker, less sample consuming and easier to perform than the COD quantification; the D-glucose monitoring was preferred across conditions and experiments. Based on the original loading of D-glucose (0.5 %, w/v), ecotoxicity assays were performed in AW with an equivalent COD loading of *ca*. 5000 mg $L^{-1}$, corresponding to a high concentration case scenario. The use of D-glucose (in the 0.5 % range, w/v) was reported before [314, 368, 369] in a similar AB trace minimal medium, minimal Davis medium or M9 medium. Similar loadings were therefore used herein to facilitate comparison with those studies. However, the monitoring of the C source utilisation and its correlation to COD information was not considered before.

## 6.3 Biosensor based assays

This work aimed to explore the putative suitability of biosensor technologies for performing testing of NPs to bacteria. Main application of NPs is the development of biosensors [16], however the use of biosensors for performing toxicity testing of NPs is not reported yet. Advantages of biosensor technologies are numerous though [370, 373, 375, 384, 385, 434]. As μCT and SPRi technologies had already shown workability for real-time growth monitoring of microorganisms (*e.g*. planktonic bacteria and yeasts as well as bacterial biofilms) trials with both approaches were envisaged in collaboration (*i.e*. short term) with experts from each domain. All assays were performed in host laboratories with the non-GMB *P. putida* KT2440 screening, when possible, toxicity of NM series NPs from the OECD in LB as a starting point.

The proof of workability of SPRi for real-time testing of NPs (Ag, ZnO, $TiO_2$) and ions (when applicable) to bacteria was demonstrated for the first time here. Additional assays based on various strains, media, and chemicals using inverted SPRi systems (with or without fluidics) and antibody or carbohydrate functionalised biochips are continuing in the host laboratory. Interestingly, the μCT approach seemed to be both very close and very far from being successful. Very close because the proof of concept in monitoring the growth of microorganisms such as yeasts had already been reported by our collaborators [377] (as well as non-published yet NP testing assays with mammalian cells) and because above all the μCTs were no more than other reactive gold coated surfaces such as the biochips used in SPRi. Very far because the μCT system was not running anymore when the collaboration started, because bacteria are simply not like yeasts (*P. putida* are motile and yeasts may be quite big compared to bacteria) and because the first (and simplest) approach did not involve surface functionalisation of the μCT (*e.g*. with antibodies as performed in SPRi) as it was not trivial procedure in the host laboratory. In addition, all the assays herein were performed on a single μCT format, whereas multiple μCTs in parallel in independent chambers would be necessary to assess several concentrations (regardless of the toxicant) at the same time; along with the appropriate light output monitoring equipment.

The μCT related literature is abundant [371, 375], forms, applications and ways of functionalisation are numerous; nonetheless the technology still seems simply too "young" compared to others, especially to SPRi. Experts agreed that μCTs were far from portable or on field applications for example (personal communication from Dr Will Shu, HWU) whereas SPRi was up to such challenges (personal communication from Thibaut Mercer, founder of PrestoDiag, French company commercialising ready to use SPRi based kits for rapid detection of bacterial pathogens in food matrices). Consequently, the μCT may be suitable for toxicity testing of NPs with bacteria, however this may require dedicated and long term projects as well as some specific developments (as aforementioned) to be demonstrated.

The possibility to exploit only part of what biosensors promise is already appealing enough to consider risking original applications, as reported herein. In the biosensor domain, any small proof of concept may thereafter lead to small technological revolutions ending on new or different ways to do things (*e.g.* test the toxicity of a chemical candidate to a bacterial target). Whereas the μCT system used was an in-house prototype system, the SPRi system (as well as the biochips which may be bought pre-functionalised if necessary) is fully commercialised for years and continuously improving making its use relatively easy nowadays. Applications in complex matrices were already reported too [381, 387]. Improved SPRi apparatus (with higher wavelength for example) may allow better resolution so higher sensibility and potentially work with, eventually, very little amount of cells. The first used of SPRi for testing of NPs to bacteria reported here is therefore likely to be challenged and further developed quickly.

## 6.4 Overall trends

As previously mentioned (§ 1.1.1), WWTPs were suggested as central but temporal recipients of manufactured NPs [29, 31, 33]. Environmental concentrations of Ag, ZnO, and $TiO_2$ NPs *ca*. $10^{-2}$ - $10^{-3}$ μg $L^{-1}$, $10^{-2}$ μg $L^{-1}$ and $10^{0}$ - $10^{-1}$ μg $L^{-1}$ were recently reported in surface waters [7, 28]. Those authors also discussed concentrations of same respective materials *ca*. $10^{-1}$ - $10^{-2}$ μg $L^{-1}$, $10^{-2}$ μg $L^{-1}$ and $10^{-1}$ μg $L^{-1}$ in effluent wastewaters.

In light of the data reported here, disregarding massive accidental or intentional discharges of NPs, there are still at least theoretically several orders of magnitude between expected or measured environmental concentrations of NPs and their threshold for toxicity on planktonic cultures (at least on bacteria). In addition, tested $TiO_2$ and ZnO NPs were not observed to be toxic in AW following the experimental approach used in this study. Their environmental adverse effects might be therefore very limited in real matrices. ZnO NPs were nonetheless observed toxic in classical laboratory medium (*i.e.* LB), hence the importance to test NPs in more realistic matrices and to promote the methodologies suitable for such assessment, as proposed here. As a counterexample, despite the erratic variability of *E. coli* in distilled water has been clearly demonstrated [217] toxicity assays in water or sodium chloride supplemented water (*i.e.* poorly representative of real matrices) have been frequently reported (§ 1.1.4.2). The case of CuO NPs could not be clearly studied herein. Conversely, Ag NPs were quite extensively studied and found to be the most toxic NPs overall. They showed consistent toxicity to planktonic cultures in LB and AW, and their further testing in real wastewaters showed they were less toxic in CWs than FWs. Their adverse effect might be therefore more detrimental to the environment if released. It is likely that the tested Ag NPs were less subject to agglomeration and more protected from matrix effects due to being provided as suspension in a dispersant compared to the other NPs which were supplied as powders. However, for industrial and commercial purposes, NPs are likely to be used (and ultimately released) in combination with dispersants or stabilisers in order to preserve or enhance their physico-chemical properties. Fate and toxicity of NPs following actual release from waste streams and industrial processes are likely to be different from their pristine counterparts especially when tested in laboratory media. Correspondingly, we demonstrated that Ag NPs were less toxic and more subject to aggregation with ageing in CWs, exclusively.

Despite morphological impacts being found from 0.01 mg $L^{-1}$ Ag NPs, we in addition demonstrated that *P. putida* mono-species biofilms exposed to pristine Ag NPs (up to 100 mg $L^{-1}$) in AW were overall capable of morphological recovery within only 24 h. The microbial activity was not found significantly affected below 1 mg $L^{-1}$ and was also subjected to recovery. Using wastewater based multi-species biofilms, preliminary assays

did not lead to clear impacts on communities composition or activity up to 1 mg $L^{-1}$ Ag NPs. Similar results were discussed with marine and wastewater multi-species biofilms elsewhere [306, 308]. Herein, the importance of the ions in the toxicity of Ag NPs to biofilms was nonetheless highlighted. The literature discussing significant impact of NPs to WWTPs refer to concentrations above the mg $L^{-1}$ range using pristine NPs [288, 308, 405, 414, 435]. Retention times of CWs may count from hours to weeks and Ag, especially, was also shown sulphidised and interacting with organic matters in natural waters and wastewaters in some hours elsewhere [411, 416, 421, 436]. Consequently, overall information suggests that the eventual impacts of released and aged Ag NPs below the mg $L^{-1}$ range to bacterial structures (*e.g.* planktonic and biofilm cultures) may be limited in real wastewaters at the present time. Although there is clearly controversy on the risks and benefits of Ag NP containing consumer and healthcare products [437], the global impact of Ag NPs to WWTPs (*i.e.* their actual toxicity in CWs) may be therefore limited at the present time [68].

The concentrations of NPs tested herein may be thought unrealistically high compared to reported environmental concentrations, but as a matter of fact they represent the range of sensitivity of bacteria to NPs as extensively reported in the literature. This current difference should rather be seen as "good news" for the environment, considering a bacterial standpoint. Interestingly, those concentrations are comparable to the effective doses (*ca.* 1 - 10 µg $mL^{-1}$ or mg $L^{-1}$ for Ag NPs) reported in nanotoxicology using mammalian cells (*e.g.* neutrophil, lymphocyte, macrophage) [174]. The membrane protecting both bacteria and mammalian cells definitively plays a crucial role in their tolerance against toxicants; maybe more again in the case of bacteria as no endocytosis mechanism is reported compared to the mammalian cells. Surprisingly, bigger and apparently more robust models such as algae or crustaceans finally appear more sensible than bacteria because of their feeding based on the filtration of their environment (*i.e.* therefore dropping their actual physical protection). Consequently, though located at the bottom of the aquatic food chain bacteria are unlikely to be the most dramatically affected by NPs at the present time. However, because of the advantages of using bacteria as bioreporters for microbiological (*e.g.* environmental and clinical) testing, they definitely

offer relevant opportunities as high throughput screening and patterning tools for standardised assessment of NPs in various matrices, including real and complex ones.

In addition, as demonstrated here, using biosensors technologies such as SPRi further developments with bacteria are possible in nanoecotoxicology. New high throughput, real time, label and GMB-free, automotised and/or portable ways of performing testing of NPs, especially investigating the kinetics of interaction between bacteria and NPs may be anticipated. Validated already using other types of cell than bacteria (*e.g*. mammalian cells), application of SPRi may be transferred in nanotoxicology. Others platforms, for example based on μCTs, optical fibres and microfluidics, are likely to emerge in near future.

# CHAPTER 7: Conclusions and Future Work

## 7.1 Conclusions

This work aimed to explore and compare (when possible) new planktonic, biofilm and biosensor based bacterial assays for NP toxicity testing with an ecotoxicological prospective.

### 7.1.1 Hypothesis 1

First, it was hypothesised that bacterial bioreporters originally isolated from environmental matrices such as the *P. putida* BS566 *lux* would be suitable for NP testing in real matrices such as wastewaters.

Ecotoxicity of various NPs (and related ions when applicable) was assessed using a switch-off methodology (*i.e*. planktonic) based on the *P. putida* BS566::luxCDABE bioreporter in LB and AW. Results showed a global ecotoxicity ranking depending on the type (*i.e*. with toxicity of Ag > ZnO > CuO and $TiO_2$ NPs) and form (*i.e*. with toxicity of ions > nanoparticles) of the tested material as well as on the matrix of exposure (*i.e*. only Ag NPs were toxic in AW). The inconsistent behaviours of the tested NPs were closely associated with, especially, versatile underlying aggregation/agglomeration and dissolution phenomena between matrices. CuO NPs (and related ions) were not found toxic due to, most likely, expressible Cu resistance genes by *P. putida*. The toxicity of Ag NPs was further reported in real wastewater samples and shown to be different in CW and FW. More specifically, Ag NPs exhibited ion based toxicity above the mg $L^{-1}$ range (*i.e*. after 1 h of exposure) in all wastewater samples with toxicity patterns occurring at significantly lower concentrations in FWs compared to CWs. The impact of the wastewater composition on toxicity was driven by related BOD, COD, TSS, bacterial plate count, ammonia, chloride and sulphide loadings which were all significantly more abundant in CWs. No significant site (*i.e*. WWTP) effect was observed on Ag NP toxicity despite clear differences in the physico-chemical characteristics between FWs and CWs. In addition, it was shown that Ag NP toxicity decreased significantly with ageing in CWs (*i.e*. due to occurring aggregation/agglomeration and complexation phenomena) but not in FWs.

Consequently, the suitability of the *P. putida* BS566::luxCDABE based planktonic assay for NP ecotoxicity screening in both artificial and real matrices was demonstrated. This was further validated *via* two published papers (Outputs I and II). The importance of the bioreporter and matrix of exposure selection was particularly emphasised (*i.e.* not all bacteria can survive in real matrices such as wastewaters), and so was the role of ageing. Possible limitations of bespoke bioreporters because they are GMB or due to endogenous resistances to particular compounds or elements were also reported herein. The potency of array development (battery test) using different bioreporters in parallel and the ease of standardisation of microplate based protocols make nonetheless such high throughput methods particularly valuable in nanoecotoxicology.

### 7.1.2 Hypothesis 2

Second, it was hypothesised that dynamic and complex microbial structures such as mono (*P. putida* based) and multi (wastewater based) species bacterial biofilms in flow-cell systems would be valuable models in nanoecotoxicology.

The temporal impact of Ag NPs (and related ions) to the dynamics of mature (*i.e.* 48 h old established and fully hydrated structures) *P. putida* mono-species biofilms was assessed in AW in parallelised flow-cells considering biofilm morphology, viability and activity related information. Sequential dose dependent toxic effects of Ag NPs were characterised on *P. putida* biofilm morphology (with impacts characterised from 0.01 mg $L^{-1}$), then activity (from 1 - 10 mg $L^{-1}$ range) and viability (from 10 mg $L^{-1}$) following a single pulse (*i.e.* exposure) of 24 h in AW. Sequential dose dependent recovery of biofilm morphology and activity were then reported 24 h after the exposure was terminated. Both "short" and "long" term effects of Ag NPs to *P. putida* biofilms were therefore questioned herein, and crucial information on biofilm recovery was reported. Ag ions also showed dose dependent impacts to biofilms but led to more efficient recovery *post* exposure despite being at least ten times more toxic than the tested Ag NPs. In light of this and of the NP characterisation information, the combined effect of NPs and ions was proposed to support the observed toxicity results of tested Ag NPs. Regardless of the methodological differences, *P. putida* biofilms were found more resilient than their planktonic counterparts. Whilst still

associated with a released ion based effect, the impact of NPs *per se* was nonetheless more evident in the biofilm case. Further assays with multi-species biofilms (*i.e*. wastewater based) were also reported herein. No clear impact of Ag NPs and ions ($\leq$ 1 mg $L^{-1}$) was concluded on biofilm composition and activity following a single pulse of 24 h in AW. Those pioneer assays with multi-species biofilms attest to the workability of the reported methodology for investigating the toxicity of NPs to highly complex and relevant biological structures.

Consequently, bacterial biofilms were shown to be valuable models as original information and new possibilities were associated with the study reported here. This was further validated *via* one published paper (Output III). In light of the above, additional works using non-static biofilms are not only desirable in nanoecotoxicology but clearly possible.

### 7.1.3 Hypothesis 3

Third, it was hypothesised that implementation of biosensor technologies such as microcantilever and surface plasmon resonance imaging would be possible with bacteria and suitable for applications in NP testing.

No toxicity testing of NPs could be eventually performed using the μCT with bacteria in spite of inputs from experienced collaborators. However, using SPRi, the impact of Ag NPs and ions on *S.* Enteritidis growth was shown; impact of Ag NPs between 1 - 10 mg $L^{-1}$ and higher toxicity of Ag ions compared to Ag NPs were reported. Workability with other types of NP (ZnO and $TiO_2$) and bacteria (*S. epidermidis*) was also reported. Unfortunately, assays with *P. putida* were not conclusive using SPRi due to the lack of specificity of the anti-*P. putida* antibodies commercially available.

Consequently, we demonstrated for the first time the workability of SPRi in nanoecotoxicology. This was further validated *via* one published paper (Output IV). In addition to several valuable intrinsic advantages (*e.g*. label-free, multiplex, bespoke and robust), SPRi is fast (*i.e*. results within a few hours) and generates kinetic data (*i.e*. real-time monitoring). A plethora of possibilities is therefore associated with the SPRi proof of concept reported herein; some possible limitations (*e.g*. availability of specific antibodies

and NP interferences) were also highlighted. SPRi occurred overall more readily available than μCT for applications in nanoecotoxicology as well as more robust for further device development or high throughput testing. The corresponding proof of concept using μCT in near future is nonetheless anticipated by the author.

### 7.1.4 Summary

This work reports on increasingly original and complex although still complementary bacteria based methodologies dedicated to the toxicity testing of NPs. From the thorough exploitation of a switch-off bioreporter to the development of bespoke biofilm assays then to the pilot implementation of biosensor technologies, various aspects of nanoecotoxicology were substantiated further (*e.g.* toxicity screening in real matrices, test of different types and related ions when relevant, impact of ageing, test of complex models such as biofilms, assessment of the possible recovery *post* exposure, etc.) if not firstly proposed (*e.g.* use of μCT and SPRi). Most of the data were subjected to peer-review; four published papers (two of which in special issues on nanoparticle ecotoxicity) are supporting this thesis which also contains relevant starting points for future applications in line with the needs recently emphasised in nanoecotoxicology using bacteria.

## 7.2 Future work

The *P. putida* BS566 *lux* bioreporter could be integrated in a larger array composed with additional bespoke GMB such as various Moraxellaceae, Aeromonadaceae or Pseudomonadaceae (to be developed mostly) for further testing in wastewaters. Alternatively, the planktonic approach could be adapted to solids such as spiked soil samples, as done before with the Microtox approach. The development of NP specific switch-on bioreporters as well as multi-bioreporters remains an open challenge in nanoecotoxicology. However, in the absence of a clear mechanism(s) of action of NPs and because of the recrudescence of inputs from analytical methods, their relevance appears limited at the present time.

Conversely, the scarce use of biofilms in nanoecotoxicology makes them particularly desirable. Pioneer works on non-static mono-species biofilms were further developed here

then upgraded to the multi-species level. A plethora of assays dedicated to the biofilm (mono or multi-species) EPS matrix, quorum sensing and metabolome behaviours in response to toxicant exposures could easily be performed based on the methodology reported here using flow-cell reactors. Similarly, alternative scenarios of exposure (*e.g.* test on established or on establishing biofilms, using coated surfaces or not, in AW or otherwise, at different flow-rates with one or several C sources testing single or multiple pulses of toxicants) are possible without additional development. Opportunities to further substantiate the topic are therefore numerous considering biofilms.

There is no doubt that dedicated projects on μCT will soon show it can be used in nanoecotoxicology; further assays using SPRi are already ongoing with inverted systems screening the toxicity of selected NPs to different bacteria in various media. Here as well, larger arrays may be anticipated. The kinetics of interactions bacteria-NPs is possibly going to be discussed soon *via* SPRi. In addition, SPRi but also other supports such as microfluidics have shown already suitability for the study of biofilms; reports on NPs testing with biofilms using SPRi is therefore anticipated in light of the proof of concept reported here.

All three above approaches could also be performed with toxicant mixtures, commercialised or directly released materials as sometimes proposed in the recent literature. Materials easily subjected to aggregation/agglomeration and sedimentation might not be suitable for use with biofilm in flow-cell reactor or biosensor based assays though. In the meantime, it is worth noticing that reported methodologies are not limited to NPs, others chemicals or drugs could easily be tested; the relevance and applicability of the work reported here go far beyond nanoecotoxicology.

In light of the above, it is recommended that further assays are performed using relevant GMB bioreporters in real matrices (*e.g.* wastewater, freshwater, seawater, soil), using mono and multi-species biofilms under hydrodynamic conditions, and using biosensor technologies in order to lead towards their standardisation whilst supporting the development (both fundamental and technical) of nanoecotoxicology. The use of well-defined NPs (and ideally their physico-chemical changes over the time of exposure) should

be further promoted (as facilitating the comparison between studies and the understanding of NP toxicity), and so are the impact of NP ageing and the potential recovery of microorganisms *post*-exposure to NPs. Finally, all successful developments here (see papers published in Outputs I to IV) resulted from the original technical transfer from ecotoxicology, biofilmology and food science; it is therefore recommended that additional implementations in nanoecotoxicology from other domains are investigated and proposed to the scientific community.

# Appendix A - Supplementary information of Chapter 1.

**Table S1.1: Comprehensive list of used *lux* GMB bioreporters in ecotoxicology.**

| Bacteria | GMB name | Switch-ON/OFF | Reference |
|---|---|---|---|
| *Acinetobacter* | ADP1_recA-*lux* | ON (DNA damage) | Song *et al*. (2009) [227] |
| | ADPWH_recA | ON (DNA damage) | Zhang *et al.* (2013) [438] |
| | DF4/PUTK2 | OFF | Abd-El-Haleem *et al*. (2006) [439] |
| *Bacillus subtilis* | BR151 (pCSS962/pBL1) | OFF | Kurvet *et al*. (2011) [440] |
| | | | Ivask *et al*. (2004) [441] |
| *Escherichia coli* | TV1068 | ON | Ben Israel *et al*. (1998) [442] |
| | | | Van Dyk *et al*. (1995) [443] |
| | GC2 | OFF | Yoo *et al*. (2007) [444] |
| | | | Mitchell *et al*. (2006) [445] |
| | | | Kim *et al*. (2005) [446] |
| | | | Chang *et al*. (2004) [447] |
| | | | Gu *et al*. (2001) [448] |
| | | | Gill *et al*. (2000) [449] |
| | MC1061 (pDN*lux*) | OFF | Kurvet *et al*. (2011) [440] |
| | | | Ivask *et al*. (2009) [450] |
| | MC1061 (pSL*lux*) | OFF | Kurvet *et al*. (2011) [440] |
| | | | Ivask *et al*. (2009) [450] |
| | K12 TG1 | OFF | Kurvet *et al*. (2011) [440] |
| | K802NR | ON | Eltzov *et al*. (2008) [451] |
| | DPD2794 | ON (DNA damage) | Eltzov *et al*. (2009) [452] |
| | | | Daniel *et al*. (2008) [453] |
| | | | Eltzov *et al*. (2008) [451] |
| | | | Lee *et al*. (2005) [454] |
| | | | Kim *et al*. (2005) [446] |
| | | | Choi *et al.* (2002) [93] |
| | | | Premkumar *et al.* (2001) [455] |
| | | | Gu *et al.* (2001) [448] |
| | | | Davidov *et al.* (2000) [456] |
| | | | Min *et al*. (2000) [457] |
| | | | Min *et al.* (1999) [458] |
| | | | Belkin *et al*. (1997) [459] |
| | | | Vollmer *et al*. (1997) [460] |
| | DPD2797 | | Pedahzur *et al*. (2004) [461] |
| | | | Davidov *et al*. (2000) [456] |

| | | | |
|---|---|---|---|
| *Escherichia coli* | DPD1718 | ON (DNA damage) | Pedahzur *et al*. (2004) [461] |
| | | | Polyak *et al.* (2001) [462] |
| | | | Davidov *et al*. (2000) [456] |
| | DPD1710 | | Mitchell *et al*. (2006) [445] |
| | DPD1714 | | Davidov *et al.* (2000) [456] |
| | DPD1709 | | Davidov *et al*. (2000) [456] |
| | DPD3063 | | Davidov *et al*. (2000) [456] |
| | DPD2818 | | Vollmer *et al.* (1997) [460] |
| | DPD2844 | | Vollmer *et al.* (1997) [460] |
| | DPD2850 | | Vollmer *et al.* (1997) [460] |
| | DPD2851 | | Vollmer *et al.* (1997) [460] |
| | BBTNrdA | | Lee *et al.* (2003) [463] |
| | MG1655 (pRecA-*lux*) | | Manukhov *et al*. (2008) [464] |
| | C600 (pPLS-1) | | Ptitsyn *et al.* (1997) [465] |
| | DO2 | | Mitchell *et al*. (2006) [445] |
| | MG1655 | | Tecon *et al.* (2010) [466] |
| | DPD2544 | ON (membrane damage) | Bechor *et al.* (2002) [467] |
| | | | Premkumar *et al.* (2001) [455] |
| | DPD2543 | | Pedahzur *et al*. (2004) [461] |
| | | | Bechor *et al.* (2002) [467] |
| | DPD2546 | | Bechor *et al.* (2002) [467] |
| | DPD2549 | | Bechor *et al.* (2002) [467] |
| | DPD1674 | | Bechor *et al.* (2002) [467] |
| | DPD2540 | | Mitchell *et al*. (2006) [445] |
| | | | Lee *et al*. (2007) [468] |
| | | | Kim *et al*. (2005) [446] |
| | | | Bechor *et al.* (2002) [467] |
| | | | Gu *et al*. (2001) [448] |
| | | | Ben Israel *et al*. (1998) [442] |
| | | | Belkin *et al*. (1997) [459] |
| | DK1 | ON (oxidative stress) | Yoo *et al.* (2007) [444] |
| | | | Mitchell *et al*. (2006) [445] |
| | | | Lee *et al*. (2005) [454] |
| | | | Mitchell *et al.* (2004) [469] |
| | MG1655 (pKatG-*lux*) | | Manukhov *et al*. (2008) [464] |
| | DPD2511 | | Pedahzur *et al*. (2004) [461] |
| | | | Lee *et al.* (2003) [463] |
| | | | Gu *et al*. (2001) [448] |
| | | | Premkumar *et al.* (2001) [455] |
| | | | Min *et al*. (2000) [457] |
| | | | Ben Israel *et al*. (1998) [442] |

| | | | |
|---|---|---|---|
| *Escherichia coli* | | ON (oxidative stress) | Belkin *et al.* (1997) [459] |
| | | | Belkin *et al*. (1996) [470] |
| | DPD2515 | | Premkumar *et al.* (2001) [455] |
| | | | Belkin *et al*. (1997) [459] |
| | DPD2519 | | Ben Israel *et al*. (1998) [442] |
| | DP1 | | Lee *et al*. (2007) [468] |
| | | | Mitchell *et al*. (2006) [445] |
| | | | Lee *et al*. (2005) [454] |
| | PGRFM | | Niazi *et al*. (2008) [471] |
| | MG1655 (pSoxS-*lux*) | | Manukhov *et al*. (2008) [464] |
| | EBSoxS | | Kim *et al*. (2005) [446] |
| | EBSoxR | | Lee *et al*. (2005) [454] |
| | | | Kim *et al*. (2005) [446] |
| | EBInaA | | Kim *et al*. (2005) [446] |
| | EBMalK | | Lee *et al*. (2007) [468] |
| | DPD1571 | | Pedahzur *et al*. (2004) [461] |
| | | | Oh *et al.* (2000) [472] |
| | EBHJ | | Lee *et al*. (2005) [454] |
| | DPD1006 | | Ben Israel *et al*. (1998) [442] |
| | | | Van Dyk *et al*. (1995) [443] |
| | DE135 | | Ben Israel *et al*. (1998) [442] |
| | | | Van Dyk *et al*. (1995) [443] |
| | DS1 | | Mitchell *et al*. (2006) [445] |
| *Escherichia coli* | ZWF | | Niazi *et al*. (2008) [471] |
| | | | Lee *et al*. (2007) [468] |
| | FPR | | Niazi *et al*. (2008) [471] |
| | | | Lee *et al*. (2007) [468] |
| | EBFumC | | Lee *et al*. (2007) [468] |
| | | | Kim *et al*. (2005) [446] |
| | EBHmp | | Lee *et al*. (2007) [468] |
| | TV1061 | ON (protein damage) | Eltzov *et al*. (2009) [452] |
| | | | Eltzov *et al*. (2008) [451] |
| | | | Mitchell *et al*. (2006) [445] |
| | | | Kim *et al*. (2005) [446] |
| | | | Pedahzur *et al.* (2004) [461] |
| | | | Bechor *et al.* (2002) [467] |
| | | | Premkumar *et al.* (2001) [455] |
| | | | Gu *et al*. (2001) [448] |
| | | | Min *et al*. (2000) [457] |
| | | | Belkin *et al.* (1997) [459] |
| | | | Rupani *et al*. (1996) [473] |

| | | | |
|---|---|---|---|
| *Escherichia coli* | | | Van Dyk *et al*. (1995) [443] |
| | DC1 | | Mitchell *et al*. (2006) [445] |
| | TV1076 | | Van Dyk *et al*. (1995) [443] |
| | WM1202 | | Van Dyk *et al*. (1995) [443] |
| | WM1302 | | Van Dyk *et al*. (1995) [443] |
| | NHEX-R | ON (DNA and protein damages) | Hever and Belkin (2006) [474] |
| | DUAL22 | ON (DNA and oxidative stresses) | Mitchell *et al.* (2004) [469] |
| *Pseudomonas aeruginosa* | RM4440 | ON (DNA damage) | Elasri *et al*. (2000) [475] |
| | | | Elasri *et al.* (1998) [476] |
| *Pseudomonas fluorescence* | 10568 (pUCD607) | OFF | Bhattacharyya *et al.* (2005) [477] |
| | | | Flynn *et al*. (2002) [478] |
| | | | Paton *et al.* (2006) [479] |
| | | | Sousa *et al*. (1998) [480] |
| | OS8 (Kn*lux*) | OFF | Ivask *et al*. (2009) [450] |
| | Shk1 | OFF | Kelly *et al*. (2004) [481] |
| | | | Lajoie *et al*. (2003) [482] |
| | | | Kelly *et al*. (1999) [483] |
| *Pseudomonas putida* | F1 (pUCD607) | OFF | Diplock *et al*. (2010) [484] |
| | | | Dawson *et al.* (2008) [485] |
| | BS566 | OFF | Wiles *et al.* (2003) [367] |
| *Salmonella typhimurium* | TA1535 (pSWITCH) | ON (DNA damage) | Baumstark-Khan *et al*. (2005) [486] |
| | Sal94 | ON (DNA damage) | Davidov *et al*. (2000) [456] |

# Appendix B - Supplementary information of Chapter 2.

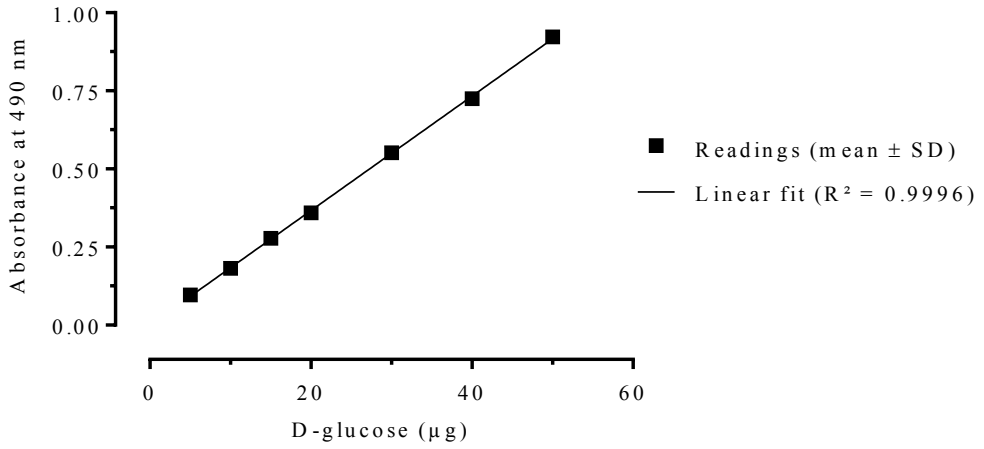


**Fig. S2.1: Calibration curve for the D-glucose quantification.** An example of obtained calibration curve whilst performing the D-glucose quantification (using a D-glucose solution at 1 mg $mL^{-1}$ as standard) *via* the phenol - sulphuric acid based method is presented above.

A.

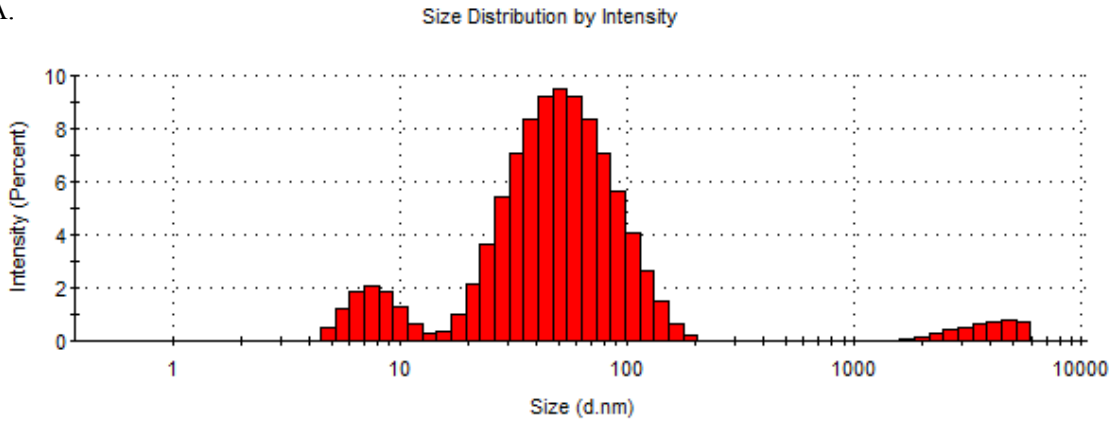


B.

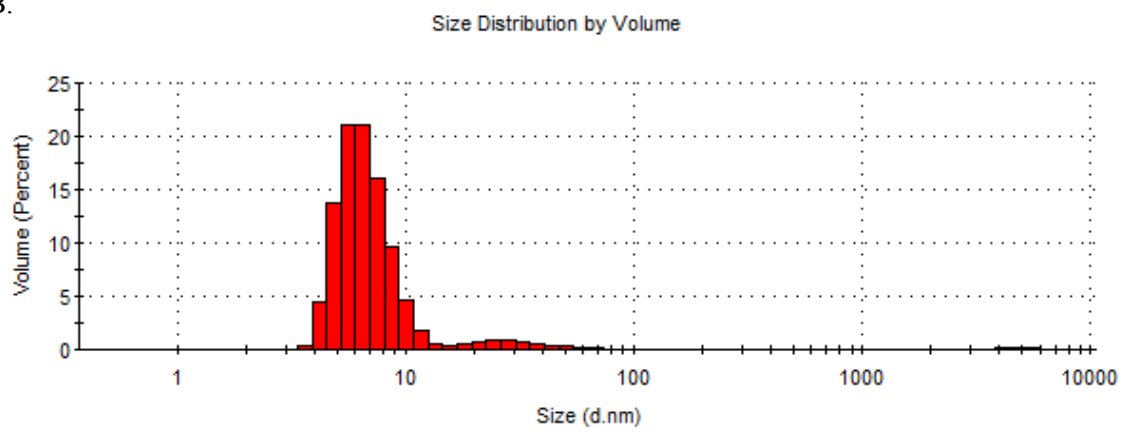


**Fig. S2.2: Generated DLS output data.** Examples of generated DLS (*i.e.* z-average) data using the pristine Ag NM-300K NPs at 10 mg $L^{-1}$ in AW are presented with a size/intensity plot in A and the corresponding size/volume plot n B (Z-average: 39.5 nm, PdI: 0.416, Intercept: 0.854, Quality: good).

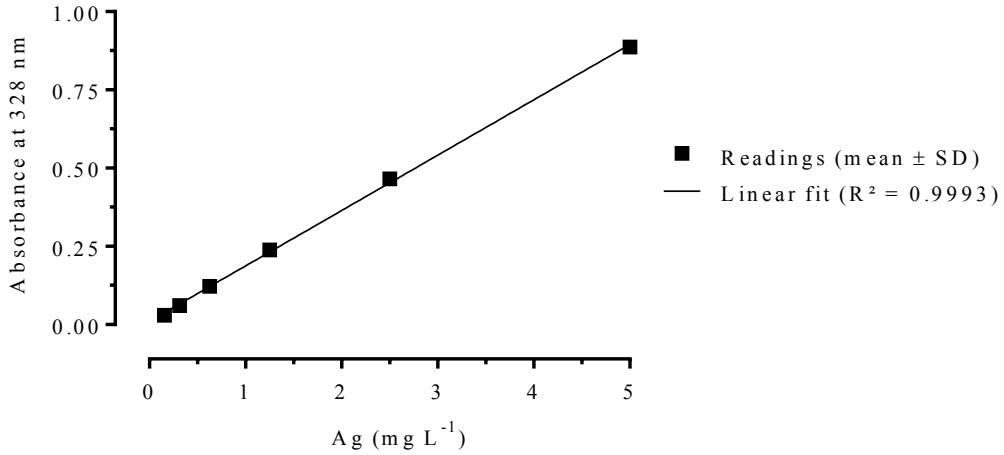


**Fig. S2.3: AAS calibration curve for Ag.** An example of calibration curve obtained by AAS using the Ag pure single element standard at concentrations of 0.156, 0.312, 0.625, 1.25, 2.5 and 5 mg $L^{-1}$is presented.

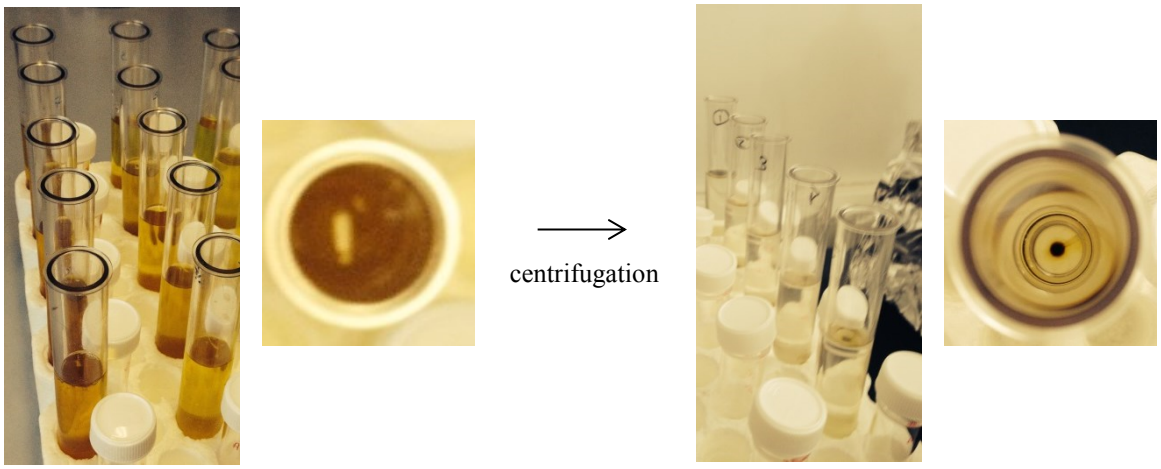


**Fig. S2.4: Ag NPs pelleting by ultracentrifugation.** Suspensions of Ag NM-300K NPs at 50 mg $L^{-1}$ in AW were ultracentrifuged at 4 °C in 15 mL open-top polycarbonate tubes at *ca*. 50 000 x g for 30 min; pictures of sample *pre* and *post* centrifugation are shown above.

# Appendix C - Supplementary information of Chapter 3.

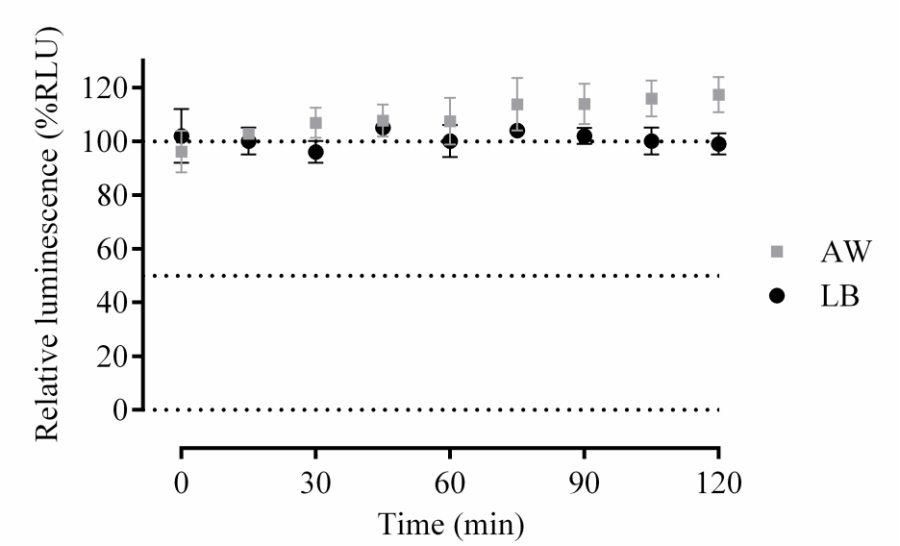


**Fig. S3.1: Toxicity of the sole Ag NM-300K dispersant in LB and AW.** Relative luminescence output evolutions over time by *P. putida* BS566::luxCDABE when challenged with 50 mg $L^{-1}$ of the sole Ag NM-300K dispersant in LB and AW are shown above. Data are mean ± SEM (n = 3).

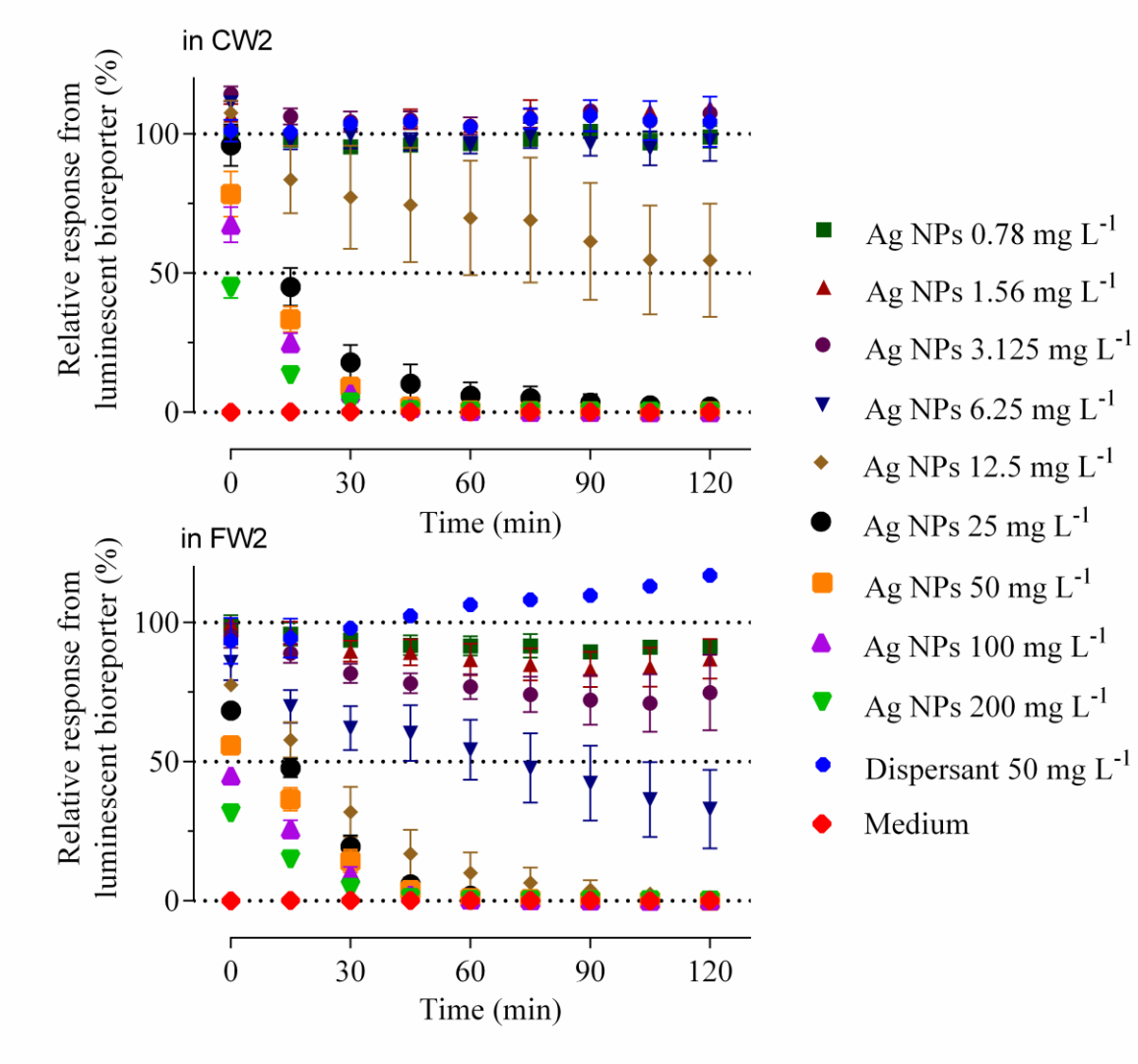


**Fig. S3.2: Real time monitoring of Ag NP toxicity in wastewaters from site 2.** Relative luminescence output evolutions over time by *P. putida* BS566::luxCDABE when challenged with 0 – 200 mg $L^{-1}$ of Ag NM-300K NPs in crude or final wastewater samples (CW2 and FW2, respectively) are shown. Background signal from used matrices and effect of Ag NM-300K dispersant (at 50 mg $L^{-1}$) are also proposed. Data are mean ± SEM (n = 4).

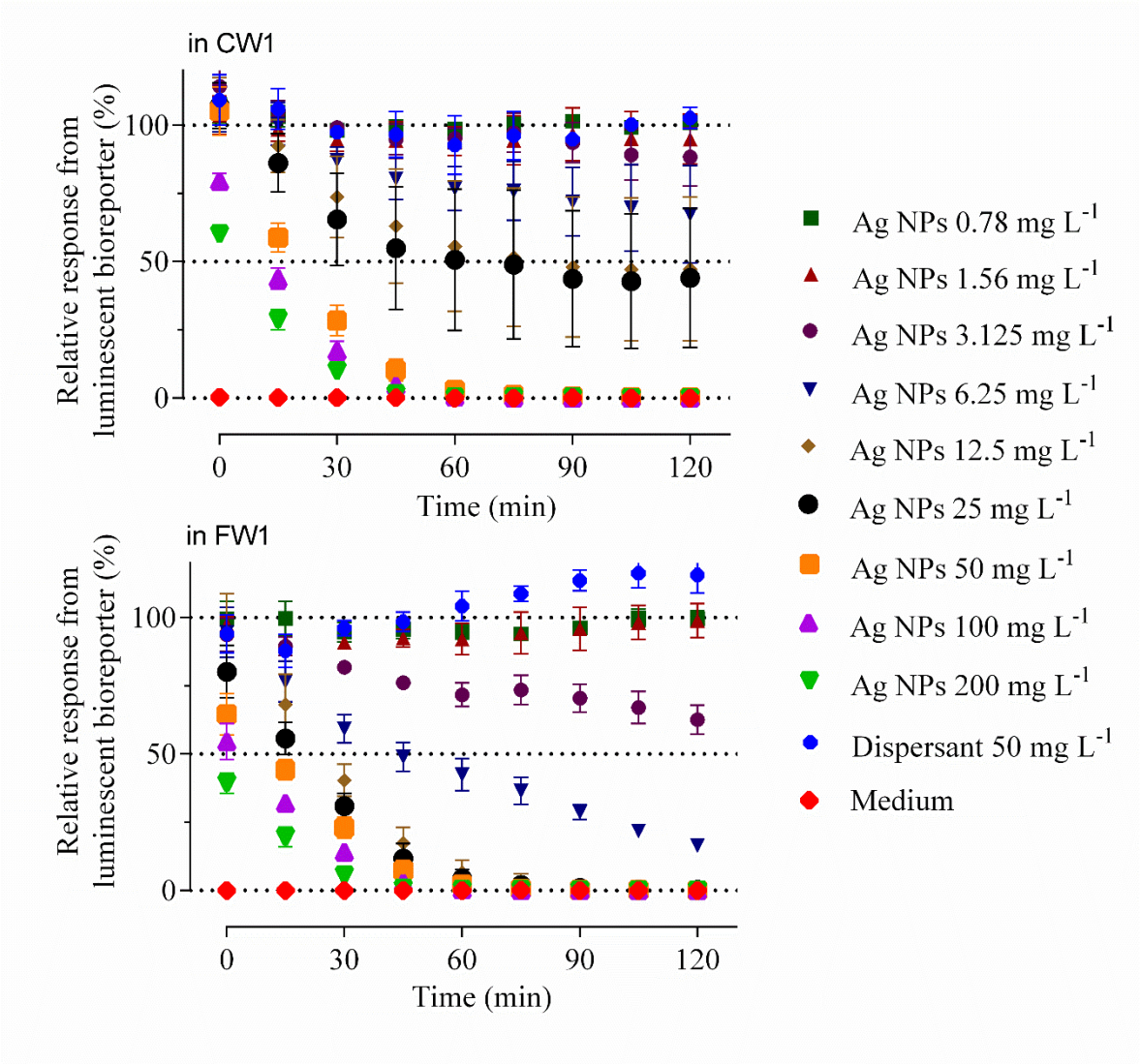


**Fig. S3.3: Real time monitoring of Ag NP toxicity in wastewaters from site 1.** Relative luminescence output evolutions over time by *P. putida* BS566::luxCDABE when challenged with 0 – 200 mg $L^{-1}$ of Ag NM-300K NPs in crude or final wastewater samples (CW1 and FW1, respectively) are shown. Background signal from used matrices and effect of Ag NM-300K dispersant (at 50 mg $L^{-1}$) are also proposed. Data are mean ± SEM (n = 4).

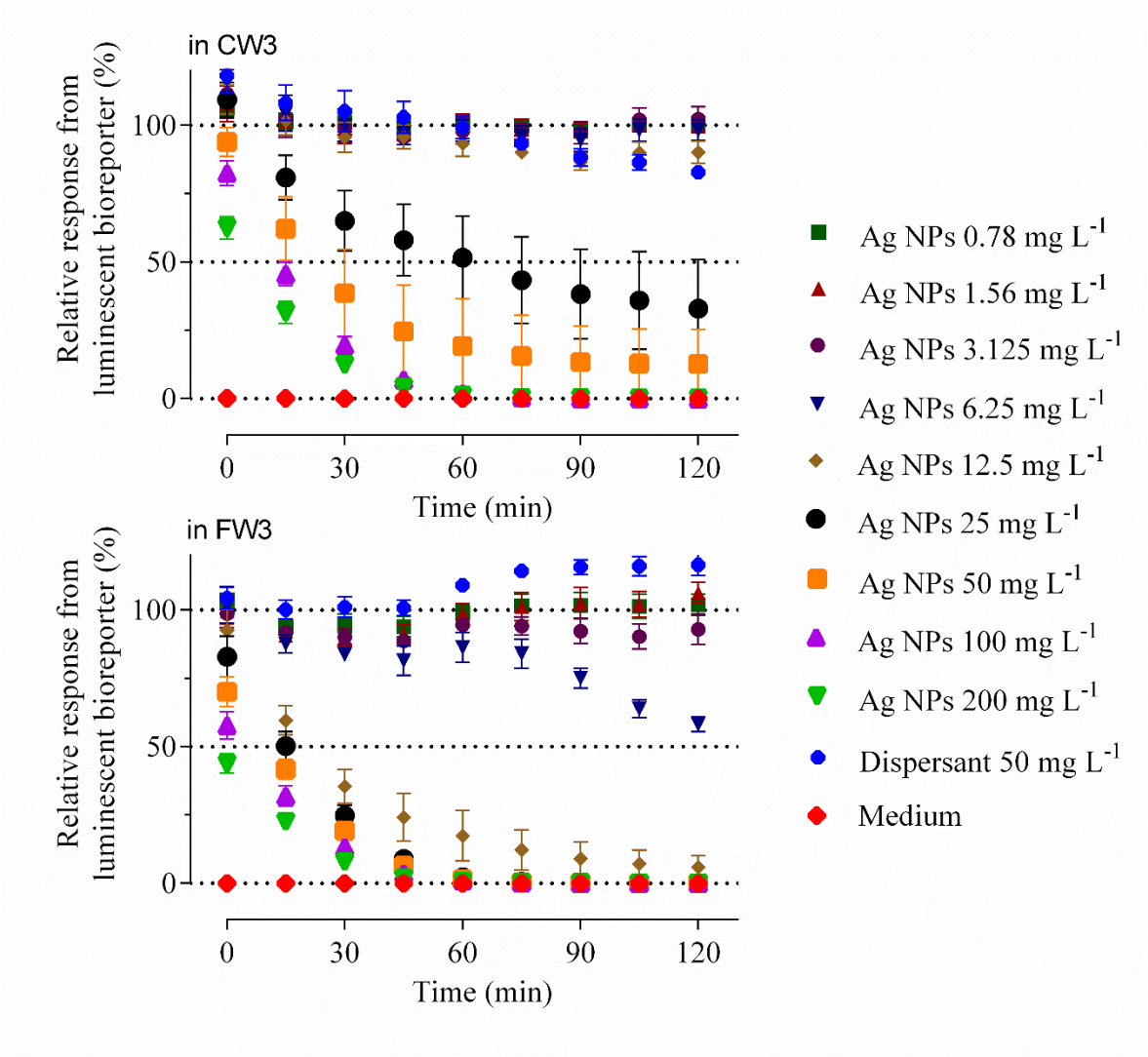


**Fig. S3.4: Real time monitoring of Ag NP toxicity in wastewaters from site 3.** Relative luminescence output evolutions over time by *P. putida* BS566::luxCDABE when challenged with 0 – 200 mg $L^{-1}$ of Ag NM-300K NPs in crude or final wastewater samples (CW3 and FW3, respectively) are shown. Background signal from used matrices and effect of Ag NM-300K dispersant (at 50 mg $L^{-1}$) are also proposed. Data are mean ± SEM (n = 4).

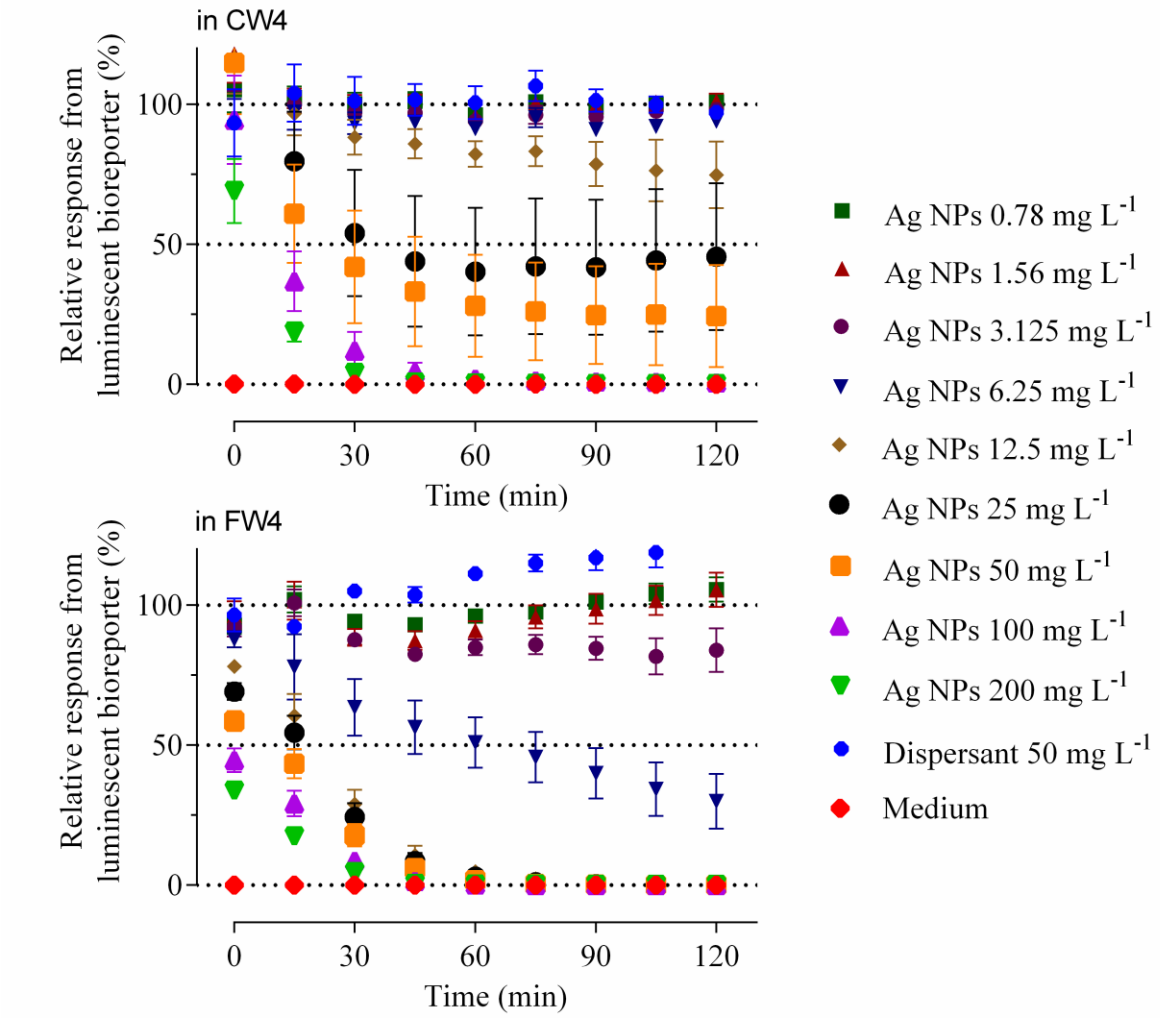


**Fig. S3.5: Real time monitoring of Ag NP toxicity in wastewaters from site 4.** Relative luminescence output evolutions over time by *P. putida* BS566::luxCDABE when challenged with 0 – 200 mg $L^{-1}$ of Ag NM-300K NPs in crude or final wastewater samples (CW4 and FW4, respectively) are shown. Background signal from used matrices and effect of Ag NM-300K dispersant (at 50 mg $L^{-1}$) are also proposed. Data are mean ± SEM (n = 4).

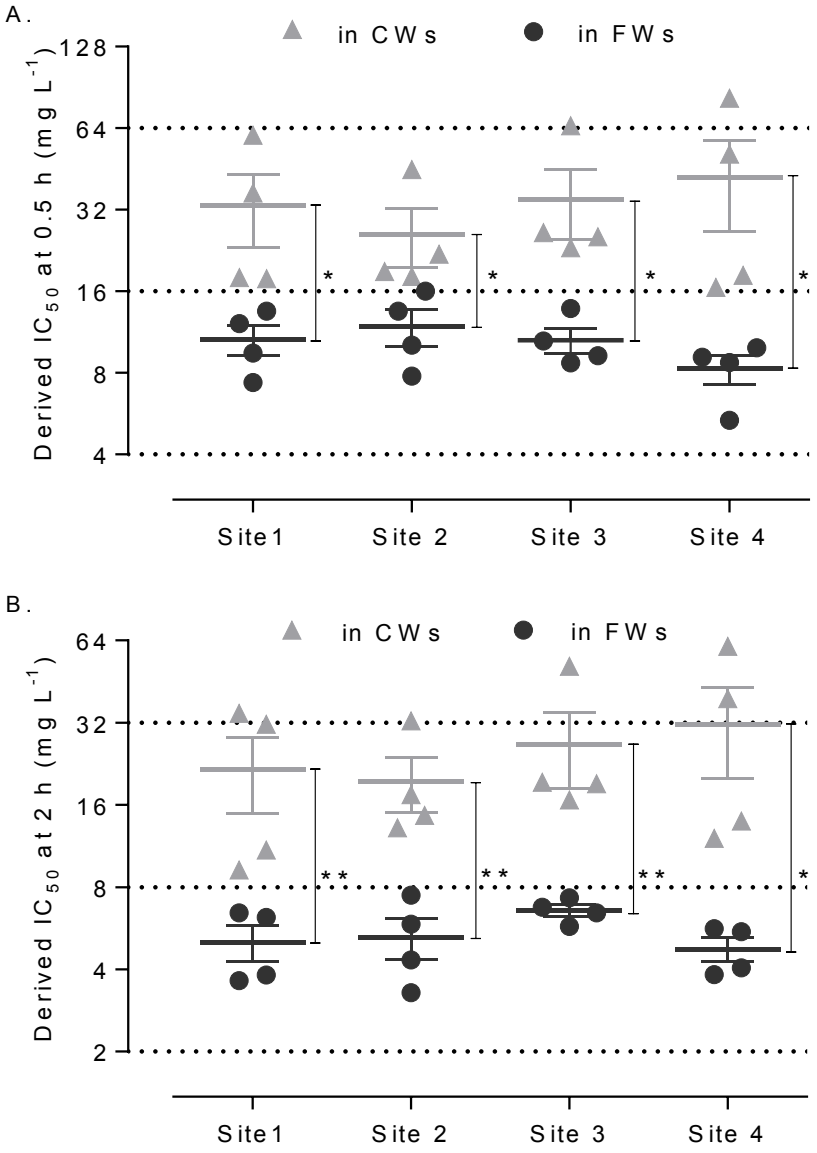


**Fig. S3.6: Derived $IC_{50}$ values.** Toxicity results from light output reductions by *P. putida* BS566::luxCDABE when exposed to Ag NM-300K NPs in crude or final wastewaters (CWs and FWs, respectively) from four different wastewater treatment plants (site 1 to 4) were plotted as (response) = f(log[Ag NPs]) for selected time points and $IC_{50}$ values were derived by fitting a four parameter dose-response model. Graphic A and B show the comparison of calculated $IC_{50}$ values at 0.5 and 2 h, respectively. Data are mean ± SEM (n = 4), significantly different by unpaired t-test with $p < 0.1$ (*) or $< 0.05$ (**).

# Appendix D - Supplementary information of Chapter 4.

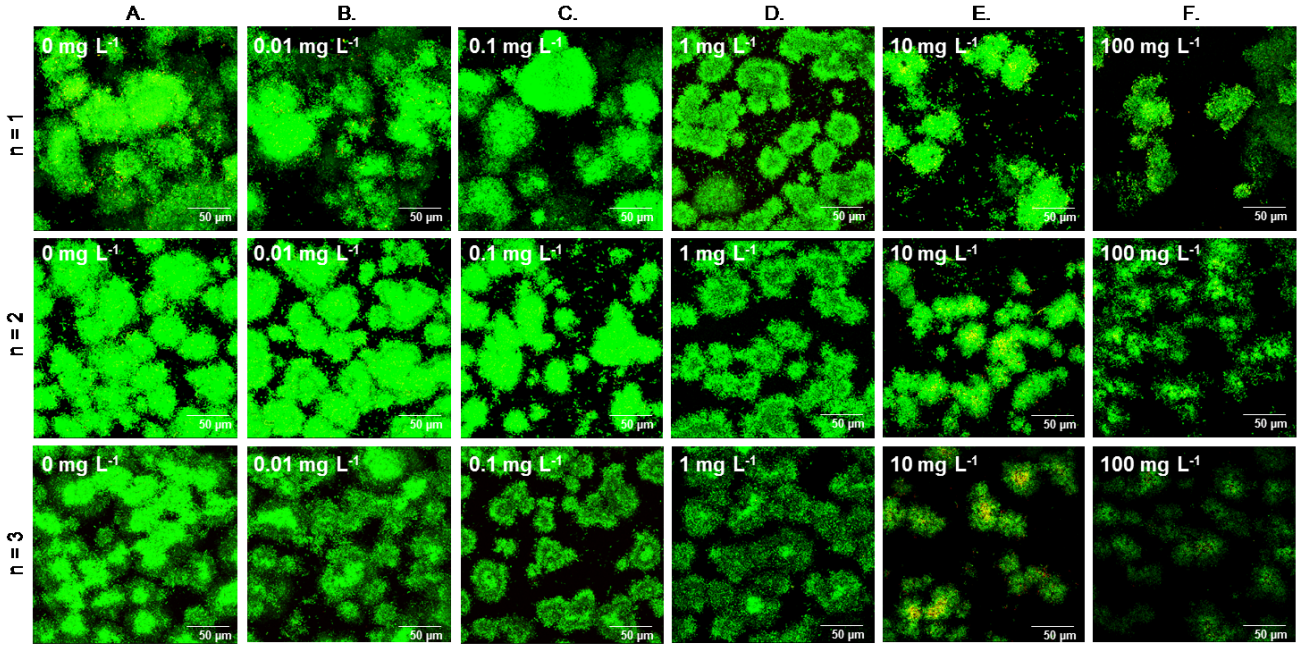


**Fig. S4.1: Biofilm morphology characterisation *post* exposure to the Ag NM-300K NPs.** Additional examples of result at 72 h (*i.e. post* exposure) from three replicated experiments are presented above as support for the Fig. 4.1 (bottom row), therefore the same caption applies.

| | 48 h vs 72 h | 72 h vs 96 h | 48 h vs 96 h |
|---|---|---|---|
| 0 mg $L^{-1}$ | **↗ | **↗ | **↗ |
| 0.01 (0.001) mg $L^{-1}$ | **↗ (**↗) | NSD (*↗) | **↗ (**↗) |
| 0.1 (0.01) mg $L^{-1}$ | *↗ (*↗) | NSD (**↗) | **↗ (**↗) |
| 1 (0.1) mg $L^{-1}$ | *↗ (*↘) | NSD (**↗) | **↗ (*↗) |
| 10 (1) mg $L^{-1}$ | NSD (**↘) | NSD (*↗) | NSD (NSD) |
| 100 (10) mg $L^{-1}$ | **↘ (**↘) | NSD (NSD) | NSD (**↘) |
| Virkon 1 % | **↘ | NSD | **↘ |

**Fig. S4.2: Statistical analysis of the reported microbial activity results.** The output results from the statistical analysis *via* multiple t-tests (corrected with the Holm-Sidak method) considering two parameters at a time are shown. The NP case is reported in blue, the ion case in red. Significantly different between time points (increased or decreased activity over time) with a $p < 0.1$ (*) or $< 0.05$ (**). Non-significantly different (NSD).

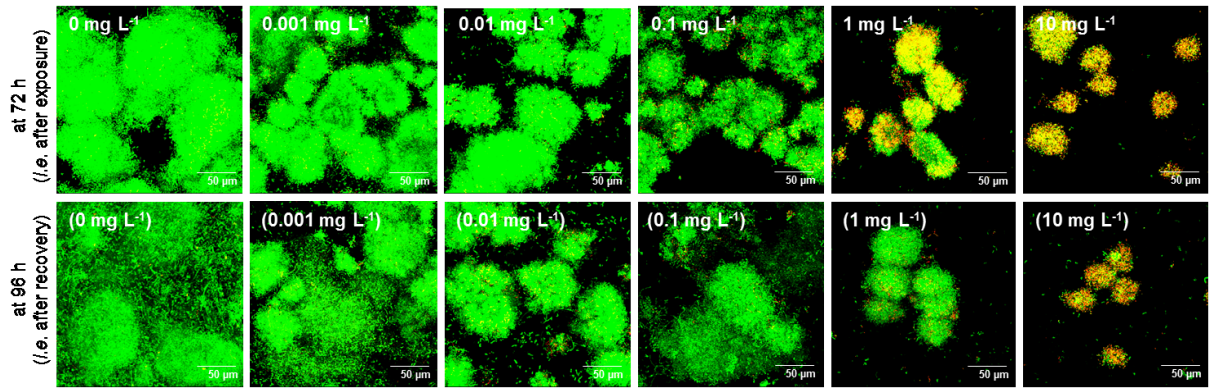


**Fig. S4.3: Biofilm morphology characterisation *post* exposure to the Ag ions.** *Pseudomonas putida* mono-species biofilms were cultured in AW in CLSM compatible flow-cells for 48 h then exposed to 0, 0.001, 0.01, 0.1, 1 and 10 mg $L^{-1}$ of Ag ions for 24 h (from A to F respectively). Biofilms were analysed by CLSM after live/dead staining at 72 h (*i.e. post* exposure, top row) and at 96 h (*i.e. post* recovery, bottom row). Representative examples of maximised z-stack are shown. Each image represents 1 out of 7 z-stacks randomly registered *per* condition for 1 experiment (n = 3). Scale is 50 µm wide.

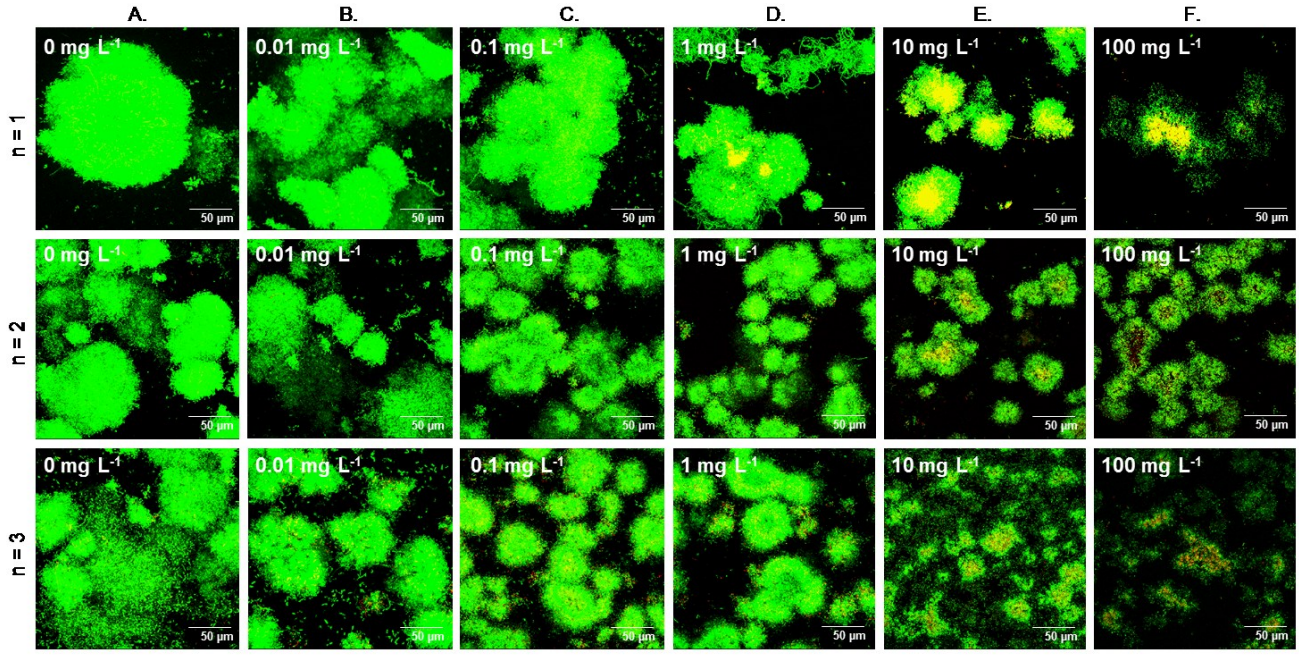


**Fig. S4.4: Biofilm recovery assessment *post* exposure to the Ag NM-300K NPs.** Supplementary examples of result at 96 h (*i.e. post* recovery) from three replicated experiments are presented above as support for the Fig. 4.5, therefore the same caption applies.

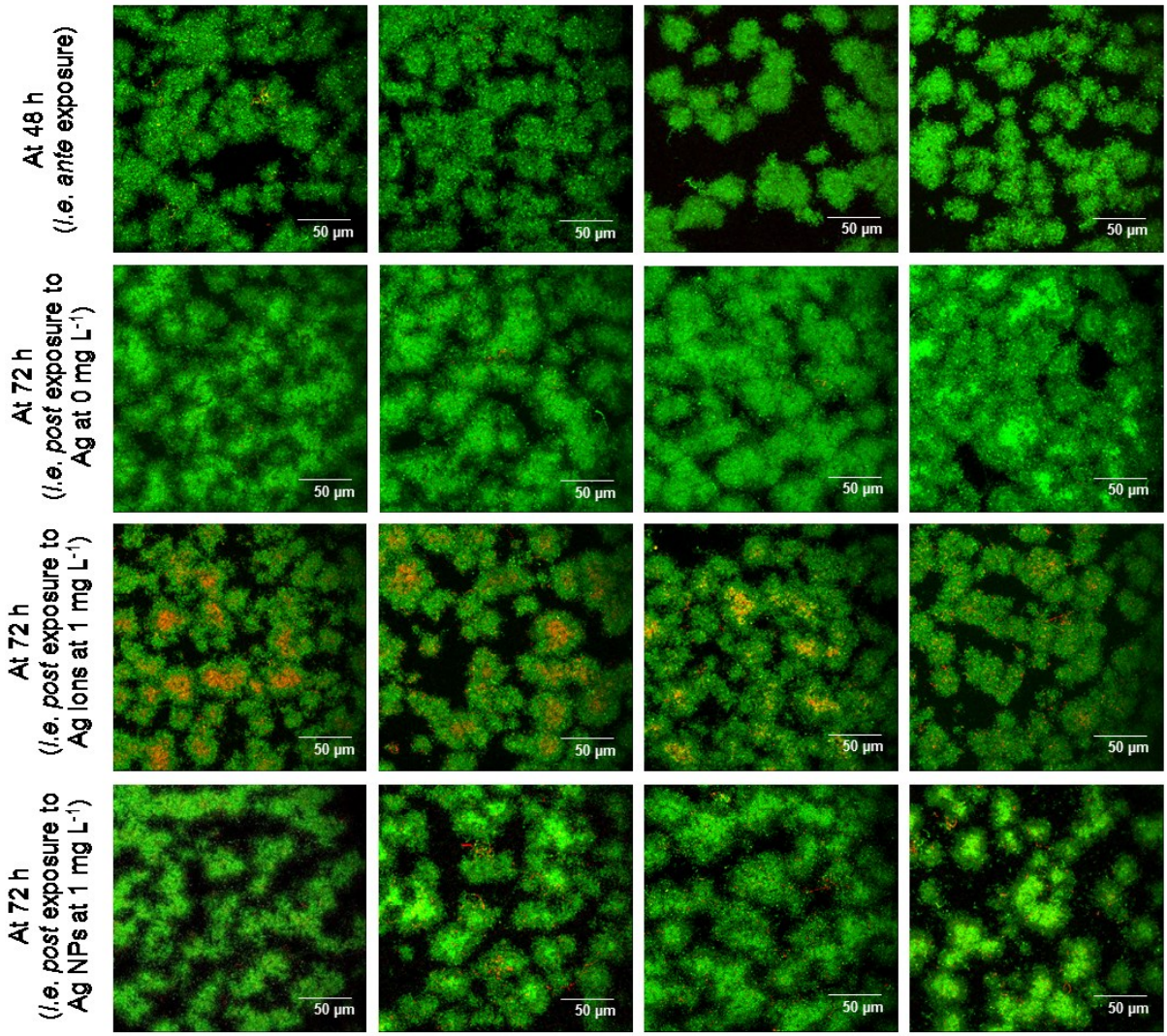


**Fig. S4.5: Morphology characterisation of D-fructose fed biofilms *ante* and *post* exposure to the Ag NPs/ions.** *Pseudomonas putida* mono-species biofilms were cultured in AW supplemented with D-fructose in CLSM compatible flow-cells for 48 h then exposed to 1 mg $L^{-1}$ of Ag NPs or Ag ions for 24 h. Biofilms were analysed by CLSM after live/dead staining at 48 h (*i.e. ante* exposure) and at 72 h (*i.e. post* exposure). Representative examples of maximised z-stack are shown. Each image represents 1 out of 7 z-stacks randomly registered *per* condition for 1 experiment (n = 4). Scale is 50 µm wide.

**Table S4.1: Template of the extracted gDNA samples sent to sequencing.**

| Sample Reference | Identification | $Abs_{260/280}$ | $Abs_{260/230}$ | Final gDNA concentration (ng/µL) | Final volume (µL) |
|---|---|---|---|---|---|
| A | original CW (no CLSM dyes) | 1.85 | 1.59 | 52.7 | 50 |
| B | pre-cultured CW (no CLSM dyes) | 2.11 | 2.12 | 75.6 | |
| C | channel 2, control 48 h, flow-cell 1 (no CLSM dyes) | 2.02 | 1.79 | 825.3 | |
| D | channel 5, control 48 h, flow-cell 2 (no CLSM dyes) | 1.99 | 1.68 | 676.2 | |
| E | channel 8, control 48 h, flow-cell 3 (no CLSM dyes) | 2.04 | 1.73 | 590.1 | |
| F | channel 10, control 48 h, flow-cell 4 (no CLSM dyes) | 1.68 | 1.11 | 40.2 | |
| G | channel 1, control 72 h, flow-cell 1 (CLSM dyes) | 2.02 | 1.84 | 726.6 | |
| H | channel 3, control 72 h, flow-cell 1 (no CLSM dyes) | 1.97 | 2.04 | 1050.0 | |
| I | channel 4, 1 µg $L^{-1}$ Ag NPs 72 h, flow-cell 2 (CLSM dyes) | 1.98 | 1.78 | 745.5 | |
| J | channel 6, 1 µg $L^{-1}$ Ag NPs 72 h, flow-cell 2 (no CLSM dyes) | 2.02 | 1.57 | 413.7 | |
| K | channel 7, 1 mg $L^{-1}$ Ag NPs 72 h, flow-cell 3 (CLSM dyes) | 1.94 | 1.79 | 858.9 | |
| L | channel 9, 1 mg $L^{-1}$ Ag NPs 72 h, flow-cell 3 (no CLSM dyes) | 1.79 | 1.07 | 96.6 | |
| M | channel 12, 1 mg $L^{-1}$ Ag ions 72 h, flow-cell 4 (CLSM dyes) | 2.03 | 1.96 | 1052.1 | |
| N | channel 11, 1 mg $L^{-1}$ Ag ions 72 h, flow-cell 4 (no CLSM dyes) | 1.99 | 2.07 | 949.2 | |

**Table S4.2: OTU table at L6.** Sample references (from A to F) are detailed in Table S4.1.

| | Sample Reference | | | | | | | | | | | | | |
|---|---|---|---|---|---|---|---|---|---|---|---|---|---|---|
| **OTU ID** | A | B | C | D | E | F | G | H | I | J | K | L | M | N |
| Acidobacteria;c__Acidobacteria-6;o__iii1-15;f__;g__ | 0,00E+00 | 0,00E+00 | 0,00E+00 | 0,00E+00 | 0,00E+00 | 0,00E+00 | 0,00E+00 | 0,00E+00 | 0,00E+00 | 0,00E+00 | 5,88E-05 | 0,00E+00 | 0,00E+00 | 1,24E-03 |
| Acidobacteria;c__Acidobacteria-6;o__iii1-15;f__RB40;g__ | 0,00E+00 | 0,00E+00 | 0,00E+00 | 0,00E+00 | 0,00E+00 | 0,00E+00 | 0,00E+00 | 0,00E+00 | 0,00E+00 | 0,00E+00 | 0,00E+00 | 0,00E+00 | 0,00E+00 | 1,18E-04 |
| Acidobacteria;c__Acidobacteria-6;o__iii1-15;f__mb2424;g__ | 0,00E+00 | 0,00E+00 | 0,00E+00 | 0,00E+00 | 0,00E+00 | 0,00E+00 | 0,00E+00 | 0,00E+00 | 0,00E+00 | 0,00E+00 | 0,00E+00 | 0,00E+00 | 0,00E+00 | 1,76E-04 |
| Acidobacteria;c__Sva0725;o__Sva0725;f__;g__ | 0,00E+00 | 0,00E+00 | 0,00E+00 | 0,00E+00 | 0,00E+00 | 0,00E+00 | 0,00E+00 | 0,00E+00 | 0,00E+00 | 0,00E+00 | 0,00E+00 | 0,00E+00 | 0,00E+00 | 3,53E-04 |
| Acidobacteria;c__[Chloracidobacteria];o__RB41;f__;g__ | 0,00E+00 | 0,00E+00 | 0,00E+00 | 5,88E-05 | 0,00E+00 | 0,00E+00 | 0,00E+00 | 0,00E+00 | 0,00E+00 | 0,00E+00 | 0,00E+00 | 0,00E+00 | 0,00E+00 | 1,71E-03 |
| Acidobacteria;c__[Chloracidobacteria];o__RB41;f__Ellin6075;g__ | 0,00E+00 | 0,00E+00 | 0,00E+00 | 0,00E+00 | 0,00E+00 | 0,00E+00 | 0,00E+00 | 0,00E+00 | 0,00E+00 | 0,00E+00 | 0,00E+00 | 0,00E+00 | 0,00E+00 | 4,71E-04 |
| Acidobacteria;c__iii1-8;o__32-20;f__;g__ | 0,00E+00 | 0,00E+00 | 0,00E+00 | 0,00E+00 | 0,00E+00 | 0,00E+00 | 0,00E+00 | 0,00E+00 | 0,00E+00 | 0,00E+00 | 0,00E+00 | 0,00E+00 | 0,00E+00 | 7,65E-04 |
| Actinobacteria;c__Acidimicrobiia;o__Acidimicrobiales;f__;g__ | 0,00E+00 | 0,00E+00 | 0,00E+00 | 0,00E+00 | 0,00E+00 | 0,00E+00 | 0,00E+00 | 0,00E+00 | 0,00E+00 | 0,00E+00 | 0,00E+00 | 0,00E+00 | 0,00E+00 | 5,29E-04 |
| Actinobacteria;c__Acidimicrobiia;o__Acidimicrobiales;f__AKIW874;g__ | 0,00E+00 | 0,00E+00 | 0,00E+00 | 0,00E+00 | 0,00E+00 | 0,00E+00 | 0,00E+00 | 0,00E+00 | 0,00E+00 | 0,00E+00 | 0,00E+00 | 0,00E+00 | 0,00E+00 | 1,76E-04 |
| Actinobacteria;c__Acidimicrobiia;o__Acidimicrobiales;f__C111;g__ | 0,00E+00 | 5,88E-05 | 0,00E+00 | 0,00E+00 | 0,00E+00 | 0,00E+00 | 5,88E-05 | 0,00E+00 | 0,00E+00 | 0,00E+00 | 0,00E+00 | 0,00E+00 | 0,00E+00 | 6,47E-04 |
| Actinobacteria;c__Acidimicrobiia;o__Acidimicrobiales;f__EB1017;g__ | 0,00E+00 | 0,00E+00 | 0,00E+00 | 0,00E+00 | 0,00E+00 | 0,00E+00 | 0,00E+00 | 0,00E+00 | 0,00E+00 | 0,00E+00 | 0,00E+00 | 0,00E+00 | 0,00E+00 | 4,71E-04 |
| Actinobacteria;c__Acidimicrobiia;o__Acidimicrobiales;f__Iamiaceae;g__Iamia | 0,00E+00 | 0,00E+00 | 0,00E+00 | 0,00E+00 | 0,00E+00 | 0,00E+00 | 0,00E+00 | 0,00E+00 | 0,00E+00 | 0,00E+00 | 5,88E-05 | 0,00E+00 | 0,00E+00 | 5,88E-05 |
| Actinobacteria;c__Actinobacteria;o__Actinomycetales;f__;g__ | 1,18E-04 | 0,00E+00 | 0,00E+00 | 0,00E+00 | 0,00E+00 | 0,00E+00 | 0,00E+00 | 0,00E+00 | 0,00E+00 | 0,00E+00 | 0,00E+00 | 0,00E+00 | 0,00E+00 | 0,00E+00 |
| Actinobacteria;c__Actinobacteria;o__Actinomycetales;f__Actinomycetaceae;g__ | 1,18E-04 | 1,18E-04 | 5,88E-05 | 0,00E+00 | 0,00E+00 | 0,00E+00 | 0,00E+00 | 0,00E+00 | 0,00E+00 | 0,00E+00 | 0,00E+00 | 0,00E+00 | 0,00E+00 | 0,00E+00 |
| Actinobacteria;c__Actinobacteria;o__Actinomycetales;f__Actinomycetaceae;g__Actinor | 2,94E-04 | 5,88E-05 | 0,00E+00 | 0,00E+00 | 0,00E+00 | 0,00E+00 | 0,00E+00 | 0,00E+00 | 0,00E+00 | 0,00E+00 | 0,00E+00 | 0,00E+00 | 0,00E+00 | 0,00E+00 |
| Actinobacteria;c__Actinobacteria;o__Actinomycetales;f__Cellulomonadaceae;Other | 5,29E-04 | 0,00E+00 | 5,88E-05 | 0,00E+00 | 0,00E+00 | 5,88E-05 | 0,00E+00 | 0,00E+00 | 0,00E+00 | 0,00E+00 | 0,00E+00 | 0,00E+00 | 0,00E+00 | 0,00E+00 |
| Actinobacteria;c__Actinobacteria;o__Actinomycetales;f__Cellulomonadaceae;g__Cellulo | 1,18E-03 | 5,88E-05 | 0,00E+00 | 0,00E+00 | 0,00E+00 | 0,00E+00 | 0,00E+00 | 0,00E+00 | 0,00E+00 | 0,00E+00 | 0,00E+00 | 0,00E+00 | 0,00E+00 | 0,00E+00 |
| Actinobacteria;c__Actinobacteria;o__Actinomycetales;f__Corynebacteriaceae;g__Coryn | 5,88E-05 | 0,00E+00 | 0,00E+00 | 0,00E+00 | 0,00E+00 | 5,88E-05 | 0,00E+00 | 0,00E+00 | 0,00E+00 | 0,00E+00 | 0,00E+00 | 0,00E+00 | 0,00E+00 | 0,00E+00 |
| Actinobacteria;c__Actinobacteria;o__Actinomycetales;f__Dermacoccaceae;g__Dermaco | 2,94E-04 | 0,00E+00 | 0,00E+00 | 0,00E+00 | 0,00E+00 | 0,00E+00 | 0,00E+00 | 0,00E+00 | 0,00E+00 | 0,00E+00 | 0,00E+00 | 0,00E+00 | 0,00E+00 | 0,00E+00 |
| Actinobacteria;c__Actinobacteria;o__Actinomycetales;f__Geodermatophilaceae;g__ | 0,00E+00 | 0,00E+00 | 0,00E+00 | 0,00E+00 | 0,00E+00 | 0,00E+00 | 0,00E+00 | 0,00E+00 | 0,00E+00 | 0,00E+00 | 0,00E+00 | 0,00E+00 | 0,00E+00 | 3,53E-04 |
| Actinobacteria;c__Actinobacteria;o__Actinomycetales;f__Intrasporangiaceae;g__ | 5,88E-05 | 5,88E-05 | 0,00E+00 | 5,88E-05 | 0,00E+00 | 0,00E+00 | 0,00E+00 | 0,00E+00 | 0,00E+00 | 0,00E+00 | 0,00E+00 | 0,00E+00 | 0,00E+00 | 4,71E-04 |
| Actinobacteria;c__Actinobacteria;o__Actinomycetales;f__Microbacteriaceae;Other | 2,94E-04 | 1,76E-04 | 0,00E+00 | 0,00E+00 | 0,00E+00 | 0,00E+00 | 0,00E+00 | 0,00E+00 | 0,00E+00 | 0,00E+00 | 0,00E+00 | 0,00E+00 | 0,00E+00 | 0,00E+00 |
| Actinobacteria;c__Actinobacteria;o__Actinomycetales;f__Microbacteriaceae;g__Agromy | 5,88E-05 | 0,00E+00 | 0,00E+00 | 0,00E+00 | 0,00E+00 | 5,88E-05 | 0,00E+00 | 0,00E+00 | 0,00E+00 | 0,00E+00 | 0,00E+00 | 0,00E+00 | 0,00E+00 | 4,12E-04 |
| Actinobacteria;c__Actinobacteria;o__Actinomycetales;f__Microbacteriaceae;g__Cryoco | 6,47E-04 | 4,47E-03 | 7,06E-04 | 0,00E+00 | 0,00E+00 | 0,00E+00 | 0,00E+00 | 0,00E+00 | 0,00E+00 | 0,00E+00 | 0,00E+00 | 0,00E+00 | 0,00E+00 | 2,35E-04 |
| Actinobacteria;c__Actinobacteria;o__Actinomycetales;f__Microbacteriaceae;g__Leucob | 2,35E-03 | 1,86E-02 | 2,00E-03 | 1,18E-04 | 0,00E+00 | 5,88E-05 | 0,00E+00 | 0,00E+00 | 0,00E+00 | 0,00E+00 | 0,00E+00 | 0,00E+00 | 0,00E+00 | 0,00E+00 |
| Actinobacteria;c__Actinobacteria;o__Actinomycetales;f__Microbacteriaceae;g__Microba | 1,29E-03 | 2,00E-03 | 1,18E-04 | 0,00E+00 | 0,00E+00 | 0,00E+00 | 1,18E-04 | 0,00E+00 | 0,00E+00 | 1,76E-04 | 0,00E+00 | 0,00E+00 | 0,00E+00 | 0,00E+00 |
| Actinobacteria;c__Actinobacteria;o__Actinomycetales;f__Micrococcaceae;g__ | 1,12E-03 | 8,82E-04 | 0,00E+00 | 0,00E+00 | 0,00E+00 | 0,00E+00 | 0,00E+00 | 0,00E+00 | 0,00E+00 | 0,00E+00 | 0,00E+00 | 5,88E-05 | 0,00E+00 | 1,18E-03 |
| Actinobacteria;c__Actinobacteria;o__Actinomycetales;f__Micromonosporaceae;Other | 0,00E+00 | 0,00E+00 | 0,00E+00 | 0,00E+00 | 0,00E+00 | 0,00E+00 | 0,00E+00 | 0,00E+00 | 0,00E+00 | 0,00E+00 | 0,00E+00 | 0,00E+00 | 0,00E+00 | 4,12E-04 |
| Actinobacteria;c__Actinobacteria;o__Actinomycetales;f__Micromonosporaceae;g__Act | 0,00E+00 | 0,00E+00 | 0,00E+00 | 0,00E+00 | 0,00E+00 | 0,00E+00 | 0,00E+00 | 0,00E+00 | 0,00E+00 | 0,00E+00 | 0,00E+00 | 0,00E+00 | 0,00E+00 | 1,76E-04 |
| Actinobacteria;c__Actinobacteria;o__Actinomycetales;f__Mycobacteriaceae;g__Mycoba | 2,35E-04 | 1,18E-04 | 0,00E+00 | 0,00E+00 | 5,88E-05 | 0,00E+00 | 0,00E+00 | 0,00E+00 | 0,00E+00 | 0,00E+00 | 0,00E+00 | 0,00E+00 | 0,00E+00 | 1,59E-03 |
| Actinobacteria;c__Actinobacteria;o__Actinomycetales;f__Nocardiaceae;g__Rhodococc | 5,88E-05 | 5,41E-03 | 8,24E-04 | 0,00E+00 | 0,00E+00 | 5,88E-05 | 0,00E+00 | 0,00E+00 | 0,00E+00 | 0,00E+00 | 0,00E+00 | 0,00E+00 | 0,00E+00 | 0,00E+00 |
| Actinobacteria;c__Actinobacteria;o__Actinomycetales;f__Nocardioidaceae;g__ | 0,00E+00 | 0,00E+00 | 0,00E+00 | 0,00E+00 | 0,00E+00 | 5,88E-05 | 0,00E+00 | 0,00E+00 | 0,00E+00 | 0,00E+00 | 0,00E+00 | 0,00E+00 | 0,00E+00 | 5,29E-04 |
| Actinobacteria;c__Actinobacteria;o__Actinomycetales;f__Nocardioidaceae;g__Kribbella | 0,00E+00 | 0,00E+00 | 0,00E+00 | 0,00E+00 | 0,00E+00 | 0,00E+00 | 0,00E+00 | 0,00E+00 | 0,00E+00 | 0,00E+00 | 0,00E+00 | 0,00E+00 | 0,00E+00 | 2,35E-04 |
| Actinobacteria;c__Actinobacteria;o__Actinomycetales;f__Nocardioidaceae;g__Nocardio | 0,00E+00 | 1,18E-04 | 0,00E+00 | 0,00E+00 | 0,00E+00 | 0,00E+00 | 0,00E+00 | 0,00E+00 | 0,00E+00 | 0,00E+00 | 0,00E+00 | 0,00E+00 | 0,00E+00 | 0,00E+00 |
| Actinobacteria;c__Actinobacteria;o__Actinomycetales;f__Nocardioidaceae;g__Pimeloba | 0,00E+00 | 5,88E-05 | 0,00E+00 | 0,00E+00 | 0,00E+00 | 0,00E+00 | 0,00E+00 | 0,00E+00 | 0,00E+00 | 0,00E+00 | 0,00E+00 | 0,00E+00 | 0,00E+00 | 0,00E+00 |
| Actinobacteria;c__Actinobacteria;o__Actinomycetales;f__Nocardioidaceae;g__Propionic | 5,88E-05 | 3,53E-04 | 1,18E-04 | 0,00E+00 | 0,00E+00 | 0,00E+00 | 0,00E+00 | 0,00E+00 | 0,00E+00 | 0,00E+00 | 0,00E+00 | 0,00E+00 | 0,00E+00 | 0,00E+00 |
| Actinobacteria;c__Actinobacteria;o__Actinomycetales;f__Propionibacteriaceae;g__ | 1,76E-04 | 0,00E+00 | 0,00E+00 | 0,00E+00 | 0,00E+00 | 0,00E+00 | 0,00E+00 | 0,00E+00 | 0,00E+00 | 0,00E+00 | 0,00E+00 | 0,00E+00 | 0,00E+00 | 0,00E+00 |
| Actinobacteria;c__Actinobacteria;o__Actinomycetales;f__Propionibacteriaceae;g__Lutec | 7,65E-04 | 2,35E-04 | 0,00E+00 | 0,00E+00 | 0,00E+00 | 0,00E+00 | 0,00E+00 | 0,00E+00 | 0,00E+00 | 0,00E+00 | 0,00E+00 | 0,00E+00 | 0,00E+00 | 0,00E+00 |
| Actinobacteria;c__Actinobacteria;o__Actinomycetales;f__Propionibacteriaceae;g__Micr | 0,00E+00 | 0,00E+00 | 0,00E+00 | 0,00E+00 | 0,00E+00 | 0,00E+00 | 0,00E+00 | 0,00E+00 | 0,00E+00 | 0,00E+00 | 0,00E+00 | 0,00E+00 | 0,00E+00 | 4,12E-04 |
| Actinobacteria;c__Actinobacteria;o__Actinomycetales;f__Propionibacteriaceae;g__Prop | 0,00E+00 | 0,00E+00 | 0,00E+00 | 0,00E+00 | 0,00E+00 | 3,53E-04 | 0,00E+00 | 0,00E+00 | 0,00E+00 | 0,00E+00 | 0,00E+00 | 0,00E+00 | 0,00E+00 | 0,00E+00 |
| Actinobacteria;c__Actinobacteria;o__Actinomycetales;f__Pseudonocardiaceae;g__Pseu | 0,00E+00 | 0,00E+00 | 0,00E+00 | 0,00E+00 | 0,00E+00 | 0,00E+00 | 0,00E+00 | 0,00E+00 | 0,00E+00 | 0,00E+00 | 0,00E+00 | 0,00E+00 | 0,00E+00 | 4,71E-04 |
| Actinobacteria;c__Actinobacteria;o__Actinomycetales;f__Streptomycetaceae;g__Strepto | 0,00E+00 | 0,00E+00 | 0,00E+00 | 0,00E+00 | 0,00E+00 | 0,00E+00 | 0,00E+00 | 0,00E+00 | 0,00E+00 | 0,00E+00 | 0,00E+00 | 0,00E+00 | 0,00E+00 | 5,88E-04 |
| Actinobacteria;c__Actinobacteria;o__Bifidobacteriales;f__Bifidobacteriaceae;g__Bifidob | 2,07E-02 | 3,53E-04 | 0,00E+00 | 0,00E+00 | 0,00E+00 | 0,00E+00 | 0,00E+00 | 0,00E+00 | 0,00E+00 | 0,00E+00 | 0,00E+00 | 0,00E+00 | 0,00E+00 | 0,00E+00 |

| | | | | | | | | | | | | | | | |
|---|---|---|---|---|---|---|---|---|---|---|---|---|---|---|---|
| Actinobacteria;c__Actinobacteria;o__Micrococcales;f__;g__ | 0,00E+00 | 0,00E+00 | 0,00E+00 | 0,00E+00 | 0,00E+00 | 0,00E+00 | 0,00E+00 | 0,00E+00 | 0,00E+00 | 0,00E+00 | 0,00E+00 | 0,00E+00 | 0,00E+00 | 0,00E+00 | 1,18E-04 |
| Actinobacteria;c__Coriobacteriia;o__Coriobacteriales;f__Coriobacteriaceae;g__ | 2,29E-03 | 5,88E-05 | 0,00E+00 | 0,00E+00 | 0,00E+00 | 0,00E+00 | 0,00E+00 | 0,00E+00 | 0,00E+00 | 0,00E+00 | 0,00E+00 | 0,00E+00 | 0,00E+00 | 0,00E+00 | 0,00E+00 |
| Actinobacteria;c__Coriobacteriia;o__Coriobacteriales;f__Coriobacteriaceae;g__Adlercre | 3,53E-04 | 0,00E+00 | 0,00E+00 | 0,00E+00 | 0,00E+00 | 0,00E+00 | 0,00E+00 | 0,00E+00 | 0,00E+00 | 0,00E+00 | 0,00E+00 | 0,00E+00 | 0,00E+00 | 0,00E+00 | 0,00E+00 |
| Actinobacteria;c__Coriobacteriia;o__Coriobacteriales;f__Coriobacteriaceae;g__Collinse | 5,98E-02 | 5,29E-04 | 1,18E-04 | 0,00E+00 | 0,00E+00 | 0,00E+00 | 0,00E+00 | 0,00E+00 | 0,00E+00 | 0,00E+00 | 0,00E+00 | 0,00E+00 | 0,00E+00 | 0,00E+00 | 0,00E+00 |
| Actinobacteria;c__Coriobacteriia;o__Coriobacteriales;f__Coriobacteriaceae;g__Eggerthe | 1,76E-04 | 0,00E+00 | 0,00E+00 | 0,00E+00 | 0,00E+00 | 0,00E+00 | 0,00E+00 | 0,00E+00 | 0,00E+00 | 0,00E+00 | 0,00E+00 | 0,00E+00 | 0,00E+00 | 0,00E+00 | 0,00E+00 |
| Actinobacteria;c__Coriobacteriia;o__Coriobacteriales;f__Coriobacteriaceae;g__Slackia | 7,65E-04 | 0,00E+00 | 0,00E+00 | 0,00E+00 | 0,00E+00 | 0,00E+00 | 0,00E+00 | 0,00E+00 | 0,00E+00 | 0,00E+00 | 0,00E+00 | 0,00E+00 | 0,00E+00 | 0,00E+00 | 0,00E+00 |
| Actinobacteria;c__MB-A2-108;o__0319-7L14;f__;g__ | 0,00E+00 | 0,00E+00 | 0,00E+00 | 0,00E+00 | 0,00E+00 | 0,00E+00 | 0,00E+00 | 0,00E+00 | 0,00E+00 | 0,00E+00 | 0,00E+00 | 0,00E+00 | 0,00E+00 | 0,00E+00 | 2,00E-03 |
| Actinobacteria;c__Thermoleophilia;o__Gaiellales;f__Gaiellaceae;g__ | 0,00E+00 | 0,00E+00 | 0,00E+00 | 0,00E+00 | 0,00E+00 | 0,00E+00 | 0,00E+00 | 0,00E+00 | 0,00E+00 | 0,00E+00 | 0,00E+00 | 0,00E+00 | 0,00E+00 | 0,00E+00 | 7,06E-04 |
| Actinobacteria;c__Thermoleophilia;o__Solirubrobacterales;f__;g__ | 0,00E+00 | 0,00E+00 | 0,00E+00 | 0,00E+00 | 0,00E+00 | 0,00E+00 | 0,00E+00 | 0,00E+00 | 0,00E+00 | 0,00E+00 | 0,00E+00 | 0,00E+00 | 0,00E+00 | 5,88E-05 | 5,88E-04 |
| Actinobacteria;c__Thermoleophilia;o__Solirubrobacterales;f__Patulibacteraceae;g__ | 0,00E+00 | 0,00E+00 | 0,00E+00 | 0,00E+00 | 0,00E+00 | 0,00E+00 | 0,00E+00 | 0,00E+00 | 0,00E+00 | 0,00E+00 | 0,00E+00 | 0,00E+00 | 0,00E+00 | 0,00E+00 | 2,35E-04 |
| Actinobacteria;c__Thermoleophilia;o__Solirubrobacterales;f__Solirubrobacteraceae;g__ | 0,00E+00 | 0,00E+00 | 0,00E+00 | 0,00E+00 | 0,00E+00 | 0,00E+00 | 0,00E+00 | 0,00E+00 | 0,00E+00 | 0,00E+00 | 0,00E+00 | 0,00E+00 | 0,00E+00 | 0,00E+00 | 1,18E-04 |
| Armatimonadetes;c__0319-6E2;o__;f__;g__ | 0,00E+00 | 0,00E+00 | 0,00E+00 | 0,00E+00 | 0,00E+00 | 0,00E+00 | 0,00E+00 | 0,00E+00 | 0,00E+00 | 0,00E+00 | 0,00E+00 | 0,00E+00 | 0,00E+00 | 0,00E+00 | 1,18E-04 |
| Bacteroidetes;Other;Other;Other;Other | 5,88E-05 | 1,07E-02 | 9,41E-04 | 0,00E+00 | 0,00E+00 | 0,00E+00 | 0,00E+00 | 0,00E+00 | 0,00E+00 | 0,00E+00 | 0,00E+00 | 0,00E+00 | 0,00E+00 | 0,00E+00 | 0,00E+00 |
| Bacteroidetes;c__Bacteroidia;o__Bacteroidales;f__;g__ | 5,29E-04 | 0,00E+00 | 0,00E+00 | 0,00E+00 | 0,00E+00 | 0,00E+00 | 0,00E+00 | 0,00E+00 | 0,00E+00 | 0,00E+00 | 0,00E+00 | 0,00E+00 | 0,00E+00 | 0,00E+00 | 0,00E+00 |
| Bacteroidetes;c__Bacteroidia;o__Bacteroidales;f__Bacteroidaceae;g__Bacteroides | 8,47E-03 | 6,47E-04 | 1,76E-04 | 0,00E+00 | 0,00E+00 | 1,18E-04 | 0,00E+00 | 0,00E+00 | 0,00E+00 | 0,00E+00 | 0,00E+00 | 0,00E+00 | 0,00E+00 | 0,00E+00 | 0,00E+00 |
| Bacteroidetes;c__Bacteroidia;o__Bacteroidales;f__Marinilabiaceae;g__ | 1,76E-04 | 0,00E+00 | 0,00E+00 | 0,00E+00 | 0,00E+00 | 0,00E+00 | 0,00E+00 | 0,00E+00 | 0,00E+00 | 0,00E+00 | 0,00E+00 | 0,00E+00 | 0,00E+00 | 0,00E+00 | 0,00E+00 |
| Bacteroidetes;c__Bacteroidia;o__Bacteroidales;f__Porphyromonadaceae;g__ | 4,71E-03 | 5,29E-04 | 5,88E-05 | 0,00E+00 | 0,00E+00 | 1,18E-04 | 0,00E+00 | 0,00E+00 | 0,00E+00 | 0,00E+00 | 0,00E+00 | 0,00E+00 | 0,00E+00 | 0,00E+00 | 0,00E+00 |
| Bacteroidetes;c__Bacteroidia;o__Bacteroidales;f__Porphyromonadaceae;g__Dysgonom | 1,76E-04 | 5,88E-05 | 0,00E+00 | 0,00E+00 | 0,00E+00 | 0,00E+00 | 0,00E+00 | 0,00E+00 | 0,00E+00 | 0,00E+00 | 0,00E+00 | 0,00E+00 | 0,00E+00 | 0,00E+00 | 0,00E+00 |
| Bacteroidetes;c__Bacteroidia;o__Bacteroidales;f__Porphyromonadaceae;g__Paludibact | 6,53E-03 | 5,88E-05 | 0,00E+00 | 0,00E+00 | 0,00E+00 | 5,88E-05 | 0,00E+00 | 0,00E+00 | 0,00E+00 | 0,00E+00 | 0,00E+00 | 0,00E+00 | 0,00E+00 | 0,00E+00 | 0,00E+00 |
| Bacteroidetes;c__Bacteroidia;o__Bacteroidales;f__Porphyromonadaceae;g__Parabacte | 7,65E-04 | 0,00E+00 | 0,00E+00 | 0,00E+00 | 0,00E+00 | 0,00E+00 | 0,00E+00 | 0,00E+00 | 0,00E+00 | 0,00E+00 | 0,00E+00 | 0,00E+00 | 0,00E+00 | 0,00E+00 | 0,00E+00 |
| Bacteroidetes;c__Bacteroidia;o__Bacteroidales;f__Prevotellaceae;g__Prevotella | 8,65E-03 | 1,18E-04 | 0,00E+00 | 0,00E+00 | 0,00E+00 | 1,18E-04 | 0,00E+00 | 0,00E+00 | 0,00E+00 | 0,00E+00 | 0,00E+00 | 0,00E+00 | 0,00E+00 | 0,00E+00 | 0,00E+00 |
| Bacteroidetes;c__Bacteroidia;o__Bacteroidales;f__Rikenellaceae;g__Blvii28 | 3,94E-03 | 0,00E+00 | 0,00E+00 | 0,00E+00 | 0,00E+00 | 5,88E-05 | 0,00E+00 | 0,00E+00 | 0,00E+00 | 0,00E+00 | 0,00E+00 | 0,00E+00 | 0,00E+00 | 0,00E+00 | 0,00E+00 |
| Bacteroidetes;c__Bacteroidia;o__Bacteroidales;f__S24-7;g__ | 2,94E-04 | 0,00E+00 | 0,00E+00 | 0,00E+00 | 0,00E+00 | 0,00E+00 | 0,00E+00 | 0,00E+00 | 0,00E+00 | 0,00E+00 | 0,00E+00 | 0,00E+00 | 0,00E+00 | 0,00E+00 | 0,00E+00 |
| Bacteroidetes;c__Bacteroidia;o__Bacteroidales;f__[Barnesiellaceae];g__ | 1,35E-03 | 0,00E+00 | 0,00E+00 | 0,00E+00 | 0,00E+00 | 0,00E+00 | 0,00E+00 | 0,00E+00 | 0,00E+00 | 0,00E+00 | 0,00E+00 | 0,00E+00 | 0,00E+00 | 0,00E+00 | 0,00E+00 |
| Bacteroidetes;c__Bacteroidia;o__Bacteroidales;f__[Paraprevotellaceae];g__Paraprevote | 5,88E-05 | 0,00E+00 | 0,00E+00 | 0,00E+00 | 0,00E+00 | 0,00E+00 | 0,00E+00 | 0,00E+00 | 0,00E+00 | 0,00E+00 | 0,00E+00 | 0,00E+00 | 0,00E+00 | 0,00E+00 | 0,00E+00 |
| Bacteroidetes;c__Bacteroidia;o__Bacteroidales;f__p-2534-18B5;g__ | 1,18E-04 | 0,00E+00 | 0,00E+00 | 0,00E+00 | 0,00E+00 | 0,00E+00 | 0,00E+00 | 0,00E+00 | 0,00E+00 | 0,00E+00 | 0,00E+00 | 0,00E+00 | 0,00E+00 | 0,00E+00 | 0,00E+00 |
| Bacteroidetes;c__Cytophagia;o__Cytophagales;f__Cytophagaceae;g__ | 0,00E+00 | 0,00E+00 | 5,88E-05 | 0,00E+00 | 0,00E+00 | 0,00E+00 | 0,00E+00 | 0,00E+00 | 0,00E+00 | 0,00E+00 | 0,00E+00 | 0,00E+00 | 0,00E+00 | 0,00E+00 | 2,35E-04 |
| Bacteroidetes;c__Cytophagia;o__Cytophagales;f__Cytophagaceae;g__Adhaeribacter | 0,00E+00 | 0,00E+00 | 0,00E+00 | 0,00E+00 | 0,00E+00 | 0,00E+00 | 0,00E+00 | 0,00E+00 | 0,00E+00 | 0,00E+00 | 0,00E+00 | 0,00E+00 | 0,00E+00 | 0,00E+00 | 2,06E-03 |
| Bacteroidetes;c__Cytophagia;o__Cytophagales;f__Cytophagaceae;g__Dyadobacter | 0,00E+00 | 5,29E-04 | 1,18E-04 | 0,00E+00 | 0,00E+00 | 0,00E+00 | 0,00E+00 | 0,00E+00 | 0,00E+00 | 0,00E+00 | 0,00E+00 | 0,00E+00 | 0,00E+00 | 0,00E+00 | 0,00E+00 |
| Bacteroidetes;c__Cytophagia;o__Cytophagales;f__Cytophagaceae;g__Hymenobacter | 0,00E+00 | 0,00E+00 | 0,00E+00 | 0,00E+00 | 0,00E+00 | 0,00E+00 | 0,00E+00 | 0,00E+00 | 0,00E+00 | 0,00E+00 | 0,00E+00 | 0,00E+00 | 0,00E+00 | 0,00E+00 | 2,94E-04 |
| Bacteroidetes;c__Cytophagia;o__Cytophagales;f__Cytophagaceae;g__Pontibacter | 0,00E+00 | 0,00E+00 | 0,00E+00 | 0,00E+00 | 0,00E+00 | 0,00E+00 | 0,00E+00 | 0,00E+00 | 0,00E+00 | 0,00E+00 | 0,00E+00 | 0,00E+00 | 0,00E+00 | 1,18E-04 | 4,18E-03 |
| Bacteroidetes;c__Flavobacteriia;o__Flavobacteriales;f__Cryomorphaceae;g__ | 0,00E+00 | 0,00E+00 | 0,00E+00 | 0,00E+00 | 0,00E+00 | 0,00E+00 | 0,00E+00 | 0,00E+00 | 0,00E+00 | 0,00E+00 | 0,00E+00 | 0,00E+00 | 0,00E+00 | 0,00E+00 | 5,88E-05 |
| Bacteroidetes;c__Flavobacteriia;o__Flavobacteriales;f__Cryomorphaceae;g__Fluviicola | 0,00E+00 | 7,29E-03 | 8,24E-04 | 0,00E+00 | 0,00E+00 | 0,00E+00 | 0,00E+00 | 0,00E+00 | 0,00E+00 | 0,00E+00 | 0,00E+00 | 0,00E+00 | 0,00E+00 | 0,00E+00 | 5,88E-05 |
| Bacteroidetes;c__Flavobacteriia;o__Flavobacteriales;f__Flavobacteriaceae;g__ | 5,88E-04 | 8,30E-02 | 1,06E-02 | 0,00E+00 | 0,00E+00 | 1,18E-04 | 0,00E+00 | 0,00E+00 | 0,00E+00 | 0,00E+00 | 0,00E+00 | 0,00E+00 | 0,00E+00 | 0,00E+00 | 0,00E+00 |
| Bacteroidetes;c__Flavobacteriia;o__Flavobacteriales;f__Flavobacteriaceae;g__Flavobac | 9,01E-02 | 1,22E-02 | 2,76E-03 | 1,71E-03 | 6,47E-04 | 4,12E-04 | 3,15E-02 | 3,29E-03 | 6,94E-03 | 5,94E-03 | 2,21E-02 | 1,18E-04 | 1,15E-02 | 2,76E-03 | |
| Bacteroidetes;c__Flavobacteriia;o__Flavobacteriales;f__Flavobacteriaceae;g__Myroides | 0,00E+00 | 1,76E-03 | 2,35E-04 | 0,00E+00 | 0,00E+00 | 0,00E+00 | 0,00E+00 | 0,00E+00 | 0,00E+00 | 0,00E+00 | 0,00E+00 | 0,00E+00 | 0,00E+00 | 0,00E+00 | 0,00E+00 |
| Bacteroidetes;c__Flavobacteriia;o__Flavobacteriales;f__[Weeksellaceae];g__ | 0,00E+00 | 1,35E-03 | 1,76E-04 | 0,00E+00 | 0,00E+00 | 0,00E+00 | 0,00E+00 | 0,00E+00 | 0,00E+00 | 0,00E+00 | 0,00E+00 | 0,00E+00 | 0,00E+00 | 0,00E+00 | 0,00E+00 |
| Bacteroidetes;c__Flavobacteriia;o__Flavobacteriales;f__[Weeksellaceae];g__Chryseoba | 7,59E-03 | 3,86E-02 | 4,00E-03 | 1,18E-04 | 0,00E+00 | 5,88E-05 | 2,94E-04 | 6,47E-04 | 2,29E-03 | 1,24E-03 | 4,12E-04 | 5,88E-05 | 2,71E-03 | 2,18E-03 | |
| Bacteroidetes;c__Flavobacteriia;o__Flavobacteriales;f__[Weeksellaceae];g__Cloacibact | 3,71E-03 | 1,18E-03 | 2,35E-04 | 0,00E+00 | 0,00E+00 | 1,18E-04 | 0,00E+00 | 0,00E+00 | 0,00E+00 | 0,00E+00 | 0,00E+00 | 0,00E+00 | 0,00E+00 | 0,00E+00 | 0,00E+00 |
| Bacteroidetes;c__Flavobacteriia;o__Flavobacteriales;f__[Weeksellaceae];g__Elizabethki | 5,88E-05 | 2,76E-03 | 4,71E-04 | 0,00E+00 | 0,00E+00 | 0,00E+00 | 0,00E+00 | 0,00E+00 | 0,00E+00 | 0,00E+00 | 2,35E-04 | 5,88E-05 | 0,00E+00 | 1,18E-04 | 0,00E+00 |
| Bacteroidetes;c__Flavobacteriia;o__Flavobacteriales;f__[Weeksellaceae];g__Wautersiell | 3,41E-03 | 6,53E-03 | 7,65E-04 | 2,65E-03 | 5,29E-04 | 1,76E-04 | 1,71E-03 | 5,88E-05 | 1,42E-02 | 6,00E-03 | 2,41E-03 | 1,76E-04 | 1,01E-02 | 4,00E-03 | |
| Bacteroidetes;c__Sphingobacteriia;o__Sphingobacteriales;f__Sphingobacteriaceae;g__ | 0,00E+00 | 1,76E-04 | 0,00E+00 | 0,00E+00 | 0,00E+00 | 0,00E+00 | 0,00E+00 | 0,00E+00 | 0,00E+00 | 0,00E+00 | 0,00E+00 | 0,00E+00 | 0,00E+00 | 0,00E+00 | 1,47E-03 |
| Bacteroidetes;c__Sphingobacteriia;o__Sphingobacteriales;f__Sphingobacteriaceae;g__P | 1,76E-04 | 3,47E-03 | 2,94E-04 | 0,00E+00 | 0,00E+00 | 0,00E+00 | 0,00E+00 | 0,00E+00 | 0,00E+00 | 0,00E+00 | 0,00E+00 | 0,00E+00 | 0,00E+00 | 0,00E+00 | 1,76E-04 |
| Bacteroidetes;c__Sphingobacteriia;o__Sphingobacteriales;f__Sphingobacteriaceae;g__S | 5,88E-05 | 4,24E-02 | 5,35E-03 | 7,65E-04 | 1,35E-03 | 0,00E+00 | 3,65E-03 | 1,81E-02 | 1,76E-02 | 6,47E-03 | 1,52E-02 | 0,00E+00 | 4,50E-02 | 3,00E-02 | |
| Bacteroidetes;c__VC2_1_Bac22;o__;f__;g__ | 0,00E+00 | 2,35E-03 | 2,35E-04 | 0,00E+00 | 0,00E+00 | 0,00E+00 | 0,00E+00 | 0,00E+00 | 0,00E+00 | 0,00E+00 | 0,00E+00 | 0,00E+00 | 0,00E+00 | 0,00E+00 | 0,00E+00 |
| Bacteroidetes;c__[Saprospirae];o__[Saprospirales];f__Chitinophagaceae;g__ | 0,00E+00 | 4,59E-03 | 6,47E-04 | 0,00E+00 | 0,00E+00 | 5,88E-05 | 0,00E+00 | 0,00E+00 | 0,00E+00 | 0,00E+00 | 5,88E-05 | 0,00E+00 | 0,00E+00 | 7,06E-04 | |
| Bacteroidetes;c__[Saprospirae];o__[Saprospirales];f__Chitinophagaceae;g__Flavisolibac | 0,00E+00 | 0,00E+00 | 0,00E+00 | 0,00E+00 | 0,00E+00 | 0,00E+00 | 0,00E+00 | 0,00E+00 | 0,00E+00 | 0,00E+00 | 0,00E+00 | 0,00E+00 | 0,00E+00 | 0,00E+00 | 6,47E-04 |
| Bacteroidetes;c__[Saprospirae];o__[Saprospirales];f__Chitinophagaceae;g__Parasegitib | 0,00E+00 | 1,18E-04 | 0,00E+00 | 0,00E+00 | 0,00E+00 | 0,00E+00 | 0,00E+00 | 0,00E+00 | 0,00E+00 | 0,00E+00 | 0,00E+00 | 0,00E+00 | 0,00E+00 | 0,00E+00 | 0,00E+00 |
| Chlorobi;c__OPB56;o__;f__;g__ | 2,94E-04 | 0,00E+00 | 0,00E+00 | 0,00E+00 | 0,00E+00 | 0,00E+00 | 0,00E+00 | 0,00E+00 | 0,00E+00 | 0,00E+00 | 0,00E+00 | 0,00E+00 | 0,00E+00 | 0,00E+00 | 0,00E+00 |
| Chloroflexi;c__Anaerolineae;o__SBR1031;f__A4b;g__ | 0,00E+00 | 0,00E+00 | 0,00E+00 | 0,00E+00 | 0,00E+00 | 0,00E+00 | 0,00E+00 | 0,00E+00 | 0,00E+00 | 0,00E+00 | 0,00E+00 | 0,00E+00 | 0,00E+00 | 0,00E+00 | 1,18E-04 |

| | | | | | | | | | | | | | | | |
|---|---|---|---|---|---|---|---|---|---|---|---|---|---|---|---|
| Chloroflexi;c__Chloroflexi;o__Herpetosiphonales;f__;g__ | 0,00E+00 | 0,00E+00 | 0,00E+00 | 0,00E+00 | 0,00E+00 | 0,00E+00 | 0,00E+00 | 0,00E+00 | 0,00E+00 | 0,00E+00 | 0,00E+00 | 0,00E+00 | 0,00E+00 | 0,00E+00 | 3,53E-04 |
| Chloroflexi;c__Chloroflexi;o__[Roseiflexales];f__[Kouleothrixaceae];g__ | 0,00E+00 | 0,00E+00 | 0,00E+00 | 0,00E+00 | 0,00E+00 | 0,00E+00 | 0,00E+00 | 0,00E+00 | 0,00E+00 | 0,00E+00 | 0,00E+00 | 0,00E+00 | 0,00E+00 | 0,00E+00 | 2,35E-04 |
| Chloroflexi;c__Ellin6529;o__;f__;g__ | 0,00E+00 | 0,00E+00 | 0,00E+00 | 0,00E+00 | 0,00E+00 | 0,00E+00 | 0,00E+00 | 0,00E+00 | 0,00E+00 | 0,00E+00 | 0,00E+00 | 0,00E+00 | 0,00E+00 | 0,00E+00 | 8,24E-04 |
| Chloroflexi;c__Thermomicrobia;o__JG30-KF-CM45;f__;g__ | 0,00E+00 | 0,00E+00 | 0,00E+00 | 0,00E+00 | 0,00E+00 | 0,00E+00 | 0,00E+00 | 0,00E+00 | 0,00E+00 | 0,00E+00 | 0,00E+00 | 0,00E+00 | 0,00E+00 | 0,00E+00 | 8,82E-04 |
| Cyanobacteria;c__Nostocophycideae;o__Nostocales;f__Nostocaceae;Other | 0,00E+00 | 0,00E+00 | 0,00E+00 | 0,00E+00 | 0,00E+00 | 0,00E+00 | 0,00E+00 | 0,00E+00 | 0,00E+00 | 0,00E+00 | 0,00E+00 | 0,00E+00 | 0,00E+00 | 0,00E+00 | 1,18E-04 |
| Firmicutes;c__Bacilli;o__Bacillales;f__Alicyclobacillaceae;g__Alicyclobacillus | 0,00E+00 | 0,00E+00 | 0,00E+00 | 0,00E+00 | 0,00E+00 | 0,00E+00 | 0,00E+00 | 0,00E+00 | 0,00E+00 | 0,00E+00 | 0,00E+00 | 0,00E+00 | 0,00E+00 | 0,00E+00 | 2,94E-04 |
| Firmicutes;c__Bacilli;o__Bacillales;f__Bacillaceae;g__Bacillus | 0,00E+00 | 0,00E+00 | 0,00E+00 | 0,00E+00 | 0,00E+00 | 0,00E+00 | 0,00E+00 | 0,00E+00 | 0,00E+00 | 0,00E+00 | 0,00E+00 | 0,00E+00 | 0,00E+00 | 0,00E+00 | 1,76E-04 |
| Firmicutes;c__Bacilli;o__Bacillales;f__Paenibacillaceae;g__Paenibacillus | 0,00E+00 | 0,00E+00 | 0,00E+00 | 0,00E+00 | 0,00E+00 | 0,00E+00 | 0,00E+00 | 0,00E+00 | 0,00E+00 | 0,00E+00 | 0,00E+00 | 0,00E+00 | 0,00E+00 | 5,88E-05 | 1,41E-03 |
| Firmicutes;c__Bacilli;o__Lactobacillales;f__Carnobacteriaceae;g__ | 1,54E-02 | 3,06E-03 | 7,06E-04 | 0,00E+00 | 0,00E+00 | 5,29E-04 | 0,00E+00 | 0,00E+00 | 0,00E+00 | 0,00E+00 | 5,88E-05 | 0,00E+00 | 0,00E+00 | 0,00E+00 | 0,00E+00 |
| Firmicutes;c__Bacilli;o__Lactobacillales;f__Lactobacillaceae;g__Lactobacillus | 1,76E-04 | 0,00E+00 | 0,00E+00 | 0,00E+00 | 0,00E+00 | 0,00E+00 | 0,00E+00 | 0,00E+00 | 0,00E+00 | 0,00E+00 | 0,00E+00 | 0,00E+00 | 0,00E+00 | 0,00E+00 | 0,00E+00 |
| Firmicutes;c__Bacilli;o__Lactobacillales;f__Streptococcaceae;g__Lactococcus | 9,35E-03 | 1,35E-02 | 1,18E-03 | 1,76E-04 | 1,76E-04 | 2,88E-03 | 1,06E-03 | 0,00E+00 | 7,06E-04 | 4,47E-03 | 0,00E+00 | 0,00E+00 | 5,88E-05 | 4,71E-04 | |
| Firmicutes;c__Bacilli;o__Lactobacillales;f__Streptococcaceae;g__Streptococcus | 2,06E-03 | 0,00E+00 | 5,88E-05 | 0,00E+00 | 0,00E+00 | 5,88E-05 | 0,00E+00 | 0,00E+00 | 0,00E+00 | 0,00E+00 | 0,00E+00 | 0,00E+00 | 0,00E+00 | 0,00E+00 | |
| Firmicutes;c__Clostridia;o__Clostridiales;Other;Other | 5,88E-05 | 0,00E+00 | 0,00E+00 | 0,00E+00 | 0,00E+00 | 0,00E+00 | 0,00E+00 | 0,00E+00 | 0,00E+00 | 0,00E+00 | 0,00E+00 | 0,00E+00 | 0,00E+00 | 0,00E+00 | 0,00E+00 |
| Firmicutes;c__Clostridia;o__Clostridiales;f__;g__ | 5,29E-03 | 5,88E-05 | 5,88E-05 | 0,00E+00 | 0,00E+00 | 0,00E+00 | 0,00E+00 | 0,00E+00 | 0,00E+00 | 0,00E+00 | 0,00E+00 | 0,00E+00 | 0,00E+00 | 0,00E+00 | 0,00E+00 |
| Firmicutes;c__Clostridia;o__Clostridiales;f__Christensenellaceae;g__ | 2,35E-04 | 0,00E+00 | 0,00E+00 | 0,00E+00 | 0,00E+00 | 0,00E+00 | 0,00E+00 | 0,00E+00 | 0,00E+00 | 0,00E+00 | 0,00E+00 | 0,00E+00 | 0,00E+00 | 0,00E+00 | 0,00E+00 |
| Firmicutes;c__Clostridia;o__Clostridiales;f__Clostridiaceae;g__Clostridium | 2,06E-03 | 2,76E-03 | 1,06E-03 | 5,29E-04 | 2,35E-04 | 8,48E-02 | 1,76E-04 | 3,53E-04 | 5,88E-05 | 0,00E+00 | 4,71E-04 | 5,88E-04 | 1,76E-04 | 1,76E-04 | |
| Firmicutes;c__Clostridia;o__Clostridiales;f__Lachnospiraceae;Other | 1,18E-04 | 0,00E+00 | 0,00E+00 | 0,00E+00 | 0,00E+00 | 0,00E+00 | 0,00E+00 | 0,00E+00 | 0,00E+00 | 0,00E+00 | 0,00E+00 | 0,00E+00 | 0,00E+00 | 0,00E+00 | 0,00E+00 |
| Firmicutes;c__Clostridia;o__Clostridiales;f__Lachnospiraceae;g__ | 5,24E-03 | 0,00E+00 | 5,88E-05 | 0,00E+00 | 0,00E+00 | 0,00E+00 | 0,00E+00 | 0,00E+00 | 0,00E+00 | 0,00E+00 | 0,00E+00 | 0,00E+00 | 0,00E+00 | 0,00E+00 | 0,00E+00 |
| Firmicutes;c__Clostridia;o__Clostridiales;f__Lachnospiraceae;g__Blautia | 7,53E-03 | 5,88E-05 | 0,00E+00 | 0,00E+00 | 0,00E+00 | 0,00E+00 | 0,00E+00 | 0,00E+00 | 0,00E+00 | 0,00E+00 | 0,00E+00 | 0,00E+00 | 0,00E+00 | 0,00E+00 | 0,00E+00 |
| Firmicutes;c__Clostridia;o__Clostridiales;f__Lachnospiraceae;g__Butyrivibrio | 1,18E-04 | 0,00E+00 | 0,00E+00 | 0,00E+00 | 0,00E+00 | 0,00E+00 | 0,00E+00 | 0,00E+00 | 0,00E+00 | 0,00E+00 | 0,00E+00 | 0,00E+00 | 0,00E+00 | 0,00E+00 | 0,00E+00 |
| Firmicutes;c__Clostridia;o__Clostridiales;f__Lachnospiraceae;g__Coprococcus | 5,29E-04 | 0,00E+00 | 0,00E+00 | 0,00E+00 | 0,00E+00 | 0,00E+00 | 0,00E+00 | 0,00E+00 | 0,00E+00 | 0,00E+00 | 0,00E+00 | 0,00E+00 | 0,00E+00 | 0,00E+00 | 0,00E+00 |
| Firmicutes;c__Clostridia;o__Clostridiales;f__Lachnospiraceae;g__Dorea | 1,12E-03 | 5,88E-05 | 0,00E+00 | 0,00E+00 | 0,00E+00 | 0,00E+00 | 0,00E+00 | 0,00E+00 | 0,00E+00 | 0,00E+00 | 0,00E+00 | 0,00E+00 | 0,00E+00 | 0,00E+00 | 0,00E+00 |
| Firmicutes;c__Clostridia;o__Clostridiales;f__Lachnospiraceae;g__[Ruminococcus] | 3,88E-03 | 5,88E-05 | 0,00E+00 | 0,00E+00 | 0,00E+00 | 5,88E-05 | 0,00E+00 | 0,00E+00 | 0,00E+00 | 0,00E+00 | 0,00E+00 | 0,00E+00 | 0,00E+00 | 0,00E+00 | 0,00E+00 |
| Firmicutes;c__Clostridia;o__Clostridiales;f__Peptostreptococcaceae;g__ | 3,12E-03 | 0,00E+00 | 0,00E+00 | 0,00E+00 | 0,00E+00 | 0,00E+00 | 0,00E+00 | 0,00E+00 | 0,00E+00 | 0,00E+00 | 0,00E+00 | 0,00E+00 | 0,00E+00 | 0,00E+00 | 0,00E+00 |
| Firmicutes;c__Clostridia;o__Clostridiales;f__Ruminococcaceae;g__ | 6,06E-03 | 2,94E-04 | 0,00E+00 | 0,00E+00 | 0,00E+00 | 0,00E+00 | 0,00E+00 | 0,00E+00 | 0,00E+00 | 0,00E+00 | 0,00E+00 | 0,00E+00 | 0,00E+00 | 0,00E+00 | 0,00E+00 |
| Firmicutes;c__Clostridia;o__Clostridiales;f__Ruminococcaceae;g__Faecalibacterium | 7,94E-03 | 0,00E+00 | 0,00E+00 | 0,00E+00 | 0,00E+00 | 0,00E+00 | 0,00E+00 | 0,00E+00 | 0,00E+00 | 0,00E+00 | 0,00E+00 | 0,00E+00 | 0,00E+00 | 0,00E+00 | 0,00E+00 |
| Firmicutes;c__Clostridia;o__Clostridiales;f__Ruminococcaceae;g__Oscillospira | 2,35E-04 | 0,00E+00 | 0,00E+00 | 0,00E+00 | 0,00E+00 | 0,00E+00 | 0,00E+00 | 0,00E+00 | 0,00E+00 | 0,00E+00 | 0,00E+00 | 0,00E+00 | 0,00E+00 | 0,00E+00 | 0,00E+00 |
| Firmicutes;c__Clostridia;o__Clostridiales;f__Ruminococcaceae;g__Ruminococcus | 3,76E-03 | 0,00E+00 | 0,00E+00 | 0,00E+00 | 0,00E+00 | 0,00E+00 | 0,00E+00 | 0,00E+00 | 0,00E+00 | 0,00E+00 | 0,00E+00 | 0,00E+00 | 5,88E-05 | 0,00E+00 | 0,00E+00 |
| Firmicutes;c__Clostridia;o__Clostridiales;f__Veillonellaceae;Other | 1,76E-04 | 0,00E+00 | 0,00E+00 | 0,00E+00 | 0,00E+00 | 0,00E+00 | 0,00E+00 | 0,00E+00 | 0,00E+00 | 0,00E+00 | 0,00E+00 | 0,00E+00 | 0,00E+00 | 0,00E+00 | 0,00E+00 |
| Firmicutes;c__Clostridia;o__Clostridiales;f__Veillonellaceae;g__ | 1,53E-03 | 0,00E+00 | 0,00E+00 | 0,00E+00 | 0,00E+00 | 0,00E+00 | 0,00E+00 | 0,00E+00 | 0,00E+00 | 0,00E+00 | 0,00E+00 | 0,00E+00 | 0,00E+00 | 0,00E+00 | 0,00E+00 |
| Firmicutes;c__Clostridia;o__Clostridiales;f__Veillonellaceae;g__Acidaminococcus | 4,71E-04 | 0,00E+00 | 0,00E+00 | 0,00E+00 | 0,00E+00 | 0,00E+00 | 0,00E+00 | 0,00E+00 | 0,00E+00 | 0,00E+00 | 0,00E+00 | 0,00E+00 | 0,00E+00 | 0,00E+00 | 0,00E+00 |
| Firmicutes;c__Clostridia;o__Clostridiales;f__Veillonellaceae;g__Dialister | 4,06E-03 | 0,00E+00 | 0,00E+00 | 0,00E+00 | 0,00E+00 | 0,00E+00 | 0,00E+00 | 0,00E+00 | 0,00E+00 | 0,00E+00 | 0,00E+00 | 0,00E+00 | 0,00E+00 | 0,00E+00 | 0,00E+00 |
| Firmicutes;c__Clostridia;o__Clostridiales;f__Veillonellaceae;g__Megamonas | 1,35E-03 | 0,00E+00 | 0,00E+00 | 0,00E+00 | 0,00E+00 | 0,00E+00 | 0,00E+00 | 0,00E+00 | 0,00E+00 | 0,00E+00 | 0,00E+00 | 0,00E+00 | 0,00E+00 | 0,00E+00 | 0,00E+00 |
| Firmicutes;c__Clostridia;o__Clostridiales;f__Veillonellaceae;g__Megasphaera | 5,29E-04 | 0,00E+00 | 0,00E+00 | 0,00E+00 | 0,00E+00 | 0,00E+00 | 0,00E+00 | 0,00E+00 | 0,00E+00 | 0,00E+00 | 0,00E+00 | 0,00E+00 | 0,00E+00 | 0,00E+00 | 0,00E+00 |
| Firmicutes;c__Clostridia;o__Clostridiales;f__Veillonellaceae;g__Pelosinus | 3,53E-04 | 0,00E+00 | 0,00E+00 | 0,00E+00 | 0,00E+00 | 0,00E+00 | 0,00E+00 | 0,00E+00 | 0,00E+00 | 0,00E+00 | 0,00E+00 | 0,00E+00 | 0,00E+00 | 0,00E+00 | 0,00E+00 |
| Firmicutes;c__Clostridia;o__Clostridiales;f__Veillonellaceae;g__Phascolarctobacterium | 2,00E-03 | 0,00E+00 | 0,00E+00 | 0,00E+00 | 0,00E+00 | 0,00E+00 | 0,00E+00 | 0,00E+00 | 0,00E+00 | 0,00E+00 | 0,00E+00 | 0,00E+00 | 0,00E+00 | 0,00E+00 | 0,00E+00 |
| Firmicutes;c__Clostridia;o__Clostridiales;f__Veillonellaceae;g__Veillonella | 5,88E-04 | 5,88E-05 | 0,00E+00 | 0,00E+00 | 0,00E+00 | 0,00E+00 | 0,00E+00 | 0,00E+00 | 0,00E+00 | 0,00E+00 | 0,00E+00 | 0,00E+00 | 0,00E+00 | 0,00E+00 | 0,00E+00 |
| Firmicutes;c__Clostridia;o__Clostridiales;f__[Acidaminobacteraceae];g__Fusibacter | 1,18E-04 | 0,00E+00 | 0,00E+00 | 0,00E+00 | 0,00E+00 | 0,00E+00 | 0,00E+00 | 0,00E+00 | 0,00E+00 | 0,00E+00 | 0,00E+00 | 0,00E+00 | 0,00E+00 | 0,00E+00 | 0,00E+00 |
| Firmicutes;c__Erysipelotrichi;o__Erysipelotrichales;f__Erysipelotrichaceae;g__ | 1,76E-03 | 0,00E+00 | 0,00E+00 | 0,00E+00 | 0,00E+00 | 0,00E+00 | 0,00E+00 | 0,00E+00 | 0,00E+00 | 0,00E+00 | 0,00E+00 | 0,00E+00 | 0,00E+00 | 0,00E+00 | 0,00E+00 |
| Firmicutes;c__Erysipelotrichi;o__Erysipelotrichales;f__Erysipelotrichaceae;g__Catenibact | 1,47E-03 | 1,18E-04 | 0,00E+00 | 0,00E+00 | 0,00E+00 | 0,00E+00 | 0,00E+00 | 0,00E+00 | 0,00E+00 | 0,00E+00 | 0,00E+00 | 0,00E+00 | 0,00E+00 | 0,00E+00 | 0,00E+00 |
| Firmicutes;c__Erysipelotrichi;o__Erysipelotrichales;f__Erysipelotrichaceae;g__[Eubacteriu | 1,12E-03 | 5,88E-05 | 5,88E-05 | 0,00E+00 | 0,00E+00 | 0,00E+00 | 0,00E+00 | 0,00E+00 | 0,00E+00 | 0,00E+00 | 0,00E+00 | 0,00E+00 | 0,00E+00 | 0,00E+00 | 0,00E+00 |
| Firmicutes;c__Erysipelotrichi;o__Erysipelotrichales;f__Erysipelotrichaceae;g__cc_115 | 5,88E-05 | 0,00E+00 | 0,00E+00 | 0,00E+00 | 0,00E+00 | 0,00E+00 | 0,00E+00 | 0,00E+00 | 0,00E+00 | 0,00E+00 | 0,00E+00 | 0,00E+00 | 0,00E+00 | 0,00E+00 | 0,00E+00 |
| Fusobacteria;c__Fusobacteriia;o__Fusobacteriales;f__;g__ | 7,00E-03 | 0,00E+00 | 0,00E+00 | 0,00E+00 | 0,00E+00 | 0,00E+00 | 0,00E+00 | 0,00E+00 | 0,00E+00 | 0,00E+00 | 0,00E+00 | 0,00E+00 | 0,00E+00 | 0,00E+00 | 0,00E+00 |
| Fusobacteria;c__Fusobacteriia;o__Fusobacteriales;f__Fusobacteriaceae;g__u114 | 1,76E-04 | 0,00E+00 | 0,00E+00 | 0,00E+00 | 0,00E+00 | 0,00E+00 | 0,00E+00 | 0,00E+00 | 0,00E+00 | 0,00E+00 | 0,00E+00 | 0,00E+00 | 0,00E+00 | 0,00E+00 | 0,00E+00 |
| Fusobacteria;c__Fusobacteriia;o__Fusobacteriales;f__Leptotrichiaceae;Other | 6,47E-04 | 0,00E+00 | 0,00E+00 | 0,00E+00 | 0,00E+00 | 0,00E+00 | 0,00E+00 | 0,00E+00 | 0,00E+00 | 0,00E+00 | 0,00E+00 | 0,00E+00 | 0,00E+00 | 0,00E+00 | 0,00E+00 |
| Fusobacteria;c__Fusobacteriia;o__Fusobacteriales;f__Leptotrichiaceae;g__ | 1,11E-02 | 5,88E-05 | 0,00E+00 | 0,00E+00 | 0,00E+00 | 5,88E-05 | 0,00E+00 | 0,00E+00 | 0,00E+00 | 0,00E+00 | 0,00E+00 | 0,00E+00 | 0,00E+00 | 0,00E+00 | 0,00E+00 |
| GN02;c__BD1-5;o__;f__;g__ | 2,35E-04 | 1,76E-04 | 5,88E-05 | 8,82E-04 | 5,88E-05 | 5,88E-05 | 1,76E-04 | 0,00E+00 | 4,12E-04 | 5,88E-05 | 5,29E-04 | 0,00E+00 | 1,18E-04 | 1,47E-03 | |
| Gemmatimonadetes;c__;o__;f__;g__ | 0,00E+00 | 0,00E+00 | 0,00E+00 | 0,00E+00 | 0,00E+00 | 0,00E+00 | 0,00E+00 | 0,00E+00 | 0,00E+00 | 0,00E+00 | 0,00E+00 | 0,00E+00 | 0,00E+00 | 0,00E+00 | 4,12E-04 |
| Gemmatimonadetes;c__Gemm-1;o__;f__;g__ | 0,00E+00 | 0,00E+00 | 0,00E+00 | 0,00E+00 | 0,00E+00 | 0,00E+00 | 0,00E+00 | 0,00E+00 | 0,00E+00 | 0,00E+00 | 0,00E+00 | 0,00E+00 | 0,00E+00 | 0,00E+00 | 4,71E-04 |
| Gemmatimonadetes;c__Gemm-3;o__;f__;g__ | 0,00E+00 | 0,00E+00 | 0,00E+00 | 0,00E+00 | 0,00E+00 | 0,00E+00 | 0,00E+00 | 0,00E+00 | 0,00E+00 | 0,00E+00 | 0,00E+00 | 0,00E+00 | 0,00E+00 | 0,00E+00 | 1,18E-04 |

| | | | | | | | | | | | | | | |
|---|---|---|---|---|---|---|---|---|---|---|---|---|---|---|
| Gemmatimonadetes;c__Gemm-5;o__;f__;g__ | 0,00E+00 | 0,00E+00 | 0,00E+00 | 0,00E+00 | 0,00E+00 | 0,00E+00 | 0,00E+00 | 0,00E+00 | 0,00E+00 | 0,00E+00 | 0,00E+00 | 0,00E+00 | 0,00E+00 | 2,35E-04 |
| Gemmatimonadetes;c__Gemmatimonadetes;o__;f__;g__ | 0,00E+00 | 0,00E+00 | 0,00E+00 | 0,00E+00 | 0,00E+00 | 0,00E+00 | 0,00E+00 | 0,00E+00 | 0,00E+00 | 0,00E+00 | 0,00E+00 | 0,00E+00 | 0,00E+00 | 2,29E-03 |
| Gemmatimonadetes;c__Gemmatimonadetes;o__Ellin5290;f__;g__ | 0,00E+00 | 0,00E+00 | 0,00E+00 | 0,00E+00 | 0,00E+00 | 0,00E+00 | 0,00E+00 | 0,00E+00 | 0,00E+00 | 0,00E+00 | 0,00E+00 | 0,00E+00 | 0,00E+00 | 5,29E-04 |
| Gemmatimonadetes;c__Gemmatimonadetes;o__Gemmatimonadales;f__Ellin5301;g__ | 0,00E+00 | 0,00E+00 | 0,00E+00 | 0,00E+00 | 0,00E+00 | 0,00E+00 | 0,00E+00 | 0,00E+00 | 0,00E+00 | 0,00E+00 | 0,00E+00 | 5,88E-05 | 0,00E+00 | 0,00E+00 | 3,00E-03 |
| Gemmatimonadetes;c__Gemmatimonadetes;o__N1423WL;f__;g__ | 0,00E+00 | 0,00E+00 | 0,00E+00 | 0,00E+00 | 0,00E+00 | 0,00E+00 | 0,00E+00 | 0,00E+00 | 0,00E+00 | 0,00E+00 | 0,00E+00 | 0,00E+00 | 0,00E+00 | 0,00E+00 | 7,06E-04 |
| Nitrospirae;c__Nitrospira;o__Nitrospirales;f__0319-6A21;g__ | 0,00E+00 | 0,00E+00 | 0,00E+00 | 0,00E+00 | 0,00E+00 | 0,00E+00 | 0,00E+00 | 0,00E+00 | 0,00E+00 | 0,00E+00 | 0,00E+00 | 0,00E+00 | 0,00E+00 | 0,00E+00 | 3,53E-04 |
| Nitrospirae;c__Nitrospira;o__Nitrospirales;f__Nitrospiraceae;g__Nitrospira | 0,00E+00 | 0,00E+00 | 0,00E+00 | 0,00E+00 | 0,00E+00 | 0,00E+00 | 0,00E+00 | 0,00E+00 | 0,00E+00 | 0,00E+00 | 0,00E+00 | 0,00E+00 | 0,00E+00 | 0,00E+00 | 1,76E-04 |
| OD1;c__ZB2;o__;f__;g__ | 0,00E+00 | 0,00E+00 | 0,00E+00 | 0,00E+00 | 0,00E+00 | 0,00E+00 | 0,00E+00 | 0,00E+00 | 0,00E+00 | 0,00E+00 | 0,00E+00 | 0,00E+00 | 0,00E+00 | 0,00E+00 | 2,35E-04 |
| Planctomycetes;c__Phycisphaerae;o__Phycisphaerales;f__;g__ | 0,00E+00 | 0,00E+00 | 0,00E+00 | 0,00E+00 | 0,00E+00 | 0,00E+00 | 0,00E+00 | 0,00E+00 | 0,00E+00 | 0,00E+00 | 0,00E+00 | 0,00E+00 | 0,00E+00 | 0,00E+00 | 1,18E-04 |
| Planctomycetes;c__Phycisphaerae;o__WD2101;f__;g__ | 0,00E+00 | 0,00E+00 | 0,00E+00 | 0,00E+00 | 0,00E+00 | 0,00E+00 | 0,00E+00 | 0,00E+00 | 0,00E+00 | 0,00E+00 | 0,00E+00 | 0,00E+00 | 0,00E+00 | 0,00E+00 | 8,82E-04 |
| Planctomycetes;c__Planctomycetia;o__Gemmatales;f__Gemmataceae;g__Gemmata | 0,00E+00 | 0,00E+00 | 0,00E+00 | 0,00E+00 | 0,00E+00 | 1,18E-04 | 0,00E+00 | 0,00E+00 | 0,00E+00 | 5,88E-05 | 0,00E+00 | 0,00E+00 | 0,00E+00 | 0,00E+00 | 1,18E-04 |
| Planctomycetes;c__Planctomycetia;o__Gemmatales;f__Isosphaeraceae;g__ | 0,00E+00 | 0,00E+00 | 0,00E+00 | 0,00E+00 | 0,00E+00 | 0,00E+00 | 0,00E+00 | 0,00E+00 | 0,00E+00 | 0,00E+00 | 0,00E+00 | 0,00E+00 | 0,00E+00 | 0,00E+00 | 5,88E-04 |
| Planctomycetes;c__Planctomycetia;o__Pirellulales;f__Pirellulaceae;g__ | 0,00E+00 | 0,00E+00 | 0,00E+00 | 0,00E+00 | 0,00E+00 | 0,00E+00 | 0,00E+00 | 0,00E+00 | 0,00E+00 | 0,00E+00 | 0,00E+00 | 0,00E+00 | 0,00E+00 | 0,00E+00 | 2,35E-04 |
| Proteobacteria;c__Alphaproteobacteria;o__;f__;g__ | 0,00E+00 | 1,76E-04 | 0,00E+00 | 0,00E+00 | 0,00E+00 | 0,00E+00 | 0,00E+00 | 0,00E+00 | 0,00E+00 | 0,00E+00 | 0,00E+00 | 0,00E+00 | 0,00E+00 | 0,00E+00 | 0,00E+00 |
| Proteobacteria;c__Alphaproteobacteria;o__Caulobacterales;f__Caulobacteraceae;g__ | 2,35E-04 | 6,47E-04 | 0,00E+00 | 0,00E+00 | 0,00E+00 | 2,35E-04 | 0,00E+00 | 0,00E+00 | 0,00E+00 | 0,00E+00 | 0,00E+00 | 0,00E+00 | 0,00E+00 | 0,00E+00 | 0,00E+00 |
| Proteobacteria;c__Alphaproteobacteria;o__Caulobacterales;f__Caulobacteraceae;g__As | 0,00E+00 | 0,00E+00 | 0,00E+00 | 0,00E+00 | 0,00E+00 | 0,00E+00 | 0,00E+00 | 0,00E+00 | 0,00E+00 | 0,00E+00 | 0,00E+00 | 0,00E+00 | 0,00E+00 | 0,00E+00 | 1,18E-04 |
| Proteobacteria;c__Alphaproteobacteria;o__Caulobacterales;f__Caulobacteraceae;g__Br | 1,76E-04 | 2,18E-03 | 2,35E-04 | 0,00E+00 | 0,00E+00 | 0,00E+00 | 0,00E+00 | 0,00E+00 | 0,00E+00 | 0,00E+00 | 0,00E+00 | 0,00E+00 | 0,00E+00 | 0,00E+00 | 0,00E+00 |
| Proteobacteria;c__Alphaproteobacteria;o__Caulobacterales;f__Caulobacteraceae;g__Ca | 3,53E-04 | 1,53E-03 | 2,35E-04 | 0,00E+00 | 0,00E+00 | 0,00E+00 | 0,00E+00 | 0,00E+00 | 0,00E+00 | 0,00E+00 | 0,00E+00 | 0,00E+00 | 0,00E+00 | 0,00E+00 | 0,00E+00 |
| Proteobacteria;c__Alphaproteobacteria;o__Caulobacterales;f__Caulobacteraceae;g__Pl | 0,00E+00 | 2,94E-04 | 0,00E+00 | 0,00E+00 | 0,00E+00 | 0,00E+00 | 0,00E+00 | 0,00E+00 | 0,00E+00 | 0,00E+00 | 0,00E+00 | 0,00E+00 | 0,00E+00 | 0,00E+00 | 1,18E-04 |
| Proteobacteria;c__Alphaproteobacteria;o__RF32;f__;g__ | 1,18E-04 | 0,00E+00 | 0,00E+00 | 0,00E+00 | 0,00E+00 | 0,00E+00 | 0,00E+00 | 0,00E+00 | 0,00E+00 | 0,00E+00 | 0,00E+00 | 0,00E+00 | 0,00E+00 | 0,00E+00 | 0,00E+00 |
| Proteobacteria;c__Alphaproteobacteria;o__Rhizobiales;f__;g__ | 0,00E+00 | 4,53E-03 | 6,47E-04 | 0,00E+00 | 0,00E+00 | 5,88E-05 | 0,00E+00 | 0,00E+00 | 0,00E+00 | 0,00E+00 | 0,00E+00 | 0,00E+00 | 0,00E+00 | 0,00E+00 | 0,00E+00 |
| Proteobacteria;c__Alphaproteobacteria;o__Rhizobiales;f__Beijerinckiaceae;g__ | 0,00E+00 | 1,18E-04 | 0,00E+00 | 0,00E+00 | 0,00E+00 | 0,00E+00 | 0,00E+00 | 0,00E+00 | 0,00E+00 | 0,00E+00 | 0,00E+00 | 0,00E+00 | 0,00E+00 | 0,00E+00 | 0,00E+00 |
| Proteobacteria;c__Alphaproteobacteria;o__Rhizobiales;f__Bradyrhizobiaceae;g__ | 5,88E-04 | 7,06E-04 | 5,88E-05 | 1,18E-04 | 5,29E-04 | 2,22E-02 | 0,00E+00 | 0,00E+00 | 0,00E+00 | 5,88E-05 | 0,00E+00 | 0,00E+00 | 0,00E+00 | 2,35E-04 |
| Proteobacteria;c__Alphaproteobacteria;o__Rhizobiales;f__Bradyrhizobiaceae;g__Balnein | 0,00E+00 | 0,00E+00 | 0,00E+00 | 0,00E+00 | 0,00E+00 | 0,00E+00 | 0,00E+00 | 0,00E+00 | 0,00E+00 | 0,00E+00 | 0,00E+00 | 0,00E+00 | 0,00E+00 | 5,88E-05 | 3,53E-04 |
| Proteobacteria;c__Alphaproteobacteria;o__Rhizobiales;f__Brucellaceae;Other | 1,76E-04 | 1,96E-02 | 1,88E-03 | 0,00E+00 | 0,00E+00 | 0,00E+00 | 1,76E-04 | 0,00E+00 | 1,76E-04 | 1,59E-03 | 5,88E-05 | 0,00E+00 | 4,12E-04 | 5,88E-05 |
| Proteobacteria;c__Alphaproteobacteria;o__Rhizobiales;f__Brucellaceae;g__Ochrobactru | 2,35E-04 | 1,72E-02 | 1,94E-03 | 5,29E-04 | 1,18E-04 | 1,18E-04 | 5,71E-03 | 1,88E-03 | 2,82E-03 | 1,24E-02 | 2,59E-03 | 0,00E+00 | 2,00E-03 | 8,82E-04 |
| Proteobacteria;c__Alphaproteobacteria;o__Rhizobiales;f__Hyphomicrobiaceae;g__ | 0,00E+00 | 0,00E+00 | 0,00E+00 | 0,00E+00 | 0,00E+00 | 0,00E+00 | 0,00E+00 | 0,00E+00 | 0,00E+00 | 0,00E+00 | 0,00E+00 | 0,00E+00 | 0,00E+00 | 0,00E+00 | 3,53E-04 |
| Proteobacteria;c__Alphaproteobacteria;o__Rhizobiales;f__Hyphomicrobiaceae;g__Devo | 0,00E+00 | 1,18E-03 | 1,76E-04 | 0,00E+00 | 0,00E+00 | 0,00E+00 | 0,00E+00 | 0,00E+00 | 0,00E+00 | 0,00E+00 | 0,00E+00 | 0,00E+00 | 0,00E+00 | 0,00E+00 | 5,88E-05 |
| Proteobacteria;c__Alphaproteobacteria;o__Rhizobiales;f__Hyphomicrobiaceae;g__Parvi | 0,00E+00 | 5,88E-05 | 0,00E+00 | 0,00E+00 | 0,00E+00 | 0,00E+00 | 0,00E+00 | 0,00E+00 | 0,00E+00 | 0,00E+00 | 0,00E+00 | 0,00E+00 | 0,00E+00 | 0,00E+00 | 0,00E+00 |
| Proteobacteria;c__Alphaproteobacteria;o__Rhizobiales;f__Hyphomicrobiaceae;g__Rhod | 0,00E+00 | 0,00E+00 | 0,00E+00 | 0,00E+00 | 0,00E+00 | 0,00E+00 | 0,00E+00 | 0,00E+00 | 0,00E+00 | 0,00E+00 | 0,00E+00 | 0,00E+00 | 0,00E+00 | 5,88E-05 | 6,47E-04 |
| Proteobacteria;c__Alphaproteobacteria;o__Rhizobiales;f__Methylobacteriaceae;g__ | 0,00E+00 | 5,88E-05 | 0,00E+00 | 0,00E+00 | 0,00E+00 | 8,24E-04 | 0,00E+00 | 0,00E+00 | 0,00E+00 | 0,00E+00 | 5,88E-05 | 0,00E+00 | 0,00E+00 | 0,00E+00 | 0,00E+00 |
| Proteobacteria;c__Alphaproteobacteria;o__Rhizobiales;f__Methylobacteriaceae;g__Met | 0,00E+00 | 0,00E+00 | 0,00E+00 | 0,00E+00 | 0,00E+00 | 2,18E-03 | 0,00E+00 | 0,00E+00 | 0,00E+00 | 0,00E+00 | 0,00E+00 | 0,00E+00 | 0,00E+00 | 0,00E+00 | 0,00E+00 |
| Proteobacteria;c__Alphaproteobacteria;o__Rhizobiales;f__Phyllobacteriaceae;g__Aminc | 0,00E+00 | 2,94E-04 | 1,18E-04 | 0,00E+00 | 0,00E+00 | 0,00E+00 | 0,00E+00 | 0,00E+00 | 0,00E+00 | 0,00E+00 | 0,00E+00 | 0,00E+00 | 0,00E+00 | 0,00E+00 | 0,00E+00 |
| Proteobacteria;c__Alphaproteobacteria;o__Rhizobiales;f__Rhizobiaceae;Other | 5,88E-05 | 2,53E-03 | 2,35E-04 | 5,88E-05 | 0,00E+00 | 0,00E+00 | 4,71E-04 | 5,88E-05 | 1,18E-04 | 2,35E-04 | 0,00E+00 | 0,00E+00 | 0,00E+00 | 2,35E-04 |
| Proteobacteria;c__Alphaproteobacteria;o__Rhizobiales;f__Rhizobiaceae;g__ | 2,35E-04 | 1,74E-02 | 1,65E-03 | 0,00E+00 | 0,00E+00 | 0,00E+00 | 0,00E+00 | 0,00E+00 | 0,00E+00 | 5,88E-05 | 0,00E+00 | 0,00E+00 | 0,00E+00 | 1,18E-04 |
| Proteobacteria;c__Alphaproteobacteria;o__Rhizobiales;f__Rhizobiaceae;g__Agrobacteri | 0,00E+00 | 2,94E-04 | 5,88E-05 | 0,00E+00 | 0,00E+00 | 5,88E-05 | 0,00E+00 | 0,00E+00 | 0,00E+00 | 0,00E+00 | 0,00E+00 | 0,00E+00 | 0,00E+00 | 0,00E+00 | 1,18E-04 |
| Proteobacteria;c__Alphaproteobacteria;o__Rhizobiales;f__Rhizobiaceae;g__Kaistia | 0,00E+00 | 1,12E-03 | 2,35E-04 | 0,00E+00 | 0,00E+00 | 0,00E+00 | 0,00E+00 | 0,00E+00 | 0,00E+00 | 0,00E+00 | 0,00E+00 | 0,00E+00 | 0,00E+00 | 0,00E+00 | 0,00E+00 |
| Proteobacteria;c__Alphaproteobacteria;o__Rhodobacterales;f__Hyphomonadaceae;g__ | 0,00E+00 | 0,00E+00 | 0,00E+00 | 0,00E+00 | 0,00E+00 | 0,00E+00 | 0,00E+00 | 0,00E+00 | 0,00E+00 | 0,00E+00 | 0,00E+00 | 0,00E+00 | 0,00E+00 | 0,00E+00 | 1,18E-04 |
| Proteobacteria;c__Alphaproteobacteria;o__Rhodobacterales;f__Rhodobacteraceae;Oth | 0,00E+00 | 1,82E-03 | 1,76E-04 | 0,00E+00 | 0,00E+00 | 0,00E+00 | 0,00E+00 | 0,00E+00 | 0,00E+00 | 0,00E+00 | 0,00E+00 | 0,00E+00 | 0,00E+00 | 0,00E+00 | 0,00E+00 |
| Proteobacteria;c__Alphaproteobacteria;o__Rhodobacterales;f__Rhodobacteraceae;g__ | 0,00E+00 | 1,29E-03 | 1,76E-04 | 0,00E+00 | 0,00E+00 | 0,00E+00 | 0,00E+00 | 0,00E+00 | 0,00E+00 | 0,00E+00 | 0,00E+00 | 0,00E+00 | 0,00E+00 | 0,00E+00 | 0,00E+00 |
| Proteobacteria;c__Alphaproteobacteria;o__Rhodobacterales;f__Rhodobacteraceae;g__ | 7,06E-04 | 3,65E-03 | 4,12E-04 | 0,00E+00 | 0,00E+00 | 5,88E-05 | 0,00E+00 | 0,00E+00 | 0,00E+00 | 0,00E+00 | 0,00E+00 | 0,00E+00 | 0,00E+00 | 0,00E+00 | 0,00E+00 |
| Proteobacteria;c__Alphaproteobacteria;o__Rhodobacterales;f__Rhodobacteraceae;g__ | 5,29E-04 | 1,42E-02 | 1,18E-03 | 0,00E+00 | 0,00E+00 | 0,00E+00 | 0,00E+00 | 0,00E+00 | 0,00E+00 | 0,00E+00 | 0,00E+00 | 0,00E+00 | 0,00E+00 | 0,00E+00 | 0,00E+00 |
| Proteobacteria;c__Alphaproteobacteria;o__Rhodospirillales;f__;g__ | 0,00E+00 | 0,00E+00 | 0,00E+00 | 0,00E+00 | 0,00E+00 | 0,00E+00 | 0,00E+00 | 0,00E+00 | 0,00E+00 | 0,00E+00 | 0,00E+00 | 0,00E+00 | 0,00E+00 | 0,00E+00 | 1,76E-04 |
| Proteobacteria;c__Alphaproteobacteria;o__Rhodospirillales;f__Rhodospirillaceae;g__ | 0,00E+00 | 0,00E+00 | 0,00E+00 | 0,00E+00 | 0,00E+00 | 0,00E+00 | 0,00E+00 | 0,00E+00 | 0,00E+00 | 0,00E+00 | 0,00E+00 | 0,00E+00 | 0,00E+00 | 0,00E+00 | 1,18E-04 |
| Proteobacteria;c__Alphaproteobacteria;o__Rhodospirillales;f__Rhodospirillaceae;g__Az | 0,00E+00 | 1,47E-03 | 5,88E-05 | 0,00E+00 | 0,00E+00 | 0,00E+00 | 0,00E+00 | 0,00E+00 | 0,00E+00 | 0,00E+00 | 0,00E+00 | 0,00E+00 | 0,00E+00 | 0,00E+00 | 0,00E+00 |
| Proteobacteria;c__Alphaproteobacteria;o__Rhodospirillales;f__Rhodospirillaceae;g__Nc | 0,00E+00 | 2,35E-04 | 0,00E+00 | 0,00E+00 | 0,00E+00 | 0,00E+00 | 0,00E+00 | 0,00E+00 | 0,00E+00 | 0,00E+00 | 0,00E+00 | 0,00E+00 | 0,00E+00 | 0,00E+00 | 0,00E+00 |
| Proteobacteria;c__Alphaproteobacteria;o__Rhodospirillales;f__Rhodospirillaceae;g__Sk | 0,00E+00 | 0,00E+00 | 0,00E+00 | 0,00E+00 | 0,00E+00 | 0,00E+00 | 0,00E+00 | 0,00E+00 | 0,00E+00 | 0,00E+00 | 0,00E+00 | 0,00E+00 | 0,00E+00 | 0,00E+00 | 2,35E-04 |
| Proteobacteria;c__Alphaproteobacteria;o__Rickettsiales;f__;g__ | 1,18E-04 | 1,34E-02 | 1,29E-03 | 0,00E+00 | 0,00E+00 | 0,00E+00 | 0,00E+00 | 0,00E+00 | 0,00E+00 | 0,00E+00 | 0,00E+00 | 0,00E+00 | 0,00E+00 | 0,00E+00 | 5,88E-05 |
| Proteobacteria;c__Alphaproteobacteria;o__Rickettsiales;f__Rickettsiaceae;g__ | 0,00E+00 | 0,00E+00 | 0,00E+00 | 0,00E+00 | 0,00E+00 | 0,00E+00 | 0,00E+00 | 0,00E+00 | 0,00E+00 | 0,00E+00 | 0,00E+00 | 0,00E+00 | 0,00E+00 | 0,00E+00 | 1,18E-04 |
| Proteobacteria;c__Alphaproteobacteria;o__Sphingomonadales;f__Erythrobacteraceae;g | 0,00E+00 | 0,00E+00 | 0,00E+00 | 0,00E+00 | 0,00E+00 | 0,00E+00 | 0,00E+00 | 0,00E+00 | 0,00E+00 | 0,00E+00 | 0,00E+00 | 0,00E+00 | 0,00E+00 | 0,00E+00 | 2,94E-04 |

| | | | | | | | | | | | | | | |
|---|---|---|---|---|---|---|---|---|---|---|---|---|---|---|
| Proteobacteria;c__Alphaproteobacteria;o__Sphingomonadales;f__Sphingomonadaceae; | 0,00E+00 | 0,00E+00 | 0,00E+00 | 5,88E-05 | 0,00E+00 | 0,00E+00 | 0,00E+00 | 0,00E+00 | 0,00E+00 | 0,00E+00 | 0,00E+00 | 0,00E+00 | 5,88E-05 | 5,65E-03 |
| Proteobacteria;c__Alphaproteobacteria;o__Sphingomonadales;f__Sphingomonadaceae; | 0,00E+00 | 3,53E-04 | 0,00E+00 | 0,00E+00 | 0,00E+00 | 0,00E+00 | 5,88E-05 | 0,00E+00 | 0,00E+00 | 0,00E+00 | 0,00E+00 | 0,00E+00 | 5,88E-05 | 5,88E-05 |
| Proteobacteria;c__Alphaproteobacteria;o__Sphingomonadales;f__Sphingomonadaceae; | 0,00E+00 | 1,76E-04 | 0,00E+00 | 0,00E+00 | 0,00E+00 | 1,76E-04 | 0,00E+00 | 5,88E-05 | 0,00E+00 | 0,00E+00 | 0,00E+00 | 5,88E-05 | 0,00E+00 | 0,00E+00 |
| Proteobacteria;c__Alphaproteobacteria;o__Sphingomonadales;f__Sphingomonadaceae; | 0,00E+00 | 0,00E+00 | 5,88E-05 | 0,00E+00 | 0,00E+00 | 0,00E+00 | 0,00E+00 | 0,00E+00 | 0,00E+00 | 0,00E+00 | 0,00E+00 | 0,00E+00 | 0,00E+00 | 5,88E-05 |
| Proteobacteria;c__Betaproteobacteria;Other;Other;Other | 5,88E-04 | 8,24E-04 | 5,88E-05 | 0,00E+00 | 5,88E-05 | 1,18E-04 | 0,00E+00 | 0,00E+00 | 0,00E+00 | 0,00E+00 | 0,00E+00 | 0,00E+00 | 0,00E+00 | 0,00E+00 |
| Proteobacteria;c__Betaproteobacteria;o__Burkholderiales;f__;g__ | 1,41E-03 | 1,76E-04 | 0,00E+00 | 0,00E+00 | 0,00E+00 | 0,00E+00 | 0,00E+00 | 0,00E+00 | 0,00E+00 | 0,00E+00 | 0,00E+00 | 0,00E+00 | 0,00E+00 | 0,00E+00 |
| Proteobacteria;c__Betaproteobacteria;o__Burkholderiales;f__Alcaligenaceae;Other | 0,00E+00 | 2,71E-03 | 2,94E-04 | 0,00E+00 | 0,00E+00 | 0,00E+00 | 0,00E+00 | 0,00E+00 | 0,00E+00 | 0,00E+00 | 0,00E+00 | 0,00E+00 | 0,00E+00 | 5,88E-05 |
| Proteobacteria;c__Betaproteobacteria;o__Burkholderiales;f__Alcaligenaceae;g__ | 0,00E+00 | 2,71E-03 | 2,94E-04 | 0,00E+00 | 0,00E+00 | 0,00E+00 | 0,00E+00 | 0,00E+00 | 0,00E+00 | 0,00E+00 | 0,00E+00 | 0,00E+00 | 0,00E+00 | 0,00E+00 |
| Proteobacteria;c__Betaproteobacteria;o__Burkholderiales;f__Alcaligenaceae;g__Denitro | 1,18E-04 | 3,65E-03 | 4,12E-04 | 0,00E+00 | 0,00E+00 | 0,00E+00 | 0,00E+00 | 0,00E+00 | 0,00E+00 | 0,00E+00 | 0,00E+00 | 0,00E+00 | 0,00E+00 | 0,00E+00 |
| Proteobacteria;c__Betaproteobacteria;o__Burkholderiales;f__Burkholderiaceae;g__Burk | 1,76E-04 | 0,00E+00 | 0,00E+00 | 0,00E+00 | 0,00E+00 | 0,00E+00 | 0,00E+00 | 0,00E+00 | 0,00E+00 | 0,00E+00 | 0,00E+00 | 0,00E+00 | 0,00E+00 | 0,00E+00 |
| Proteobacteria;c__Betaproteobacteria;o__Burkholderiales;f__Burkholderiaceae;g__Pan | 0,00E+00 | 1,76E-03 | 5,88E-05 | 0,00E+00 | 0,00E+00 | 0,00E+00 | 0,00E+00 | 0,00E+00 | 0,00E+00 | 0,00E+00 | 0,00E+00 | 0,00E+00 | 0,00E+00 | 0,00E+00 |
| Proteobacteria;c__Betaproteobacteria;o__Burkholderiales;f__Comamonadaceae;g__ | 3,80E-02 | 2,56E-02 | 3,71E-03 | 1,65E-03 | 2,94E-04 | 4,71E-04 | 4,65E-03 | 3,47E-03 | 8,88E-03 | 6,24E-03 | 2,18E-03 | 0,00E+00 | 7,59E-03 | 5,53E-03 |
| Proteobacteria;c__Betaproteobacteria;o__Burkholderiales;f__Comamonadaceae;g__Co | 1,82E-03 | 8,41E-03 | 1,53E-03 | 1,29E-03 | 1,18E-04 | 5,88E-05 | 1,82E-03 | 1,12E-03 | 4,88E-03 | 2,53E-03 | 1,18E-03 | 5,88E-05 | 5,06E-03 | 1,29E-03 |
| Proteobacteria;c__Betaproteobacteria;o__Burkholderiales;f__Comamonadaceae;g__De | 5,36E-02 | 2,65E-02 | 3,71E-03 | 2,59E-03 | 5,29E-04 | 3,53E-04 | 2,05E-02 | 1,21E-02 | 1,38E-02 | 7,41E-03 | 1,61E-02 | 1,18E-04 | 1,59E-02 | 1,36E-02 |
| Proteobacteria;c__Betaproteobacteria;o__Burkholderiales;f__Comamonadaceae;g__Hy | 7,06E-03 | 5,88E-05 | 0,00E+00 | 0,00E+00 | 0,00E+00 | 5,88E-05 | 0,00E+00 | 0,00E+00 | 0,00E+00 | 0,00E+00 | 0,00E+00 | 0,00E+00 | 5,88E-05 | 0,00E+00 |
| Proteobacteria;c__Betaproteobacteria;o__Burkholderiales;f__Comamonadaceae;g__Lim | 1,18E-04 | 0,00E+00 | 0,00E+00 | 0,00E+00 | 0,00E+00 | 0,00E+00 | 0,00E+00 | 0,00E+00 | 0,00E+00 | 0,00E+00 | 0,00E+00 | 0,00E+00 | 0,00E+00 | 0,00E+00 |
| Proteobacteria;c__Betaproteobacteria;o__Burkholderiales;f__Oxalobacteraceae;g__ | 1,06E-03 | 7,94E-03 | 7,65E-04 | 0,00E+00 | 5,88E-05 | 5,88E-05 | 5,88E-05 | 0,00E+00 | 0,00E+00 | 0,00E+00 | 0,00E+00 | 0,00E+00 | 0,00E+00 | 6,65E-03 |
| Proteobacteria;c__Betaproteobacteria;o__Burkholderiales;f__Oxalobacteraceae;g__Jant | 1,02E-02 | 1,18E-04 | 5,88E-05 | 0,00E+00 | 0,00E+00 | 0,00E+00 | 0,00E+00 | 0,00E+00 | 0,00E+00 | 0,00E+00 | 0,00E+00 | 0,00E+00 | 0,00E+00 | 1,18E-03 |
| Proteobacteria;c__Betaproteobacteria;o__Burkholderiales;f__Oxalobacteraceae;g__Poly | 1,76E-04 | 0,00E+00 | 0,00E+00 | 0,00E+00 | 0,00E+00 | 0,00E+00 | 0,00E+00 | 0,00E+00 | 0,00E+00 | 0,00E+00 | 0,00E+00 | 0,00E+00 | 0,00E+00 | 0,00E+00 |
| Proteobacteria;c__Betaproteobacteria;o__Methylophilales;f__Methylophilaceae;Other | 1,76E-04 | 1,89E-02 | 2,59E-03 | 0,00E+00 | 0,00E+00 | 0,00E+00 | 0,00E+00 | 0,00E+00 | 0,00E+00 | 0,00E+00 | 0,00E+00 | 0,00E+00 | 0,00E+00 | 5,88E-05 |
| Proteobacteria;c__Betaproteobacteria;o__Methylophilales;f__Methylophilaceae;g__ | 2,35E-04 | 0,00E+00 | 0,00E+00 | 0,00E+00 | 0,00E+00 | 0,00E+00 | 0,00E+00 | 0,00E+00 | 0,00E+00 | 0,00E+00 | 0,00E+00 | 0,00E+00 | 0,00E+00 | 5,88E-05 |
| Proteobacteria;c__Betaproteobacteria;o__Neisseriales;f__Neisseriaceae;Other | 1,71E-03 | 0,00E+00 | 0,00E+00 | 0,00E+00 | 0,00E+00 | 0,00E+00 | 0,00E+00 | 0,00E+00 | 0,00E+00 | 0,00E+00 | 0,00E+00 | 0,00E+00 | 0,00E+00 | 0,00E+00 |
| Proteobacteria;c__Betaproteobacteria;o__Neisseriales;f__Neisseriaceae;g__ | 7,06E-04 | 7,65E-04 | 5,88E-05 | 0,00E+00 | 0,00E+00 | 2,35E-04 | 0,00E+00 | 0,00E+00 | 0,00E+00 | 0,00E+00 | 0,00E+00 | 0,00E+00 | 0,00E+00 | 0,00E+00 |
| Proteobacteria;c__Betaproteobacteria;o__Neisseriales;f__Neisseriaceae;g__Microvirgul | 1,18E-03 | 5,88E-05 | 0,00E+00 | 0,00E+00 | 0,00E+00 | 0,00E+00 | 0,00E+00 | 0,00E+00 | 0,00E+00 | 0,00E+00 | 0,00E+00 | 0,00E+00 | 0,00E+00 | 0,00E+00 |
| Proteobacteria;c__Betaproteobacteria;o__Neisseriales;f__Neisseriaceae;g__Vitreoscilla | 9,41E-04 | 1,76E-04 | 0,00E+00 | 5,88E-05 | 0,00E+00 | 0,00E+00 | 0,00E+00 | 0,00E+00 | 0,00E+00 | 0,00E+00 | 0,00E+00 | 0,00E+00 | 0,00E+00 | 0,00E+00 |
| Proteobacteria;c__Betaproteobacteria;o__Procabacteriales;f__Procabacteriaceae;g__ | 5,94E-03 | 0,00E+00 | 0,00E+00 | 0,00E+00 | 0,00E+00 | 0,00E+00 | 0,00E+00 | 0,00E+00 | 0,00E+00 | 0,00E+00 | 0,00E+00 | 0,00E+00 | 0,00E+00 | 0,00E+00 |
| Proteobacteria;c__Betaproteobacteria;o__Rhodocyclales;f__Rhodocyclaceae;Other | 5,88E-05 | 0,00E+00 | 0,00E+00 | 0,00E+00 | 0,00E+00 | 0,00E+00 | 0,00E+00 | 0,00E+00 | 0,00E+00 | 0,00E+00 | 0,00E+00 | 0,00E+00 | 0,00E+00 | 1,18E-04 |
| Proteobacteria;c__Betaproteobacteria;o__Rhodocyclales;f__Rhodocyclaceae;g__Dechl | 4,35E-03 | 0,00E+00 | 0,00E+00 | 0,00E+00 | 0,00E+00 | 0,00E+00 | 0,00E+00 | 0,00E+00 | 0,00E+00 | 0,00E+00 | 0,00E+00 | 0,00E+00 | 0,00E+00 | 0,00E+00 |
| Proteobacteria;c__Betaproteobacteria;o__Rhodocyclales;f__Rhodocyclaceae;g__Propi | 3,53E-03 | 0,00E+00 | 0,00E+00 | 0,00E+00 | 0,00E+00 | 0,00E+00 | 0,00E+00 | 0,00E+00 | 0,00E+00 | 0,00E+00 | 0,00E+00 | 0,00E+00 | 0,00E+00 | 0,00E+00 |
| Proteobacteria;c__Betaproteobacteria;o__Rhodocyclales;f__Rhodocyclaceae;g__Thaue | 1,18E-03 | 1,06E-03 | 0,00E+00 | 5,88E-05 | 5,88E-05 | 1,18E-04 | 0,00E+00 | 0,00E+00 | 0,00E+00 | 5,88E-05 | 5,88E-04 | 0,00E+00 | 5,88E-05 | 0,00E+00 |
| Proteobacteria;c__Betaproteobacteria;o__Rhodocyclales;f__Rhodocyclaceae;g__Uligino | 1,18E-04 | 0,00E+00 | 0,00E+00 | 0,00E+00 | 0,00E+00 | 0,00E+00 | 0,00E+00 | 0,00E+00 | 0,00E+00 | 0,00E+00 | 0,00E+00 | 0,00E+00 | 0,00E+00 | 0,00E+00 |
| Proteobacteria;c__Betaproteobacteria;o__Rhodocyclales;f__Rhodocyclaceae;g__Zoogl | 7,35E-03 | 2,94E-04 | 5,88E-05 | 0,00E+00 | 0,00E+00 | 0,00E+00 | 0,00E+00 | 0,00E+00 | 0,00E+00 | 0,00E+00 | 0,00E+00 | 0,00E+00 | 0,00E+00 | 0,00E+00 |
| Proteobacteria;c__Betaproteobacteria;o__SC-I-84;f__;g__ | 0,00E+00 | 0,00E+00 | 0,00E+00 | 0,00E+00 | 0,00E+00 | 0,00E+00 | 0,00E+00 | 0,00E+00 | 0,00E+00 | 0,00E+00 | 0,00E+00 | 0,00E+00 | 0,00E+00 | 1,41E-03 |
| Proteobacteria;c__Deltaproteobacteria;o__Bdellovibrionales;f__Bacteriovoracaceae;g__ | 5,29E-04 | 1,76E-04 | 5,88E-05 | 0,00E+00 | 0,00E+00 | 0,00E+00 | 0,00E+00 | 0,00E+00 | 0,00E+00 | 0,00E+00 | 0,00E+00 | 0,00E+00 | 0,00E+00 | 0,00E+00 |
| Proteobacteria;c__Deltaproteobacteria;o__Desulfobacterales;f__Desulfobacteraceae;g_ | 5,88E-05 | 1,18E-04 | 0,00E+00 | 0,00E+00 | 0,00E+00 | 0,00E+00 | 0,00E+00 | 0,00E+00 | 0,00E+00 | 0,00E+00 | 0,00E+00 | 0,00E+00 | 0,00E+00 | 0,00E+00 |
| Proteobacteria;c__Deltaproteobacteria;o__Desulfobacterales;f__Desulfobulbaceae;g__ | 2,94E-04 | 0,00E+00 | 0,00E+00 | 0,00E+00 | 0,00E+00 | 0,00E+00 | 0,00E+00 | 0,00E+00 | 0,00E+00 | 0,00E+00 | 0,00E+00 | 0,00E+00 | 0,00E+00 | 0,00E+00 |
| Proteobacteria;c__Deltaproteobacteria;o__Desulfovibrionales;f__Desulfomicrobiaceae;g | 2,35E-04 | 0,00E+00 | 0,00E+00 | 0,00E+00 | 0,00E+00 | 0,00E+00 | 0,00E+00 | 0,00E+00 | 0,00E+00 | 0,00E+00 | 0,00E+00 | 0,00E+00 | 0,00E+00 | 0,00E+00 |
| Proteobacteria;c__Deltaproteobacteria;o__Desulfovibrionales;f__Desulfovibrionaceae;g | 2,94E-04 | 0,00E+00 | 0,00E+00 | 0,00E+00 | 0,00E+00 | 0,00E+00 | 0,00E+00 | 0,00E+00 | 0,00E+00 | 0,00E+00 | 0,00E+00 | 0,00E+00 | 0,00E+00 | 0,00E+00 |
| Proteobacteria;c__Deltaproteobacteria;o__Desulfovibrionales;f__Desulfovibrionaceae;g | 2,35E-04 | 0,00E+00 | 0,00E+00 | 0,00E+00 | 0,00E+00 | 0,00E+00 | 0,00E+00 | 0,00E+00 | 0,00E+00 | 0,00E+00 | 0,00E+00 | 0,00E+00 | 0,00E+00 | 0,00E+00 |
| Proteobacteria;c__Deltaproteobacteria;o__Desulfuromonadales;Other;Other | 1,18E-04 | 0,00E+00 | 0,00E+00 | 0,00E+00 | 0,00E+00 | 0,00E+00 | 0,00E+00 | 0,00E+00 | 0,00E+00 | 0,00E+00 | 0,00E+00 | 0,00E+00 | 0,00E+00 | 0,00E+00 |
| Proteobacteria;c__Deltaproteobacteria;o__Myxococcales;Other;Other | 0,00E+00 | 0,00E+00 | 0,00E+00 | 0,00E+00 | 0,00E+00 | 0,00E+00 | 0,00E+00 | 0,00E+00 | 0,00E+00 | 0,00E+00 | 0,00E+00 | 0,00E+00 | 0,00E+00 | 4,71E-04 |
| Proteobacteria;c__Deltaproteobacteria;o__Myxococcales;f__;g__ | 0,00E+00 | 0,00E+00 | 0,00E+00 | 0,00E+00 | 0,00E+00 | 0,00E+00 | 0,00E+00 | 0,00E+00 | 0,00E+00 | 0,00E+00 | 0,00E+00 | 0,00E+00 | 0,00E+00 | 1,18E-04 |
| Proteobacteria;c__Deltaproteobacteria;o__[Entotheonellales];f__[Entotheonellaceae];g_ | 0,00E+00 | 0,00E+00 | 0,00E+00 | 0,00E+00 | 0,00E+00 | 0,00E+00 | 0,00E+00 | 0,00E+00 | 0,00E+00 | 0,00E+00 | 0,00E+00 | 0,00E+00 | 0,00E+00 | 4,12E-04 |
| Proteobacteria;c__Epsilonproteobacteria;o__Campylobacterales;f__Campylobacteracea | 1,33E-01 | 6,47E-04 | 1,18E-04 | 5,29E-03 | 1,76E-04 | 2,59E-03 | 1,18E-04 | 0,00E+00 | 6,38E-02 | 5,29E-04 | 1,82E-03 | 5,88E-05 | 6,81E-02 | 8,21E-02 |
| Proteobacteria;c__Epsilonproteobacteria;o__Campylobacterales;f__Campylobacteracea | 9,41E-04 | 0,00E+00 | 0,00E+00 | 0,00E+00 | 0,00E+00 | 0,00E+00 | 0,00E+00 | 0,00E+00 | 0,00E+00 | 0,00E+00 | 0,00E+00 | 0,00E+00 | 0,00E+00 | 0,00E+00 |
| Proteobacteria;c__Epsilonproteobacteria;o__Campylobacterales;f__Helicobacteraceae;g | 3,53E-04 | 0,00E+00 | 0,00E+00 | 0,00E+00 | 0,00E+00 | 0,00E+00 | 0,00E+00 | 0,00E+00 | 0,00E+00 | 0,00E+00 | 0,00E+00 | 0,00E+00 | 0,00E+00 | 0,00E+00 |
| Proteobacteria;c__Epsilonproteobacteria;o__Campylobacterales;f__Helicobacteraceae;g | 1,76E-04 | 0,00E+00 | 0,00E+00 | 0,00E+00 | 0,00E+00 | 0,00E+00 | 0,00E+00 | 0,00E+00 | 0,00E+00 | 0,00E+00 | 0,00E+00 | 0,00E+00 | 0,00E+00 | 0,00E+00 |
| Proteobacteria;c__Epsilonproteobacteria;o__Campylobacterales;f__Helicobacteraceae;g | 3,53E-04 | 0,00E+00 | 0,00E+00 | 0,00E+00 | 0,00E+00 | 0,00E+00 | 0,00E+00 | 0,00E+00 | 0,00E+00 | 0,00E+00 | 0,00E+00 | 0,00E+00 | 0,00E+00 | 0,00E+00 |
| Proteobacteria;c__Gammaproteobacteria;o__Aeromonadales;f__Aeromonadaceae;g__ | 5,92E-02 | 1,50E-01 | 3,26E-01 | 3,56E-01 | 3,47E-01 | 4,76E-03 | 2,69E-01 | 3,09E-01 | 2,68E-01 | 2,00E-01 | 2,74E-01 | 1,24E-03 | 2,35E-01 | 2,29E-01 |
| Proteobacteria;c__Gammaproteobacteria;o__Aeromonadales;f__Aeromonadaceae;g__ | 8,47E-03 | 5,29E-04 | 3,53E-04 | 1,18E-04 | 1,76E-04 | 5,88E-05 | 2,94E-04 | 5,88E-05 | 1,18E-04 | 0,00E+00 | 2,35E-04 | 0,00E+00 | 1,18E-04 | 2,35E-04 |

| | | | | | | | | | | | | | | |
|---|---|---|---|---|---|---|---|---|---|---|---|---|---|---|
| Proteobacteria;c__Gammaproteobacteria;o__Alteromonadales;f__21lds20;g__ | 0,00E+00 | 0,00E+00 | 0,00E+00 | 0,00E+00 | 0,00E+00 | 0,00E+00 | 0,00E+00 | 0,00E+00 | 0,00E+00 | 0,00E+00 | 0,00E+00 | 0,00E+00 | 0,00E+00 | 1,18E-04 |
| Proteobacteria;c__Gammaproteobacteria;o__Alteromonadales;f__Shewanellaceae;g__S | 3,29E-03 | 5,53E-03 | 8,06E-03 | 1,39E-02 | 6,82E-03 | 2,76E-03 | 1,60E-02 | 1,81E-02 | 1,36E-02 | 1,56E-02 | 7,53E-03 | 8,82E-04 | 1,38E-02 | 1,26E-02 |
| Proteobacteria;c__Gammaproteobacteria;o__Alteromonadales;f__[Chromatiaceae];g__I | 0,00E+00 | 2,94E-04 | 0,00E+00 | 0,00E+00 | 0,00E+00 | 0,00E+00 | 0,00E+00 | 0,00E+00 | 0,00E+00 | 5,88E-05 | 0,00E+00 | 0,00E+00 | 0,00E+00 | 5,88E-05 |
| Proteobacteria;c__Gammaproteobacteria;o__Enterobacteriales;f__Enterobacteriaceae;g | 7,53E-03 | 4,95E-02 | 6,18E-02 | 5,70E-02 | 1,42E-01 | 7,00E-01 | 1,11E-01 | 7,97E-02 | 8,04E-02 | 2,08E-01 | 1,03E-01 | 4,50E-01 | 5,22E-02 | 7,84E-02 |
| Proteobacteria;c__Gammaproteobacteria;o__Enterobacteriales;f__Enterobacteriaceae;g | 0,00E+00 | 7,06E-04 | 5,76E-03 | 1,94E-03 | 7,65E-04 | 5,88E-05 | 1,94E-03 | 1,76E-04 | 3,00E-03 | 4,12E-04 | 8,12E-03 | 0,00E+00 | 4,47E-03 | 2,82E-03 |
| Proteobacteria;c__Gammaproteobacteria;o__Legionellales;f__Legionellaceae;g__Legion | 0,00E+00 | 1,76E-04 | 5,88E-05 | 0,00E+00 | 0,00E+00 | 0,00E+00 | 0,00E+00 | 0,00E+00 | 0,00E+00 | 0,00E+00 | 0,00E+00 | 0,00E+00 | 0,00E+00 | 0,00E+00 |
| Proteobacteria;c__Gammaproteobacteria;o__Pseudomonadales;f__Moraxellaceae;Othe | 1,11E-02 | 1,76E-04 | 0,00E+00 | 0,00E+00 | 0,00E+00 | 0,00E+00 | 0,00E+00 | 0,00E+00 | 0,00E+00 | 0,00E+00 | 0,00E+00 | 0,00E+00 | 0,00E+00 | 0,00E+00 |
| Proteobacteria;c__Gammaproteobacteria;o__Pseudomonadales;f__Moraxellaceae;g__ | 1,18E-03 | 5,88E-05 | 0,00E+00 | 0,00E+00 | 0,00E+00 | 0,00E+00 | 0,00E+00 | 0,00E+00 | 0,00E+00 | 0,00E+00 | 0,00E+00 | 0,00E+00 | 0,00E+00 | 0,00E+00 |
| Proteobacteria;c__Gammaproteobacteria;o__Pseudomonadales;f__Moraxellaceae;g__A | 1,83E-01 | 2,09E-01 | 3,08E-01 | 3,33E-01 | 3,00E-01 | 2,16E-02 | 1,77E-01 | 1,44E-01 | 1,78E-01 | 1,53E-01 | 1,68E-01 | 1,56E-01 | 2,33E-01 | 1,50E-01 |
| Proteobacteria;c__Gammaproteobacteria;o__Pseudomonadales;f__Moraxellaceae;g__P | 5,12E-03 | 1,18E-04 | 0,00E+00 | 0,00E+00 | 0,00E+00 | 0,00E+00 | 0,00E+00 | 0,00E+00 | 0,00E+00 | 0,00E+00 | 0,00E+00 | 0,00E+00 | 0,00E+00 | 0,00E+00 |
| Proteobacteria;c__Gammaproteobacteria;o__Pseudomonadales;f__Moraxellaceae;g__P | 4,12E-04 | 1,76E-03 | 5,88E-05 | 0,00E+00 | 0,00E+00 | 0,00E+00 | 0,00E+00 | 0,00E+00 | 0,00E+00 | 0,00E+00 | 0,00E+00 | 0,00E+00 | 0,00E+00 | 0,00E+00 |
| Proteobacteria;c__Gammaproteobacteria;o__Pseudomonadales;f__Pseudomonadacea | 1,82E-03 | 1,55E-02 | 5,82E-02 | 5,44E-02 | 3,43E-02 | 4,71E-04 | 8,11E-02 | 1,31E-01 | 4,38E-02 | 4,93E-02 | 1,21E-01 | 4,81E-02 | 6,62E-02 | 6,62E-02 |
| Proteobacteria;c__Gammaproteobacteria;o__Pseudomonadales;f__Pseudomonadacea | 8,57E-02 | 4,53E-02 | 1,66E-01 | 1,62E-01 | 1,62E-01 | 1,41E-01 | 2,42E-01 | 2,73E-01 | 2,51E-01 | 3,08E-01 | 2,39E-01 | 3,42E-01 | 2,08E-01 | 2,26E-01 |
| Proteobacteria;c__Gammaproteobacteria;o__Thiotrichales;f__Thiotrichaceae;g__Thioth | 7,06E-04 | 0,00E+00 | 0,00E+00 | 0,00E+00 | 0,00E+00 | 0,00E+00 | 0,00E+00 | 0,00E+00 | 0,00E+00 | 0,00E+00 | 0,00E+00 | 0,00E+00 | 0,00E+00 | 0,00E+00 |
| Proteobacteria;c__Gammaproteobacteria;o__Xanthomonadales;f__Sinobacteraceae;g__ | 0,00E+00 | 0,00E+00 | 0,00E+00 | 0,00E+00 | 0,00E+00 | 0,00E+00 | 0,00E+00 | 0,00E+00 | 0,00E+00 | 0,00E+00 | 0,00E+00 | 0,00E+00 | 0,00E+00 | 8,82E-04 |
| Proteobacteria;c__Gammaproteobacteria;o__Xanthomonadales;f__Xanthomonadaceae | 1,18E-04 | 1,76E-04 | 5,88E-05 | 5,88E-05 | 0,00E+00 | 0,00E+00 | 5,88E-05 | 0,00E+00 | 0,00E+00 | 0,00E+00 | 0,00E+00 | 0,00E+00 | 0,00E+00 | 8,18E-03 |
| Proteobacteria;c__Gammaproteobacteria;o__Xanthomonadales;f__Xanthomonadaceae | 5,88E-05 | 4,12E-04 | 0,00E+00 | 0,00E+00 | 0,00E+00 | 0,00E+00 | 0,00E+00 | 0,00E+00 | 0,00E+00 | 0,00E+00 | 0,00E+00 | 0,00E+00 | 0,00E+00 | 0,00E+00 |
| Proteobacteria;c__Gammaproteobacteria;o__Xanthomonadales;f__Xanthomonadaceae | 1,76E-03 | 3,66E-02 | 4,88E-03 | 9,41E-04 | 4,71E-04 | 1,18E-04 | 2,54E-02 | 3,24E-03 | 2,28E-02 | 5,35E-03 | 1,17E-02 | 2,94E-04 | 1,79E-02 | 1,75E-02 |
| Proteobacteria;c__Gammaproteobacteria;o__Xanthomonadales;f__Xanthomonadaceae | 0,00E+00 | 0,00E+00 | 0,00E+00 | 0,00E+00 | 0,00E+00 | 0,00E+00 | 0,00E+00 | 0,00E+00 | 0,00E+00 | 0,00E+00 | 0,00E+00 | 0,00E+00 | 0,00E+00 | 1,18E-04 |
| Spirochaetes;c__[Leptospirae];o__[Leptospirales];f__Leptospiraceae;g__Turneriella | 1,18E-04 | 0,00E+00 | 0,00E+00 | 0,00E+00 | 0,00E+00 | 0,00E+00 | 0,00E+00 | 0,00E+00 | 0,00E+00 | 0,00E+00 | 0,00E+00 | 0,00E+00 | 0,00E+00 | 0,00E+00 |
| Synergistetes;c__Synergistia;o__Synergistales;f__Synergistaceae;g__vadinCA02 | 3,53E-04 | 0,00E+00 | 0,00E+00 | 0,00E+00 | 0,00E+00 | 0,00E+00 | 0,00E+00 | 0,00E+00 | 0,00E+00 | 0,00E+00 | 0,00E+00 | 0,00E+00 | 0,00E+00 | 0,00E+00 |
| Tenericutes;c__Mollicutes;o__Mycoplasmatales;f__Mycoplasmataceae;g__Mycoplasma | 1,18E-04 | 2,35E-04 | 1,35E-03 | 2,18E-03 | 1,41E-03 | 8,65E-03 | 3,82E-03 | 3,53E-04 | 1,71E-03 | 5,76E-03 | 1,24E-03 | 1,06E-03 | 8,82E-04 | 1,76E-04 |
| Verrucomicrobia;c__Opitutae;o__Opitutales;f__Opitutaceae;g__ | 1,18E-04 | 0,00E+00 | 0,00E+00 | 0,00E+00 | 0,00E+00 | 0,00E+00 | 0,00E+00 | 0,00E+00 | 0,00E+00 | 0,00E+00 | 0,00E+00 | 0,00E+00 | 0,00E+00 | 0,00E+00 |
| Verrucomicrobia;c__Opitutae;o__Opitutales;f__Opitutaceae;g__Opitutus | 0,00E+00 | 0,00E+00 | 0,00E+00 | 0,00E+00 | 0,00E+00 | 0,00E+00 | 0,00E+00 | 0,00E+00 | 0,00E+00 | 0,00E+00 | 0,00E+00 | 0,00E+00 | 0,00E+00 | 1,18E-04 |
| Verrucomicrobia;c__Verrucomicrobiae;o__Verrucomicrobiales;f__Verrucomicrobiaceae;g | 3,41E-03 | 1,18E-04 | 0,00E+00 | 0,00E+00 | 0,00E+00 | 0,00E+00 | 0,00E+00 | 0,00E+00 | 0,00E+00 | 0,00E+00 | 0,00E+00 | 0,00E+00 | 0,00E+00 | 0,00E+00 |
| Verrucomicrobia;c__[Spartobacteria];o__[Chthoniobacterales];f__[Chthoniobacteraceae | 0,00E+00 | 0,00E+00 | 0,00E+00 | 0,00E+00 | 0,00E+00 | 0,00E+00 | 0,00E+00 | 0,00E+00 | 0,00E+00 | 0,00E+00 | 0,00E+00 | 0,00E+00 | 0,00E+00 | 1,18E-04 |
| Verrucomicrobia;c__[Spartobacteria];o__[Chthoniobacterales];f__[Chthoniobacteraceae | 0,00E+00 | 0,00E+00 | 0,00E+00 | 0,00E+00 | 0,00E+00 | 0,00E+00 | 0,00E+00 | 5,88E-05 | 0,00E+00 | 0,00E+00 | 0,00E+00 | 0,00E+00 | 0,00E+00 | 1,41E-03 |
| [Thermi];c__Deinococci;o__Thermales;f__Thermaceae;g__Thermus | 0,00E+00 | 0,00E+00 | 0,00E+00 | 0,00E+00 | 0,00E+00 | 5,88E-05 | 0,00E+00 | 0,00E+00 | 0,00E+00 | 0,00E+00 | 0,00E+00 | 0,00E+00 | 0,00E+00 | 0,00E+00 |

# Appendix E - Supplementary information of Chapter 5.

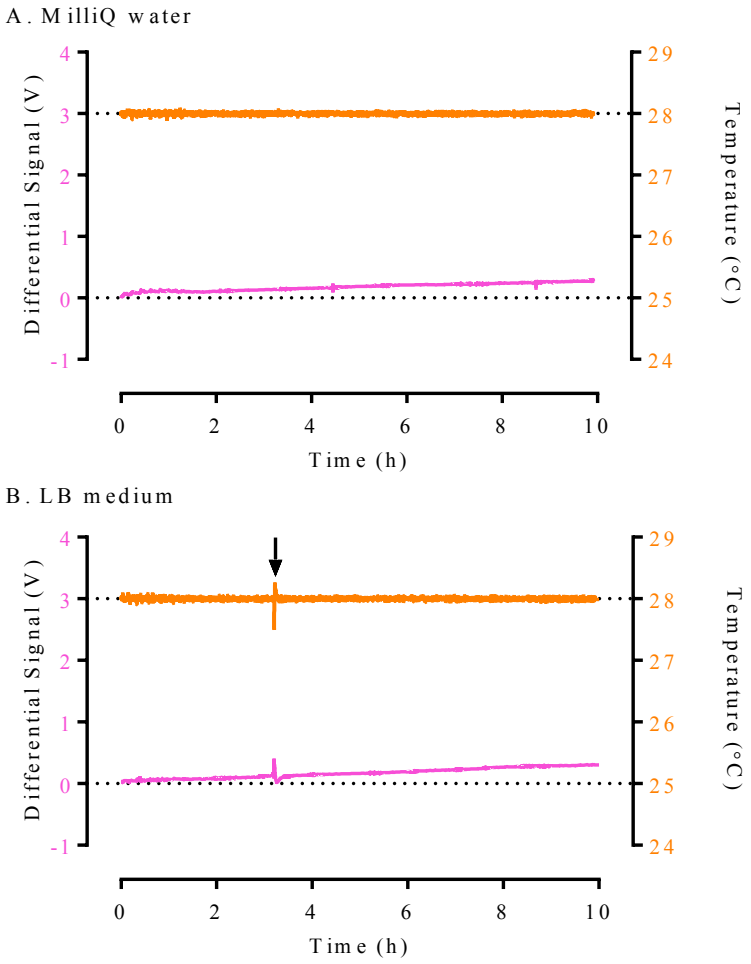


**Fig. S5.1: Behaviour of the µCT system in water and LB medium.** In the absence of the bacteria the µCT system was set-up in milliQ water (A) and in LB medium (B). The impact of time and medium types on the output µCT differential signal (pink curve) was assessed. Similarly, the perturbations created by the injection of fresh medium (arrow) and the overall quality of the temperature control (orange curve) over time were questioned.

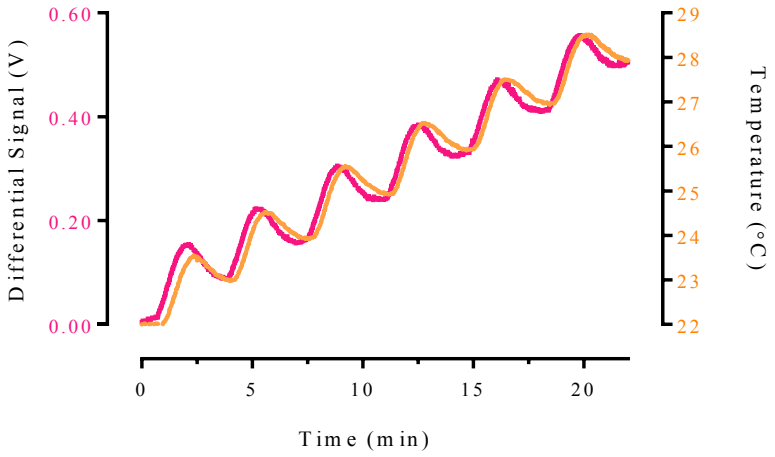


**Fig. S5.2: The µCT response to credential temperature stresses.** In the absence of the bacteria the set-up µCT system in LB medium was subjected to deliberate temperature variations (*i.e.* pulses of temperature using steps of 1 °C) in order to assess its response potency (*i.e.* associated to its surface stress). The above plot shows the µCT output differential signal variation along with the temperature evolution over time.

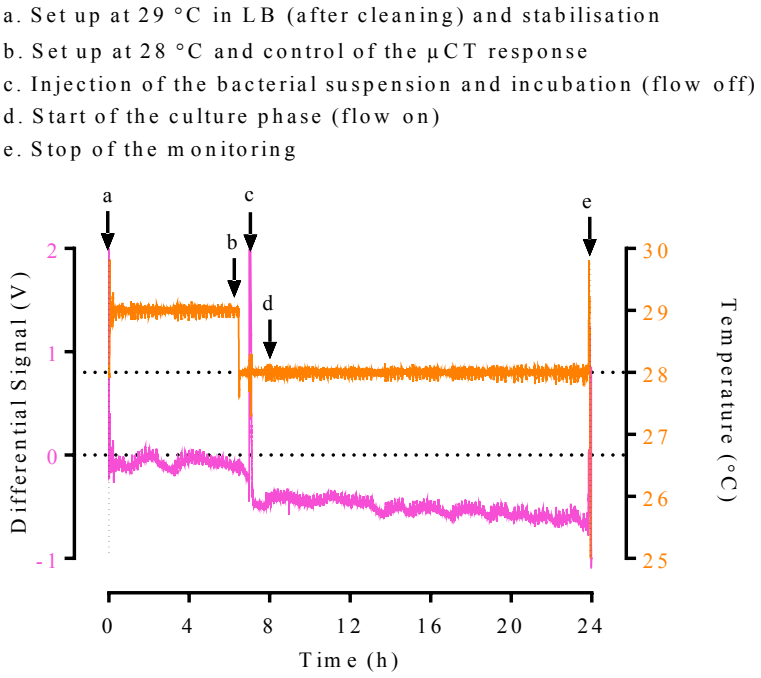


**Fig. S5.3: Growth monitoring of *P. putida* using the µCT system.** In the absence of the NPs (or related ions) the growth monitoring (in pink) of *P. putida* KT2440 was undertaken in LB medium using the set-up µCT following the main phases (from "a" to "e") reported on the above plot. The applied temperature (in orange) over time is equally shown.

# References

[1] European Commission, Official Journal of the European Union (2011/696/EU), OJ L 275/38, http://ec.europa.eu/environment/chemicals/nanotech/faq/definition_en.htm, last seen 01/12/15, last updated 11/11/15.

[2] Klaine, S. J., Alvarez, P. J. J., Batley, G. E., Fernandes, T. F.*, et al.*, Nanomaterials in the environment: Behavior, fate, bioavailability, and effects. *Environmental Toxicology and Chemistry* 2008, *27*, 1825-1851.

[3] Auffan, M., Rose, J., Bottero, J.-Y., Lowry, G. V.*, et al.*, Towards a definition of inorganic nanoparticles from an environmental, health and safety perspective. *Nature Nanotechnology* 2009, *4*, 634-641.

[4] British Standards Institution, Nanoparticles - Vocabulary, BSI Standards Publication, PAS71:2011, ISBN 978 0 580 70137 5.

[5] Ju-Nam, Y., Lead, J. R., Manufactured nanoparticles: An overview of their chemistry, interactions and potential environmental implications. *Science of the Total Environment* 2008, *400*, 396-414.

[6] Farre, M., Gajda-Schrantz, K., Kantiani, L., Barcelo, D., Ecotoxicity and analysis of nanomaterials in the aquatic environment. *Analytical and Bioanalytical Chemistry* 2009, *393*, 81-95.

[7] Sun, T. Y., Gottschalk, F., Hungerbuhler, K., Nowack, B., Comprehensive probabilistic modelling of environmental emissions of engineered nanomaterials. *Environmental Pollution* 2014, *185*, 69-76.

[8] Sardar, M., Mishra, A., Ahmad, R., Biosynthesis of Metal Nanoparticles and Their Applications. *Biosensors Nanotechnology* 2014, 239-266.

[9] Tinkle, S. S., Maximizing safe design of engineered nanomaterials: the NIH and NIEHS research perspective. *Wiley Interdisciplinary Reviews-Nanomedicine and Nanobiotechnology* 2010, *2*, 88-98.

[10] Piccinno, F., Gottschalk, F., Seeger, S., Nowack, B., Industrial production quantities and uses of ten engineered nanomaterials in Europe and the world. *Journal of Nanoparticle Research* 2012, *14*, 11.

[11] Kumar, S. A., Khan, M. I., Heterofunctional Nanomaterials: Fabrication, Properties and Applications in Nanobiotechnology. *Journal of Nanoscience and Nanotechnology* 2010, *10*, 4124-4134.

[12] Vance, M. E., Kuiken, T., Vejerano, E. P., McGinnis, S. P.*, et al.*, Nanotechnology in the real world: Redeveloping the nanomaterial consumer products inventory. *Beilstein Journal of Nanotechnology* 2015, *6*, 1769-1780.

[13] Brar, S. K., Verma, M., Tyagi, R. D., Surampalli, R. Y., Engineered nanoparticles in wastewater and wastewater sludge - Evidence and impacts. *Waste Management* 2010, *30*, 504-520.

[14] Kahru, A., Dubourguier, H.-C., From ecotoxicology to nanoecotoxicology. *Toxicology* 2010, *269*, 105-119.

[15] Rai, M., Birla, S., Ingle, A. P., Gupta, I.*, et al.*, Nanosilver: an inorganic nanoparticle with myriad potential applications. *Nanotechnology Reviews* 2014, *3*, 281-309.

[16] Juganson, K., Ivask, A., Blinova, I., Mortimer, M., Kahru, A., NanoE-Tox: New and in-depth database concerning ecotoxicity of nanomaterials. *Beilstein Journal of Nanotechnology* 2015, *6*, 1788-1804.

[17] Dizaj, S. M., Lotfipour, F., Barzegar-Jalali, M., Zarrintan, M. H., Adibkia, K., Antimicrobial activity of the metals and metal oxide nanoparticles. *Materials Science & Engineering C-Materials for Biological Applications* 2014, *44*, 278-284.

[18] Hajipour, M. J., Fromm, K. M., Ashkarran, A. A., Jimenez de Aberasturi, D.*, et al.*, Antibacterial properties of nanoparticles (vol 30, pg 499, 2012). *Trends in Biotechnology* 2013, *31*, 61-62.

[19] Doane, T. L., Burda, C., The unique role of nanoparticles in nanomedicine: imaging, drug delivery and therapy. *Chemical Society Reviews* 2012, *41*, 2885-2911.

[20] Aitken, R. J., Chaudhry, M. Q., Boxall, A. B. A., Hull, M., Manufacture and use of nanomaterials: current status in the UK and global trends. *Occupational Medicine-Oxford* 2006, *56*, 300-306.

[21] Matsuda, M., Hunt, G., Research on the societal impacts of nanotechnology: A preliminary comparison of USA, Europe and Japan. *Bio-Medical Materials and Engineering* 2009, *19*, 259-267.

[22] Lu, L. Y. Y., Lin, B. J. Y., Liu, J. S., Yu, C. Y., Ethics in Nanotechnology: What's Being Done? What's Missing? *Journal of Business Ethics* 2012, *109*, 583-598.

[23] Gavankar, S., Anderson, S., Keller, A. A., Critical Components of Uncertainty Communication in Life Cycle Assessments of Emerging Technologies: Nanotechnology as a Case Study. *Journal of Industrial Ecology* 2015, *19*, 468-479.

[24] Gottschalk, F., Nowack, B., The release of engineered nanomaterials to the environment. *Journal of Environmental Monitoring* 2011, *13*, 1145-1155.

[25] Yang, Y., Westerhoff, P., Presence in, and Release of, Nanomaterials from Consumer Products. *Nanomaterial: Impacts on Cell Biology and Medicine* 2014, *811*, 1-17.

[26] Nowack, B., Ranville, J. F., Diamond, S., Gallego-Urrea, J. A.*, et al.*, Potential scenarios for nanomaterial release and subsequent alteration in the environment. *Environmental Toxicology and Chemistry* 2012, *31*, 50-59.

[27] Handy, R. D., von der Kammer, F., Lead, J. R., Hassellov, M.*, et al.*, The ecotoxicology and chemistry of manufactured nanoparticles. *Ecotoxicology* 2008, *17*, 287-314.

[28] Gottschalk, F., Sun, T. Y., Nowack, B., Environmental concentrations of engineered nanomaterials: Review of modeling and analytical studies. *Environmental Pollution* 2013, *181*, 287-300.

[29] Marcoux, M. A., Matias, M., Olivier, F., Keck, G., Review and prospect of emerging contaminants in waste - Key issues and challenges linked to their presence in waste treatment schemes: General aspects and focus on nanoparticles. *Waste Management* 2013, *33*, 2147-2156.

[30] Gottschalk, F., Sonderer, T., Scholz, R. W., Nowack, B., Modeled Environmental Concentrations of Engineered Nanomaterials (TiO2, ZnO, Ag, CNT, Fullerenes) for Different Regions. *Environmental Science & Technology* 2009, *43*, 9216-9222.

[31] Chernousova, S., Epple, M., Silver as Antibacterial Agent: Ion, Nanoparticle, and Metal. *Angewandte Chemie-International Edition* 2013, *52*, 1636-1653.

[32] Westerhoff, P. K., Kiser, A., Hristovski, K., Nanomaterial Removal and Transformation During Biological Wastewater Treatment. *Environmental Engineering Science* 2013, *30*, 109-117.

[33] Duester, L., Burkhardt, M., Gutleb, A. C., Kaegi, R.*, et al.*, Toward a comprehensive and realistic risk evaluation of engineered nanomaterials in the urban water system. *Frontiers in chemistry* 2014, *2*, 39.

[34] Scown, T. M., van Aerle, R., Tyler, C. R., Review: Do engineered nanoparticles pose a significant threat to the aquatic environment? *Critical Reviews in Toxicology* 2010, *40*, 653-670.

[35] Kinsner-Ovaskainen, A., Colpo, P., Ponti, J., Rossi, F., Nanotoxicology. *In Vitro Toxicology Systems* 2014, 481-499.

[36] Seabra, A. B., Duran, N., Nanotoxicology of Metal Oxide Nanoparticles. *Metals* 2015, *5*, 934-975.

[37] Kahru, A., Ivask, A., Mapping the Dawn of Nanoecotoxicological Research. *Accounts of Chemical Research* 2013, *46*, 823-833.

[38] Zook, J. M., Long, S. E., Cleveland, D., Geronimo, C. L. A., MacCuspie, R. I., Measuring silver nanoparticle dissolution in complex biological and environmental matrices using UV-visible absorbance. *Analytical and Bioanalytical Chemistry* 2011, *401*, 1993-2002.

[39] MacCuspie, R. I., Rogers, K., Patra, M., Suo, Z.*, et al.*, Challenges for physical characterization of silver nanoparticles under pristine and environmentally relevant conditions. *Journal of Environmental Monitoring* 2011, *13*, 1212-1226.

[40] Djurisic, A. B., Leung, Y. H., Ng, A. M. C., Xu, X. Y.*, et al.*, Toxicity of Metal Oxide Nanoparticles: Mechanisms, Characterization, and Avoiding Experimental Artefacts. *Small* 2015, *11*, 26-44.

[41] Dhawan, A., Sharma, V., Toxicity assessment of nanomaterials: methods and challenges. *Analytical and Bioanalytical Chemistry* 2010, *398*, 589-605.

[42] Hassan, P. A., Rana, S., Verma, G., Making Sense of Brownian Motion: Colloid Characterization by Dynamic Light Scattering. *Langmuir* 2015, *31*, 3-12.

[43] Suresh, A. K., Pelletier, D. A., Doktycz, M. J., Relating nanomaterial properties and microbial toxicity. *Nanoscale* 2013, *5*, 463-474.

[44] Garner, K. L., Keller, A. A., Emerging patterns for engineered nanomaterials in the environment: a review of fate and toxicity studies. *Journal of Nanoparticle Research* 2014, *16*.

[45] Gottschalk, F., Kost, E., Nowack, B., Engineered nanomaterials in water and soils: A risk quantification based on probabilistic exposure and effect modeling. *Environmental Toxicology and Chemistry* 2013, *32*, 1278-1287.

[46] von der Kammer, F., Ferguson, P. L., Holden, P. A., Masion, A.*, et al.*, Analysis of engineered nanomaterials in complex matrices (environment and biota): General considerations and conceptual case studies. *Environmental Toxicology and Chemistry* 2012, *31*, 32-49.

[47] Notter, D. A., Mitrano, D. M., Nowack, B., ARE NANOSIZED OR DISSOLVED METALS MORE TOXIC IN THE ENVIRONMENT? A META-ANALYSIS. *Environmental Toxicology and Chemistry* 2014, *33*, 2733-2739.

[48] Duran, N., Silveira, C. P., Duran, M., Martinez, D. S. T., Silver nanoparticle protein corona and toxicity: a mini-review. *Journal of Nanobiotechnology* 2015, *13*.

[49] Xiu, Z.-M., Ma, J., Alvarez, P. J. J., Differential Effect of Common Ligands and Molecular Oxygen on Antimicrobial Activity of Silver Nanoparticles versus Silver Ions. *Environmental Science & Technology* 2011, *45*, 9003-9008.

[50] Lin, X., Li, J., Ma, S., Liu, G.*, et al.*, Toxicity of TiO2 Nanoparticles to Escherichia coli: Effects of Particle Size, Crystal Phase and Water Chemistry. *Plos One* 2014, *9*.

[51] Ma, R., Levard, C., Marinakos, S. M., Cheng, Y.*, et al.*, Size-Controlled Dissolution of Organic-Coated Silver Nanoparticles. *Environmental Science & Technology* 2012, *46*, 752-759.

[52] Laha, D., Pramanik, A., Laskar, A., Jana, M.*, et al.*, Shape-dependent bactericidal activity of copper oxide nanoparticle mediated by DNA and membrane damage. *Materials Research Bulletin* 2014, *59*, 185-191.

[53] Pal, S., Tak, Y. K., Song, J. M., Does the antibacterial activity of silver nanoparticles depend on the shape of the nanoparticle? A study of the gram-negative bacterium Escherichia coli. *Applied and Environmental Microbiology* 2007, *73*, 1712-1720.

[54] Silva, T., Pokhrel, L. R., Dubey, B., Tolaymat, T. M.*, et al.*, Particle size, surface charge and concentration dependent ecotoxicity of three organo-coated silver nanoparticles: Comparison between general linear model-predicted and observed toxicity. *Science of the Total Environment* 2014, *468*, 968-976.

[55] Simon-Deckers, A., Loo, S., Mayne-L'Hermite, M., Herlin-Boime, N.*, et al.*, Size-, Composition- and Shape-Dependent Toxicological Impact of Metal Oxide Nanoparticles and Carbon Nanotubes toward Bacteria. *Environmental Science & Technology* 2009, *43*, 8423-8429.

[56] Keller, A. A., Wang, H. T., Zhou, D. X., Lenihan, H. S.*, et al.*, Stability and Aggregation of Metal Oxide Nanoparticles in Natural Aqueous Matrices. *Environmental Science & Technology* 2010, *44*, 1962-1967.

[57] Fabrega, J., Fawcett, S. R., Renshaw, J. C., Lead, J. R., Silver Nanoparticle Impact on Bacterial Growth: Effect of pH, Concentration, and Organic Matter. *Environmental Science & Technology* 2009, *43*, 7285-7290.

[58] French, R. A., Jacobson, A. R., Kim, B., Isley, S. L.*, et al.*, Influence of Ionic Strength, pH, and Cation Valence on Aggregation Kinetics of Titanium Dioxide Nanoparticles. *Environmental Science & Technology* 2009, *43*, 1354-1359.

[59] Pokhrel, L. R., Dubey, B., Scheuerman, P. R., Natural water chemistry (dissolved organic carbon, pH, and hardness) modulates colloidal stability, dissolution, and antimicrobial activity of citrate functionalized silver nanoparticles. *Environmental Science-Nano* 2014, *1*, 45-54.

[60] Ng, A. M. C., Chan, C. M. N., Guo, M. Y., Leung, Y. H.*, et al.*, Antibacterial and photocatalytic activity of TiO2 and ZnO nanomaterials in phosphate buffer and saline solution. *Applied Microbiology and Biotechnology* 2013, *97*, 5565-5573.

[61] Jomini, S., Labille, J., Bauda, P., Pagnout, C., Modifications of the bacterial reverse mutation test reveals mutagenicity of TiO2 nanoparticles and byproducts from a sunscreen TiO2-based nanocomposite. *Toxicology Letters* 2012, *215*, 54-61.

[62] Pagnout, C., Jomini, S., Dadhwal, M., Caillet, C.*, et al.*, Role of electrostatic interactions in the toxicity of titanium dioxide nanoparticles toward Escherichia coli. *Colloids and Surfaces B-Biointerfaces* 2012, *92*, 315-321.

[63] He, X., Kuang, Y., Li, Y., Zhang, H.*, et al.*, Changing exposure media can reverse the cytotoxicity of ceria nanoparticles for Escherichia coli. *Nanotoxicology* 2012, *6*, 233-240.

[64] Lesniak, A., Salvati, A., Santos-Martinez, M. J., Radomski, M. W.*, et al.*, Nanoparticle Adhesion to the Cell Membrane and Its Effect on Nanoparticle Uptake Efficiency. *Journal of the American Chemical Society* 2013, *135*, 1438-1444.

[65] Lv, J., Zhang, S., Luo, L., Han, W.*, et al.*, Dissolution and Microstructural Transformation of ZnO Nanoparticles under the Influence of Phosphate. *Environmental Science & Technology* 2012, *46*, 7215-7221.

[66] Kaekinen, A., Bondarenko, O., Ivask, A., Kahru, A., The Effect of Composition of Different Ecotoxicological Test Media on Free and Bioavailable Copper from CuSO4 and CuO Nanoparticles: Comparative Evidence from a Cu-Selective Electrode and a Cu-Biosensor. *Sensors* 2011, *11*, 10502-10521.

[67] Cupi, D., Hartmann, N. B., Baun, A., The influence of natural organic matter and aging on suspension stability in guideline toxicity testing of silver, zinc oxide, and titanium dioxide nanoparticles with daphnia magna. *Environmental Toxicology and Chemistry* 2015, *34*, 497-506.

[68] Yang, Y., Zhang, C. Q., Hu, Z. Q., Impact of metallic and metal oxide nanoparticles on wastewater treatment and anaerobic digestion. *Environmental Science-Processes & Impacts* 2013, *15*, 39-48.

[69] Krug, H. F., Nanosafety Research-Are We on the Right Track? *Angewandte Chemie-International Edition* 2014, *53*, 12304-12319.

[70] Paterson, G., Macken, A., Thomas, K. V., The need for standardized methods and environmental monitoring programs for anthropogenic nanoparticles. *Analytical Methods* 2011, *3*, 1461-1467.

[71] Saleh, N. B., Chambers, B., Aich, N., Plazas-Tuttle, J.*, et al.*, Mechanistic lessons learned from studies of planktonic bacteria with metallic nanomaterials: implications for interactions between nanomaterials and biofilm bacteria. *Frontiers in Microbiology* 2015, *6*.

[72] Handy, R. D., van den Brink, N., Chappell, M., Muehling, M.*, et al.*, Practical considerations for conducting ecotoxicity test methods with manufactured nanomaterials: what have we learnt so far? *Ecotoxicology* 2012, *21*, 933-972.

[73] Hartmann, N. B., Jensen, K. A., Baun, A., Rasmussen, K.*, et al.*, Techniques and protocols for dispersing nanoparticle powders in aqueous media. Is there a rationale for harmonization? *Journal of Toxicology and Environmental Health-Part B-Critical Reviews* 2015, *18*, 299-326.

[74] Zhang, L., Jiang, Y., Ding, Y., Povey, M., York, D., Investigation into the antibacterial behaviour of suspensions of ZnO nanoparticles (ZnO nanofluids). *Journal of Nanoparticle Research* 2007, *9*, 479-489.

[75] Oomen, A. G., Bos, P. M. J., Fernandes, T. F., Hund-Rinke, K.*, et al.*, Concern-driven integrated approaches to nanomaterial testing and assessment - report of the NanoSafety Cluster Working Group 10. *Nanotoxicology* 2014, *8*, 334-348.

[76] Costerton, J. W., Lewandowski, Z., Caldwell, D. E., Korber, D. R., Lappinscott, H. M., Microbial biofilms. *Annual Review of Microbiology* 1995, *49*, 711-745.

[77] Stewart, P. S., Franklin, M. J., Physiological heterogeneity in biofilms. *Nature Reviews Microbiology* 2008, *6*, 199-210.

[78] Lopez, D., Vlamakis, H., Kolter, R., Biofilms. *Cold Spring Harbor Perspectives in Biology* 2010, *2*, 11.

[79] Booth, S. C., Workentine, M. L., Wen, J., Shaykhutdinov, R.*, et al.*, Differences in Metabolism between the Biofilm and Planktonic Response to Metal Stress. *Journal of Proteome Research* 2011, *10*, 3190-3199.

[80] Sampathkumar, B., Napper, S., Carrillo, C. D., Willson, P.*, et al.*, Transcriptional and translational expression patterns associated with immobilized growth of Campylobacter jejuni. *Microbiology-Sgm* 2006, *152*, 567-577.

[81] Doetsch, A., Eckweiler, D., Schniederjans, M., Zimmermann, A.*, et al.*, The Pseudomonas aeruginosa Transcriptome in Planktonic Cultures and Static Biofilms Using RNA Sequencing. *Plos One* 2012, *7*.

[82] Bridier, A., Briandet, R., Thomas, V., Dubois-Brissonnet, F., Resistance of bacterial biofilms to disinfectants: a review. *Biofouling* 2011, *27*, 1017-1032.

[83] Mah, T. F. C., O'Toole, G. A., Mechanisms of biofilm resistance to antimicrobial agents. *Trends in Microbiology* 2001, *9*, 34-39.

[84] Robbens, J., Dardenne, F., Devriese, L., De Coen, W., Blust, R., Escherichia coli as a bioreporter in ecotoxicology. *Applied Microbiology and Biotechnology* 2010, *88*, 1007-1025.

[85] Girotti, S., Ferri, E. N., Fumo, M. G., Maiolini, E., Monitoring of environmental pollutants by bioluminescent bacteria. *Analytica Chimica Acta* 2008, *608*, 2-29.

[86] Tecon, R., van der Meer, J. R., Bacterial biosensors for measuring availability of environmental pollutants. *Sensors* 2008, *8*, 4062-4080.

[87] Xu, T. T., Close, D. M., Sayler, G. S., Ripp, S., Genetically modified whole-cell bioreporters for environmental assessment. *Ecological Indicators* 2013, *28*, 125-141.

[88] Struss, A. K., Pasini, P., Daunert, S., Biosensing Systems Based on Genetically Engineered Whole Cells. *Recognition Receptors in Biosensors* 2010, 565-598.

[89] Su, L. A., Jia, W. Z., Hou, C. J., Lei, Y., Microbial biosensors: A review. *Biosensors & Bioelectronics* 2011, *26*, 1788-1799.

[90] van der Meer, J. R., Belkin, S., Where microbiology meets microengineering: design and applications of reporter bacteria. *Nature Reviews Microbiology* 2010, *8*, 511-522.

[91] Michelini, E., Cevenini, L., Calabretta, M. M., Spinozzi, S.*, et al.*, Field-deployable whole-cell bioluminescent biosensors: so near and yet so far. *Analytical and Bioanalytical Chemistry* 2013, *405*, 6155-6163.

[92] Cerminati, S., Soncini, F. C., Checa, S. K., A sensitive whole-cell biosensor for the simultaneous detection of a broad-spectrum of toxic heavy metal ions. *Chemical Communications* 2015, *51*, 5917-5920.

[93] Choi, S. H., Gu, M. B., A portable toxicity biosensor using freeze-dried recombinant bioluminescent bacteria. *Biosensors & Bioelectronics* 2002, *17*, 433-440.

[94] Close, D. M., Ripp, S., Sayler, G. S., Reporter Proteins in Whole-Cell Optical Bioreporter Detection Systems, Biosensor Integrations, and Biosensing Applications. *Sensors* 2009, *9*, 9147-9174.

[95] Melamed, S., Ceriotti, L., Weigel, W., Rossi, F.*, et al.*, A printed nanolitre-scale bacterial sensor array. *Lab on a Chip* 2011, *11*, 139-146.

[96] Roda, A., Mirasoli, M., Michelini, E., Di Fusco, M.*, et al.*, Progress in chemical luminescence-based biosensors: A critical review. *Biosensors & Bioelectronics* 2016, *76*, 164-179.

[97] Holden, P. A., Schimel, J. P., Godwin, H. A., Five reasons to use bacteria when assessing manufactured nanomaterial environmental hazards and fates. *Current Opinion in Biotechnology* 2014, *27*, 73-78.

[98] von Moos, N., Slaveykova, V. I., Oxidative stress induced by inorganic nanoparticles in bacteria and aquatic microalgae - state of the art and knowledge gaps. *Nanotoxicology* 2014, *8*, 605-630.

[99] Bondarenko, O., Juganson, K., Ivask, A., Kasemets, K.*, et al.*, Toxicity of Ag, CuO and ZnO nanoparticles to selected environmentally relevant test organisms and mammalian cells in vitro: a critical review. *Archives of Toxicology* 2013, *87*, 1181-1200.

[100] Thannickal, V. J., Fanburg, B. L., Reactive oxygen species in cell signaling. *American Journal of Physiology-Lung Cellular and Molecular Physiology* 2000, *279*, L1005-L1028.

[101] Apel, K., Hirt, H., Reactive oxygen species: Metabolism, oxidative stress, and signal transduction. *Annual Review of Plant Biology* 2004, *55*, 373-399.

[102] Jiang, W., Mashayekhi, H., Xing, B., Bacterial toxicity comparison between nano- and micro-scaled oxide particles. *Environmental Pollution* 2009, *157*, 1619-1625.

[103] Feris, K., Otto, C., Tinker, J., Wingett, D.*, et al.*, Electrostatic Interactions Affect Nanoparticle-Mediated Toxicity to Gram-Negative Bacterium Pseudomonas aeruginosa PAO1. *Langmuir* 2010, *26*, 4429-4436.

[104] Applerot, G., Lellouche, J., Lipovsky, A., Nitzan, Y.*, et al.*, Understanding the Antibacterial Mechanism of CuO Nanoparticles: Revealing the Route of Induced Oxidative Stress. *Small* 2012, *8*, 3326-3337.

[105] Thill, A., Zeyons, O., Spalla, O., Chauvat, F.*, et al.*, Cytotoxicity of CeO2 nanoparticles for Escherichia coli. Physico-chemical insight of the cytotoxicity mechanism. *Environmental Science & Technology* 2006, *40*, 6151-6156.

[106] Marambio-Jones, C., Hoek, E. M. V., A review of the antibacterial effects of silver nanomaterials and potential implications for human health and the environment. *Journal of Nanoparticle Research* 2010, *12*, 1531-1551.

[107] Ma, H. B., Williams, P. L., Diamond, S. A., Ecotoxicity of manufactured ZnO nanoparticles - A review. *Environmental Pollution* 2013, *172*, 76-85.

[108] Chambers, B. A., Afrooz, A. R. M. N., Bae, S., Aich, N.*, et al.*, Effects of Chloride and Ionic Strength on Physical Morphology, Dissolution, and Bacterial Toxicity of Silver Nanoparticles. *Environmental Science & Technology* 2014, *48*, 761-769.

[109] Feng, Q. L., Wu, J., Chen, G. Q., Cui, F. Z.*, et al.*, A mechanistic study of the antibacterial effect of silver ions on Escherichia coli and Staphylococcus aureus. *Journal of Biomedical Materials Research* 2000, *52*, 662-668.

[110] Reyes, V. C., Li, M., Hoek, E. M. V., Mahendra, S., Damoiseaux, R., Genome-Wide Assessment in Escherichia coli Reveals Time-Dependent Nanotoxicity Paradigms. *Acs Nano* 2012, *6*, 9402-9415.

[111] Cui, Y., Zhao, Y., Tian, Y., Zhang, W.*, et al.*, The molecular mechanism of action of bactericidal gold nanoparticles on Escherichia coli. *Biomaterials* 2012, *33*, 2327-2333.

[112] Lu, J., Struewing, I., Buse, H. Y., Kou, J.*, et al.*, Legionella pneumophila Transcriptional Response following Exposure to CuO Nanoparticles. *Applied and Environmental Microbiology* 2013, *79*, 2713-2720.

[113] Picado, A., Paixao, S. M., Moita, L., Silva, L.*, et al.*, A multi-integrated approach on toxicity effects of engineered TiO2 nanoparticles. *Frontiers of Environmental Science & Engineering* 2015, *9*, 793-803.

[114] Jung, Y., Park, C.-B., Kim, Y., Kim, S.*, et al.*, Application of Multi-Species Microbial Bioassay to Assess the Effects of Engineered Nanoparticles in the Aquatic Environment: Potential of a Luminous Microbial Array for Toxicity Risk Assessment (LumiMARA) on Testing for Surface-Coated Silver Nanoparticles. *International Journal of Environmental Research and Public Health* 2015, *12*, 8172-8186.

[115] Nam, S.-H., Shin, Y.-J., Lee, W.-M., Kim, S. W.*, et al.*, Conducting a battery of bioassays for gold nanoparticles to derive guideline value for the protection of aquatic ecosystems. *Nanotoxicology* 2015, *9*, 326-335.

[116] Kaweeteerawat, C., Chang, C. H., Roy, K. R., Liu, R.*, et al.*, Cu Nanoparticles Have Different Impacts in Escherichia coli and Lactobacillus brevis than Their Microsized and Ionic Analogues. *Acs Nano* 2015, *9*, 7215-7225.

[117] Kaweeteerawat, C., Ivask, A., Liu, R., Zhang, H.*, et al.*, Toxicity of Metal Oxide Nanoparticles in Escherichia coli Correlates with Conduction Band and Hydration Energies. *Environmental Science & Technology* 2015, *49*, 1105-1112.

[118] Farkas, J., Peter, H., Ciesielski, T. M., Thomas, K. V.*, et al.*, Impact of TiO2 nanoparticles on freshwater bacteria from three Swedish lakes. *Science of the Total Environment* 2015, *535*, 85-93.

[119] Erdem, A., Metzler, D., Cha, D., Huang, C. P., Inhibition of bacteria by photocatalytic nano-TiO2 particles in the absence of light. *International Journal of Environmental Science and Technology* 2015, *12*, 2987-2996.

[120] Leung, Y. H., Yung, M. M. N., Ng, A. M. C., Ma, A. P. Y.*, et al.*, Toxicity of CeO2 nanoparticles - The effect of nanoparticle properties. *Journal of Photochemistry and Photobiology B-Biology* 2015, *145*, 48-59.

[121] Ng, A. M. C., Guo, M. Y., Leung, Y. H., Chan, C. M. N.*, et al.*, Metal oxide nanoparticles with low toxicity. *Journal of Photochemistry and Photobiology B-Biology* 2015, *151*, 17-24.

[122] Velimirovic, M., Simons, Q., Bastiaens, L., Use of CAH-degrading bacteria as test-organisms for evaluating the impact of fine zerovalent iron particles on the anaerobic subsurface environment. *Chemosphere* 2015, *134*, 338-345.

[123] Chu Thi Thanh, B., Tong, T., Gaillard, J.-F., Gray, K. A., Kelly, J. J., Acute Effects of TiO2 Nanomaterials on the Viability and Taxonomic Composition of Aquatic Bacterial Communities Assessed via High-Throughput Screening and Next Generation Sequencing. *Plos One* 2014, *9*.

[124] Lan, J., Gou, N., Gao, C., He, M., Gu, A. Z., Comparative and Mechanistic Genotoxicity Assessment of Nanomaterials via a Quantitative Toxicogenomics Approach across Multiple Species. *Environmental Science & Technology* 2014, *48*, 12937-12945.

[125] Pakrashi, S., Kumar, D., Iswarya, V., Bhuvaneshwari, M*., et al.*, A comparative ecotoxicity analysis of alpha- and gamma-phase aluminium oxide nanoparticles towards a freshwater bacterial isolate Bacillus licheniformis. *Bioprocess and Biosystems Engineering* 2014, *37*, 2415-2423.

[126] Engelke, M., Koeser, J., Hackmann, S., Zhang, H*., et al.*, A miniaturized solid contact test with arthrobacter globiformis for the assessment of the environmental impact of silver nanoparticles. *Environmental Toxicology and Chemistry* 2014, *33*, 1142-1147.

[127] Chu Thi Thanh, B., Tong, T., Gaillard, J.-F., Gray, K. A., Kelly, J. J., Common freshwater bacteria vary in their responses to short-term exposure to nano-TiO2. *Environmental Toxicology and Chemistry* 2014, *33*, 317-327.

[128] Concha-Guerrero, S. I., Souza Brito, E. M., Pinon-Castillo, H. A., Tarango-Rivero, S. H*., et al.*, Effect of CuO Nanoparticles over Isolated Bacterial Strains from Agricultural Soil. *Journal of Nanomaterials* 2014.

[129] Weber, K. P., Petersen, E. J., Bissegger, S., Koch, I*., et al.*, Effect of gold nanoparticles and ciprofloxacin on microbial catabolism: a community-based approach. *Environmental Toxicology and Chemistry* 2014, *33*, 44-51.

[130] Hachicho, N., Hoffmann, P., Ahlert, K., Heipieper, H. J., Effect of silver nanoparticles and silver ions on growth and adaptive response mechanisms of Pseudomonas putida mt-2. *Fems Microbiology Letters* 2014, *355*, 71-77.

[131] Beddow, J., Stolpe, B., Cole, P., Lead, J. R*., et al.*, Effects of engineered silver nanoparticles on the growth and activity of ecologically important microbes. *Environmental Microbiology Reports* 2014, *6*, 448-458.

[132] Boenigk, J., Beisser, D., Zimmermann, S., Bock, C*., et al.*, Effects of Silver Nitrate and Silver Nanoparticles on a Planktonic Community: General Trends after Short-Term Exposure. *Plos One* 2014, *9*.

[133] Kumari, J., Kumar, D., Mathur, A., Naseer, A*., et al.*, Cytotoxicity of TiO2 nanoparticles towards freshwater sediment microorganisms at low exposure concentrations. *Environmental Research* 2014, *135*, 333-345.

[134] Kumar, D., Kumari, J., Pakrashi, S., Dalai, S*., et al.*, Qualitative toxicity assessment of silver nanoparticles on the fresh water bacterial isolates and consortium at low level of exposure concentration. *Ecotoxicology and Environmental Safety* 2014, *108*, 152-160.

[135] Goix, S., Leveque, T., Xiong, T.-T., Schreck, E*., et al.*, Environmental and health impacts of fine and ultrafine metallic particles: Assessment of threat scores. *Environmental Research* 2014, *133*, 185-194.

[136] Burkowska-But, A., Sionkowski, G., Walczak, M., Influence of stabilizers on the antimicrobial properties of silver nanoparticles introduced into natural water. *Journal of Environmental Sciences-China* 2014, *26*, 542-549.

[137] Kwon, J. Y., Lee, S. Y., Koedrith, P., Lee, J. Y*., et al.*, Lack of genotoxic potential of ZnO nanoparticles in in vitro and in vivo tests. *Mutation Research-Genetic Toxicology and Environmental Mutagenesis* 2014, *761*, 1-9.

[138] Kwon, J. Y., Kim, H. L., Lee, J. Y., Ju, Y. H., *et al.*, Undetactable levels of genotoxicity of SiO2 nanoparticles in in vitro and in vivo tests. *International Journal of Nanomedicine* 2014, *9*, 173-181.

[139] Leung, Y. H., Ng, A. M. C., Xu, X., Shen, Z., *et al.*, Mechanisms of Antibacterial Activity of MgO: Non-ROS Mediated Toxicity of MgO Nanoparticles Towards Escherichia coli. *Small* 2014, *10*, 1171-1183.

[140] Starodub, N. F., Shavanova, K. E., Taran, M. V., Katsev, A. M., *et al.*, *8th International Conference on Advanced Optical Materials and Devices (AOMD)*, Riga, LATVIA 2014.

[141] Mallevre, F., Fernandes, T. F., Aspray, T. J., Silver, zinc oxide and titanium dioxide nanoparticle ecotoxicity to bioluminescent Pseudomonas putida in laboratory medium and artificial wastewater. *Environmental Pollution* 2014, *195*, 218-225.

[142] Wang, D., Lin, Z., Yao, Z., Yu, H., Surfactants present complex joint effects on the toxicities of metal oxide nanoparticles. *Chemosphere* 2014, *108*, 70-75.

[143] Loza, K., Diendorf, J., Sengstock, C., Ruiz-Gonzalez, L., *et al.*, The dissolution and biological effects of silver nanoparticles in biological media. *Journal of Materials Chemistry B* 2014, *2*, 1634-1643.

[144] Ko, K.-S., Kong, I. C., Toxic effects of nanoparticles on bioluminescence activity, seed germination, and gene mutation. *Applied Microbiology and Biotechnology* 2014, *98*, 3295-3303.

[145] Ivask, A., ElBadawy, A., Kaweeteerawat, C., Boren, D., *et al.*, Toxicity Mechanisms in Escherichia coli Vary for Silver Nanoparticles and Differ from Ionic Silver. *Acs Nano* 2014, *8*, 374-386.

[146] Santimano, M. C., Kowshik, M., Altered growth and enzyme expression profile of ZnO nanoparticles exposed non-target environmentally beneficial bacteria. *Environmental Monitoring and Assessment* 2013, *185*, 7205-7214.

[147] Li, F. F., Lei, C. Y., Shen, Q. P., Li, L. J., *et al.*, Analysis of copper nanoparticles toxicity based on a stress-responsive bacterial biosensor array. *Nanoscale* 2013, *5*, 653-662.

[148] Doudi, M., Naghsh, N., Setorki, M., Comparison of the effects of silver nanoparticles on pathogenic bacteria resistant to beta-lactam antibiotics (ESBLs) as a prokaryote model and Wistar rats as a eukaryote model. *Medical science monitor basic research* 2013, *19*, 103-110.

[149] Chudobova, D., Nejdl, L., Gumulec, J., Krystofova, O., *et al.*, Complexes of Silver(I) Ions and Silver Phosphate Nanoparticles with Hyaluronic Acid and/or Chitosan as Promising Antimicrobial Agents for Vascular Grafts. *International Journal of Molecular Sciences* 2013, *14*, 13592-13614.

[150] Casado, M. P., Macken, A., Byrne, H. J., Ecotoxicological assessment of silica and polystyrene nanoparticles assessed by a multitrophic test battery. *Environment International* 2013, *51*, 97-105.

[151] Allard, P., Darnajoux, R., Phalyvong, K., Bellenger, J.-P., Effects of Tungsten and Titanium Oxide Nanoparticles on the Diazotrophic Growth and Metals Acquisition by Azotobacter vinelandii under Molybdenum Limiting Condition. *Environmental Science & Technology* 2013, *47*, 2061-2068.

[152] Kim, J. S., Song, K. S., Sung, J. H., Ryu, H. R., *et al.*, Genotoxicity, acute oral and dermal toxicity, eye and dermal irritation and corrosion and skin sensitisation evaluation of silver nanoparticles. *Nanotoxicology* 2013, *7*, 953-960.

[153] Karunakaran, G., Suriyaprabha, R., Manivasakan, P., Yuvakkumar, R.*, et al.*, Impact of Nano and Bulk ZrO2, TiO2 Particles on Soil Nutrient Contents and PGPR. *Journal of Nanoscience and Nanotechnology* 2013, *13*, 678-685.

[154] Yang, Y., Wang, J., Xiu, Z., Alvarez, P. J. J., Impacts of silver nanoparticles on cellular and transcriptional activity of nitrogen-cycling bacteria. *Environmental Toxicology and Chemistry* 2013, *32*, 1488-1494.

[155] Gunawan, C., Teoh, W. Y., Marquis, C. P., Amal, R., Induced Adaptation of Bacillus sp. to Antimicrobial Nanosilver. *Small* 2013, *9*, 3554-3560.

[156] Planchon, M., Ferrari, R., Guyot, F., Gelabert, A.*, et al.*, Interaction between Escherichia coli and TiO2 nanoparticles in natural and artificial waters. *Colloids and Surfaces B-Biointerfaces* 2013, *102*, 158-164.

[157] Filser, J., Arndt, D., Baumann, J., Geppert, M.*, et al.*, Intrinsically green iron oxide nanoparticles? From synthesis via (eco-)toxicology to scenario modelling. *Nanoscale* 2013, *5*, 1034-1046.

[158] Zhao, J., Wang, Z., Dai, Y., Xing, B., Mitigation of CuO nanoparticle-induced bacterial membrane damage by dissolved organic matter. *Water Research* 2013, *47*, 4169-4178.

[159] Ansari, M. A., Khan, H. M., Khan, A. A., Sultan, A., Azam, A., Characterization of clinical strains of MSSA, MRSA and MRSE isolated from skin and soft tissue infections and the antibacterial activity of ZnO nanoparticles. *World Journal of Microbiology & Biotechnology* 2012, *28*, 1605-1613.

[160] Krishnamoorthy, K., Manivannan, G., Kim, S. J., Jeyasubramanian, K., Premanathan, M., Antibacterial activity of MgO nanoparticles based on lipid peroxidation by oxygen vacancy. *Journal of Nanoparticle Research* 2012, *14*.

[161] Vargas-Reus, M. A., Memarzadeh, K., Huang, J., Ren, G. G., Allaker, R. P., Antimicrobial activity of nanoparticulate metal oxides against peri-implantitis pathogens. *International Journal of Antimicrobial Agents* 2012, *40*, 135-139.

[162] Hassan, M. S., Amna, T., Yang, O. B., El-Newehy, M. H.*, et al.*, Smart copper oxide nanocrystals: Synthesis, characterization, electrochemical and potent antibacterial activity. *Colloids and Surfaces B-Biointerfaces* 2012, *97*, 201-206.

[163] Hossain, S. T., Mukherjee, S. K., CdO Nanoparticle Toxicity on Growth, Morphology, and Cell Division in Escherichia coli. *Langmuir* 2012, *28*, 16614-16622.

[164] Neal, A. L., Kabengi, N., Grider, A., Bertsch, P. M., Can the soil bacterium Cupriavidus necator sense ZnO nanomaterials and aqueous Zn2+ differentially? *Nanotoxicology* 2012, *6*, 371-380.

[165] Perreault, F., Melegari, S. P., Fuzinatto, C. F., Bogdan, N.*, et al.*, Toxicity of PAMAM-Coated Gold Nanoparticles in Different Unicellular Models. *Environmental Toxicology* 2014, *29*, 328-336.

[166] Yang, Y., Mathieu, J. M., Chattopadhyay, S., Miller, J. T.*, et al.*, Defense Mechanisms of Pseudomonas aeruginosa PAO1 against Quantum Dots and Their Released Heavy Metals. *Acs Nano* 2012, *6*, 6091-6098.

[167] Yang, Y., Wang, J., Zhu, H., Colvin, V. L., Alvarez, P. J., Relative Susceptibility and Transcriptional Response of Nitrogen Cycling Bacteria to Quantum Dots. *Environmental Science & Technology* 2012, *46*, 3433-3441.

[168] Kim, S. W., An, Y. J., Effect of ZnO and TiO2 nanoparticles preilluminated with UVA and UVB light on Escherichia coli and Bacillus subtilis. *Applied Microbiology and Biotechnology* 2012, *95*, 243-253.

[169] Li, Y., Zhang, W., Niu, J., Chen, Y., Mechanism of Photogenerated Reactive Oxygen Species and Correlation with the Antibacterial Properties of Engineered Metal-Oxide Nanoparticles. *Acs Nano* 2012, *6*, 5164-5173.

[170] Pokhrel, L. R., Silva, T., Dubey, B., El Badawy, A. M.*, et al.*, Rapid screening of aquatic toxicity of several metal-based nanoparticles using the MetPLATE (TM) bioassay. *Science of the Total Environment* 2012, *426*, 414-422.

[171] Xu, H., Qu, F., Xu, H., Lai, W.*, et al.*, Role of reactive oxygen species in the antibacterial mechanism of silver nanoparticles on Escherichia coli O157:H7. *Biometals* 2012, *25*, 45-53.

[172] Dutta, R. K., Nenavathu, B. P., Gangishetty, M. K., Reddy, A. V. R., Studies on antibacterial activity of ZnO nanoparticles by ROS induced lipid peroxidation. *Colloids and Surfaces B-Biointerfaces* 2012, *94*, 143-150.

[173] Hessler, C. M., Wu, M.-Y., Xue, Z., Choi, H., Seo, Y., The influence of capsular extracellular polymeric substances on the interaction between TiO2 nanoparticles and planktonic bacteria. *Water Research* 2012, *46*, 4687-4696.

[174] Greulich, C., Braun, D., Peetsch, A., Diendorf, J.*, et al.*, The toxic effect of silver ions and silver nanoparticles towards bacteria and human cells occurs in the same concentration range. *Rsc Advances* 2012, *2*, 6981-6987.

[175] Lopes, I., Ribeiro, R., Antunes, F. E., Rocha-Santos, T. A. P.*, et al.*, Toxicity and genotoxicity of organic and inorganic nanoparticles to the bacteria Vibrio fischeri and Salmonella typhimurium. *Ecotoxicology* 2012, *21*, 637-648.

[176] Stevanovic, M. M., Skapin, S. D., Bracko, I., Milenkovic, M.*, et al.*, Poly(lactide-co-glycolide)/silver nanoparticles: Synthesis, characterization, antimicrobial activity, cytotoxicity assessment and ROS-inducing potential. *Polymer* 2012, *53*, 2818-2828.

[177] Binaeian, E., Attar, H., Safekordi, A. A., Saber, R., Chaichi, M. J., Study on Toxicity of Seven Manufactured Nano Particles and Two Phenolic Compounds to Bacteria Vibrio fischeri Using Homemade Luminometer. *Asian Journal of Chemistry* 2012, *24*, 5211-5218.

[178] Kumar, A., Pandey, A. K., Singh, S. S., Shanker, R., Dhawan, A., A Flow Cytometric Method to Assess Nanoparticle Uptake in Bacteria. *Cytometry Part A* 2011, *79A*, 707-712.

[179] Kumar, A., Pandey, A. K., Singh, S. S., Shanker, R., Dhawan, A., Cellular Response to Metal Oxide Nanoparticles in Bacteria. *Journal of Biomedical Nanotechnology* 2011, *7*, 102-103.

[180] Kumar, A., Pandey, A. K., Singh, S. S., Shanker, R., Dhawan, A., Cellular uptake and mutagenic potential of metal oxide nanoparticles in bacterial cells. *Chemosphere* 2011, *83*, 1124-1132.

[181] Kumar, A., Pandey, A. K., Singh, S. S., Shanker, R., Dhawan, A., Engineered ZnO and TiO2 nanoparticles induce oxidative stress and DNA damage leading to reduced viability of Escherichia coli. *Free Radical Biology and Medicine* 2011, *51*, 1872-1881.

[182] Gou, N., Gu, A. Z., A New Transcriptional Effect Level Index (TELI) for Toxicogenomics-based Toxicity Assessment. *Environmental Science & Technology* 2011, *45*, 5410-5417.

[183] Garcia, A., Espinosa, R., Delgado, L., Casals, E.*, et al.*, Acute toxicity of cerium oxide, titanium oxide and iron oxide nanoparticles using standardized tests. *Desalination* 2011, *269*, 136-141.

[184] Johnson, A. C., Bowes, M. J., Crossley, A., Jarvie, H. P.*, et al.*, An assessment of the fate, behaviour and environmental risk associated with sunscreen TiO2 nanoparticles in UK field scenarios. *Science of the Total Environment* 2011, *409*, 2503-2510.

[185] Dams, R. I., Biswas, A., Olesiejuk, A., Fernandes, T., Christofi, N., Silver nanotoxicity using a light-emitting biosensor Pseudomonas putida isolated from a wastewater treatment plant. *Journal of Hazardous Materials* 2011, *195*, 68-72.

[186] Carpenter, A. W., Slomberg, D. L., Rao, K. S., Schoenfisch, M. H., Influence of Scaffold Size on Bactericidal Activity of Nitric Oxide-Releasing Silica Nanoparticles. *Acs Nano* 2011, *5*, 7235-7244.

[187] Xie, Y., He, Y., Irwin, P. L., Jin, T., Shi, X., Antibacterial Activity and Mechanism of Action of Zinc Oxide Nanoparticles against Campylobacter jejuni. *Applied and Environmental Microbiology* 2011, *77*, 2325-2331.

[188] Emami-Karvani, Z., Chehrazi, P., Antibacterial activity of ZnO nanoparticle on gram-positive and gram-negative bacteria. *African Journal of Microbiology Research* 2011, *5*, 1368-1373.

[189] Kim, S. W., Baek, Y.-W., An, Y.-J., Assay-dependent effect of silver nanoparticles to Escherichia coli and Bacillus subtilis. *Applied Microbiology and Biotechnology* 2011, *92*, 1045-1052.

[190] Gunawan, C., Teoh, W. Y., Marquis, C. P., Amal, R., Cytotoxic Origin of Copper(II) Oxide Nanoparticles: Comparative Studies with Micron-Sized Particles, Leachate, and Metal Salts. *Acs Nano* 2011, *5*, 7214-7225.

[191] Pakrashi, S., Dalai, S., Sabat, D., Singh, S.*, et al.*, Cytotoxicity of Al2O3 Nanoparticles at Low Exposure Levels to a Freshwater Bacterial Isolate. *Chemical Research in Toxicology* 2011, *24*, 1899-1904.

[192] Chatterjee, S., Bandyopadhyay, A., Sarkar, K., Effect of iron oxide and gold nanoparticles on bacterial growth leading towards biological application. *Journal of Nanobiotechnology* 2011, *9*.

[193] Radniecki, T. S., Stankus, D. P., Neigh, A., Nason, J. A., Semprini, L., Influence of liberated silver from silver nanoparticles on nitrification inhibition of Nitrosomonas europaea. *Chemosphere* 2011, *85*, 43-49.

[194] Luna-delRisco, M., Orupold, K., Dubourguier, H.-C., Particle-size effect of CuO and ZnO on biogas and methane production during anaerobic digestion. *Journal of Hazardous Materials* 2011, *189*, 603-608.

[195] Pereira, R., Rocha-Santos, T. A. P., Antunes, F. E., Rasteiro, M. G.*, et al.*, Screening evaluation of the ecotoxicity and genotoxicity of soils contaminated with organic and inorganic nanoparticles: The role of ageing. *Journal of Hazardous Materials* 2011, *194*, 345-354.

[196] Premanathan, M., Karthikeyan, K., Jeyasubramanian, K., Manivannan, G., Selective toxicity of ZnO nanoparticles toward Gram-positive bacteria and cancer cells by apoptosis through lipid peroxidation. *Nanomedicine-Nanotechnology Biology and Medicine* 2011, *7*, 184-192.

[197] Raghupathi, K. R., Koodali, R. T., Manna, A. C., Size-Dependent Bacterial Growth Inhibition and Mechanism of Antibacterial Activity of Zinc Oxide Nanoparticles. *Langmuir* 2011, *27*, 4020-4028.

[198] Funfak, A., Cao, J., Knauer, A., Martin, K., Koehler, J. M., Synergistic effects of metal nanoparticles and a phenolic uncoupler using microdroplet-based two-dimensional approach. *Journal of Environmental Monitoring* 2011, *13*, 410-415.

[199] Li, M., Zhu, L. Z., Lin, D. H., Toxicity of ZnO Nanoparticles to Escherichia coli: Mechanism and the Influence of Medium Components. *Environmental Science & Technology* 2011, *45*, 1977-1983.

[200] Jiang, G. X., Shen, Z. Y., Niu, J. F., Bao, Y. P.*, et al.*, Toxicological assessment of TiO2 nanoparticles by recombinant Escherichia coli bacteria. *Journal of Environmental Monitoring* 2011, *13*, 42-48.

[201] Dimkpa, C. O., Calder, A., Britt, D. W., McLean, J. E., Anderson, A. J., Responses of a soil bacterium, Pseudomonas chlororaphis O6 to commercial metal oxide nanoparticles compared with responses to metal ions. *Environmental Pollution* 2011, *159*, 1749-1756.

[202] Syed, M. A., Manzoor, U., Shah, I., Bukhari, S. H. A., Antibacterial effects of Tungsten nanoparticles on the Escherichia coli strains isolated from catheterized urinary tract infection (UTI) cases and Staphylococcus aureus. *New Microbiologica* 2010, *33*, 329-335.

[203] Banerjee, M., Mallick, S., Paul, A., Chattopadhyay, A., Ghosh, S. S., Heightened Reactive Oxygen Species Generation in the Antimicrobial Activity of a Three Component Iodinated Chitosan-Silver Nanoparticle Composite. *Langmuir* 2010, *26*, 5901-5908.

[204] Blinova, I., Ivask, A., Heinlaan, M., Mortimer, M., Kahru, A., Ecotoxicity of nanoparticles of CuO and ZnO in natural water. *Environmental Pollution* 2010, *158*, 41-47.

[205] Dasari, T. P., Hwang, H.-M., The effect of humic acids on the cytotoxicity of silver nanoparticles to a natural aquatic bacterial assemblage. *Science of the Total Environment* 2010, *408*, 5817-5823.

[206] Dumas, E., Gao, C., Suffern, D., Bradforth, S. E.*, et al.*, Interfacial Charge Transfer between CdTe Quantum Dots and Gram Negative Vs Gram Positive Bacteria. *Environmental Science & Technology* 2010, *44*, 1464-1470.

[207] Ivask, A., Bondarenko, O., Jepihhina, N., Kahru, A., Profiling of the reactive oxygen species-related ecotoxicity of CuO, ZnO, TiO2, silver and fullerene nanoparticles using a set of recombinant luminescent Escherichia coli strains: differentiating the impact of particles and solubilised metals. *Analytical and Bioanalytical Chemistry* 2010, *398*, 701-716.

[208] Jiang, W., Yang, K., Vachet, R. W., Xing, B., Interaction between Oxide Nanoparticles and Biomolecules of the Bacterial Cell Envelope As Examined by Infrared Spectroscopy. *Langmuir* 2010, *26*, 18071-18077.

[209] Jin, X., Li, M., Wang, J., Marambio-Jones, C.*, et al.*, High-Throughput Screening of Silver Nanoparticle Stability and Bacterial Inactivation in Aquatic Media: Influence of Specific Ions. *Environmental Science & Technology* 2010, *44*, 7321-7328.

[210] Pelletier, D. A., Suresh, A. K., Holton, G. A., McKeown, C. K., *et al.*, Effects of Engineered Cerium Oxide Nanoparticles on Bacterial Growth and Viability. *Applied and Environmental Microbiology* 2010, *76*, 7981-7989.

[211] Suresh, A. K., Pelletier, D. A., Wang, W., Moon, J.-W., *et al.*, Silver Nanocrystallites: Biofabrication using Shewanella oneidensis, and an Evaluation of Their Comparative Toxicity on Gram-negative and Gram-positive Bacteria. *Environmental Science & Technology* 2010, *44*, 5210-5215.

[212] Wu, B., Wang, Y., Lee, Y.-H., Horst, A., *et al.*, Comparative Eco-Toxicities of Nano-ZnO Particles under Aquatic and Aerosol Exposure Modes. *Environmental Science & Technology* 2010, *44*, 1484-1489.

[213] Lara, H. H., Ayala-Nunez, N. V., Ixtepan Turrent, L. d. C., Rodriguez Padilla, C., Bactericidal effect of silver nanoparticles against multidrug-resistant bacteria. *World Journal of Microbiology & Biotechnology* 2010, *26*, 615-621.

[214] Khan, S., Mukherjee, A., Chandrasekaran, N., Silver nanoparticles tolerant bacteria from sewage environment. *Journal of Environmental Sciences-China* 2011, *23*, 346-352.

[215] Barrena, R., Casals, E., Colon, J., Font, X., *et al.*, Evaluation of the ecotoxicity of model nanoparticles. *Chemosphere* 2009, *75*, 850-857.

[216] Brunet, L., Lyon, D. Y., Hotze, E. M., Alvarez, P. J. J., Wiesner, M. R., Comparative Photoactivity and Antibacterial Properties of C-60 Fullerenes and Titanium Dioxide Nanoparticles. *Environmental Science & Technology* 2009, *43*, 4355-4360.

[217] Cushnie, T. P. T., Robertson, P. K. J., Officer, S., Pollard, P. M., *et al.*, Variables to be considered when assessing the photocatalytic destruction of bacterial pathogens. *Chemosphere* 2009, *74*, 1374-1378.

[218] Dror-Ehre, A., Mamane, H., Belenkova, T., Markovich, G., Adin, A., Silver nanoparticle-E. coli colloidal interaction in water and effect on E-coli survival. *Journal of Colloid and Interface Science* 2009, *339*, 521-526.

[219] Gajjar, P., Pettee, B., Britt, D. W., Huang, W., *et al.*, Antimicrobial activities of commercial nanoparticles against an environmental soil microbe, Pseudomonas putida KT2440. *Journal of biological engineering* 2009, *3*, 9-9.

[220] Lee, S., Lee, J., Kim, K., Sim, S.-J., *et al.*, Eco-toxicity of Commercial Silver Nanopowders to Bacterial and Yeast Strains. *Biotechnology and Bioprocess Engineering* 2009, *14*, 490-495.

[221] Liu, Y., He, L., Mustapha, A., Li, H., *et al.*, Antibacterial activities of zinc oxide nanoparticles against Escherichia coli O157:H7. *Journal of Applied Microbiology* 2009, *107*, 1193-1201.

[222] Park, H.-J., Kim, J. Y., Kim, J., Lee, J.-H., *et al.*, Silver-ion-mediated reactive oxygen species generation affecting bactericidal activity. *Water Research* 2009, *43*, 1027-1032.

[223] Priester, J. H., Stoimenov, P. K., Mielke, R. E., Webb, S. M., *et al.*, Effects of Soluble Cadmium Salts Versus CdSe Quantum Dots on the Growth of Planktonic Pseudomonas aeruginosa. *Environmental Science & Technology* 2009, *43*, 2589-2594.

[224] Ren, G., Hu, D., Cheng, E. W. C., Vargas-Reus, M. A., *et al.*, Characterisation of copper oxide nanoparticles for antimicrobial applications. *International Journal of Antimicrobial Agents* 2009, *33*, 587-590.

[225] Sadiq, I. M., Chowdhury, B., Chandrasekaran, N., Mukherjee, A., Antimicrobial sensitivity of Escherichia coli to alumina nanoparticles. *Nanomedicine-Nanotechnology Biology and Medicine* 2009, *5*, 282-286.

[226] Slaveykova, V. I., Startchev, K., Roberts, J., Amine- and Carboxyl- Quantum Dots Affect Membrane Integrity of Bacterium Cupriavidus metallidurans CH34. *Environmental Science & Technology* 2009, *43*, 5117-5122.

[227] Song, Y., Li, G., Thornton, S. F., Thompson, I. P.*, et al.*, Optimization of Bacterial Whole Cell Bioreporters for Toxicity Assay of Environmental Samples. *Environmental Science & Technology* 2009, *43*, 7931-7938.

[228] Sovova, T., Koci, V., Kochankova, L., Tanger, L. C. M. N. M. S., Ecotoxicity of nano and bulk forms of metal oxides. *Nanocon 2009, Conference Proceedings* 2009, 341-347.

[229] Strigul, N., Vaccari, L., Galdun, C., Wazne, M.*, et al.*, Acute toxicity of boron, titanium dioxide, and aluminum nanoparticles to Daphnia magna and Vibrio fischeri. *Desalination* 2009, *248*, 771-782.

[230] Zeyons, O., Thill, A., Chauvat, F., Menguy, N.*, et al.*, Direct and indirect CeO2 nanoparticles toxicity for Escherichia coli and Synechocystis. *Nanotoxicology* 2009, *3*, 284-295.

[231] Applerot, G., Lipovsky, A., Dror, R., Perkas, N.*, et al.*, Enhanced Antibacterial Activity of Nanocrystalline ZnO Due to Increased ROS-Mediated Cell Injury. *Advanced Functional Materials* 2009, *19*, 842-852.

[232] Auffan, M., Achouak, W., Rose, J., Roncato, M.-A.*, et al.*, Relation between the redox state of iron-based nanoparticles and their cytotoxicity toward Escherichia coli. *Environmental Science & Technology* 2008, *42*, 6730-6735.

[233] Blaise, C., Gagne, F., Ferard, J. F., Eullaffroy, P., Ecotoxicity of selected nano-materials to aquatic organisms. *Environmental Toxicology* 2008, *23*, 591-598.

[234] Choi, O., Hu, Z., Size dependent and reactive oxygen species related nanosilver toxicity to nitrifying bacteria. *Environmental Science & Technology* 2008, *42*, 4583-4588.

[235] Choi, O., Deng, K. K., Kim, N.-J., Ross, L., Jr.*, et al.*, The inhibitory effects of silver nanoparticles, silver ions, and silver chloride colloids on microbial growth. *Water Research* 2008, *42*, 3066-3074.

[236] Heinlaan, M., Ivask, A., Blinova, I., Dubourguier, H.-C., Kahru, A., Toxicity of nanosized and bulk ZnO, CuO and TiO2 to bacteria Vibrio fischeri and crustaceans Daphnia magna and Thamnocephalus platyurus. *Chemosphere* 2008, *71*, 1308-1316.

[237] Huang, Z., Zheng, X., Yan, D., Yin, G.*, et al.*, Toxicological effect of ZnO nanoparticles based on bacteria. *Langmuir* 2008, *24*, 4140-4144.

[238] Hwang, E., Lee, J., Chae, Y., Kim, Y.*, et al.*, Analysis of the toxic mode of action of silver nanoparticles using stress-specific bioluminescent bacteria. *Small* 2008, *4*, 746-750.

[239] Limbach, L. K., Bereiter, R., Mueller, E., Krebs, R.*, et al.*, Removal of oxide nanoparticles in a model wastewater treatment plant: Influence of agglomeration and surfactants on clearing efficiency. *Environmental Science & Technology* 2008, *42*, 5828-5833.

[240] Lu, Z., Li, C. M., Bao, H., Qiao, Y., *et al.*, Mechanism of antimicrobial activity of CdTe quantum dots. *Langmuir* 2008, *24*, 5445-5452.

[241] Mahendra, S., Zhu, H., Colvin, V. L., Alvarez, P. J., Quantum Dot Weathering Results in Microbial Toxicity. *Environmental Science & Technology* 2008, *42*, 9424-9430.

[242] Martinez-Castanon, G. A., Nino-Martinez, N., Martinez-Gutierrez, F., Martinez-Mendoza, J. R., Ruiz, F., Synthesis and antibacterial activity of silver nanoparticles with different sizes. *Journal of Nanoparticle Research* 2008, *10*, 1343-1348.

[243] Mortimer, M., Kasemets, K., Heinlaan, M., Kurvet, I., Kahru, A., High throughput kinetic Vibrio fischeri bioluminescence inhibition assay for study of toxic effects of nanoparticles. *Toxicology in Vitro* 2008, *22*, 1412-1417.

[244] Padmavathy, N., Vijayaraghavan, R., Enhanced bioactivity of ZnO nanoparticles-an antimicrobial study. *Science and Technology of Advanced Materials* 2008, *9*.

[245] Paschoalino, M., Guedes, N. C., Jardim, W., Mieluarski, E., *et al.*, Inactivation of E-coli mediated by high surface area CuO accelerated by light irradiation > 360 nm. *Journal of Photochemistry and Photobiology a-Chemistry* 2008, *199*, 105-111.

[246] Raffi, M., Hussain, F., Bhatti, T. M., Akhter, J. I., *et al.*, Antibacterial characterization of silver nanoparticles against E. coli ATCC-15224. *Journal of Materials Science & Technology* 2008, *24*, 192-196.

[247] Ruparelia, J. P., Chatteriee, A. K., Duttagupta, S. P., Mukherji, S., Strain specificity in antimicrobial activity of silver and copper nanoparticles. *Acta Biomaterialia* 2008, *4*, 707-716.

[248] Velzeboer, I., Hendriks, A. J., Ragas, A. M. J., Van de Meent, D., Aquatic ecotoxicity tests of some nanomaterials. *Environmental Toxicology and Chemistry* 2008, *27*, 1942-1947.

[249] Francisco Hernandez-Sierra, J., Ruiz, F., Cruz Pena, D. C., Martinez-Gutierrez, F., *et al.*, The antimicrobial sensitivity of Streptococcus mutans to nanoparticles of silver, zinc oxide, and gold. *Nanomedicine-Nanotechnology Biology and Medicine* 2008, *4*, 237-240.

[250] Gogniat, G., Dukan, S., TiO2 photocatalysis causes DNA damage via Fenton reaction-generated hydroxyl radicals during the recovery period. *Applied and Environmental Microbiology* 2007, *73*, 7740-7743.

[251] Kim, J. S., Kuk, E., Yu, K. N., Kim, J.-H., *et al.*, Antimicrobial effects of silver nanoparticles. *Nanomedicine-Nanotechnology Biology and Medicine* 2007, *3*, 95-101.

[252] Mitoraj, D., Janczyk, A., Strus, M., Kisch, H., *et al.*, Visible light inactivation of bacteria and fungi by modified titanium dioxide. *Photochemical & Photobiological Sciences* 2007, *6*, 642-648.

[253] Reddy, K. M., Feris, K., Bell, J., Wingett, D. G., *et al.*, Selective toxicity of zinc oxide nanoparticles to prokaryotic and eukaryotic systems. *Applied Physics Letters* 2007, *90*.

[254] Yoon, K.-Y., Byeon, J. H., Park, J.-H., Hwang, J., Susceptibility constants of Escherichia coli and Bacillus subtilis to silver and copper nanoparticles. *Science of the Total Environment* 2007, *373*, 572-575.

[255] Adams, L. K., Lyon, D. Y., Alvarez, P. J. J., Comparative eco-toxicity of nanoscale TiO2, SiO2, and ZnO water suspensions. *Water Research* 2006, *40*, 3527-3532.

[256] Brayner, R., Ferrari-Iliou, R., Brivois, N., Djediat, S.*, et al.*, Toxicological impact studies based on Escherichia coli bacteria in ultrafine ZnO nanoparticles colloidal medium. *Nano Letters* 2006, *6*, 866-870.

[257] Gogniat, G., Thyssen, M., Denis, M., Pulgarin, C., Dukan, S., The bactericidal effect of TiO2 photocatalysis involves adsorption onto catalyst and the loss of membrane integrity. *Fems Microbiology Letters* 2006, *258*, 18-24.

[258] Gogoi, S. K., Gopinath, P., Paul, A., Ramesh, A.*, et al.*, Green fluorescent protein-expressing Escherichia coli as a model system for investigating the antimicrobial activities of silver nanoparticles. *Langmuir* 2006, *22*, 9322-9328.

[259] Lok, C. N., Ho, C. M., Chen, R., He, Q. Y.*, et al.*, Proteomic analysis of the mode of antibacterial action of silver nanoparticles. *Journal of Proteome Research* 2006, *5*, 916-924.

[260] Nadtochenko, V., Denisov, N., Sarkisov, O., Gumy, D.*, et al.*, Laser kinetic spectroscopy of the interfacial charge transfer between membrane cell walls of E-coli and TiO2. *Journal of Photochemistry and Photobiology a-Chemistry* 2006, *181*, 401-407.

[261] Panacek, A., Kvitek, L., Prucek, R., Kolar, M.*, et al.*, Silver colloid nanoparticles: Synthesis, characterization, and their antibacterial activity. *Journal of Physical Chemistry B* 2006, *110*, 16248-16253.

[262] Huang, L., Li, D. Q., Lin, Y. J., Wei, M.*, et al.*, Controllable preparation of nano-MgO and investigation of its bactericidal properties. *Journal of Inorganic Biochemistry* 2005, *99*, 986-993.

[263] Kubo, M., Onodera, R., Shibasaki-Kitakawa, N., Tsumoto, K., Yonemoto, T., Kinetics of ultrasonic disinfection of Escherichia coli in the presence of titanium dioxide particles. *Biotechnology Progress* 2005, *21*, 897-901.

[264] Lei, H., Li, D. Q., Lin, Y. J., Evans, D. G., Xue, D., Influence of nano-MgO particle size on bactericidal action against Bacillus subtilis var. niger. *Chinese Science Bulletin* 2005, *50*, 514-519.

[265] Morones, J. R., Elechiguerra, J. L., Camacho, A., Holt, K.*, et al.*, The bactericidal effect of silver nanoparticles. *Nanotechnology* 2005, *16*, 2346-2353.

[266] Nadtochenko, V. A., Rincon, A. G., Stanca, S. E., Kiwi, J., Dynamics of E-coli membrane cell peroxidation during TiO2 photocatalysis studied by ATR-FTIR spectroscopy and AFM microscopy. *Journal of Photochemistry and Photobiology a-Chemistry* 2005, *169*, 131-137.

[267] Cho, M., Chung, H. M., Choi, W. Y., Yoon, J. Y., Different inactivation Behaviors of MS-2 phage and Escherichia coli in TiO2 photocatalytic disinfection. *Applied and Environmental Microbiology* 2005, *71*, 270-275.

[268] Ansari, Evaluation of antibacterial activity of silver nanoparticles against MSSA and MRSA on isolates from skin infections. 2011.

[269] Gokulakrishnan, In vitro antibacterial potential of metal oxide nanoparticles against antibiotic resistant bacterial pathogens. 2012.

[270] Freire, P. L. L., Stamford, T. C. M., Albuquerque, A. J. R., Sampaio, F. C.*, et al.*, Action of silver nanoparticles towards biological systems: cytotoxicity evaluation using hen's egg test and inhibition of Streptococcus mutans biofilm formation. *International Journal of Antimicrobial Agents* 2015, *45*, 183-187.

[271] Salem, W., Leitner, D. R., Zingl, F. G., Schratter, G.*, et al.*, Antibacterial activity of silver and zinc nanoparticles against Vibrio cholerae and enterotoxic Escherichia coli. *International Journal of Medical Microbiology* 2015, *305*, 85-95.

[272] Singh, A., Ahmed, A., Prasad, K. N., Khanduja, S.*, et al.*, Antibiofilm and Membrane-Damaging Potential of Cuprous Oxide Nanoparticles against Staphylococcus aureus with Reduced Susceptibility to Vancomycin. *Antimicrobial agents and chemotherapy* 2015, *59*, 6882-6890.

[273] Khiralla, G. M., El-Deeb, B. A., Antimicrobial and antibiofilm effects of selenium nanoparticles on some foodborne pathogens. *Lwt-Food Science and Technology* 2015, *63*, 1001-1007.

[274] Beatrice, S., Wei, L., Alain, T., Aurelien, A.*, et al.*, Design of a live biochip for in situ nanotoxicology studies: a proof of concept. *Rsc Advances* 2015, *5*, 82169-82178.

[275] Boda, S. K., Broda, J., Schiefer, F., Weber-Heynemann, J.*, et al.*, Cytotoxicity of Ultrasmall Gold Nanoparticles on Planktonic and Biofilm Encapsulated Gram-Positive Staphylococci. *Small* 2015, *11*, 3183-3193.

[276] Gambino, M., Marzano, V., Villa, F., Vitali, A.*, et al.*, Effects of sublethal doses of silver nanoparticles on Bacillus subtilis planktonic and sessile cells. *Journal of Applied Microbiology* 2015, *118*, 1103-1115.

[277] Gonzalez, A. G., Mombo, S., Leflaive, J., Lamy, A.*, et al.*, Silver nanoparticles impact phototrophic biofilm communities to a considerably higher degree than ionic silver. *Environmental Science and Pollution Research* 2015, *22*, 8412-8424.

[278] Hou, J., You, G., Xu, Y., Wang, C.*, et al.*, Effects of CeO2 nanoparticles on biological nitrogen removal in a sequencing batch biofilm reactor and mechanism of toxicity. *Bioresource Technology* 2015, *191*, 73-78.

[279] Hsueh, Y.-H., Ke, W.-J., Hsieh, C.-T., Lin, K.-S.*, et al.*, ZnO Nanoparticles Affect Bacillus subtilis Cell Growth and Biofilm Formation. *Plos One* 2015, *10*.

[280] Jomini, S., Clivot, H., Bauda, P., Pagnout, C., Impact of manufactured TiO2 nanoparticles on planktonic and sessile bacterial communities. *Environmental Pollution* 2015, *202*, 196-204.

[281] Khanal, M., Raks, V., Issa, R., Chernyshenko, V.*, et al.*, Selective Antimicrobial and Antibiofilm Disrupting Properties of Functionalized Diamond Nanoparticles Against Escherichia coli and Staphylococcus aureus. *Particle & Particle Systems Characterization* 2015, *32*, 822-830.

[282] Mohanty, A., Liu, Y., Yang, L., Cao, B., Extracellular biogenic nanomaterials inhibit pyoverdine production in Pseudomonas aeruginosa: a novel insight into impacts of metal(loid)s on environmental bacteria. *Applied Microbiology and Biotechnology* 2015, *99*, 1957-1966.

[283] Reyes, V. C., Opot, S. O., Mahendra, S., Planktonic and biofilm-grown nitrogen-cycling bacteria exhibit different susceptibilities to copper nanoparticles. *Environmental Toxicology and Chemistry* 2015, *34*, 887-897.

[284] Vidovic, S., Elder, J., Medihala, P., Lawrence, J. R.*, et al.*, ZnO Nanoparticles Impose a Panmetabolic Toxic Effect Along with Strong Necrosis, Inducing Activation of the Envelope Stress Response in Salmonella enterica Serovar Enteritidis. *Antimicrobial Agents and Chemotherapy* 2015, *59*, 3317-3328.

[285] Agarwala, M., Choudhury, B., Yadav, R. N. S., Comparative Study of Antibiofilm Activity of Copper Oxide and Iron Oxide Nanoparticles Against Multidrug Resistant Biofilm Forming Uropathogens. *Indian Journal of Microbiology* 2014, *54*, 365-368.

[286] Ammendolia, M. G., Iosi, F., De Berardis, B., Guccione, G.*, et al.*, Listeria monocytogenes Behaviour in Presence of Non-UV-Irradiated Titanium Dioxide Nanoparticles. *Plos One* 2014, *9*.

[287] Chrzanowska, N., Zaleska-Radziwill, M., The impacts of aluminum and zirconium nano-oxides on planktonic and biofilm bacteria. *Desalination and Water Treatment* 2014, *52*, 3680-3689.

[288] Hou, J., Miao, L., Wang, C., Wang, P.*, et al.*, Inhibitory effects of ZnO nanoparticles on aerobic wastewater biofilms from oxygen concentration profiles determined by microelectrodes. *Journal of Hazardous Materials* 2014, *276*, 164-170.

[289] Raftery, T. D., Kerscher, P., Hart, A. E., Saville, S. L.*, et al.*, Discrete nanoparticles induce loss of Legionella pneumophila biofilms from surfaces. *Nanotoxicology* 2014, *8*, 477-484.

[290] Schug, H., Isaacson, C. W., Sigg, L., Ammann, A. A., Schirmer, K., Effect of TiO2 Nanoparticles and UV Radiation on Extracellular Enzyme Activity of Intact Heterotrophic Biofilms. *Environmental Science & Technology* 2014, *48*, 11620-11628.

[291] Flores, C. Y., Minan, A. G., Grillo, C. A., Salvarezza, R. C.*, et al.*, Citrate-Capped Silver Nanoparticles Showing Good Bactericidal Effect against Both Planktonic and Sessile Bacteria and a Low Cytotoxicity to Osteoblastic Cells. *Acs Applied Materials & Interfaces* 2013, *5*, 3149-3159.

[292] Hartmann, T., Mühling, M., Wolf, A., Mariana, F.*, et al.*, A chip-calorimetric approach to the analysis of Ag nanoparticle caused inhibition and inactivation of beads-grown bacterial biofilms. *J Microbiol Methods* 2013, *95*, 129-137.

[293] Inbakandan, D., Kumar, C., Abraham, L. S., Kirubagaran, R.*, et al.*, Silver nanoparticles with anti microfouling effect: A study against marine biofilm forming bacteria. *Colloids and Surfaces B-Biointerfaces* 2013, *111*, 636-643.

[294] Martinez-Gutierrez, F., Boegli, L., Agostinho, A., Sanchez, E. M.*, et al.*, Anti-biofilm activity of silver nanoparticles against different microorganisms. *Biofouling* 2013, *29*, 651-660.

[295] Maurer-Jones, M. A., Gunsolus, I. L., Meyer, B. M., Christenson, C. J., Haynes, C. L., Impact of TiO2 Nanoparticles on Growth, Biofilm Formation, and Flavin Secretion in Shewanella oneidensis. *Analytical Chemistry* 2013, *85*, 5810-5818.

[296] Miller, J. K., Neubig, R., Clemons, C. B., Kreider, K. L.*, et al.*, Nanoparticle Deposition onto Biofilms. *Annals of Biomedical Engineering* 2013, *41*, 53-67.

[297] Park, H. J., Park, S., Roh, J., Kim, S.*, et al.*, Biofilm-inactivating activity of silver nanoparticles: A comparison with silver ions. *Journal of Industrial and Engineering Chemistry* 2013, *19*, 614-619.

[298] Radzig, M. A., Nadtochenko, V. A., Koksharova, O. A., Kiwi, J.*, et al.*, Antibacterial effects of silver nanoparticles on gram-negative bacteria: Influence on the growth and biofilms formation, mechanisms of action. *Colloids and Surfaces B-Biointerfaces* 2013, *102*, 300-306.

[299] Ronen, A., Semiat, R., Dosoretz, C. G., Antibacterial efficiency of composite nano-ZnO in biofilm development in flow-through systems. *Desalination and Water Treatment* 2013, *51*, 988-996.

[300] Sathyanarayanan, M. B., Balachandranath, R., Genji Srinivasulu, Y., Kannaiyan, S. K., Subbiahdoss, G., The effect of gold and iron-oxide nanoparticles on biofilm-forming pathogens. *ISRN microbiology* 2013, *2013*, 272086.

[301] Slomberg, D. L., Lu, Y., Broadnax, A. D., Hunter, R. A.*, et al.*, Role of size and shape on biofilm eradication for nitric oxide-releasing silica nanoparticles. *ACS applied materials & interfaces* 2013, *5*, 9322-9329.

[302] Joshi, N., Ngwenya, B. T., French, C. E., Enhanced resistance to nanoparticle toxicity is conferred by overproduction of extracellular polymeric substances. *Journal of Hazardous Materials* 2012, *241*, 363-370.

[303] Mohanty, S., Mishra, S., Jena, P., Jacob, B.*, et al.*, An investigation on the antibacterial, cytotoxic, and antibiofilm efficacy of starch-stabilized silver nanoparticles. *Nanomedicine-Nanotechnology Biology and Medicine* 2012, *8*, 916-924.

[304] Wirth, S. M., Lowry, G. V., Tilton, R. D., Natural Organic Matter Alters Biofilm Tolerance to Silver Nanoparticles and Dissolved Silver. *Environmental Science & Technology* 2012, *46*, 12687-12696.

[305] Raftery, T. D., Lindler, H., McNealy, T. L., Altered Host Cell-Bacteria Interaction due to Nanoparticle Interaction with a Bacterial Biofilm. *Microbial Ecology* 2013, *65*, 496-503.

[306] Fabrega, J., Zhang, R., Renshaw, J. C., Liu, W. T., Lead, J. R., Impact of silver nanoparticles on natural marine biofilm bacteria. *Chemosphere* 2011, *85*, 961-966.

[307] Peulen, T. O., Wilkinson, K. J., Diffusion of Nanoparticles in a Biofilm. *Environmental Science & Technology* 2011, *45*, 3367-3373.

[308] Sheng, Z. Y., Liu, Y., Effects of silver nanoparticles on wastewater biofilms. *Water Research* 2011, *45*, 6039-6050.

[309] Stojak, A. R., Raftery, T., Klaine, S. J., McNealy, T. L., Morphological responses of Legionella pneumophila biofilm to nanoparticle exposure. *Nanotoxicology* 2011, *5*, 730-742.

[310] Choi, O. Y., Yu, C. P., Fernandez, G. E., Hu, Z. Q., Interactions of nanosilver with Escherichia coli cells in planktonic and biofilm cultures. *Water Research* 2010, *44*, 6095-6103.

[311] Kalishwaralal, K., BarathManiKanth, S., Pandian, S. R. K., Deepak, V., Gurunathan, S., Silver nanoparticles impede the biofilm formation by Pseudomonas aeruginosa and Staphylococcus epidermidis. *Colloids and Surfaces B-Biointerfaces* 2010, *79*, 340-344.

[312] Battin, T. J., Kammer, F. V. D., Weilhartner, A., Ottofuelling, S., Hofmann, T., Nanostructured TiO2: Transport Behavior and Effects on Aquatic Microbial Communities under Environmental Conditions. *Environmental Science & Technology* 2009, *43*, 8098-8104.

[313] Emtiazi, G., Shahrokh, S., Ieee, Unusual biological behavior of Staphylococci with nano silver assayed by microtiter-plate. *2009 9th Ieee Conference on Nanotechnology (Ieee-Nano)* 2009, 394-396.

[314] Fabrega, J., Renshaw, J. C., Lead, J. R., Interactions of Silver Nanoparticles with Pseudomonas putida Biofilms. *Environmental Science & Technology* 2009, *43*, 9004-9009.

[315] Taylor, E. N., Webster, T. J., The use of superparamagnetic nanoparticles for prosthetic biofilm prevention. *International Journal of Nanomedicine* 2009, *4*, 145-152.

[316] Xu, C., Peng, C., Sun, L., Zhang, S.*, et al.*, Distinctive effects of TiO2 and CuO nanoparticles on soil microbes and their community structures in flooded paddy soil. *Soil Biology & Biochemistry* 2015, *86*, 24-33.

[317] Chai, H., Yao, J., Sun, J., Zhang, C.*, et al.*, The Effect of Metal Oxide Nanoparticles on Functional Bacteria and Metabolic Profiles in Agricultural Soil. *Bulletin of Environmental Contamination and Toxicology* 2015, *94*, 490-495.

[318] Echavarri-Bravo, V., Paterson, L., Aspray, T. J., Porter, J. S.*, et al.*, Shifts in the metabolic function of a benthic estuarine microbial community following a single pulse exposure to silver nanoparticles. *Environmental Pollution* 2015, *201*, 91-99.

[319] Fajardo, C., Gil-Diaz, M., Costa, G., Alonso, J.*, et al.*, Residual impact of aged nZVI on heavy metal-polluted soils. *Science of the Total Environment* 2015, *535*, 79-84.

[320] Schlich, K., Hund-Rinke, K., Influence of soil properties on the effect of silver nanomaterials on microbial activity in five soils. *Environmental Pollution* 2015, *196*, 321-330.

[321] Simonin, M., Guyonnet, J. P., Martins, J. M. F., Ginot, M., Richaume, A., Influence of soil properties on the toxicity of TiO2 nanoparticles on carbon mineralization and bacterial abundance. *Journal of Hazardous Materials* 2015, *283*, 529-535.

[322] Ge, Y., Priester, J. H., Van de Werfhorst, L. C., Walker, S. L.*, et al.*, Soybean Plants Modify Metal Oxide Nanoparticle Effects on Soil Bacterial Communities. *Environmental Science & Technology* 2014, *48*, 13489-13496.

[323] Kumar, N., Palmer, G. R., Shah, V., Walker, V. K., The Effect of Silver Nanoparticles on Seasonal Change in Arctic Tundra Bacterial and Fungal Assemblages. *Plos One* 2014, *9*.

[324] Ludovica Sacca, M., Fajardo, C., Costa, G., Lobo, C.*, et al.*, Integrating classical and molecular approaches to evaluate the impact of nanosized zero-valent iron (nZVI) on soil organisms. *Chemosphere* 2014, *104*, 184-189.

[325] Masrahi, A., VandeVoort, A. R., Arai, Y., Effects of Silver Nanoparticle on Soil-Nitrification Processes. *Archives of Environmental Contamination and Toxicology* 2014, *66*, 504-513.

[326] Mohanty, S. R., Rajput, P., Kollah, B., Chourasiya, D.*, et al.*, Methane oxidation and abundance of methane oxidizers in tropical agricultural soil (vertisol) in response to CuO and ZnO nanoparticles contamination. *Environmental Monitoring and Assessment* 2014, *186*, 3743-3753.

[327] Shah, V., Collins, D., Walker, V. K., Shah, S., The impact of engineered cobalt, iron, nickel and silver nanoparticles on soil bacterial diversity under field conditions. *Environmental Research Letters* 2014, *9*.

[328] Wakelin, S., Gerard, E., Black, A., Hamonts, K.*, et al.*, Mechanisms of pollution induced community tolerance in a soil microbial community exposed to Cu. *Environmental Pollution* 2014, *190*, 1-9.

[329] Frenk, S., Ben-Moshe, T., Dror, I., Berkowitz, B., Minz, D., Effect of Metal Oxide Nanoparticles on Microbial Community Structure and Function in Two Different Soil Types. *Plos One* 2013, *8*.

[330] Colman, B. P., Arnaout, C. L., Anciaux, S., Gunsch, C. K.*, et al.*, Low Concentrations of Silver Nanoparticles in Biosolids Cause Adverse Ecosystem Responses under Realistic Field Scenario. *Plos One* 2013, *8*.

[331] Colman, B. P., Wang, S.-Y., Auffan, M., Wiesner, M. R., Bernhardt, E. S., Antimicrobial effects of commercial silver nanoparticles are attenuated in natural streamwater and sediment. *Ecotoxicology* 2012, *21*, 1867-1877.

[332] Collins, D., Luxton, T., Kumar, N., Shah, S.*, et al.*, Assessing the Impact of Copper and Zinc Oxide Nanoparticles on Soil: A Field Study. *Plos One* 2012, *7*.

[333] Das, P., Xenopoulos, M. A., Williams, C. J., Hoque, M. E., Metcalfe, C. D., Effects of silver nanoparticles on bacterial activity in natural waters. *Environmental Toxicology and Chemistry* 2012, *31*, 122-130.

[334] Ge, Y., Schimel, J. P., Holden, P. A., Identification of Soil Bacteria Susceptible to TiO2 and ZnO Nanoparticles. *Applied and Environmental Microbiology* 2012, *78*, 6749-6758.

[335] Kumar, N., Shah, V., Walker, V. K., Influence of a nanoparticle mixture on an arctic soil community. *Environmental Toxicology and Chemistry* 2012, *31*, 131-135.

[336] Lee, S., Kim, S., Kim, S., Lee, I., Effects of Soil-Plant Interactive System on Response to Exposure to ZnO Nanoparticles. *Journal of Microbiology and Biotechnology* 2012, *22*, 1264-1270.

[337] Rousk, J., Ackermann, K., Curling, S. F., Jones, D. L., Comparative Toxicity of Nanoparticulate CuO and ZnO to Soil Bacterial Communities. *Plos One* 2012, *7*.

[338] Wang, Y., Westerhoff, P., Hristovski, K. D., Fate and biological effects of silver, titanium dioxide, and C-60 (fullerene) nanomaterials during simulated wastewater treatment processes. *Journal of Hazardous Materials* 2012, *201*, 16-22.

[339] Calder, A. J., Dimkpa, C. O., McLean, J. E., Britt, D. W.*, et al.*, Soil components mitigate the antimicrobial effects of silver nanoparticles towards a beneficial soil bacterium, Pseudomonas chlororaphis O6. *Science of the Total Environment* 2012, *429*, 215-222.

[340] Gao, J., Wang, Y., Hovsepyan, A., Bonzongo, J.-C. J., Effects of engineered nanomaterials on microbial catalyzed biogeochemical processes in sediments. *Journal of Hazardous Materials* 2011, *186*, 940-945.

[341] Ge, Y., Schimel, J. P., Holden, P. A., Evidence for Negative Effects of TiO2 and ZnO Nanoparticles on Soil Bacterial Communities. *Environmental Science & Technology* 2011, *45*, 1659-1664.

[342] Kumar, N., Shah, V., Walker, V. K., Perturbation of an arctic soil microbial community by metal nanoparticles. *Journal of Hazardous Materials* 2011, *190*, 816-822.

[343] Pradhan, A., Seena, S., Pascoal, C., Cassio, F., Can Metal Nanoparticles Be a Threat to Microbial Decomposers of Plant Litter in Streams? *Microbial Ecology* 2011, *62*, 58-68.

[344] He, S., Feng, Y., Ren, H., Zhang, Y.*, et al.*, The impact of iron oxide magnetic nanoparticles on the soil bacterial community. *Journal of Soils and Sediments* 2011, *11*, 1408-1417.

[345] Barnes, R. J., van der Gast, C. J., Riba, O., Lehtovirta, L. E.*, et al.*, The impact of zero-valent iron nanoparticles on a river water bacterial community. *Journal of Hazardous Materials* 2010, *184*, 73-80.

[346] Bradford, A., Handy, R. D., Readman, J. W., Atfield, A., Muehling, M., Impact of Silver Nanoparticle Contamination on the Genetic Diversity of Natural Bacterial Assemblages in Estuarine Sediments. *Environmental Science & Technology* 2009, *43*, 4530-4536.

[347] Beddow, J., Stoelpe, B., Cole, P. A., Lead, J. R.*, et al.*, Estuarine sediment hydrocarbon-degrading microbial communities demonstrate resilience to nanosilver. *International Biodeterioration & Biodegradation* 2014, *96*, 206-215.

[348] Ali, K., Ahmed, B., Dwivedi, S., Saquib, Q.*, et al.*, Microwave Accelerated Green Synthesis of Stable Silver Nanoparticles with Eucalyptus globulus Leaf Extract and Their Antibacterial and Antibiofilm Activity on Clinical Isolates. *Plos One* 2015, *10*.

[349] Elumalai, K., Velmurugan, S., Ravi, S., Kathiravan, V., Ashokkumar, S., Green synthesis of zinc oxide nanoparticles using Moringa oleifera leaf extract and evaluation of its antimicrobial activity. *Spectrochimica Acta Part a-Molecular and Biomolecular Spectroscopy* 2015, *143*, 158-164.

[350] Arokiyaraj, S., Arasu, M. V., Vincent, S., Prakash, N. U.*, et al.*, Rapid green synthesis of silver nanoparticles from Chrysanthemum indicum L and its antibacterial and cytotoxic effects: an in vitro study. *International Journal of Nanomedicine* 2014, *9*, 379-388.

[351] Nguyen Thi Mai, T., Tran Nguyen Minh, A., Mai Dinh, T., Sreekanth, T. V. M.*, et al.*, Green Synthesis of Silver Nanoparticles Using Nelumbo nucifera Seed Extract and its Antibacterial Activity. *Acta Chimica Slovenica* 2013, *60*, 673-678.

[352] Birla, S. S., Tiwari, V. V., Gade, A. K., Ingle, A. P.*, et al.*, Fabrication of silver nanoparticles by Phoma glomerata and its combined effect against Escherichia coli, Pseudomonas aeruginosa and Staphylococcus aureus. *Letters in Applied Microbiology* 2009, *48*, 173-179.

[353] Wu, B., Huang, R., Sahu, M., Feng, X.*, et al.*, Bacterial responses to Cu-doped TiO2 nanoparticles. *Science of the Total Environment* 2010, *408*, 1755-1758.

[354] Nhung Thi-Tuyet, H., Nguyen Van, S., The-Vinh, N., Bactericidal activities and synergistic effects of Ag-TiO2 and Ag-TiO2-SiO2 nanomaterials under UV-C and dark conditions. *International Journal of Nanotechnology* 2015, *12*, 367-379.

[355] Cherchi, C., Miljkovic, M., Diem, M., Gu, A. Z., nTiO(2) induced changes in intracellular composition and nutrient stoichiometry in primary producer - cyanobacteria. *Science of the Total Environment* 2015, *512*, 345-352.

[356] Rodea-Palomares, I., Gonzalo, S., Santiago-Morales, J., Leganes, F.*, et al.*, An insight into the mechanisms of nanoceria toxicity in aquatic photosynthetic organisms. *Aquatic Toxicology* 2012, *122*, 133-143.

[357] Voelker, D., Schlich, K., Hohndorf, L., Koch, W.*, et al.*, Approach on environmental risk assessment of nanosilver released from textiles. *Environmental Research* 2015, *140*, 661-672.

[358] Pan, H. M., Zhang, Y. B., He, G. X., Katagori, N., Chen, H. Z., A comparison of conventional methods for the quantification of bacterial cells after exposure to metal oxide nanoparticles. *Bmc Microbiology* 2014, *14*.

[359] Oostingh, G. J., Casals, E., Italiani, P., Colognato, R.*, et al.*, Problems and challenges in the development and validation of human cell-based assays to determine nanoparticle-induced immunomodulatory effects. *Particle and Fibre Toxicology* 2011, *8*.

[360] Bondarenko, O., Ivask, A., Kakinen, A., Kahru, A., Sub-toxic effects of CuO nanoparticles on bacteria: Kinetics, role of Cu ions and possible mechanisms of action. *Environmental Pollution* 2012, *169*, 81-89.

[361] Buckingham-Meyer, K., Goeres, D. M., Hamilton, M. A., Comparative evaluation of biofilm disinfectant efficacy tests. *Journal of Microbiological Methods* 2007, *70*, 236-244.

[362] Crusz, S. A., Popat, R., Rybtke, M. T., Camara, M.*, et al.*, Bursting the bubble on bacterial biofilms: a flow cell methodology. *Biofouling* 2012, *28*, 835-842.

[363] Weiss Nielsen, M., Sternberg, C., Molin, S., Regenberg, B., Pseudomonas aeruginosa and Saccharomyces cerevisiae biofilm in flow cells. *Journal of visualized experiments : JoVE* 2011.

[364] Turner, A. P. F., Karube, I., Wilson, G. S., Biosensors. Fundamentals and applications. *Biosensors. Fundamentals and applications.* 1987, i-xvi, 1-770.

[365] Deryabin, D. G., Aleshina, E. S., Efremova, L. V., Application of the inhibition of bacterial bioluminescence test for assessment of toxicity of carbon-based nanomaterials. *Microbiology* 2012, *81*, 492-497.

[366] Sotiriou, G. A., Pratsinis, S. E., Antibacterial Activity of Nanosilver Ions and Particles. *Environmental Science & Technology* 2010, *44*, 5649-5654.

[367] Wiles, S., Whiteley, A. S., Philp, J. C., Bailey, M. J., Development of bespoke bioluminescent reporters with the potential for in situ deployment within a phenolic-remediating wastewater treatment system. *Journal of Microbiological Methods* 2003, *55*, 667-677.

[368] Bjarnsholt, T., Kirketerp-Moller, K., Kristiansen, S., Phipps, R.*, et al.*, Silver against Pseudomonas aeruginosa biofilms. *Apmis* 2007, *115*, 921-928.

[369] Halan, B., Schmid, A., Buehler, K., Real-Time Solvent Tolerance Analysis of Pseudomonas sp Strain LB120 Delta C Catalytic Biofilms. *Applied and Environmental Microbiology* 2011, *77*, 1563-1571.

[370] Nguyen, H. H., Park, J., Kang, S., Kim, M., Surface Plasmon Resonance: A Versatile Technique for Biosensor Applications. *Sensors* 2015, *15*, 10481-10510.

[371] Alvarez, M., Lechuga, L. M., Microcantilever-based platforms as biosensing tools. *Analyst* 2010, *135*, 827-836.

[372] Zhang, H.-Y., Pan, H.-Q., Zhang, B.-L., Tang, J.-L., Microcantilever Sensors for Chemical and Biological Applications in Liquid. *Chinese Journal of Analytical Chemistry* 2012, *40*, 801-807.

[373] Waggoner, P. S., Craighead, H. G., Micro- and nanomechanical sensors for environmental, chemical, and biological detection. *Lab on a Chip* 2007, *7*, 1238-1255.

[374] Binnig, G., Quate, C. F., Gerber, C., ATOMIC FORCE MICROSCOPE. *Physical Review Letters* 1986, *56*, 930-933.

[375] Buchapudi, K. R., Huang, X., Yang, X., Ji, H.-F., Thundat, T., Microcantilever biosensors for chemicals and bioorganisms. *Analyst* 2011, *136*, 1539-1556.

[376] Shu, W. M., Laue, E. D., Seshia, A. A., Investigation of biotin-streptavidin binding interactions using microcantilever sensors. *Biosensors & Bioelectronics* 2007, *22*, 2003-2009.

[377] Liu, Y. F., Schweizer, L. M., Wang, W. X., Reuben, R. L.*, et al.*, Label-free and real-time monitoring of yeast cell growth by the bending of polymer microcantilever biosensors. *Sensors and Actuators B-Chemical* 2013, *178*, 621-626.

[378] Wu, C. W., Chang, S. P., Wu, C. J., Huang, S. H., Cells adhered and cultured on microcantilevers. *Microsystem Technologies-Micro-and Nanosystems-Information Storage and Processing Systems* 2013, *19*, 105-112.

[379] Riedel, T., Majek, P., Rodriguez-Emmenegger, C., Brynda, E., Surface plasmon resonance: advances of label-free approaches in the analysis of biological samples. *Bioanalysis* 2014, *6*, 3325-3336.

[380] Wang, X., Xu, J. Y., Chen, Y., Surface Plasmon Resonance Methodology for Interaction Kinetics of Biomolecules. *Progress in Chemistry* 2015, *27*, 550-558.

[381] Bouguelia, S., Roupioz, Y., Slimani, S., Mondani, L.*, et al.*, On-chip microbial culture for the specific detection of very low levels of bacteria. *Lab on a Chip* 2013, *13*, 4024-4032.

[382] Kodoyianni, V., Label-free analysis of biomolecular interactions using SPR imaging. *Biotechniques* 2011, *50*, 32-40.

[383] Abadian, P. N., Kelley, C. P., Goluch, E. D., Cellular Analysis and Detection Using Surface Plasmon Resonance Techniques. *Analytical Chemistry* 2014, *86*, 2799-2812.

[384] Hill, R. T., Plasmonic biosensors. *Wiley Interdisciplinary Reviews-Nanomedicine and Nanobiotechnology* 2015, *7*, 152-168.

[385] Rich, R. L., Myszka, D. G., Survey of the 2009 commercial optical biosensor literature. *Journal of Molecular Recognition* 2011, *24*, 892-914.

[386] Bulard, E., Bouchet-Spinelli, A., Chaud, P., Roget, A.*, et al.*, Carbohydrates as New Probes for the Identification of Closely Related Escherichia coli Strains Using Surface Plasmon Resonance Imaging. *Analytical Chemistry* 2015, *87*, 1804-1811.

[387] Mondani, L., Roupioz, Y., Delannoy, S., Fach, P., Livache, T., Simultaneous enrichment and optical detection of low levels of stressed Escherichia coli O157:H7 in food matrices. *Journal of Applied Microbiology* 2014, *117*, 537-546.

[388] Abadian, P. N., Tandogan, N., Jamieson, J. J., Goluch, E. D., Using surface plasmon resonance imaging to study bacterial biofilms. *Biomicrofluidics* 2014, *8*.

[389] Klein, C., Comero, S., Stahlmecke, B., Romazanov, J., Kuhlbusch, T., van Doren, E., Wick, P., Locoro, G., Koerdel, W., Gawlik, B., Mast, J., Krug, H. F., Hund-Rinke, K., Friedrichs, S., Maier, G., Werner, J., Linsinger, T., NM-300 silver characterisation, stability, homogeneity. EUR - Scientific and Toxicological Sciences 2011, Technical Research Reports, JRC Publication No. JRC60709, EUR 24693 EN, Publications Office of the European Union.

[390] Gaiser, B. K., Hirn, S., Kermanizadeh, A., Kanase, N.*, et al.*, Effects of Silver Nanoparticles on the Liver and Hepatocytes In Vitro. *Toxicological Sciences* 2013, *131*, 537-547.

[391] Kermanizadeh, A., Gaiser, B. K., Hutchison, G. R., Stone, V., An in vitro liver model - assessing oxidative stress and genotoxicity following exposure of hepatocytes to a panel of engineered nanomaterials. *Particle and Fibre Toxicology* 2012, *9*.

[392] Martin, M. M. B., Perez, J. A. S., Fernandez, F. G. A., Sanchez, J. L. G.*, et al.*, A kinetics study on the biodegradation of synthetic wastewater simulating effluent from an advanced oxidation process using Pseudomonas putida CECT 324. *Journal of Hazardous Materials* 2008, *151*, 780-788.

[393] Shim, H., Hwang, B., Lee, S. S., Kong, S. H., Kinetics of BTEX biodegradation by a coculture of Pseudomonas putida and Pseudomonas fluorescens under hypoxic conditions. *Biodegradation* 2005, *16*, 319-327.

[394] Aspray, T. J., Hansen, S. K., Burns, R. G., A soil-based microbial biofilm exposed to 2,4-D: bacterial community development and establishment of conjugative plasmid pJP4. *Fems Microbiology Ecology* 2005, *54*, 317-327.

[395] Fournier, E., Colorimetric quantification of carbohydrates, in: Wrolstad, R.E., Acree, T.E., Decker, E.A., Penner, M.H., Reid, D.S., Schwartz, S.J., Shoemaker, C.F, Smith, D.M., Sporns, P. (Eds.), *Current Protocols in Food Analytical Chemistry* 2001. John Wiley and Sons Inc., Unit E1.1.

[396] Faure, D., Joly, D., Next-generation sequencing as a powerful motor for advances in the biological and environmental sciences. *Genetica* 2015, *143*, 129-132.

[397] Buermans, H. P. J., den Dunnen, J. T., Next generation sequencing technology: Advances and applications. *Biochimica Et Biophysica Acta-Molecular Basis of Disease* 2014, *1842*, 1932-1941.

[398] Caporaso, J. G., Lauber, C. L., Walters, W. A., Berg-Lyons, D.*, et al.*, Ultra-high-throughput microbial community analysis on the Illumina HiSeq and MiSeq platforms. *Isme Journal* 2012, *6*, 1621-1624.

[399] Bolger, A. M., Lohse, M., Usadel, B., Trimmomatic: a flexible trimmer for Illumina sequence data. *Bioinformatics* 2014, *30*, 2114-2120.

[400] Edgar, R. C., Haas, B. J., Clemente, J. C., Quince, C., Knight, R., UCHIME improves sensitivity and speed of chimera detection. *Bioinformatics* 2011, *27*, 2194-2200.

[401] Edgar, R. C., Search and clustering orders of magnitude faster than BLAST. *Bioinformatics* 2010, *26*, 2460-2461.

[402] DeSantis, T. Z., Hugenholtz, P., Larsen, N., Rojas, M.*, et al.*, Greengenes, a chimera-checked 16S rRNA gene database and workbench compatible with ARB. *Applied and Environmental Microbiology* 2006, *72*, 5069-5072.

[403] Heydorn, A., Nielsen, A. T., Hentzer, M., Sternberg, C.*, et al.*, Quantification of biofilm structures by the novel computer program COMSTAT. *Microbiology-Uk* 2000, *146*, 2395-2407.

[404] Cherif, B., Roget, A., Villiers, C. L., Calemczuk, R.*, et al.*, Clinically related protein-peptide interactions monitored in real time on novel peptide chips by surface plasmon resonance imaging. *Clinical Chemistry* 2006, *52*, 255-262.

[405] Eduok, S., Martin, B., Villa, R., Nocker, A.*, et al.*, Evaluation of engineered nanoparticle toxic effect on wastewater microorganisms: Current status and challenges. *Ecotoxicology and Environmental Safety* 2013, *95*, 1-9.

[406] Damoiseaux, R., George, S., Li, M., Pokhrel, S.*, et al.*, No time to lose-high throughput screening to assess nanomaterial safety. *Nanoscale* 2011, *3*, 1345-1360.

[407] Losasso, C., Belluco, S., Cibin, V., Zavagnin, P.*, et al.*, Antibacterial activity of silver nanoparticles: sensitivity of different Salmonella serovars. *Frontiers in Microbiology* 2014, *5*.

[408] Jeong, E., Im, W.-T., Kim, D.-H., Kim, M.-S.*, et al.*, Different susceptibilities of bacterial community to silver nanoparticles in wastewater treatment systems. *Journal of Environmental Science and Health Part a-Toxic/Hazardous Substances & Environmental Engineering* 2014, *49*, 685-693.

[409] Smijs, T. G., Pavel, S., Titanium dioxide and zinc oxide nanoparticles in sunscreens: focus on their safety and effectiveness. *Nanotechnol Sci Appl* 2011, *4*, 95-112.

[410] Wu, X., Monchy, S., Taghavi, S., Zhu, W.*, et al.*, Comparative genomics and functional analysis of niche-specific adaptation in Pseudomonas putida. *Fems Microbiology Reviews* 2011, *35*, 299-323.

[411] Impellitteri, C. A., Harmon, S., Silva, R. G., Miller, B. W.*, et al.*, Transformation of silver nanoparticles in fresh, aged, and incinerated biosolids. *Water Research* 2013, *47*, 3878-3886.

[412] Levard, C., Hotze, E. M., Lowry, G. V., Brown, G. E., Jr., Environmental Transformations of Silver Nanoparticles: Impact on Stability and Toxicity. *Environmental Science & Technology* 2012, *46*, 6900-6914.

[413] Chen, Y. G., Chen, H., Zheng, X., Mu, H., The impacts of silver nanoparticles and silver ions on wastewater biological phosphorous removal and the mechanisms. *Journal of Hazardous Materials* 2012, *239*, 88-94.

[414] Priester, J. H., Van De Werfhorst, L. C., Ge, Y., Adeleye, A. S.*, et al.*, Effects of TiO2 and Ag Nanoparticles on Polyhydroxybutyrate Biosynthesis By Activated Sludge Bacteria. *Environmental Science & Technology* 2014, *48*, 14712-14720.

[415] El Badawy, A. M., Luxton, T. P., Silva, R. G., Scheckel, K. G.*, et al.*, Impact of Environmental Conditions (pH, Ionic Strength, and Electrolyte Type) on the Surface Charge and Aggregation of Silver Nanoparticles Suspensions. *Environmental Science & Technology* 2010, *44*, 1260-1266.

[416] Kaegi, R., Voegelin, A., Ort, C., Sinnet, B.*, et al.*, Fate and transformation of silver nanoparticles in urban wastewater systems. *Water Research* 2013, *47*, 3866-3877.

[417] Kaegi, R., Voegelin, A., Sinnet, B., Zuleeg, S.*, et al.*, Behavior of Metallic Silver Nanoparticles in a Pilot Wastewater Treatment Plant. *Environmental Science & Technology* 2011, *45*, 3902-3908.

[418] Kiser, M. A., Ryu, H., Jang, H., Hristovski, K., Westerhoff, P., Biosorption of nanoparticles to heterotrophic wastewater biomass. *Water Research* 2010, *44*, 4105-4114.

[419] Ma, R., Levard, C., Judy, J. D., Unrine, J. M.*, et al.*, Fate of Zinc Oxide and Silver Nanoparticles in a Pilot Wastewater Treatment Plant and in Processed Biosolids. *Environmental Science & Technology* 2014, *48*, 104-112.

[420] Kent, R. D., Oser, J. G., Vikesland, P. J., Controlled Evaluation of Silver Nanoparticle Sulfidation in a Full-Scale Wastewater Treatment Plant. *Environmental Science & Technology* 2014, *48*, 8564-8572.

[421] Levard, C., Hotze, E. M., Colman, B. P., Dale, A. L.*, et al.*, Sulfidation of Silver Nanoparticles: Natural Antidote to Their Toxicity. *Environmental Science & Technology* 2013, *47*, 13440-13448.

[422] Hall-Stoodley, L., Costerton, J. W., Stoodley, P., Bacterial biofilms: From the natural environment to infectious diseases. *Nature Reviews Microbiology* 2004, *2*, 95-108.

[423] Bester, E., Kroukamp, O., Hausner, M., Edwards, E. A., Wolfaardt, G. M., Biofilm form and function: carbon availability affects biofilm architecture, metabolic activity and planktonic cell yield. *Journal of Applied Microbiology* 2011, *110*, 387-398.

[424] Dror-Ehre, A., Adin, A., Markovich, G., Mamane, H., Control of biofilm formation in water using molecularly capped silver nanoparticles. *Water Research* 2010, *44*, 2601-2609.

[425] Skogman, M. E., Vuorela, P. M., Fallarero, A., Combining biofilm matrix measurements with biomass and viability assays in susceptibility assessments of antimicrobials against Staphylococcus aureus biofilms. *Journal of Antibiotics* 2012, *65*, 453-459.

[426] Tote, K., Horemans, T., Vanden Berghe, D., Maes, L., Cos, P., Inhibitory Effect of Biocides on the Viable Masses and Matrices of Staphylococcus aureus and Pseudomonas aeruginosa Biofilms. *Applied and Environmental Microbiology* 2010, *76*, 3135-3142.

[427] Habimana, O., Steenkeste, K., Fontaine-Aupart, M.-P., Bellon-Fontaine, M.-N.*, et al.*, Diffusion of Nanoparticles in Biofilms Is Altered by Bacterial Cell Wall Hydrophobicity. *Applied and Environmental Microbiology* 2011, *77*, 367-368.

[428] Jahn, A., Griebe, T., Nielsen, P. H., Composition of Pseudomonas putida biofilms: Accumulation of protein in the biofilm matrix. *Biofouling* 1999, *14*, 49-57.

[429] Crabbe, A., Leroy, B., Wattiez, R., Aertsen, A.*, et al.*, Differential proteomics and physiology of Pseudomonas putida KT2440 under filament-inducing conditions. *Bmc Microbiology* 2012, *12*.

[430] Jensen, R. H., Woolfolk, C. A., FORMATION OF FILAMENTS BY PSEUDOMONAS-PUTIDA. *Applied and Environmental Microbiology* 1985, *50*, 364-372.

[431] Justice, S. S., Hunstad, D. A., Cegelski, L., Hultgren, S. J., Morphological plasticity as a bacterial survival strategy. *Nature Reviews Microbiology* 2008, *6*, 162-168.

[432] Weimer, M., Applying Precaution in EU Authorisation of Genetically Modified Products-Challenges and Suggestions for Reform. *European Law Journal* 2010, *16*, 624-657.

[433] Lok, C.-N., Ho, C.-M., Chen, R., He, Q.-Y.*, et al.*, Silver nanoparticles: partial oxidation and antibacterial activities. *Journal of Biological Inorganic Chemistry* 2007, *12*, 527-534.

[434] Li, X., Lee, D.-W., Integrated microcantilevers for high-resolution sensing and probing. *Measurement Science & Technology* 2012, *23*.

[435] Otero-Gozalez, L., Field, J. A., Sierra-Alvarez, R., Inhibition of anaerobic wastewater treatment after long-term exposure to low levels of CuO nanoparticles. *Water Research* 2014, *58*, 160-168.

[436] Thalmann, B., Voegelin, A., Sinnet, B., Morgenroth, E., Kaegi, R., Sulfidation Kinetics of Silver Nanoparticles Reacted with Metal Sulfides. *Environmental Science & Technology* 2014, *48*, 4885-4892.

[437] Boholm, M., Arvidsson, R., Controversy over antibacterial silver: implications for environmental and sustainability assessments. *Journal of Cleaner Production* 2014, *68*, 135-143.

[438] Zhang, D., Ding, A., Cui, S., Hu, C.*, et al.*, Whole cell bioreporter application for rapid detection and evaluation of crude oil spill in seawater caused by Dalian oil tank explosion. *Water Research* 2013, *47*, 1191-1200.

[439] Abd-El-Haleem, D., Zaki, S., Abulhamd, A., Elbery, H., Abu-Elreesh, G., Acinetobacter bioreporter assessing heavy metals toxicity. *Journal of Basic Microbiology* 2006, *46*, 339-347.

[440] Kurvet, I., Ivask, A., Bondarenko, O., Sihtmaee, M., Kahru, A., LuxCDABE-Transformed Constitutively Bioluminescent Escherichia coli for Toxicity Screening: Comparison with Naturally Luminous Vibrio fischeri. *Sensors* 2011, *11*, 7865-7878.

[441] Ivask, A., Francois, M., Kahru, A., Dubourguier, H. C.*, et al.*, Recombinant luminescent bacterial sensors for the measurement of bioavailability of cadmium and lead in soils polluted by metal smelters. *Chemosphere* 2004, *55*, 147-156.

[442] Ben-Israel, O., Ben-Israel, H., Ulitzur, S., Identification and quantification of toxic chemicals by use of Escherichia coli carrying lux genes fused to stress promoters. *Applied and Environmental Microbiology* 1998, *64*, 4346-4352.

[443] Vandyk, T. K., Reed, T. R., Vollmer, A. C., Larossa, R. A., Synergistic induction of the heat-shock response in Escherichia coli by simultaneous treatment with chemical inducers. *Journal of Bacteriology* 1995, *177*, 6001-6004.

[444] Yoo, S. K., Lee, J. H., Yun, S.-S., Gu, M. B., Lee, J. H., Fabrication of a bio-MEMS based cell-chip for toxicity monitoring. *Biosensors & Bioelectronics* 2007, *22*, 1586-1592.

[445] Mitchell, R. J., Gu, M. B., Characterization and optimization of two methods in the immobilization of 12 bioluminescent strains. *Biosensors & Bioelectronics* 2006, *22*, 192-199.

[446] Kim, B. C., Gu, M. B., A multi-channel continuous water toxicity monitoring system: Its evaluation and application to water discharged from a power plant. *Environmental Monitoring and Assessment* 2005, *109*, 123-133.

[447] Chang, S. T., Lee, H. J., Gu, M. B., Enhancement in the sensitivity of an immobilized cell-based soil biosensor for monitoring PAH toxicity. *Sensors and Actuators B-Chemical* 2004, *97*, 272-276.

[448] Gu, M. B., Kim, B. C., Cho, J., Hansen, P. D., The continuous monitoring of field water samples with a novel multi-channel two-stage mini-bioreactor system. *Environmental Monitoring and Assessment* 2001, *70*, 71-81.

[449] Gill, R. T., Valdes, J. J., Bentley, W. E., A Comparative Study of Global Stress Gene Regulation in Response to Overexpression of Recombinant Proteins in Escherichia coli. *Metabolic Engineering* 2000, *2*, 178-189.

[450] Ivask, A., Rolova, T., Kahru, A., A suite of recombinant luminescent bacterial strains for the quantification of bioavailable heavy metals and toxicity testing. *Bmc Biotechnology* 2009, *9*, 15.

[451] Eltzov, E., Ben-Yosef, D. Z., Kushmaro, A., Marks, R., Detection of sub-inhibitory antibiotic concentrations via luminescent sensing bacteria and prediction of their mode of action. *Sensors and Actuators B-Chemical* 2008, *129*, 685-692.

[452] Eltzov, E., Marks, R. S., Voost, S., Wullings, B. A., Heringa, M. B., Flow-through real time bacterial biosensor for toxic compounds in water. *Sensors and Actuators B-Chemical* 2009, *142*, 11-18.

[453] Daniel, R., Almog, R., Ron, A., Belkin, S., Diamand, Y. S., Modeling and measurement of a whole-cell bioluminescent biosensor based on a single photon avalanche diode. *Biosensors & Bioelectronics* 2008, *24*, 882-887.

[454] Lee, J. H., Gu, M. B., An integrated mini biosensor system for continuous water toxicity monitoring. *Biosensors & Bioelectronics* 2005, *20*, 1744-1749.

[455] Premkumar, J. R., Lev, O., Marks, R. S., Polyak, B.*, et al.*, Antibody-based immobilization of bioluminescent bacterial sensor cells. *Talanta* 2001, *55*, 1029-1038.

[456] Davidov, Y., Rozen, R., Smulski, D. R., Van Dyk, T. K.*, et al.*, Improved bacterial SOS promoter:: lux fusions for genotoxicity detection. *Mutation Research-Genetic Toxicology and Environmental Mutagenesis* 2000, *466*, 97-107.

[457] Min, J. H., Lee, C. W., Moon, S. H., LaRossa, R. A., Gu, M. B., Detection of radiation effects using recombinant bioluminescent Escherichia coli strains. *Radiation and Environmental Biophysics* 2000, *39*, 41-45.

[458] Min, J. H., Kim, E. J., LaRossa, R. A., Gu, M. B., Distinct responses of a recA :: luxCDABE Escherichia coli strain to direct and indirect DNA damaging agents. *Mutation Research-Genetic Toxicology and Environmental Mutagenesis* 1999, *442*, 61-68.

[459] Belkin, S., Smulski, D. R., Dadon, S., Vollmer, A. C.*, et al.*, A panel of stress-responsive luminous bacteria for the detection of selected classes of toxicants. *Water Research* 1997, *31*, 3009-3016.

[460] Vollmer, A. C., Belkin, S., Smulski, D. R., VanDyk, T. K., LaRossa, R. A., Detection of DNA damage by use of Escherichia coli carrying recA'-lux, uvrA'-lux, or alkA'-lux reporter plasmids. *Applied and Environmental Microbiology* 1997, *63*, 2566-2571.

[461] Pedahzur, R., Polyak, B., Marks, R. S., Belkin, S., Water toxicity detection by a panel of stress-responsive luminescent bacteria. *Journal of Applied Toxicology* 2004, *24*, 343-348.

[462] Polyak, B., Bassis, E., Novodvorets, A., Belkin, S., Marks, R. S., Bioluminescent whole cell optical fiber sensor to genotoxicants: system optimization. *Sensors and Actuators B-Chemical* 2001, *74*, 18-26.

[463] Lee, H. Y., Choi, S. H., Gu, M. B., Response of bioluminescent bacteria to sixteen azo dyes. *Biotechnology and Bioprocess Engineering* 2003, *8*, 101-105.

[464] Manukhov, I. V., Kotova, V. Y., Mal'dov, D. G., Il'ichev, A. V.*, et al.*, Induction of oxidative stress and SOS response in Escherichia coli by vegetable extracts: the role of hydroperoxides and the synergistic effect of simultaneous treatment with cisplatinum. *Microbiology* 2008, *77*, 523-529.

[465] Ptitsyn, L. R., Horneck, G., Komova, O., Kozubek, S.*, et al.*, A biosensor for environmental genotoxin screening based on an SOS lux assay in recombinant Escherichia coli cells. *Applied and Environmental Microbiology* 1997, *63*, 4377-4384.

[466] Tecon, R., Beggah, S., Czechowska, K., Sentchilo, V.*, et al.*, Development of a Multistrain Bacterial Bioreporter Platform for the Monitoring of Hydrocarbon Contaminants in Marine Environments. *Environmental Science & Technology* 2010, *44*, 1049-1055.

[467] Bechor, O., Smulski, D. R., Van Dyk, T. K., LaRossa, R. A., Belkin, S., Recombinant microorganisms as environmental biosensors: pollutants detection by Escherichia coli bearing fabA ':: lux fusions. *Journal of Biotechnology* 2002, *94*, 125-132.

[468] Lee, J. H., Youn, C. H., Kim, B. C., Gu, M. B., An oxidative stress-specific bacterial cell array chip for toxicity analysis. *Biosensors & Bioelectronics* 2007, *22*, 2223-2229.

[469] Mitchell, R. J., Gu, M. B., An Escherichia coli biosensor capable of detecting both genotoxic and oxidative damage. *Applied Microbiology and Biotechnology* 2004, *64*, 46-52.

[470] Belkin, S., Smulski, D. R., Vollmer, A. C., VanDyk, T. K., LaRossa, R. A., Oxidative stress detection with Escherichia coli harboring a katG'::lux fusion. *Applied and Environmental Microbiology* 1996, *62*, 2252-2256.

[471] Niazi, J. H., Kim, B. C., Ahn, J.-M., Gu, M. B., A novel bioluminescent bacterial biosensor using the highly specific oxidative stress-inducible pgi gene. *Biosensors & Bioelectronics* 2008, *24*, 670-675.

[472] Oh, J. T., Cajal, Y., Skowronska, E. M., Belkin, S.*, et al.*, Cationic peptide antimicrobials induce selective transcription of micF and osmY in Escherichia coli. *Biochimica Et Biophysica Acta-Biomembranes* 2000, *1463*, 43-54.

[473] Rupani, S. P., Gu, M. R., Konstantinov, K. B., Dhurjati, P. S.*, et al.*, Characterization of the stress response of a bioluminescent biological sensor in batch and continuous cultures. *Biotechnology Progress* 1996, *12*, 387-392.

[474] Hever, N., Belkin, S., A dual-color bacterial reporter strain for the detection of toxic and genotoxic effects. *Engineering in Life Sciences* 2006, *6*, 319-323.

[475] Elasri, M. O., Reid, T., Hutchens, S., Miller, R. V., Response of a Pseudomonas aeruginosa biofilm community to DNA-damaging chemical agents. *Fems Microbiology Ecology* 2000, *33*, 21-25.

[476] Elasri, M. O., Miller, R. V., A Pseudomonas aeruginosa biosensor responds to exposure to ultraviolet radiation. *Applied Microbiology and Biotechnology* 1998, *50*, 455-458.

[477] Bhattacharyya, J., Read, D., Amos, S., Dooley, S.*, et al.*, Biosensor-based diagnostics of contaminated groundwater: assessment and remediation strategy. *Environmental Pollution* 2005, *134*, 485-492.

[478] Flynn, H. C., McMahon, V., Diaz, G. C., Demergasso, C. S.*, et al.*, Assessment of bioavailable arsenic and copper in soils and sediments from the Antofagasta region of northern Chile. *Science of the Total Environment* 2002, *286*, 51-59.

[479] Paton, G. I., Viventsova, E., Kumpene, J., Wilson, M. J.*, et al.*, An ecotoxicity assessment of contaminated forest soils from the Kola Peninsula. *Science of the Total Environment* 2006, *355*, 106-117.

[480] Sousa, S., Duffy, C., Weitz, H., Glover, L. A., Bar, E., Use of a lux-modified bacterial, biosensor to identify constraints to bioremediation of BTEX-contaminated sites. *Environmental Toxicology and Chemistry* 1998, *17*, 1039-1045.

[481] Kelly, C. J., Tumsaroj, N., Lajoie, C. A., Assessing wastewater metal toxicity with bacterial bioluminescence in a bench-scale wastewater treatment system. *Water Research* 2004, *38*, 423-431.

[482] Lajoie, C. A., Lin, S. C., Kelly, C. J., Comparison of bacterial bioluminescence with activated sludge oxygen uptake rates during zinc toxic shock loads in a wastewater treatment system. *Journal of Environmental Engineering-Asce* 2003, *129*, 879-883.

[483] Kelly, C. J., Lajoie, C. A., Layton, A. C., Sayler, G. S., Bioluminescent reporter bacterium for toxicity monitoring in biological wastewater treatment systems. *Water Environment Research* 1999, *71*, 31-35.

[484] Diplock, E. E., Alhadrami, H. A., Paton, G. I., Application of Microbial Bioreporters in Environmental Microbiology and Bioremediation. *Whole Cell Sensing Systems Ii: Applications* 2010, *118*, 189-209.

[485] Dawson, J. J. C., Iroegbu, C. O., Maciel, H., Paton, G. I., Application of luminescent biosensors for monitoring the degradation and toxicity of BTEX compounds in soils. *Journal of Applied Microbiology* 2008, *104*, 141-151.

[486] Baumstark-Khan, C., Cioara, K., Rettberg, P., Horneck, G., Determination of geno- and cytotoxicity of groundwater and sediments using the recombinant SWITCH test. *Journal of Environmental Science and Health Part a-Toxic/Hazardous Substances & Environmental Engineering* 2005, *40*, 245-263.

## Output I - Published paper 1

Title: "Silver, zinc oxide and titanium dioxide nanoparticle ecotoxicity to bioluminescent *Pseudomonas putida* in laboratory medium and artificial wastewater"

Journal: *Environmental Pollution* (2014), doi:10.1016/j.envpol.2014.09.002

Authors: Florian Mallevre (Main author, Main experimenter), Teresa F. Fernandes, Thomas J. Aspray (Corresponding author)

Institution: NanoSafety Research Group, School of Life Sciences, Heriot-Watt University, Edinburgh EH14 4AS, UK

Abstract: Bacteria based ecotoxicology assessment of manufactured nanoparticles is largely restricted to *Escherichia coli* bioreporters in laboratory media. Here, toxicity effects of model OECD nanoparticles (Ag NM-300K, ZnO NM-110 and $TiO_2$ NM-104) were assessed using the switch-off luminescent *Pseudomonas putida* BS566::luxCDABE bioreporter in Luria Bertani (LB) medium and artificial wastewater (AW). $IC_{50}$ values ~4 mg $L^{-1}$, 100 mg $L^{-1}$ and >200 mg $L^{-1}$ at 1 h were observed in LB for Ag NM-300K, ZnO NM-110 and $TiO_2$ NM-104, respectively. Similar results were obtained in AW for Ag NM-300K ($IC_{50}$ ~5 mg $L^{-1}$) and $TiO_2$ NM-104 (IC50 >200 mg $L^{-1}$) whereas ZnO NM-110 was significantly higher ($IC_{50}$ >200 mg $L^{-1}$). Lower ZnO NM-110 toxicity in AW compared to LB was associated with differences in agglomeration status and dissolution rate. This work demonstrates the importance of nanoecotoxicological studies in environmentally relevant matrices.

## Output II - Published paper 2

Title: "Toxicity testing of pristine and aged silver nanoparticles in real wastewaters using bioluminescent *Pseudomonas putida*"

Journal: *Nanomaterials* (2016), doi:10.3390/nano6030049

Special issue: "Engineered nanomaterials in the environment"

Authors: Florian Mallevre[1] (Main author, Main experimenter), Camille Alba[2] (Co-Main experimenter), Craig Milne[3], Simon Gillespie[3], Teresa F. Fernandes[1], Thomas J. Aspray[1] (Corresponding author)

Institutions: (1) NanoSafety Research Group, School of Life Sciences, Heriot-Watt University, Edinburgh EH14 4AS, UK; (2) Lille 1 University, Sciences and Technologies, Villeneuve d'Ascq 59650, France; (3) Scottish Water, Juniper House, Heriot-Watt Research Park, Edinburgh EH14 4AP, Scotland, UK

Abstract: The toxicity of pristine and aged silver nanoparticles (Ag NPs) to a bioluminescent *Pseudomonas putida* bioreporter was measured in spiked crude (CWs) and final (FWs) wastewater samples collected from four wastewater treatment plants (WWTPs). Results showed lower toxicity of pristine Ag NPs in CWs than in FWs. The effect of the matrix on the eventual Ag NP toxicity was related to multiple physico-chemical parameters (BOD, COD, TSS, pH, ammonia, sulphide and chloride) based on multivariate analysis. However, no site effect was concluded. Aged Ag NPs (up to 8 weeks) were found less toxic than pristine Ag NPs in CWs; evident increased aggregation and decreased dissolution were associated with ageing. Ag NPs exhibited consistent toxicity in FWs in spite of ageing; comparable results were obtained in artificial wastewater (AW) simulating effluent. The study demonstrates the value of performing nanoparticle acute toxicity testing in real and complex matrices such as wastewaters using relevant bacterial bioreporters.

## Output III - Published paper 3

Title: "*Pseudomonas putida* biofilm dynamics following a single pulse of silver nanoparticles"

Journal: *Chemosphere* (2016), doi:10.1016/j.chemosphere.2016.03.060

Special issue: "Thermodynamics and kinetics of emerging contaminants in the environment"

Authors: Florian Mallevre (Main author, Main experimenter), Teresa F. Fernandes, Thomas J. Aspray (Corresponding author)

Institution: NanoSafety Research Group, School of Life Sciences, Heriot-Watt University, Edinburgh EH14 4AS, UK

Abstract: *Pseudomonas putida* mono-species biofilms were exposed to silver nanoparticles (Ag NPs) in artificial wastewater (AW) under hydrodynamic conditions. Specifically, 48 h old biofilms received a single pulse of Ag NPs at 0, 0.01, 0.1, 1, 10 and 100 mg $L^{-1}$ for 24 h in confocal laser scanning microscopy (CLSM) compatible flow-cells. The biofilm dynamics (in terms of morphology, viability and activity) were characterised at 48, 72 and 96 h. Consistent patterns were found across flow-cells and experiments at 48 h. Dose dependent impacts of NPs were then shown at 72 h on biofilm morphology (*e.g.* biomass, surface area and roughness) from 0.01 mg $L^{-1}$. The microbial viability was not altered below 10 mg $L^{-1}$ Ag NPs. The activity (based on the D-glucose utilisation) was impacted by concentrations of Ag NPs equal and superior to 10 mg $L^{-1}$. Partial recovery of morphology, viability and activity were finally observed at 96 h. Comparatively, exposure to Ag salts resulted in *ca*. one order of magnitude higher toxicity when compared to Ag NPs. Consequently, the use of a continuous culture system and incorporation of a recovery stage extends the value of biofilm assays beyond the standard acute toxicity assessment.

## Output IV - Published paper 4

Title: "Real-time toxicity testing of silver nanoparticles to *Salmonella* Enteritidis using Surface Plasmon Resonance imaging: a proof of concept"

Journal: *NanoImpact* (2016), doi:10.1016/j.impact.2016.02.004

Authors: Florian Mallevre[1] (Main author, Main experimenter), Vincent Templier[2], Raphael Mathey[2], Loic Leroy[2], Yoann Roupioz[2], Teresa F. Fernandes[1], Thomas J. Aspray[1] (Corresponding author), Thierry Livache[2]

Institutions: (1) NanoSafety Research Group, School of Life Sciences, Heriot-Watt University, Edinburgh EH14 4AS, UK; (2) INAC - SPRAM, UMR CEA CNRS Univ. Grenoble Alpes, F-38000 Grenoble, France

Abstract: In this paper we report for the first time on the suitability of surface plasmon resonance imaging (SPRi) for performing ecotoxicity testing of nanoparticles (NPs). Specifically, the impact of silver NPs (using Ag NM-300K) and ions (using $AgNO_3$ salt) on *Salmonella* Enteritidis growth was assessed in Luria Bertani medium using the culture-capture- measure (CCM) based SPRi method. Clear effects were observed at 10 mg $L^{-1}$ Ag NPs characterised by shifted SPRi detection times ($T_D$) by *ca*. 2.6 h compared to the control. Comparable results were obtained using 1 mg $L^{-1}$ Ag ions. No clear effects were observed at 1 mg $L^{-1}$ Ag NPs and 0.1 mg $L^{-1}$ Ag ions. Overall results match the current trend in nanoecotoxicology using bacteria (*e.g*. impact of Ag NPs between 1 and 10 mg $L^{-1}$ and higher toxicity of Ag ions compared to Ag NPs). The dose dependent patterns of toxicity were coherent with those obtained using a standard plating method; however, the SPRi approach was faster (*i.e*. results within a few hours) and generated kinetic data (*i.e*. real-time monitoring). In addition, SPRi presents many valuable intrinsic advantages (*e.g*. label-free, multiplex, bespoke and robust) over current approaches. Consequently, a plethora of opportunities for future developments and applications of SPRi in NP testing is associated with the proof of concept reported herein.

## Output V - List of events/presentations and poster portfolio

Society of Environmental Toxicology and Chemistry conference 2013, Glasgow, UK (helper)

School of Life Sciences conference 2013, HWU, Edinburgh, UK (co-organiser, talk presentation)

Society of Environmental Toxicology and Chemistry conference 2014, Basel, Switzerland (poster n°1 presentation)

HWU Post Graduate conference 2014, Edinburgh, UK (poster n°1 presentation)

Scottish Environmental Technology Network meeting 2014, Glasgow, UK (poster n°2 presentation)

NanoSafe conference 2014, Grenoble, France (poster n°3 presentation)

Centre for Marine Biodiversity and Biotechnology away day 2014, UK (talk presentation, best talk award)

Microfluidics conference 2014, Limerick, UK (poster n°4 presentation by W. Mielczarek)

Biofilm network meeting 2015, Glasgow, UK (talk presentation)

World Water conference 2015, Edinburgh, UK (e-poster n°5 presentation)

Poster n°1

# Nanoparticle ecotoxicity testing in laboratory media and wastewater using a *lux*-based switch-off *Pseudomonas putida* bioreporter

Florian Mallevre*, Thomas J. Aspray, Teresa F. Fernandes

*Corresponding author: fm203@hw.ac.uk

Nano-Safety Research Group, School of Life Sciences, Heriot-Watt University, Edinburgh, EH14 4AS, Scotland, UK

## INTRODUCTION

Manufactured nanoparticles (NPs), defined as anthropogenic materials exhibiting all three external dimensions at the nanoscale, are being increasingly used in commercial products and industrial processes. Although offering benefits, the wide use of NPs has raised health and safety concerns regarding their potential release to and impact in the environment.[1,2] However, fate and ecotoxicity of NPs are still largely unknown on account of, notably, the challenge for establishing suitable, harmonised and reproducible nanoecotoxicological methodologies as currently much debated in the literature.[3,4]

In this context, genetically modified bacteria (GMB) represent particularly interesting screening tools already validated in ecotoxicology for drug and chemical testing.[5,6] Readily available, GMB definitively offer advantages (e.g. cheap, easy to handle, potentially integrable into devices and multiplexable, etc.) to help establishing suitable screening approaches in nanoecotoxicology. However to date, studies have been restricted to assays in laboratory rich media, as such information in real matrices such as wastewaters is lacking.[7,8]

### Emerging Nanoecotoxicology

### GMB Bioreporters

### Delicate Applications

## OBJECTIVES

A *Pseudomonas putida* strain (*P. putida* BS566::luxCDABE), originally isolated from wastewater and subsequently tagged with a full *lux* cassette to generate a constitutive (i.e. switch-off) luminescent GMB bioreporter, was recently proposed for nanoparticle testing.[11] Only applied for silver nanoparticle assessment in laboratory rich medium so far, this *P. putida* GMB bioreporter, though remarkable, remains weakly validated.

The aims of this work were thus:

1) to assess the ecotoxicity of three OECD standard inorganic nanoparticles (Ag NM-300K, ZnO NM-110 and $TiO_2$ NM-104) in two different laboratory matrices (Luria-Bertani as rich medium and Artificial Wastewater as minimal medium) to *P. putida* BS566::luxCDABE;

2) to correlate ecotoxicity results to nanoparticle characterisation information in both matrices;

3) to trial nanoparticle ecotoxicity testing in real crude and final wastewaters from wastewater treatment plants.

## APPROACH

Constitutive (switch-off) luminescent *P. putida* bioreporter (precultured overnight) (used at $10^8$ cell $mL^{-1}$ per well)

NPs freshly prepared in media along with characterisation (i.e. UV-Vis, DLS, AAS) (sonicated 2 x 8 min then used at 0-200 mg $L^{-1}$)

Black flat bottomed 96-well plate (final volume 100 µL per well)

28°C for 120 min (measure every 15 min)

Luminescence = f(Time)

Relative Luminescence = f(Concentration of NPs)

$IC_{50}$

## OBJECTIVE 1

### Toxicity in Luria-Bertani

Toxicity of Ag NM-300K, ZnO NM-110 and $TiO_2$ NM-104 OECD standard nanoparticles was tested on *P. putida* BS566::luxCDABE in Luria-Bertani (LB, rich medium) and Artificial Wastewater (AW, minimal medium).

### Toxicity in Artificial Wastewater

Relative luminescence output reduction by *P. putida* when challenged with 0 - 200 mg $L^{-1}$ of Ag (blue), ZnO (red) and $TiO_2$ (green) nanoparticles in LB (ABOVE) or in AW (LEFT) for three selected time points (0 h, 1 h and 2 h). Data are mean ± standard error of the mean with n = 3.

### Derived $IC_{50}$ overtime

ABOVE: Calculated $IC_{50}$ for various time points by fitting a four parameter dose-response model to the logarithm of the concentration. Derivation of $IC_{50}$ for ZnO in AW and for $TiO_2$ in both matrices was not applicable. Data are mean ± standard error of the mean with n = 3.

- Ag NPs showed comparable toxicity patterns between matrices with non significantly different $IC_{50}$ at 1 h close to 4-6 mg $L^{-1}$.
- ZnO NPs showed exclusive and temporary toxicity in LB with $IC_{50}$ from 60 to 100 mg $L^{-1}$ during the first hour of exposure.
- No toxicity was monitorable for $TiO_2$ NPs in both matrices.

## OBJECTIVE 2

### Agglomeration / Aggregation status

Agglomeration / Aggregation status were evaluated in LB and AW by UV-Vis and DLS. ABOVE: Specific absorption spectra of 10 mg $L^{-1}$ Ag (A.), 200 mg $L^{-1}$ ZnO (B.), 10 mg $L^{-1}$ $TiO_2$ (C.) and z-average (Δ) and polydispersity index (PDI, ○) of 10 mg $L^{-1}$ Ag, ZnO, and $TiO_2$ (D.). Data are mean ± standard error of the mean with n = 3. Significantly different at $^{**}p < 0.01$ and $^{****}p < 0.0001$.

- All NPs showed specific spectra with unique peak by UV-Vis. DLS analysis showed polydispersity of all NPs in both matrices (PDI ~0.3-0.6). Ag showed comparable z-averages in both matrices. ZnO and $TiO_2$ showed significantly higher z-averages in AW attesting to agglomeration / aggregation in this matrix.

### Dissolution / Ion release rates

Dissolution rates were calculated as ratios between the AAS measured concentration of released element from NPs in supernatant after ultracentrifugation and the original prepared concentration of NPs. LEFT: Dissolution rates of 50 mg $L^{-1}$ of Ag (A.) and 200 mg $L^{-1}$ of ZnO (B.) after 0 h or 1 h of incubation. Data are mean ± standard error of the mean with n = 3. Significantly different at $^{***}p < 0.0001$. No dissolution study was carried out for $TiO_2$ since it was considered not relevant.

- Ag NPs showed low and time independent dissolution rates ~ 2-4 % in both matrices which were not found significantly different. ZnO NPs showed matrix dependent and time independent dissolution rates close to 40 % in LB and to 2.5 % in AW.

## OBJECTIVE 3

### Toxicity in Real Wastewaters

Toxicity of Ag NPs was tested in fresh real crude (RCW) and final (RFW) wastewaters. LEFT: Derived $IC_{50}$ overtime from *P. putida* when challenged with 0 - 200 mg $L^{-1}$ of Ag NPs in LB, AW, RCW and RFW. Data are mean ± standard error of the mean with n = 3.

### Wastewater sample parameters

ABOVE: A list of key and common wastewater parameters is recorded besides toxicity results.

- Though lower in more complex matrices, the toxicity of Ag NM-300K NPs persisted in real wastewaters.
- Proposed approach based on a remarkable *P. putida* bioreporter is suitable for assays in real matrices such as wastewaters.
- Assays are continuing over wastewaters from different treatment plants in collaboration with Scottish Water along with NP and wastewater characterisation.

## CONCLUSIONS

Ecotoxicity of Ag NM-300K, ZnO NM-110 and $TiO_2$ NM-104 OECD standard nanoparticles was assessed in various matrices using a constitutively luminescent *P. putida* BS566::luxCDABE bioreporter based methodology. Toxicity results were correlated with matrix dependent nanoparticle fate characterised by DLS, UV-visible and AAS when applicable. Overall results showed:

1) the suitability and reproducibility of the switch-off *P. putida* BS566::luxCDABE bioreporter based approach for NP testing, even in real and complex matrices such as wastewaters;

2) a global ecotoxicity ranking (Ag > ZnO > $TiO_2$ NPs) correlating to known information on bacteria in the literature with versatile underlying NP fates depending on the particle material and the matrix of exposure;

3) the persisting ecotoxicity of Ag NM-300K NPs in real environmental matrices;

4) the importance of further assays in real matrices along with characterisation information in order to lead towards fate and toxicity forecast.

## REFERENCES

1. K. Johnston et al. 2013, doi: 10.3109/17435390.2012.736107.
2. T.M. Benn et al. 2010, doi: 10.1016/j.watres.2010.04.036.
3. B.J. Kahru et al. 2008, doi: 10.1007/s00253-008-1.
4. A. Kahru et al. 2013, doi: 10.1021/es304037c.
5. S. D. Petersen et al. 2001, doi: 10.1023/A:1014599.1374.
6. A.S. Ozmen et al. 2004, doi: 10.1016/j.ejps.2003.10.
7. T.T. Su et al. 2013, doi: 10.1016/j.ecoenv.2012.01.
8. C.A. Reilly et al. 2008, doi: 10.1128/AEM.
9. A. R. Pilsbeck et al. 2003, doi: 10.1016/j.enzmictec.2003.
10. J.R. Van der Meer et al. 2010, doi: 10.1038/nrmicro2.
11. R.J. Dams et al. 2011, doi: 10.1016/j.jhazmat.2011.06.

## FUNDINGS

Work funded by: James Watt Scholarship (HWU)

Communication sponsored by: Alumni Annual Fund Grant (HWU)

Poster n°2

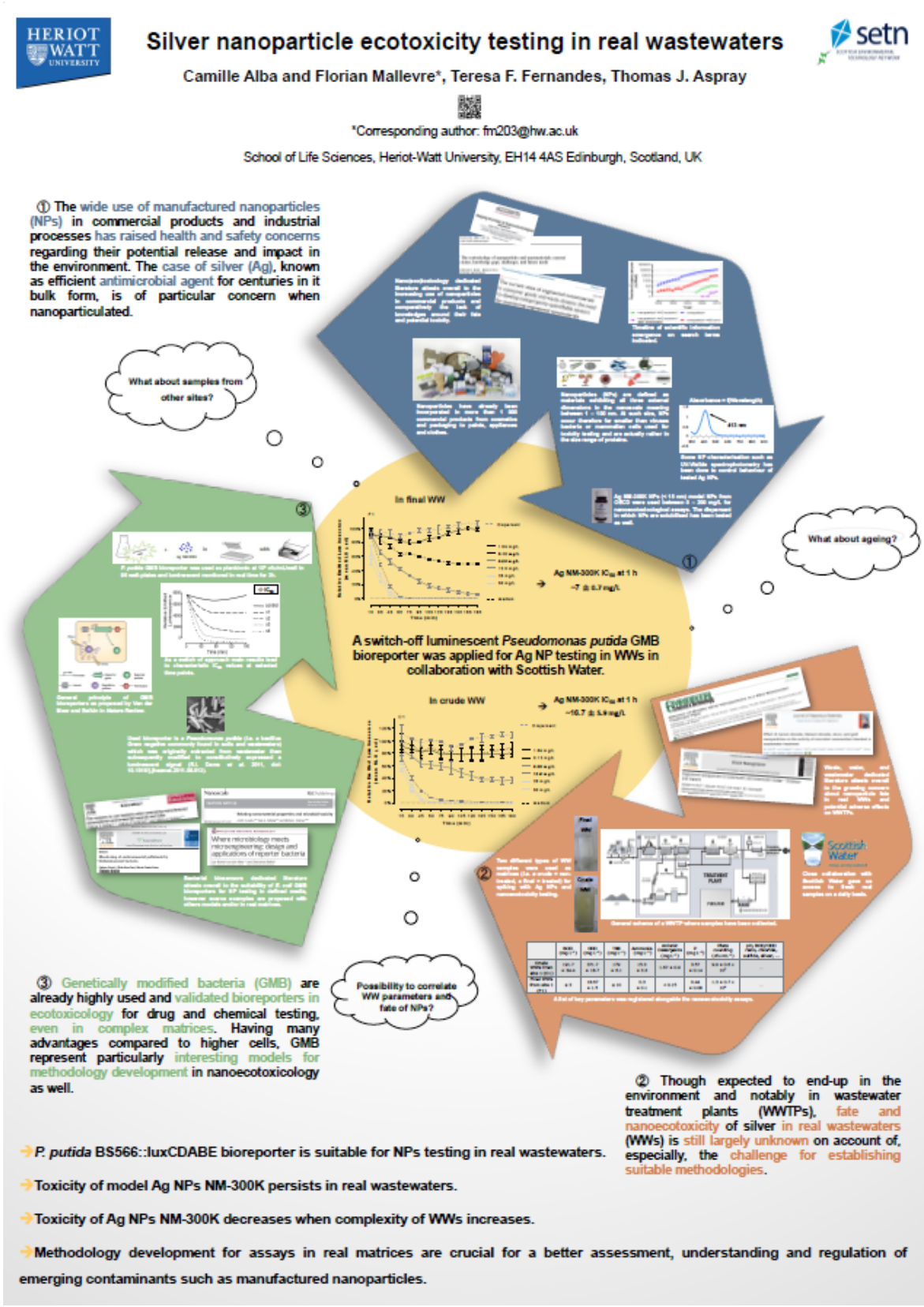
Silver nanoparticle ecotoxicity testing in real wastewaters
Camille Alba and Florian Mallevre*, Teresa F. Fernandes, Thomas J. Aspray
*Corresponding author: fm203@hw.ac.uk
School of Life Sciences, Heriot-Watt University, EH14 4AS Edinburgh, Scotland, UK
① The wide use of manufactured nanoparticles (NPs) in commercial products and industrial processes has raised health and safety concerns regarding their potential release and impact in the environment. The case of silver (Ag), known as efficient antimicrobial agent for centuries in it bulk form, is of particular concern when nanoparticulated.
What about samples from other sites?
What about ageing?
In final WW
Ag NM-300K IC50 at 1 h ~7 (± 0.7 mg/L
A switch-off luminescent Pseudomonas putida GMB bioreporter was applied for Ag NP testing in WWs in collaboration with Scottish Water.
In crude WW
Ag NM-300K IC50 at 1 h ~16.7 (± 5.9 mg/L
Scottish Water
③ Genetically modified bacteria (GMB) are already highly used and validated bioreporters in ecotoxicology for drug and chemical testing, even in complex matrices. Having many advantages compared to higher cells, GMB represent particularly interesting models for methodology development in nanoecotoxicology as well.
Possibility to correlate WW parameters and fate of NPs?
② Though expected to end-up in the environment and notably in wastewater treatment plants (WWTPs), fate and nanoecotoxicity of silver in real wastewaters (WWs) is still largely unknown on account of, especially, the challenge for establishing suitable methodologies.
P. putida BS566::luxCDABE bioreporter is suitable for NPs testing in real wastewaters.
Toxicity of model Ag NPs NM-300K persists in real wastewaters.
Toxicity of Ag NPs NM-300K decreases when complexity of WWs increases.
Methodology development for assays in real matrices are crucial for a better assessment, understanding and regulation of emerging contaminants such as manufactured nanoparticles.

Poster n°3

# Silver nanoparticle toxicity to *Pseudomonas putida* mono-species biofilms under flow conditions

Florian Mallevre*, Teresa F. Fernandes, Thomas J. Aspray

*Corresponding author: fm203@hw.ac.uk

Nano-Safety Research Group, Heriot-Watt University, Edinburgh, EH14 4AS, Scotland, UK

**INTRODUCTION.** Biofilms, defined as "matrix-enclosed microbial accretions that adhere to biological or non-biological surfaces", are structurally complex and dynamic systems with major implications in natural environments as well as in various sectors such as the water/wastewater sector [1,2].

Manufactured nanoparticles (NPs), defined as "anthropogenic materials exhibiting all three external dimensions at the nanoscale", are being increasingly used for various purposes with raising health and safety concerns regarding their potential adverse effect [3,4].

Evidences of released NPs in wastewaters are emerging [5] however their actual impact to relevant structures such as biofilms, especially under flow conditions, is still poorly addressed. Consequently, main aims of this work were to:

→ assess the toxicity of Ag NM-300K NPs under flow conditions in artificial wastewater (AW) to *P. putida* mono-species biofilms,

→ compare with Ag ion based toxicity under the same conditions.

**EXPERIMENTAL PROCEDURE.** Followed method and used materials [6,7].

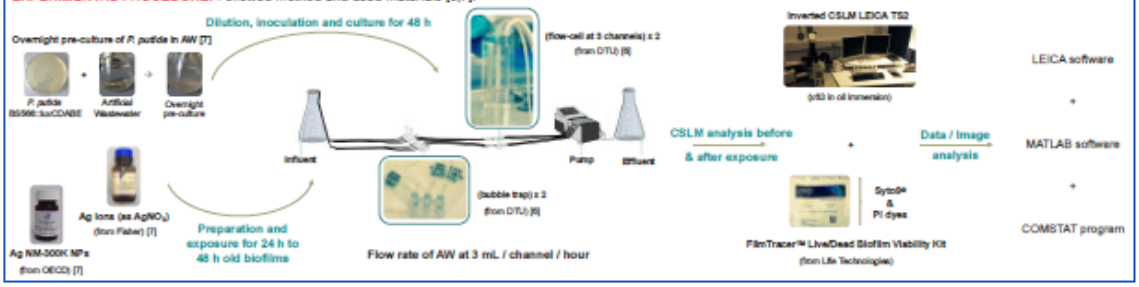


**RESULTS 1.** Ag NM-300K NP toxicity to *P. putida* biofilms

Biofilm culture in flow conditions (result at 48 h)

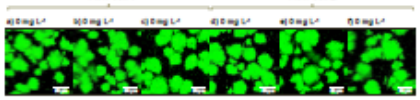


Example of maximized z-stacks registered at 48 h (i.e. ante exposure) over all channels for 1 exp.

→ Consistent biofilm growth across channels and experiments

(also based on matlab / comstat analysis, data table not shown)

→ No dual staining

Exposure for 24 h to Ag NM-300K NPs (result at 72 h)

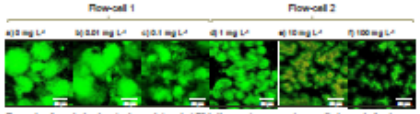


Example of maximized z-stacks registered at 72 h (i.e. post exposure) over all channels for 1 exp.

→ Dose dependant toxicity pattern

(also based on matlab / comstat analysis, data table not shown)

→ Dual staining

(visible at 10 mg $L^{-1}$ exclusively for 3 out of 5 experiments)

Analysis as (result at 72 h - result at 48 h) / (result at 48 h) per condition considering 420 z-stacks over 5 independent exp.

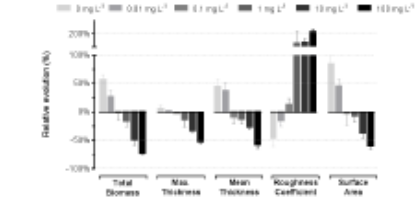


→ Impacts include:

↓ biomass, thickness, surface area

↑ roughness

→ Altered biofilm morphology from the lowest tested concentrations

Histogram of the relative evolution (in %) of characteristic parameters of biofilms post exposure to Ag NPs for 24 h. Data, calculated per condition as (result at 72 h - result at 48 h) / (result at 48 h), are mean ± SEM with n = 6. For each experiment 7 random z-stacks were registered per condition at both 48 h and 72 h.

**RESULTS 2.** Ag ion toxicity to *P. putida* biofilms

Exposure for 24 h to Ag ions ($AgNO_3$)

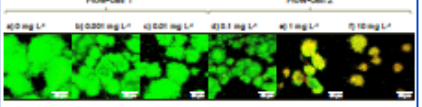


Example of maximized z-stacks registered at 72 h (i.e. post exposure) over all channels for 1 exp.

→ Dose dependant toxicity pattern for Ag ions as well

→ Ag ions are at least 1 order of magnitude more toxic

→ Dual staining more presents

(visible at 1 and 10 mg $L^{-1}$ for all experiments)

**RESULTS 3.** Ag NM-300K NP characterization in AW

UV-visible, DLS and AAS analysis related information

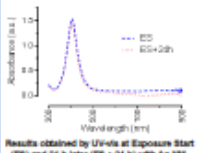


Results obtained by UV-vis at Exposure Start (ES) and 24 h later (ES + 24 h) with Ag NM-300K NPs at 10 mg $L^{-1}$.

| | ES | ES + 24 h |
|---|---|---|
| Z-average (nm) | 50.4 ± 2.3 | 42.8 ± 2.7 |
| PDI | 0.47 ± 0.03 | 0.52 ± 0.06 |
| Zeta potential (mV) | - 8 ± 1.3 | - 10 ± 0.6 |
| Dissolution (%) | ~ 2.6 (lbs) | ~ 2.6 (lbs) |

Results obtained by DLS and AAS at Exposure Start (ES) and 24 h later (ES + 24 h) with Ag NM-300K NPs at 10 mg $L^{-1}$.

→ Sole peak at ~ 413 nm, z-average of ~ 60 nm, zeta potential of ~ - 9 mV, dissolution of ~ 2.6-3 %

→ Comparable status overall of NPs at ES and ES + 24 h

**CONCLUSIONS.** The ecotoxicity of Ag NM-300K NPs and Ag ions was assessed on *P. putida* mono-species biofilms in artificial wastewater simulating effluent using a CSLM compatible flow-cell system based methodology. Two-day old mature biofilms were exposed for 24 h and characterised by CLSM before and after exposure.

Main conclusions drawn:

→ dose-dependent toxicity patterns to *P. putida* biofilms in AW with measurable effects occurring from the lowest doses tested,

→ toxicity patterns mainly driven by released-ions from NPs.

Future applications:

→ test other NPs and ions / with mono- and multi-species biofilms / with bespoke scenarios of exposure / in different matrices.

**REFERENCES.**

[1] Hall-Stoodley *et al.* 2004, doi:10.1038/nrmicro821; [2] Karunakaran *et al.* 2011, doi: 10.1007/s00253-011-3293-4; [3] Ju-Nam *et al.* 2008, doi: 10.1016/j.scitotenv.2008.06.042; [4] Klaine *et al.* 2008, doi: 10.1897/08-090.1; [5] Gottschalk *et al.* 2013, doi: 10.1002/wnan.2177; [6] Tolker-Nielsen *et al.* 2011, doi: 10.1002/9780471729259.mc01b02s21; [7] Mallevre *et al.* 2014, doi: 10.1016/j.envpol.2014.09.002.

More information about ongoing research here

**ACKNOWLEDGMENTS.**

Heriot-Watt University for providing FM with a James Watt scholarship.

European Union's Seventh Framework Programme [FP7 2007-2013] under EC-GA No. 263215 'MARINA' for the provision of the nanomaterials used in this study.

Poster n°4

# "Microworld and Microflows" Initiating School Children to Microfluidics

W. Mielczarek*[1], T. J. Aspray[2], F. Mallevre[2], M. Jimenez[1], J. McGrath[1], P. Cameron[3], H. Bridle[1] and M. Kersaudy-Kerhoas*[1]

Institute of Biological Chemistry, Biophysics and Bioengineering

[1]Heriot-Watt University - Institute of Biological Chemistry, Biophysics and Bioengineering, School of Engineering and Physical Sciences - Edinburgh Campus, EH14 4AS Edinburgh, UK
[2]Heriot Watt University, School of Life Sciences - Edinburgh Campus, EH14 4AS Edinburgh, UK
[3]Novo Science Ltd, 3 Hatton Mains Cottages, Dalmahoy, EH27 8EB Edinburgh, UK
* Corresponding authors: wsm30@hw.ac.uk, m.kersaudy-kerhoas@hw.ac.uk

## Summary


- Increasing popularity of microfluidics in research and commercially available applications contrasts with its modest recognition among the public.
- Outreach activities such as science festivals and school workshops are efficient in popularising microfluidics as well as science and engineering in general.
- Microfluidics is attractive for the public due to its varied, multidisciplinary and applied nature.
- Children and their families benefit from public engagement but so does the whole science and engineering community.


## Planning public engagement

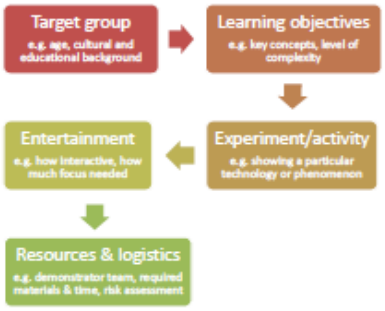


Main challenges of planning a science festival workshop:
- diversity of participants' ages and backgrounds,
- short time dedicated to each activity,
- balance between entertainment and education.

## Microworld and Microflows at Bang Goes The Borders 2013


- Local annual science festival at Melrose, Scottish Borders.
- Attended by families with children aged 3-15.
- Positive reception of our microfluidics workshop.

## Ingenious

ROYAL ACADEMY OF ENGINEERING

We were awarded Royal Academy of Engineering Ingenious grant for project "Small Plumbing: Empowering the next-generation of Microfluidic Engineers" to push ahead with our outreach work taking it into schools:
- Changing public perception of Engineering.
- Encouraging studying STEM subjects.
- Enabling high school pupils to design microfluidic chips.

## Microworld and Microflows Workshop structure

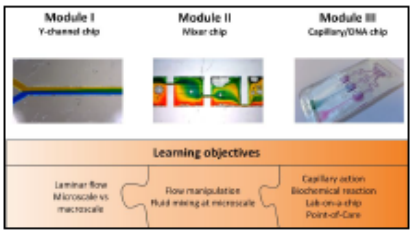


Chip fabrication: simple sandwich of 3-4 laser-cut PMMA layers.
Workflow: from basic concepts of fluid flow at the microscale, through flow handling, to portable sensing.

## Conclusion

- Hands-on and visual microfluidic experiments prove to be highly popular among school children.
- Demonstrations can be attractive despite their simplicity in terms of the involved science and technology.
- Children are able to grasp the key concepts in a field they are exposed to for the first time.
- The public is keen to learn about new technologies, the microfluidics community needs to come out!

Poster n°5

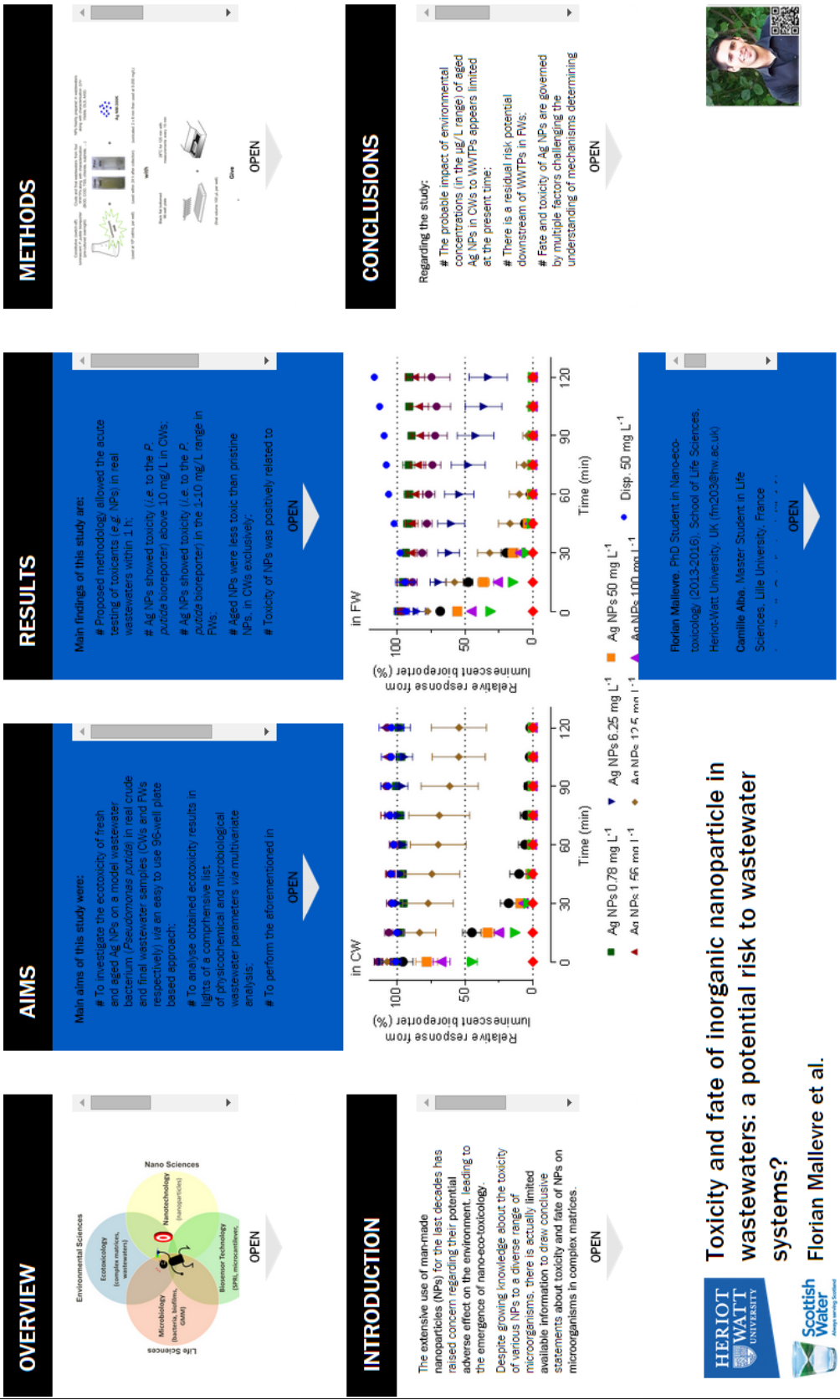
OVERVIEW
Environmental Sciences
Nano Sciences
Life Sciences
Ecotoxicology (complex matrices, wastewaters)
Nanotechnology (nanoparticles)
Microbiology (bacteria, biofilms, GMM)
Biosensor Technology (SPRi, microcantilever,
OPEN
INTRODUCTION
The extensive use of man-made nanoparticles (NPs) for the last decades has raised concern regarding their potential adverse effect on the environment, leading to the emergence of nano-eco-toxicology.
Despite growing knowledge about the toxicity of various NPs to a diverse range of microorganisms, there is actually limited available information to draw conclusive statements about toxicity and fate of NPs on microorganisms in complex matrices.
OPEN
AIMS
Main aims of this study were:
# To investigate the ecotoxicity of fresh and aged Ag NPs on a model wastewater bacterium (*Pseudomonas putida*) in real crude and final wastewater samples (CWs and FWs respectively) via an easy to use 96-well plate based approach;
# To analyse obtained ecotoxicity results in lights of a comprehensive list of physicochemical and microbiological wastewater parameters via multivariate analysis;
# To perform the aforementioned in
OPEN
RESULTS
Main findings of this study are:
# Proposed methodology allowed the acute testing of toxicants (e.g. NPs) in real wastewaters within 1 h;
# Ag NPs showed toxicity (i.e. to the *P. putida* bioreporter) above 10 mg/L in CWs;
# Ag NPs showed toxicity (i.e. to the *P. putida* bioreporter) in the 1-10 mg/L range in FWs;
# Aged NPs were less toxic than pristine NPs, in CWs exclusively;
# Toxicity of NPs was positively related to
OPEN
in CW
in FW
Relative response from luminescent bioreporter (%)
Time (min)
Ag NPs 0.78 mg L-1
Ag NPs 6.25 mg L-1
Ag NPs 50 mg L-1
Disp. 50 mg L-1
METHODS
OPEN
CONCLUSIONS
Regarding the study:
# The probable impact of environmental concentrations (in the µg/L range) of aged Ag NPs in CWs to WWTPs appears limited at the present time;
# There is a residual risk potential downstream of WWTPs in FWs;
# Fate and toxicity of Ag NPs are governed by multiple factors challenging the understanding of mechanisms determining
OPEN
Toxicity and fate of inorganic nanoparticle in wastewaters: a potential risk to wastewater systems?
Florian Mallevre et al.
fm203@hw.ac.uk
Florian Mallevre, PhD Student in Nano-eco-toxicology (2013-2016), School of Life Sciences, Heriot-Watt University, UK (fm203@hw.ac.uk)
Camille Alba, Master Student in Life Sciences, Lille University, France
OPEN
HERIOT WATT UNIVERSITY
Scottish Water